Polymerization of Vinyl Acetate by High Energy Radiation

By Seizo OKAMURA, Takao YAMASHITA and
Toshinobu HIGASHIMURA

(Received February 22, 1956)

Introduction

While extensive work has been carried out on the radiation polymerization of vinyl compounds, there has been comparatively little attention paid to that of vinyl acetate. One of the reasons for this seems to be that in the case of vinyl acetate the reproducibility was very poor as shown by the work of Chapiro[1]. It is, however, even more attractive for us to study the radiation polymerization of vinyl acetate, because the considerations on the degree of polymerization are done more easily from two sides as polyvinyl acetate and also as polyvinyl alcohol. Manowitz et al.[2] had recognized that the degree of polymerization increased during polymerization and this could be explained by the branching or the cross-linking of polymers. Attempts have now been made to clarify the chain transfer mechanism of polymer molecules in the radiation polymerization of vinyl acetate. This leads to some preliminary conclusion that the increase of the molecular weight during polymerization is coming from the branching at the acetyl side chain of polyvinyl acetate. The degree of polymerization of polyvinyl alcohol was found to be comparatively higher than that in the thermal polymerization. This reason, however, has not yet been clarified in this paper.

Experimental

Vinyl acetate (VAc), methyl acrylate (MA) and methyl methacrylate (MMA) were polymerized in sealed tubes, in which gas phase was replaced by vacuum and thereafter by nitrogen. Sources of gamma-rays were 20 and 0.5 curies of Cobalt-60, and its doses were measured by the method of Weiss[3]. X-ray from a 180 kV.-20 mA. apparatus were filtered by 0.3 mm. Cu and 0.5 mm. Al, and the dose rate at 12.5 cm. distance from target, that is at the middle point of reaction vessel, was 977 r/min. The average degrees of polymerization were calculated by the following equations,

PVAc in acetone: $\bar{P}_{AC}=(\text{antilog}\ \frac{[\eta]}{0.28}-1)\cdot 2000$

PMMA in chloroform: $[\eta]=2.52\cdot 10^{-3}\bar{P}^{0.80}$

PVA in water: $\log \bar{P}_A=1.613\log\frac{[\eta]\times 10^4}{8.87}$

1) A. Chapiro, *J. chim. phys.*, **47**, 764 (1950).
2) D.S. Ballantine, P. Colombo, A. Glines and B. Manowitz, *Chem. Eng. Prog. Symp.*, **50**, No. 11, 267 (1954).
3) J. Weiss, *Nucleonics*, **10**, (7). 28 (1952).

Results

The rates of polymerization were shown in Figs 1 and 2. In both cases of gamma- and X-rays, the polymerization of MMA showed

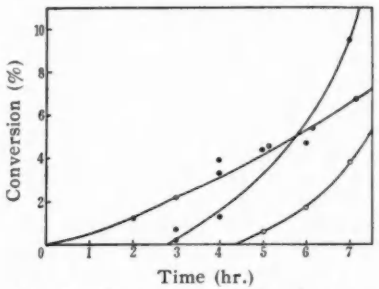

Fig. 1. Gamma-ray polymerization of VAc (●), MMA (⊙) and MA (○). 2 cm from 20 curie Co-60., 10±2°C, dose rate; about 15×10^3 r/hr.

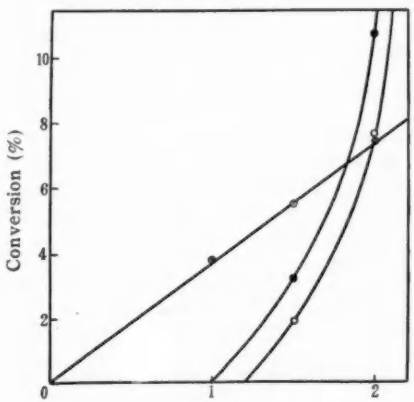

Fig. 2. X-ray polymerization of VAc (○ and ●) and MMA (⊙). 18±2°C, dose rate; 977 r/min.

no induction period, that of VAc showed a moderate one and that of MA a long one. The order of the rates of polymerization was VAc>MA>MMA, in accordance with the results obtained by Chapiro[1]. Table I repre-

CHEMISTRY HALL LIBRARY

TABLE I

THE DEGREES OF POLYMERIZATION OF POLYVINYL ACETATE

Expt. No.	Condition of Irradiation	Polym. Time (hr.)	Polym. Yields (%)	Viscosity [η]	$\bar{P}_{AC}$	Huggins Constants k'
gamma-4	2 cm. from 20 curies Co-60	4	3.35	0.232	11480	0.28
gamma-5	〃 〃 〃	5	4.41	0.248	13370	0.31
gamma-7	〃 〃 〃	7	9.53	0.290	19710	0.37
X-1	X-rays	1.5	3.20	0.158	5330	0.30
X-2	〃	2	10.70	0.187	7190	0.32

sents the degrees of polymerization of polyvinyl acetate obtained by gamma- and X-rays.

As shown in Table I, the degrees of polymerization were found to increase rapidly during polymerization. In the case of MA, the intrinsic viscosities were measured as 0.38 and 0.73 at the polymerization yields of 1.7 and 3.9 respectively. The degrees of polymerization of PMMA were 6000–7000 independent of the polymerization yields in the range of 1–7. Table II shows the degrees of polymerization of polyvinyl alcohol obtained by the saponification of PVAc.

The degrees of polymerization of the polyvinyl alcohol were found to be very high compared with those obtained by the thermal polymerization. The content of 1,2 glycol bond in PVA, measured by the comsumption of periodic acid[4] was found to be 1.23% in the sample S-1.

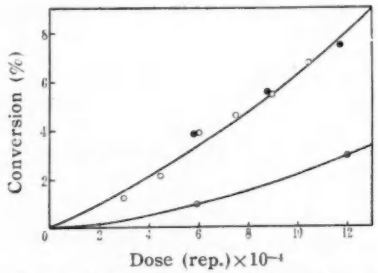

Fig. 3. The relationship between dose and conversion of gamma- and X-ray polymerization of MMA.
○; gamma-ray polym. (15000 r/hr. 10°C)
●; X-ray polym. (58600 r/hr. 18°C)
⊙; gamma-ray polym. (Manowitz et al.[2] 250000 r/hr. room temperature).

TABLE II

THE DEGREES OF POLYMERIZATION OF POLYVINYL ALCOHOL

Expt. No.	Condition of Irradiation	Polym. Time (hr.)	Polym. Yields (%)	Polym. Temp. (°C)	Viscosity [η]	$\bar{P}_A$	k'
gamma-7'	Same as gamma-7 in Table I	7	9.53	10	0.223	7440	0.77
gamma-15*	〃	15	95	〃	0.219	6710	0.75
gamma-24*	〃	24	100	〃	0.195	5990	0.63
X-2'	Same as X-2 in Table I	2	10.70	18	0.155	4140	0.90
S-1	at 3.5 cm. from 0.5 curies Co-60,	ca. 8 days	27	0–5	0.269	10070	0.82
S-2	〃	ca. 9 days	92	〃	0.234	7980	0.75
H-1*	Same as gamma-7	7	95.6	51	0.144	3680	0.80
L-III*	Upper of test tube at	15	Average		0.255	9230	—
L-M*	Middle 1–6.4 cm. from	〃	75	10	0.232	7950	—
L-d*	Under 20 curies Co-60	〃			0.202	6420	—

* Marks indicate that PVAc forms gel in acetone.

Discussion

The relationships between the rates of polymerization and the total doses of radiation are shown in Fig. 3. In these conditions, that was 15,000 r/hr., 10°C at gamma-rays and 58,600 r/hr. 18°C at X-rays respectively, just the same rates were obtained in both cases of gamma- and X-rays. The results of Manowitz[2] were considerably low, as shown in Fig. 3. It has been reported that the lower rates of polymerization were obtained at a higher dose rate in the same total doses[5].

4) I. Sakurada and G. Takahashi, Private communications, Sep., 10, 1955.

5) I.A. Berstein, E.C. Farmer, W.G. Rothschild and F.F. Spalding, *J. Chem. Phys.*, **21**, 1303 (1953).

These situations were just the same as those shown in Fig. 3.

The degrees of polymerization of PVAc increase during polymerization, and the extrapolated values of degrees of polymerization to zero yields coincide well with that of PVA. This relation is just the same as in thermal or catalysed polymerization.

From the following equation[6], we could obtain the branching reactivity of polymer (k'_b/k_b) and that of monomer (k''_b/k_b).

$$\left(\frac{1}{P_A}-\frac{1}{P_{AC}}\right)$$

$$=-\frac{k'_b}{k_b}\left\{1+\frac{1}{X}\ln(1-X)\right\}+\frac{k''_b}{k_b}$$

where X was the polymerization yield, k'_b and k''_b were the branching velocity constants of polymer and of monomer respectively, and k_b was the propagating velocity constant.

As shown in Table III, the branching reaction by monomer is of the same order as the normal one $(k''_b/k_b \fallingdotseq 0.5\times10^{-4})$, but the branching by polymer (k'_b/k_b) occurs more rapidly than in the thermal or catalyzed polymerization $(k'_b/k_b \fallingdotseq 2.5\times10^{-4})$.

TABLE III

VELOSITY CONSTANTS RATIOS OF SECONDARY POLYMERIZATION BY GAMMA- AND X-RAYS

Conditions of polymerization	k'_b/k_b	k''_b/k_b
gamma-rays	$12.0\cdot10^{-4}$	$0.33\cdot10^{-4}$
X-rays	$13.9\cdot10^{-4}$	$0.36\cdot10^{-4}$

One of the observed complexities, hitherto reported in the case of styrene, methyl acrylate and so on, was found to be related to the branching reactions, which occurred during the radiation polymerization. Much further work, however, is of course necessary in these important points.

The authors wish to express their heartfelt thanks to Prof. Ichiro Sakurada and also to Prof. Tadashi Fukuda for kind advice and encouragement.

Department of Textile-chemistry, Faculty of Engineering, Kyoto University, Kyoto

6) S. Okamura and T. Yamashita, *Bull. of the Institute for Chemical Research*, Kyoto University, **18**, 46 (1949).

*The Oxygen Equilibrium of Denatured Hemoglobin and the Mechanism of Denaturation**

By Masaji KUBO

(Received April 5, 1956)

Hemoglobin is perhaps one of the most interesting compounds known to biochemists. The development of the physico-chemical methods, such as x-ray analysis[1] and magneto-chemical investigation[2], has led to a considerable increase of knowledge in regard to the structure of the molecule of this important compound. The problem of the structure could also be tackled with the aid of chemical equilibria involving hemoglobin molecules capable of undergoing a great variety of reactions with other molecules and ions. Since, however, the normal physiological function of hemolobin is the transport of oxygen, the combination thereof with hemoglobin has been studied in the most extensive way. From the analysis of the oxygen equilibrium curve, it has been concluded that the four hemes in a hemoglobin molecule are located at the corners of a square (or a rectangle) and that stabilizing interaction exists between the hemes along the sides of the square[3,4,5]. The effect of pH on the oxygen equilibrium, i.e., Bohr effect, has clarified the existence of oxygen-linked acid groups[6].

* The substance of this paper was presented in a lecture delivered before the annual meeting of the Chemical Society of Japan on April 4, 1956.

1) M.F. Perutz, *Nature*, **143**, 731 (1939); ibid., **149**, 491 (1942). J. Boyes-Watson and M.F. Perutz, ibid., **151**, 714 (1943). J. Boyes-Watson, E. Davidson and M.F. Perutz, *Proc. Roy. Soc. London*, **A 191**, 83 (1947).

2) L. Pauling and C.D. Coryell, *Proc. Natl. Acad. Sci. U. S.*, **22**, 159, 210 (1936).

3) L. Pauling, *Proc. Natl. Acad. Sci. U. S.*, **21**, 186 (1936).

4) J. Wyman, *Adv. Protein Chem.*, **4**, 407 (1948).

5) D. Allen, K.F. Guthe and J. Wyman, *J. Biol. Chem.*, **187**, 393 (1950).

6) B. German and J. Wyman, *J. Biol. Chem.*, **117**, 533 (1937).

From the temperature dependence of the oxygen equilibrium[7], the heat of oxygenation has been evaluated.

The effect of denaturation has attracted little attention[8], probably because the oxygen equilibrium curve of denatured homoglobin can be less easily interpreted than that of a fresh preparation. Although denaturation is a property common to a large group of proteins, it is doubtful whether a general theory can be worked out which would be universally applicable to all proteins. In view of this point, any theory of denaturation for a particular protein, if the theory is definite and detailed, will lead to a better understanding of this important phenomenon. The present investigations has been undertaken in order to infer the mechanism of denaturation of hemoglobin from its oxygen equilibrium curve.

Experimental Method and Results

Experiments were carried out at the Biological Laboratories of Harvard University. The experimental procedure was essentially the same as that used by Wyman and his collaborators[5]. Hemoglobin solutions were prepared from cow blood and were buffered with a phosphate mixture, pH being equal to 6.8. Slight denaturation took place while the preparations were left to stand in an ice-box for a few days or more. The degree of partial saturation with oxygen was determined at 20°C by the spectrophotometric method described in a previous paper[9].

The oxygen equilibrium curve depends upon the degree of denaturation. A typical example in the case of slight denaturation is shown in Fig. 1, in which Y, the degree of partial saturation with oxygen, is plotted against $\log p$, the logarithm of the partial pressure of oxygen in equilibrium with the hemoglobin solution. It will be seen that the curve is not exactly symmetric across the center at $Y=1/2$ and $\log p=\log p_0$, where p_0 denotes the partial pressure of oxygen corresponding to 50% saturation. Therefore the data cannot be fitted by any symmetric curve of whatever shape. If a symmetric curve is drawn through the center in accordance with Hill's empirical equation described below, both sets of data lie above the curve for large as well as small values of saturation. This feature of the curve is characteristic of the denatured hemoglobin irrespective of the degree of denaturation. The deviation from symmetry seems to lie within the fringe of experimental errors in the case of a fresh preparation, but increases with increasing degree of denaturation, until it becomes apparent and indubitable in view of the accuracy of measurements.

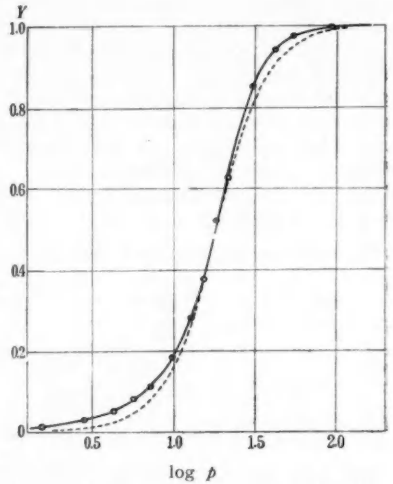

Fig. 1. The degree of partial saturation with oxygen of a slightly denatured cow hemoglobin plotted against the logarithm of the partial pressure of oxygen. The dotted curve depicts the symmetric equilibrium curve of Equation (2), which is applicable to a fresh preparation.

It should be mentioned in this connection that the same trend of asymmetry can also be seen in the oxygen equilibrium curves obtained by Forbes and Roughton[10] on sheep hemoglobin and by Courtice and Douglas[11] on human hemoglobin. Both employed a gasometric method. Their data were considered to be most accurate before the advent of the spectrophotometric method, which shortened the time required for measurements and thus minimized the effect of denaturation.

Discussion

The oxygen equilibrium of a fresh preparation of hemoglobin accords, to a fair degree of accuracy, with Hill's empirical equation[12].

$$Y=Kp^n/(1+Kp^n), \qquad (1)$$

where K and n are constants. The present writer[13] proposed an equation of the following form.

$$Y=\frac{1}{2}+\frac{1}{2}\tanh\left(\frac{n}{2}\ln\frac{p}{p_0}\right). \qquad (2)$$

The relation between the two sets of constants is $K=p_0^{-n}$. Eq. (2) is mathematically equivalent to Hill's original equation but expresses the property of symmetry with greater clearness. The hyperbolic tangent curve has

7) J. Wyman, *J. Biol. Chem.*, **127**, 581 (1939).
8) A.E. Mirsky and L. Pauling, *Proc. Natl. Acad. Sci. U. S.*, **22**, 439 (1936).
9) M. Kubo, This Bulletin, **26**, 189 (1953).
10) W.H. Forbes and F.J.W. Roughton, *J. Physiol.*, **71**, 229 (1931).
11) F.C. Courtice and C.G. Douglas, *J. Physiol.*, **105**, 345 (1947).
12) A.V. Hill, *Biochem. J.*, **7**, 471 (1913).
13) M. Kubo, *Proc. Japan Acad.*, **29**, 156 (1953).

a center of symmetry, the existence of which has been confirmed very carefully by the experimental data of Wyman et al.[5]. From Eq. (2), the following relation can be derived.

$$\ln[Y/(1-Y)]=n(\ln p-\ln p_0). \quad (3)$$

Therefore a plot of $\ln[Y/(1-Y)]$ against $\ln p$ yields a straight line, the inclination of which gives the value of n. In the case of denatured hemoglobin a similar plot gives a slightly curved line, which is convex towards the abscissa.

Obviously the experimental points can never be fitted by an empirical equation having two constants. One must resort to the more general expression for Y of the following form first proposed by Adair[14].

$$Y=\frac{L_1p+2L_2p^2+3L_3p^3+4L_4p^4}{4(1+L_1p+L_2p^2+L_3p^3+L_4p^4)}. \quad (4)$$

The meaning of this equation becomes clear from the following considerations. At any given partial pressure of oxygen, hemoglobin will be present in five different forms distinguished by i, the number of molecules of oxygen combined with each molecule of hemoglobin. The different forms may be referred to by Hb, HbO_2, $Hb(O_2)_2$, $Hb(O)_3$, and $Hb(O_2)_4$, which are present in relative amounts, $1:L_1p:L_2p^2:L_3p^3:L_4p^4$. Obviously L_i is the equilibrium constant of the formation of $Hb(O_2)_i$ from Hb and i molecules of oxygen. Accordingly the equilibrium constant of oxygenation,

$$Hb(O_2)_{i-1}+O_2=Hb(O_2)_i,$$

is given by $K_i=L_i/L_{i-1}$. By definition, $L_0=1$.

Although Eq. (4) is general and theoretically sound, it is difficult to determine the four constants uniquely from a rather smooth curve, because the equation contains too many constants. Let the discussion be opened with a consideration of symmetry, which is realized, at least approximately, even in the case of slightly denatured hemoglobin.

If the relation (4) is plotted in a Y versus $\ln p$ diagram and if the origin of the coordinates is shifted to the center of symmetry at $Y=1/2$ and $\ln p=\ln p_0$ according to the relations,

$$y=Y-1/2,\ x=\ln p-\ln p_0,$$

one has

$$\begin{aligned} y&=\frac{-2-L_1p+L_3p^3+2L_4p^4}{4(1+L_1p+L_2p^2+L_3p^3+L_4p^4)}\\ &=\frac{-2-L_1p_0e^x+L_3p_0^3e^{3x}+2L_4p_0^4e^{4x}}{4(1+L_1p_0e^x+L_2p_0^2e^{2x}+L_3p_0^3e^{3x}+L_4p_0^4e^{4x}}\\ &=\frac{-2e^{-2x}-L_1p_0e^{-x}+L_3p_0^3e^x+2L_4p_0^4e^{2x}}{4(e^{-2x}+L_1p_0e^{-x}+L_2p_0^2+L_3p_0^3e^x+L_4p_0^4e^{2x})}. \end{aligned} \quad (5)$$

The condition of symmetry implies that y is an odd function of x.

$$y=\frac{2L_4p_0^4e^{-2x}+L_3p_0^3e^{-x}-L_1p_0e^x-2e^{2x}}{4(L_4p_0^4e^{-2x}+L_3p_0^3e^{-x}+L_2p_0^2+L_1p^0e^x+e^{2x})}. \quad (6)$$

The right hand sides of Eqs. (5) and (6) are identically equal to each other, irrespective of the value of x. Hence

$$1=L_4p_0^4,\ L_1p_0=L_3p_0^3,$$

or

$$\Delta\equiv L_3^2-L_1^2L_4=0. \quad (7)$$

Eq. (7) embodies the necessary and sufficient condition of symmetry of the equilibrium curve[4].

The same relation can be obtained in a different way, which is more instructive. The oxygenation of hemoglobin is analogous to acid-base titration in that the former represents progressive saturation of hemoglobin with oxygen while the latter is nothing but a process in which the negative charges of a base are successively neutralized with protons. The analogy is complete if one considers the reverse process of the dissociation of a polybasic acid, H_2R, and compares it with oxygenation in the following way:

$$R^{--}+2H^+=HR^-+H^+=H_2R,$$

$$Hb+4O_2=HbO_2+3O_2=\cdots=Hb(O_2)_4.$$

Just as pK_1 (or pK_2) of the polybasic acid is the value of pH at which the amounts of H_2R and HR^- (or HR^- and R^{--}) are equal to each other, one may define pO_i** as the value of $\ln p$ at which the amount of $Hb(O_2)_{i-1}$ is equal to that of $Hb(O_2)_i$. Since the equilibrium constant of oxygenation of $Hb(O_2)_{i-1}$ is $K_i=L_i/L_{i-1}$ as mentioned above, it follows that

$$pO_i=-\ln K_i=\ln(L_{i-1}/L_i). \quad (8)$$

If pO_i increases with increasing i and the four values of pO_i are far apart from each other, the oxygen equilibrium curve would show seven inflection points at each of the pO_i's and also between the neighboring pO_i's. Then it would bear striking resemblance to a titration curve. If the pO_i's approach towards each other or if their order is reversed, a number of inflection points disappear leaving only one, as is actually found in the oxygen equilibrium curve of hemoglobin.

The condition of symmetry of the curve is that the middle point of pO_1 and pO_4 coincides with that of pO_2 and pO_3. In other words, pO_4-pO_3 is equal to pO_2-pO_1. This, in terms of the constants L in Eq. (8), is the following:

14) G.S. Adair, *Proc. Roy. Soc. London*, A 109, 292 (1925); *J. Biol. Chem.*, 63, 529 (1925).

** This p should not be confused with p denoting the partial pressure of oxygen.

$$\frac{L_3}{L_4} \Big/ \frac{L_2}{L_3} = \frac{L_1}{L_2} \Big/ \frac{1}{L_1} \quad \text{or} \quad L_3^2 = L_1^2 L_4, \tag{9}$$

which is identical with the relation (7). It will be seen that the constant L_2 has nothing to do with the symmetry property, although it affects the slope of the curve at the center, or at $Y=1/2$.

If, on the other hand, $L_3^2 - L_1^2 L_4$ is not equal to zero, the Y-ln p curve of Eq. (4) loses its symmetry. If the difference is positive, $pO_4 - pO_3$ is greater than $pO_2 - pO_1$ and the whole curve, except the point at $Y=1/2$, lies below the curve of Eq. (2) with the suitable choice of the constant n. Conversely if the difference is negative, the curve of Eq. (4) is above the symmetric curve of Eq. (2), as was actually found for denatured hemoglobin in the present experiment. How can the condition:

$$\Delta \equiv L_3^2 - L_1^2 L_4 < 0 \tag{10}$$

be realized? One must look for the solution of this inequality.

Pauling[3] has given an analysis of the oxygen equilibrium curve obtained by Ferry and Green[15] on horse hemoglobin, assuming the four hemes to interact in pairs as if located at the corners of a square with interactions between adjacent hemes along the sides of the square but with no interactions along diagonals. His formula for the degree of oxygenation is as follows.

$$Y = \frac{kp + (2\alpha+1)k^2p^2 + 3\alpha^2k^3p^3 + \alpha^1k^4p^4}{1 + 4kp + (4\alpha+2)k^2p^2 + 4\alpha^2k^3p^3 + \alpha^1k^4p^4}. \tag{11}$$

Here k is the equilibrium constant of oxygenation of a single heme unaffected by the reaction of its neighbors, that is to say, RT ln k is the decrease in free energy accompanying the combination of a heme with oxygen. Since there are four hemes in a hemoglobin molecule, $K_1 = L_1 = 4k$. The constant α has the following significance. The equilibrium constant of the combination of two oxygen molecules with a hemoglobin molecule would be k^2 provided that no interaction exists between the hemes, but it is αk^2 if the two hemes are adjacent, because the equilibrium constant of the second heme is increased by the factor α as a result of the reaction of the first. In other words, RT ln α is the additional free energy stabilizing two interacting oxygen-combining centers. The factors 2 and 4 in Eq. (11) result from the symmetry numbers. Pauling's model involves only two constants, and it is remarkable that with a suitable choice of these constants ($k=0.033$ and $\alpha=12$) it may be made to fit the data of the fresh preparation of hemoglobin apparently within the allowable limit of errors of observation.

From the comparison of Eq. (11) with Eq. (4), one has for Pauling's model,

$$L_1 = 4k, \; L_3 = 4\alpha^2k^3, \; L_4 = \alpha^1k^4. \tag{12}$$

Inasmuch as $\Delta = 0$, Pauling's formula satisfies the symmetry condition (7). Therefore his formula cannot be applied to denatured hemoglobin. When denaturation takes place, the oxygen equilibrium curve changes its shape. There are two conceivable causes bearing on this matter. One involves the effect of the change of the equilibrium constant k, the other the effect of the interaction constant α, on the form of the oxygen equilibrium curve. Therefore a number of conceivable cases will be subjected to critical examination to see what change in k or α leads to the required condition (10) of asymmetry actually found.

(1) Let it be assumed that k's, the equilibrium constants of the four hemes, are equivalent to each other, while the interactions between different pairs of hemes are not mutually equivalent. In other words, supposing interactions to be represented by distances, Pauling's model may be depicted by a square, while this more general model having different interaction constants, α_1, α_2, α_3, and α_4, between the successive pairs of oxygen-combining centers would be represented by a quadrilateral having unequal sides. A case in which one of the stabilizing interactions of Pauling's model is annihilated would be a special case of this general model. For this model, the equilibrium constants L_i are given by the following equations.

$$L_1 = 4k, \; L_3 = (\alpha_1\alpha_2 + \alpha_2\alpha_3 + \alpha_3\alpha_4 + \alpha_4\alpha_1)k^3, \quad L_4 = \alpha_1\alpha_2\alpha_3\alpha_4 k^4. \tag{13}$$

Accordingly,

$$\begin{aligned}\Delta &= [(\alpha_1\alpha_2 + \alpha_2\alpha_3 + \alpha_3\alpha_4 + \alpha_4\alpha_1)^2 - 16\alpha_1\alpha_2\alpha_3\alpha_4]k^6 \\ &= [(\alpha_1\alpha_2 + \alpha_2\alpha_3 - \alpha_3\alpha_4 - \alpha_4\alpha_1)^2 \\ &\qquad + 4\alpha_2\alpha_4(\alpha_1 - \alpha_3)^2]k^6.\end{aligned} \tag{14}$$

The right hand side of Eq. (14) is either zero (when $\alpha_1 = \alpha_3$ and $\alpha_2 = \alpha_4$) or positive (otherwise). In the former case, Y-ln p curve would be symmetric. In the latter case, although the curve is asymmetric it would lie below the symmetric curve of Eq. (2). In any way, this model does not satisfy the required condition (10). It is worth mentioning that even if interactions are assumed to exist along diagonals, Δ always turns out to be either positive or zero.

(2) Having seen that the changes in α do not lead to the required condition provided that k remains unchanged, one must inquire

15) R. M. Ferry and A. A. Green, *J. Biol. Chem.*, 81, 175 (1929).

into the effect of change in k. The next case taken up is that in which each of the k's, the equilibrium constants of the four hemes, is slightly altered by an amount δk_i independently of others, while the interaction constant is tentatively assumed to be unchanged. The equilibrium constants L_i are given by

$$L_1=(k+\delta k_1)+\text{three similar terms},$$
$$L_3=\alpha^2(k+\delta k_1)(k+\delta k_2)(k+\delta k_3)+\text{three similar terms},$$
$$L_4=\alpha^1(k+\delta k_1)(k+\delta k_2)(k+\delta k_3)(k+\delta k_4).$$

Disregarding higher powers in δk, one has

$$\begin{aligned} L_1&=4k(1+\textstyle\sum^1 \delta k_i/4k),\\ L_3&=4\alpha^2k^3(1+3\textstyle\sum^1 \delta k_i/4k),\\ L_4&=\alpha^1k^4(1+\textstyle\sum^1 \delta k_i/k). \end{aligned} \qquad (15)$$

Accordingly $\Delta=0$, which is the condition (7) of symmetry. That is to say, small changes in k do not affect the symmetry property of Pauling's curve in any appreciable manner.

(3) Pauling's model was modified in such a way that the equilibrium constant of one of the four hemes is increased (or decreased) to βk. Then the constants L_i are given by

$$L_1=k(\beta+3),\ L_3=\alpha^2k^3(3\beta+1),\ L_4=\alpha^1k^4\beta. \quad (16)$$

Therefore

$$\Delta=\alpha^4k^5[(3\beta+1)^2-(\beta+3)^2\beta]=\alpha^4k^5(1-\beta)^3.$$

If $\beta>1$, this expression is negative, satisfying the required condition (10). At first sight, it may appear rather surprising that the oxygen affinity of a heme increases as a result of denaturation. It is, however, a remarkable fact that in almost every case in which hemes are separated, there appears to be an increase of oxygen affinity, i.e., the decrease of p_0. For example, the data of Altschul and Hogness[16] on hemoglobin in dilute solutions, where the molecules may be expected to dissociate, show a decrease in p_0. The same effect is seen in the results of Hill and Wolvekamp[17] on diluted hemoglobin and of Taylor and Hastings[18] on spilt hemoglobin. The latter authors found that p_0 is considerably less for horse hemoglobin split in urea solution than for native hemoglogin.

(4) If two of the four hemes have an increased equilibrium constant βk relative to the remaining two, one has

$$L_1=k(2\beta+2),\ L_3=\alpha^2k^3(2\beta^2+2\beta),\ L_4=\alpha^1k^4\beta^2. \quad (17)$$

Hence

$$\Delta=\alpha^4k^5[(2\beta^2+2\beta)^2-(2\beta+2)^2\beta^1]=0.$$

Again a symmetric Y-$\ln p$ curve would result.

(5) Finally let the case be considered, in which one of the four oxygen-combining centers has lost its ability to combine with oxygen. In this case,

$$L_1=3k,\ L_2=(2\alpha+1)k^2,\ L_3=\alpha^2k^3,\ L_4=0. \quad (18)$$

Since $L_4=0$, the condition of symmetry of the equilibrium curve must be altered, which in terms of the constants L_i, is

$$\frac{L_2}{L_3}\Big/\frac{L_1}{L_2}=\frac{L_1}{L_2}\Big/\frac{1}{L_1} \text{ or } L_2^3-L_1^3L_3=0, \quad (19)$$

rather than Eq. (9), and the condition of asymmetry in conformity with experiment is

$$L_2^3-L_1^3L_3<0,$$

in place of Eq. (10). Introducing the values given by (18) into the left hand side of this equation, one is led to

$$\begin{aligned} L_2^3-L_1^3L_3&=[(2\alpha+1)^3-3^3\alpha^2]k^3\\ &=(8\alpha+1)(\alpha-1)^2k^3. \end{aligned}$$

The right hand side of this equation is positive inasmuch as $\alpha>1$ for stabilizing interaction. Here again the required condition is not fulfilled. It is of course possible that the changes of molecules due of denaturation take place only partly, leaving unchanged molecules. However, a mixture of two kinds of such molecules, one giving a symmetric oxygen equilibrium curve, the other an asymmetric one having a trend contrary to experimental observations, would never yield a curve even in qualitative agreement with experiments.

So far a numbers of conceivable cases have been examined for the change of k as well as of α. Although they cover by no means all the possible combinations of changes in k and α, yet relatively simple changes appropriate for the first stage of denaturation seem to have been taken into account. It was found that the condition of asymmetry (10) is so severe that it can rule out almost all except case (3). Therefore one may conclude that the increase in the equilibrium constant of the combination with oxygen of one of the four hemes takes place in the first stage of the denaturation of hemoglobin.

Summary

The oxygen equilibrium curve of a slightly denatured preparation of hemoglobin solution was determined by the spectrophotometric method. The plot of Y, the degree of partial saturation with oxygen, against $\log p$, the logarithm of the partial pressure of oxygen, was not symmetric across the point at 50% saturation. The trend of asymmetry was

16) A. M. Altschul and T. R. Hogness, *J. Biol. Chem.*, 139, 315 (1939).
17) R. Hill and H. R. Wolvekamp, *Proc. Roy. Soc. London*, B107, 286 (1930).
18) J. F. Taylor and A. B. Hastings, *J. Biol. Chem.*, 144, 1 (1942).

such that if the lower left portion of the curve was rotated through 180° about the point at $Y=1/2$, it lay below the upper right portion of the original curve. The condition of this trend of asymmetry was derived from the theory of chemical equilibrium. This condition was tested with various conceivable changes in k, the equilibrium constant of oxygenation of a single heme, as well as in α, the constant of interaction stabilizing the combination of each of two adjacent hemes with an oxygen molecule. It was found that the deviation from the equivalence of α, of whetever kind and degree, can never satisfy the required condition, provided that the k's of the four hemes remain equivalent to each other. A number of other conceivable cases were subjected to critical examination. The condition of asymmetry was so severe that it could rule out almost all except the case in which one of the four hemes increases its affinity towards an oxygen molecule compared with the other three. This conclusion is in conformity with the results on hemoglobin dissociated in a dilute solution or split in a urea solution.

Chemical Department, Faculty of Science
Nagoya University, Nagoya

Synthetic Amphoteric Polypeptide. I. Syntheses and Some Properties of Linear Amphoteric Polypeptides

By Heimei YUKI, Shumpei SAKAKIBARA and Hisaya TANI

(Received February 27, 1956)

Introduction

The behavior of synthetic amphoteric polypeptides is of great interest, because of their relationship to those of proteins. With this in mind, Akabori, Tani and Noguchi[1] have synthesized copoly-1:1-(L-glutamic acid, DL-lysine), the first synthetic amphoteric polypeptide. This substance, unfortunately, had some unfavorable properties as a "model protein". Its solubility in water was too great, due to its relatively low molecular weight; also it differed from proteins in that all of the component amino acid residues had the ionisable side chain groups.

It would be desirable to obtain a high molecular weight polypeptide having acidic, basic and neutral amino acid residues in proportions nearly equal to those in protein. Therefore, copoly-1:1:3-(DL-glutamic acid, DL-lysine, DL-phenylalanine) (A) and copoly-1:1:1.9-(L-glutamic acid, L-lysine, L-leucine) (B) have been synthesized and some properties of their solutions investigated.

Preparations

The copolymerizations were carried out with mixtures of N-carboxy anhydrides of γ-benzyl DL-glutamate, ε-N-carbobenzoxy-DL-lysine and DL-phenylalanine (I, II, III respectively) and of γ-benzyl L-glutamate, ε-N-carbobenzoxy-L-lysine and L-leucine (IV, V, VI respectively). To obtain a homogeneous high molecular polypeptide, a suitable solvent must be used for the polymerization. The results obtained with several solvents tried in these experiments are shown in Table I. It was found that chlorobenzene was the most suitable solvent, giving the polymers having the highest specific viscosities. In nitrobenzene and in ethyl phenylacetate, the reaction mixtures formed transparent gels or highly viscous solutions. The polymer produced in benzene and its reduction product were found to be heterogeneous in their solubility behavior. In dioxane and tetrahydrofuran the polymerization could not proceed; after evaporating the solvents in vacuo the crystalline masses, supposedly mixtures of the N-carboxy anhydrides, were recovered. These could now be polymerized in any of the suitable solvents mentioned above, the polymerization proceeding apparently in the same manner as when fresh monomer mixtures were used. It has been observed previously[2] that N-carboxy-α-amino acid anhydride was very stable in purified acetone. The dioxane and tetrahydrofuran used in these experiments contained traces of an aldehydic substance, which might have some stabilizing effect on the monomers.

The polymers were reduced with phosphonium iodide and converted into the hydriodides of corresponding amphoteric polypeptides. The hydriodides gave the free polypeptides quantitatively on treatment with triethylamine. Dialyses of these hydriodides were also carried out to remove

1) S. Akabori, H. Tani and J. Noguchi, *Nature*, **167**, 159 (1951); H. Tani and J. Noguchi, *Chem. High Polymers, Japan*, **8**, 57 (1951).

2) H. Tani and H. Yuki, *Chem. High Polymers, Japan*, **8**, 62 (1951).

TABLE I

Monomers	Solvents	Results	Yield (%)	η_{sp} *3)
(A) I, II, III*1) (1 : 1 : 3)	Nitrobenzene	Transparent gel	100	
	Ethyl Phenylacetate	Opalescent gel	100	
	Benzene	Gel particles in viscous soln.	94	
	Dioxane	No change		
(B) IV, V, VI*2) (1 : 1 : 2)	Chlorobenzene	Clear viscous soln.	94	0.48
	Nitrobenzene	Viscous soln., partially gelling	70	0.15
	Ethyl Phenylacetate	Transparent gel	95	0.31
	Chloroform	Soln. of low viscosity		
	Tetrahydrofuran	No change		

*1) The polymerizations were carried out by heating at 70°C for 60 hr.
*2) The polymerizations were carried out with about 8% solution at 60°C for 8 hr. and then at room temperature for ten days.
*3) The specific viscosities of 0.1% solution of the polymers in chloroform at 30°C.

hydriodic acid, but the polypeptides obtained here still contained a small amount of hydrogen iodide and about half of the polypeptides were lost. Such fractionation caused during dialysis may produce changes in the ratios of the amino acid residues composing the polypeptides, if, in each case, the compositions of the individual molecules are not the same. However, the elementary analyses and the amounts of lysine residues estimated from van Slyke's amino-nitrogen determinations indicated that these polypeptides contained the amino acid residues in the same molar ratios as those of the starting monomer mixtures.

Titration curves (see Fig. 1) of these polypeptides in aqueous solutions showed typical amphoteric properties and the carboxyl group contents calculated from the hydrogen ion combining capacities corresponded to the values obtained from analytical data. These polypeptides were soluble in dilute mineral acids and in dilute alkalis, but were insoluble in water over a rather wide range of pH, i.e., 4.0–10.8 for polypeptide A and 4.5–10.2 for polypeptide B, respectively.

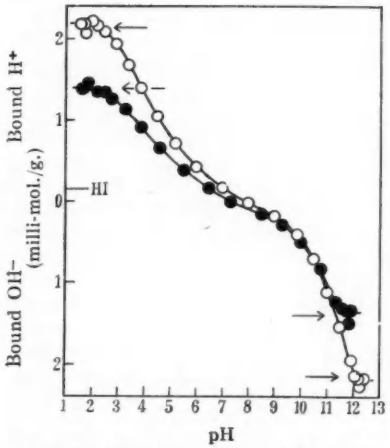

Fig. 1. Titration curves of free amphoteric polypeptides.
●: Copoly-1 : 1 : 3-(DL-glutamic acid, DL-lysine, DL-phenylalanine).
○: Copoly-1 : 1 : 1.9-(L-glutamic acid, L-lysine, L-leucine).
Arrows represent the theoretical end points respectively.

Properties of the Solution

The properties of the aqueous solution of polypeptide B were studied, using the dialysed solution of the hydriodide. The dialysed solution had

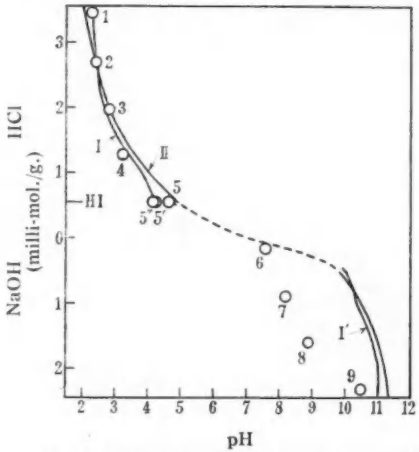

Fig. 2. Titration curves of copoly-1 : 1 : 1.9-(L-glutamic acid, L-lysine, L-leucine).
Curves I and I′: Titration of the dialysed solution by 0.1 N HCl and 0.1 N NaOH respectively. Curve II: Titration of a solution of the dry sample in hydrochloric acid with 0.1 N NaOH. The dotted line indicates the insoluble region. The numbered circles represent the pH of the solutions for viscosity measurements, 400 hr. after the preparation of solutions.

a pH value of 4.3. It contained 0.27 mol. of hydriodic acid per lysine residue of the polypeptide. The resulting polypeptide had an isoelectric point at about pH 7.3 as shown in the titration curve in Fig. 2.

The relation of the reduced viscosity to the concentration of the polypeptide was linear in the concentration below about 1%. The intrinsic viscosity was 0.70 (see Fig. 3).

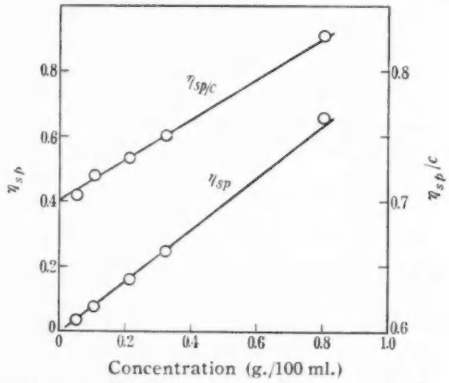

Fig. 3. Relationship between viscosity and concentration.

Because of the insolubility of this polypeptide in the pH range near its isoelectric point, the pH-dependence of viscosity could be measured only outside of this insoluble region. The results (see Fig. 4) showed that the viscosity increased gradually towards its isoelectric point from both sides and that it was considerably higher in the acidic than in the alkaline region.

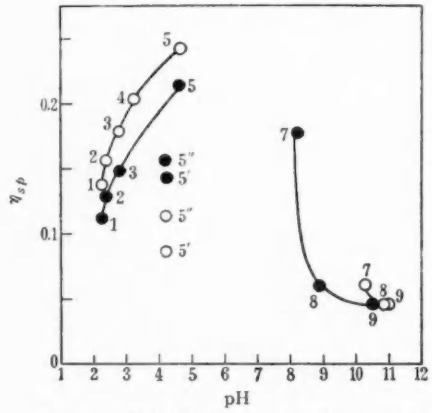

Fig. 4. Relationship between specific viscosity and pH: ○, at 17–52 hr.; ●, at 305–355 hr., after the preparation of the solutions.

The viscosities of solutions of this polypeptide changed gradually with time. In acidic solution the growth of mould was found occasionally, but it is not certain whether or not such bacterial decomposition of the polypeptide caused this decrease in viscosity (see Fig. 5). In alkaline solution the viscosity remained constant for a rather long period and then suddenly began to increase linearly with time. The final solution exhibited thixotropy (see Fig. 6). It was observed also that at the beginning of this increase in viscosity the solution began to show opalescence, which became gradually strong with time, and that the

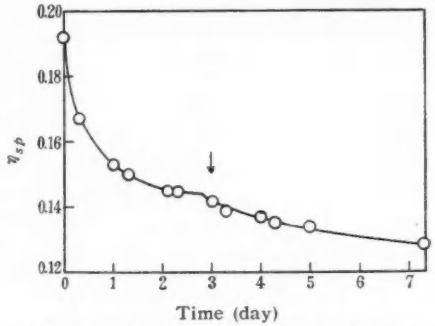

Fig. 5. Change of specific viscosity of solution No. 1. The arrow represents the appearance of mould.

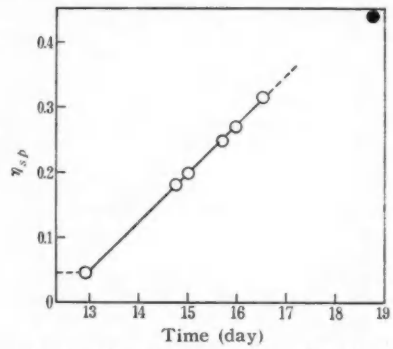

Fig. 6. Change of specific viscosity of solution No. 7.
●: Thixotropy.

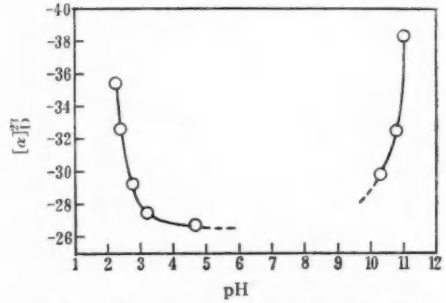

Fig. 7. Relationship between optical rotation and pH.

pH of the solution shifted toward neutrality, as a result of absorption of atmospheric carbon dioxide.

The pH dependence of optical rotatory power of this polypeptide was observed in the soluble region. All of the observed values were laevorotatory, the absolute magnitudes decreasing toward the isoelectric region (see Fig. 7).

Discussion

From the results of studies[7] on synthetic vinyl polymers, it has been stated that polyampholytes are insoluble in water in any pH range, if the dissociation constant of either the acidic or the basic group is very small, or if the number of one of these groups is much less than that of the other. In the polypeptides obtained in this research, the acidic and basic groups have pK′ values of 4.3 and 10.5 respectively[4], and hence have sufficient dissociation constants to form dipolar ions in their isoelectric regions; moreover, the numbers of these groups are equal. Although the insolubility of these polypeptides in the isoelectric regions may be presumed to be due to the large contribution of the hydrophobic side chain groups of leucine or phenylalanine residues, which are contained in relatively high proportions, high molecular weight copoly-1 : 1-(L-glutamic acid, L-lysine)[5], which contains no such hydrophobic side chain group, also had a wide insoluble region around its isoelectric point.

For solutions of synthetic amphoteric vinyl polymers[3,6,7] and of some of natural proteins[8], it has been reported that viscosity exhibits a minimum at the isoelectric point and a maximum on each side. This viscometric behavior has been interpreted as due to the coiling and stretching of long chain molecules caused by the electrostatic attraction and repulsion between positive and/or negative charges of ionized groups distributed along the molecular chains.

In these experiments the viscosity could be measured only on the outsides of both maxima, because of the insolubility of polypeptide in the neutral region. The lower viscosity in an alkaline region than that of an acidic region may be due to sodium iodide, which was present as extra-salt in the alkaline solutions. It has been shown that a small amount of neutral salt caused a considerable decrease in the viscosity of vinyl polyelectrolyte solutions[3].

The change of viscosity on ageing has been observed in cases of the solution of proteins, such as gelatin[9], but the cause remains obscure.

The increase in viscosity as the pH approaches that of the insoluble region from either side and the appearance of turbidity in the alkaline solution, together with the shift of pH of the solution caused by ageing, suggest that the aggregation of the solute polypeptide becomes greater as the solution approaches to its isoelectric point. Likewise, the insolubility of these amphoteric polypeptides in the neutral region may be due to this aggregation.

As one of the factors causing such an inter-molecular association, the formation of inter-molecular salt-linkages, such as have been assumed by Isemura and Hamaguchi[10] on the basis of their studies of the surface viscosity of these polypeptides, might be considered. Further, the role of hydrogen bonds formed between large numbers of carbonyl and imino groups distributed in the polypeptide chains can not be ignored, since these amphoteric polypeptides differ essentially from the vinyl polyampholytes only in having peptide bonds in their skeletal molecular chains. The large intrinsic viscosity of the polypeptide suggests that it had a more-or-less rigid and highly extended structure in solution.

The behavior of the solution of the polypeptide with regard to optical rotation is quite similar to that of natural proteins[11].

All of these properties of the polypeptides in solution, together with their surface chemical properties reported by Isemura and Hamaguchi[10] and by Davies and Llopis[12] show that they are interesting substances, similar in many respects to polypeptides of natural proteins.

Experimental

γ-Benzyl DL-Glutamate.—A mixture of 30 ml. of conc. hydrochloric acid, 12 ml. of water, 30 g. of powdered DL-glutamic acid and 300 ml. of benzyl alcohol was heated to 95°C for 1/2 hr. with stirring.

3) T. Alfrey, Jr. and H. Morawetz, *J. Am. Chem. Soc.*, 74, 436 (1952); T. Alfrey, Jr., R.M. Fuoss, H. Morawetz and H. Pinner, ibid., 74, 438 (1954).
4) E. J. Cohn and J. T. Edsall, "Proteins, Amino Acids, and Peptides as Ions and Dipolar Ions", Reinhold, New York (1943), p. 84.
5) H. Yuki and H. Tani, Unpublished.
6) T. Matsumoto, *Chem. High Polymers, Japan*, 8, 412 (1951).
7) A. Katchalsky and I. R. Miller, *J. Polymer Sci.*, 13, 57 (1954).
8) S. Akabori and S. Mizushima, "Protein Chemistry", Vol. 2, Kyoritsushuppan, Tokyo (1954), p. 390.
9) S. Akabori, "Amino Acids and Proteins", Kyoritsushuppan, Tokyo (1944), p. 463.
10) T. Isemura and K. Hamaguchi, This Bulletin, 27, 339 (1954); K. Hamaguchi and T. Isemura, ibid., 28, 9 (1955).
11) W. Pauli and E. Valko, "Kolloidchemie der Proteine", T. Steinkopff, Dresden (1933).
12) J. T. Davies, *Biochem. J.*, 56, 509 (1954); J. T. Davies and J. Llopis, *Proc. Roy. Soc.*, A 227, 537 (1955).

The resultant clear solution gave no phase-separation on cooling. The cooled solution was neutralized by an aqueous solution of 30 g. of sodium bicarbonate, and 500 ml. of ether was added with stirring. The precipitated crystals were filtered and washed with a small amount of water, ethanol, and ether. Plates, m.p. 163–163.5°C; no change in m.p. was observed by recrystallization from 520 ml. of water. Yield 26 g. (54% of the theor.)

Anal. Found: N, 5.97. Calcd. for $C_{12}H_{15}NO_4$: N, 5.91%.

γ-Benzyl L-Glutamate[13].—A mixture of 14.5 g. of powdered L-glutamic acid, 24 ml. of conc. hydrochloric acid and 150 ml. of benzyl alcohol was treated as above, and the product was recrystallized from 370 ml. of water to give 12.6 g. (53% of the theor.). Plates, m.p. 173°C, $[\alpha]_D^{17}$ 20.7° (glacial acetic acid, *c* 6.76).

Anal. Found: N, 5.85. Calcd. for $C_{12}H_{15}NO_4$: N, 5.91%.

γ-Benzyl N-Carboxy-DL-glutamate Anhydride (I).—Phosgene was passed for one hour into a suspension of 13 g. of powdered γ-benzyl DL-glutamate in 260 ml. of anhydrous dioxane with stirring at room temperature. After excess phosgene was removed by passing dry air through the solution, it was concentrated to a syrup in vacuo at 40°C and finally at 50°C. The ethyl acetate solution of this syrup gave colorless needles on the addition of petroleum ether. Yield 12 g. (77% of the theor.), m.p. 70–83°C.

Recrystallization from ethyl acetate and petroleum ether gave 8.5 g. of crystals (Ia) of m.p. 70–71°C, and the concentrated mother liquor gave 2 g. of crystals (Ib) of m.p. 83–85°C by adding petroleum ether. Ia and Ib are supposed to be different crystallographic modifications of the same substance, because neither of them showed optical rotation in ethyl acetate solution and both gave the same infra-red absorption spectra.

Anal. Found: N, (Ia) 5.35; (Ib) 5.39. Calcd. for $C_{13}H_{13}NO_5$: N, 5.32%.

γ-Benzyl N-Carboxy-L-glutamate Anhydride (IV).—A suspension of 10 g. of powdered γ-benzyl L-glutamate in 300 ml. of dry dioxane was treated with phosgene as described above. The crystalline product was recrystallized from ethyl acetate and petroleum ether to give 10.5 g. (95% of the theor.) of needles, m.p. 91–92.5°C. Further recrystallization from ethyl acetate raised the m.p. to 93.5–94.5°C. $[\alpha]_D^{29}$ −17.0° (ethyl acetate, *c* 3.65).

Anal. Found: N, 5.28. Calcd. for $C_{13}H_{13}NO_5$: N, 5.32%.

α-N-Carboxy-ε-N-carbobenzoxy-DL-lysine Anhydride[14] **(II).**—This compound was prepared from 12 g. of N, N′-dicarbobenzoxy-DL-lysine and 20 ml. of thionyl chloride and recrystallized several times from ethyl acetate and petroleum ether. Yield 2.4 g. (27% of the theor.), m.p. 103°C.

α-N-Carboxy-ε-N-carbobenzoxy-L-lysine Anhydride[14] **(V).**—A solution of 15 g. of crystalline N, N′-dicarbobenzoxy-L-lysine in 20 ml. of dry dioxane and 30 ml. of dry ether was cooled to 0°C and 8.8 g. of phosphorus pentachloride was added. After shaking for 1/2 hr., the supernatant liquid was decanted and concentrated in vacuo at 40°C. The resultant crystalline mass was decolorized by washing with a small amount of dry ether. Yield 10 g. (80% of the theor.). Recrystallization from ethyl acetate and petroleum ether gave crystals of m.p. 100°C, $[\alpha]_D^9$ −24.1° (ethyl acetate, *c* 6.22).

N-Carboxy-DL-phenylalanine Anhydride[15] **(III).**—This compound was prepared from 14 g. of N-carbobenzoxy-DL-phenylalanine and 20 ml. of thionyl chloride, and repeatedly recrystallized from ethyl acetate and petroleum ether. Yield 6 g. (72% of the theor.), m.p. 123°C.

N-Carboxy-L-leucine Anhydride[16] **(VI).**—Phosgene was passed for two hours into a suspension of 5 g. of powdered L-leucine in 200 ml. of dry dioxane at 40°C. The crystals, which were obtained in the same manner as described above, were recrystallized from ethyl acetate and petroleum ether. Yield 4.8 g. (80% of the theor.), m.p. 76.5–77.5°C. $[\alpha]_D^{11}$ −42.2° (benzene, *c* 0.95).

Anal. Found: N, 8.83, Calcd. for $C_7H_{11}NO_3$: N, 8.91%.

The Effect of Solvent on the Copolymerization.—All the solvents were purified by distillation, and benzene, dioxane and tetrahydrofuran were further dried over metallic sodium. Dioxane and tetrahydrofuran were colored by Schiff's reagent.

The mixtures of N-carboxy anhydrides in the ratio shown in Table I were dissolved in each solvent in a sealed glass tube, and heated to polymerize them.

The solutions of dioxane and tetrahydrofuran showed no change, and on evaporating the solvents in vacuo the crystalline residues were obtained. These residues were dissolved in nitrobenzene or chlorobenzene and heated in sealed tubes. They polymerized rapidly and formed transparent gels or viscous solutions.

The polymers (B) listed in Table I were precipitated by adding ether and petroleum ether to each reaction mixture and reprecipitated from chloroform solutions by petroleum ether. The viscosities of 0.1% chloroform solutions were determined at 30±0.1°C using an Ostwald viscometer.

Copolymer of I, II and III (VII).—The copolymerization was carried out for the mixture of 0.413 g. (1.57 m mol.) of I, 0.480 g. (1.57 m mol.) of II, and 0.900 g. (4.71 m mol.) of III in 20 ml. of each of the solvents listed in Table I, (A). The dioxane solution was evaporated off, and the residual crystals were polymerized in nitrobenzene. Each polymer was precipitated by adding petroleum ether and reprecipitated from tetrahydrofuran by petroleum ether and ether. All the polymers, excepting that from benzene solution, were collected and dried; white powder, 4.35 g.

13) W.E. Hanby et al. (*J. Chem. Soc.*, 1950, 3239) obtained this compound with a considerably lower yield, using hydriodic acid instead of hydrochloric acid.

14) M. Bergmann, L. Zervas and W.F. Ross, *J. Biol. Chem.*, **111**, 245 (1935).

15) H. Leuchs and W. Geiger, *Ber.*, **41**, 1721 (1908).

16) A.C. Farthing, *J. Chem. Soc.*, 1950, 3213; D. Coleman, ibid., 1950, 3222.

(100% of the theor.), soluble in dioxane, tetrahydrofuran, hot glacial acetic acid, and hot chloroform.

Anal. Found: C, 68.71; H, 5.99; N, 9.07. Calcd. for $[(C_{12}H_{13}NO_3)$, $(C_{14}H_{18}N_2O_3)$, $3(C_9H_9NO)]_n$: C, 68.94; H, 6.34; N, 9.11%.

The polymer obtained from benzene solution (N, 9.16%) contained a small amount of material which was insoluble in the above solvents.

Copoly-1: 1: 3-(DL-glutamic acid, DL-lysine, DL-phenylalanine) (VIII).—A mixture of 4 g. of VII and 100 ml. of glacial acetic acid was heated until a complete solution was obtained. Six grams of phosphonium iodide was then added in portions during 4.5 hr. at 60–70°C with passing through dry hydrogen. After cooling, the precipitate formed was separated by decantation and washed with dry ether. Repeated reprecipitation from absolute ethanol and dry ether gave 3.3 g. (95% of the theor.) of polypeptide hydriodide as white powder. This was hygroscopic and was soluble in ethanol, methanol, water, wet dioxane and wet tetrahydrofuran.

This hydriodide was dissolved in 100 ml. of water and dialysed against distilled water. The solution obtained had a pH of 5.5 and an osmotic pressure of about 30 mm-H_2O (*c*, 6 g./l.); it coagulated to a white gelatinous precipitate on warming to 30°C. After evaporating the solution in an evacuated desiccator at room temperature, 1.6 g. (53% based on the polymer) of pale yellow glassy solid was obtained. This was soluble in dilute mineral acids and in dilute alkalis, but insoluble in water and conc. hydrochloric acid. It was also insoluble in methanol, ethanol and dioxane, but readily soluble in any of these containing hydrochloric acid. It was also soluble in hot, but not in cold, aqueous pyridine. It gave a positive biuret reaction in aqueous solution and foamed even in dilute solution.

Anal. Found*: C, 62.38; H, 6.62; N, 11.12; amino-N, 1.87; I, 3.70. Calcd. for $[(C_5H_7NO_3)$, $(C_5H_{12}N_2O)$, $3(C_9H_9NO)$, 0.21 HI$]_n$: C, 62.90; H, 6.40; N, 11.59; amino-N, 1.93; I, 3.68%.

The polymer obtained from benzene solution was reduced and treated in the same manner as described above, but the product contained a small amount of matter which was insoluble in dilute alkali.

Copolymer of IV, V and VI (IX).—A solution of 2.63 g. (0.01 mol.) of IV, 3.06 g. (0.01 mol.) of V and 2.98 g. (0.019 mol.) of VI in 100 ml. of chlorobenzene was sealed in a glass tube and heated for several hours at 80°C and then for 135 hr. at 60°C. The polymer was precipitated from the clear viscous solution by ether and petroleum ether and then reprecipitated from acetone and petroleum ether. The dried white powder weighed 6.90 g. (99% of the theor.). This polymer was easily soluble in chloroform and dioxane, and soluble in tetrahydrofuran, ethyl acetate, acetone and hot glacial acetic acid.

Anal. Found: C, 64.24; H, 7.18; N, 9.96. Calcd. for $[(C_{12}H_{13}NO_3)$, $(C_{14}H_{18}N_2O_3)$, $1.9(C_5H_{11}NO)]_n$: C, 64.51; H, 7.52; N, 9.86%.

Copoly-1: 1: 1.9-(L-glutamic acid, L-lysine, L-leucine) Hydriodide (X).—As described for the preparation of VIII the solution of 2 g. of IX in 75 ml. of glacial acetic acid was treated with 4.2 g. of phosphonium iodide (with stirring), and the resultant precipitate was repeatedly reprecipitated from absolute ethanol and ether, and dried. The polypeptide hydriodide was obtained as a pale yellow powder. Yield 1.66 g. (96% of the theor.). Its solubility was similar to that of the hydriodide of VIII described above.

Anal. Found*: C, 43.56; H, 6.55; N, 10.62; amino-N, 2.32; I, 22.7. Calcd. for $[(C_5H_5NO_3)$, $(C_6H_{12}N_2O\cdot HI)$, $1.9(C_5H_{11}NO)]_n$: C, 44.80; H, 6.87; N, 11.43; amino-N, 2.33; I, 21.2%.

Copoly-1: 1: 1.9-(L-glutamic acid, L-lysine, L-leucine) (XI).—To the solution of 1.4 g. of X in 15 ml. of methanol, 0.75 g. of triethylamine was added. The precipitated polypeptide was washed with methanol repeatedly until no halogen was detectable, then washed with ether and dried. The white powder weighed 1.04 g. (94% of the theor.). It was slightly soluble in water and methanol, and considerably soluble in hot water. In dilute mineral acids and in dilute alkalis, it gave a very foamy and viscous solution and gave a positive biuret reaction.

Anal. Found*: C, 56.16; H, 8.03; N, 14.42; amino-N, 3.03. Calcd. for $[(C_5H_7NO_3)$, $(C_6H_{12}N_2O)$, $1.9(C_5H_{11}NO)]_n$: C, 56.94; H, 8.52; N, 14.53; amino-N, 2.97%.

Dialysis of the Solution of X.—A solution of 1.3 g. of X in 50 ml. of water was dialysed against distilled water for four days. This was concentrated in an evacuated desiccator at room temperature to 65 ml. and used in the following experiments as the "original solution". The concentration of this solution was determined using 5 ml.; making the correction of the content of hydrogen iodide, the concentration of free polypeptide was 8.07 mg./ml. and its yield was 51% of the theoretical value. The dried substance was transparent glassy solid, soluble in dilute mineral acids or in dilute alkalis, but not in water.

Anal. Found*: C, 52.96; H, 8.11; N, 13.69; amino-N, 2.78; I, 6.8. Calcd. for $[(C_5H_7NO_3)$, $(C_6H_{12}N_2O)$, $1.9(C_5H_{11}NO)$, 0.27 HI$]_n$: C, 53.05; H, 7.99; N, 13.54; amino-N, 2.76; I, 6.79%.

Electrometric Titrations.—Titrations were made on solutions containing a known weight of the sample (*c*, ca. 10 mg./ml.) dissolved in a known amount of hydrochloric acid with 0.1 N NaOH using a Beckman G pH meter. During the titrations, insoluble precipitates appeared at pH 4.0–10.8 and 4.5–10.2 for VIII and XI. Blank titrations were made under the same conditions. The hydrogen ion and hydroxyl ion combining capacities were estimated from the differences between the measurements for the unknowns (VIII and XI) and those for the blanks[17] (Fig. 1). Curve II in Fig. 2 represents the titration of a dry sample obtained from the "original solution," and curves I and I′ in Fig. 2 are the titration curves.

* The analytical samples were dried over phosphorus pentoxide for several hours at 108°/3 mmHg.

17) T. V. Parke and W. W. Davis, *Anal. Chem*, **26**, 642 (1954).

of the "original solution" with 0.1 N HCl and 0.1 N NaOH respectively.

The Solution Used for Measurements.—Twenty ml. of the "original solution" was diluted to 50 ml.; this was designated as "solution-N". Each 0.25 m mol. of hydrochloric acid and sodium hydroxide were added to each 10 ml. of the "original solution" and these were diluted with water to 25 ml., giving "solution-A" and "solution-B", respectively. By mixing these solutions the following eleven solutions were made. The numbers inserted in Figs. 2, 4, and 7 represent these solution numbers.

Solution No.	1,	2,	3,	4,	5,	5′,	5″,	6,	7,	8,	9
Solution A (ml.)	11	6	5	3	0	3	2	0	0	0	0
Solution N (〃)	0	2	5	9	10	0	4	9	5	2	0
Solution B (〃)	0	0	0	0	0	3	2	3	5	6	11

In solution No. 6, precipitation occurred.

Measurement of Viscosity.—The measurements were carried out at 25±0.01°C using an Ostwald viscometer. As viscosity changes with time, the time intervals between the measurements and the preparation of the solution were noted.

(1) The effect of concentration.—The measurements were carried out on the "original solution," solution No. 5, and its diluted solution 17–24 hr. after their preparation.

(2) The effect of the time.—Solutions No. 1 and 9 were placed, respectively, in the viscometers held in a thermostat, and the measurements were made at appropriate intervals.

(3) The effect of pH.—The measurements were carried out twice on solutions No. 1–9 at 17–52 hr. and at 305–355 hr.

In Fig. 2 the points numbered 1–9 represent the pH of each solution about 400 hr. after their preparations.

Measurement of Optical Rotation.—The measurements were made 43–48 hr. after the preparation of solution.

Measurement of Osmotic Pressure.—The measurement was carried out on solution No. 5 (c, 3.23 mg./ml.) using a Bull and Currie type osmometer at 25±0.01°C. The observed osmotic pressure was 22.8 mm-H_2O**.

Summary

1. Two linear highmolecular amphoteric polypeptides were synthesized.

2. The pH-dependences of viscosity and optical rotation were measured. Some of these properties resembled that of vinyl polyampholytes and some proteins.

The authors express their hearty thanks to Prof. S. Akabori and Prof. S. Murahashi for their interest and encouragement throughout the work, to Dr M. L. Huggins for reading the manuscript, and to Mr. C. Oizumi for a part of the experimental work. This research was financially supported by the Institute for Fiber Research.

Department of Chemistry, Faculty of Science, Osaka University, Osaka

** Using van't Hoff's equation and neglecting the presence of hydrogen iodide, this corresponds to a molecular weight of about 3.6×10^4. Davies et al.[12] reported the molecular weight of this substance being 35,000 from their measurements of the surface pressure.

Addition of Trichlorosilane to Acetylene and to Vinyltrichlorosilane[1]

By Shunichi NOZAKURA

(Received March 29, 1956)

The addition of trichlorosilane to acetylene is one of the well-known methods for the preparation of organosilicon compounds, and is known to be accelerated in the presence of peroxides or platin catalyst[2].

$$HSiCl_3+CH\equiv CH \longrightarrow CH_2=CHSiCl_3$$
$$CH_2=CHSiCl_3+HSiCl_3 \longrightarrow Cl_3SiCH_2CH_2SiCl_3$$

In the course of our study on the additional reactions of trichlorosilane to various vinyl compounds, it was observed in the previous paper[3] that cyanoethylation of trichlorosilane took place easily in the presence of organic bases as well as platin or benzoylperoxide. All these catalysts resulted in the formation of β-cyanoethyltrichlorosilane. On the contrary, when the reactions were carried out either in the presence of pyridine in an autoclave, or in the presence of tetrapyridine nickel (II) chloride in sealed glass tubes, the reversal of the orientation of addition was observed[4].

1) Paper VI in a series on the study of organosilicon compounds.

2) G.H. Wagner and C.O. Strother, Brit. Pat. 670, 617, Apr. 23, 1952; *C.A.*, **46**, 8894c.

3) S. Nozakura and S. Konotsune, This Bulletin, **29**, 322 (1956).

4) S. Nozakura and S. Konotsune, ibid., **29**, 326 (1956).

$$HSiCl_3 + CH_2{=}CHCN \xrightarrow[\text{Pryidine (in autoclave) or } NiCl_2 \cdot 4C_5H_5N]{\text{Base, Pt, or peroxide}} \begin{cases} Cl_3SiCH_2CH_2CN \\ Cl_3SiCHCN \\ \quad\quad | \\ \quad\quad CH_3 \end{cases}$$

The present work was undertaken to see if the same base catalyst could hold its effect in the above reaction, i. e., the reaction between acetylene and trichlorosilane, and to see if the reverse orientation of addition would also take place in this case. In fact, the reverse addition took place, and there obtained 1,1-di(trimethylsilyl) ethane which otherwise would not be obtainable.

Addition of Trichlorosilane to Acetylene.—For the comparison of the reactions, the reaction in an autoclave was carried out in the first place according to the procedure described by Wagner and Strother[2]. Thus, in the presence of platinized asbestos, the reaction started at about 170°C. When an excess amount of trichlorosilane over acetylene was used, the principal product was found to be di(trichlorosilyl) ethane. On the other hand, when a sufficient amount of acetylene was supplied to the reaction system, the main product was vinyltrichlorosilane. These results confirmed the description of Wagner and Strother.

In the presence of a catalytic amount of pyridine, on the contrary, the reaction was observed to be initiated at temperatures as high as 180–185°C. Since it was rather tedious to handle the reaction mixture directly, the chlorine atoms attached to silicon atoms were replaced by methyl groups and the mixture of silico-hydrocarbons thus obtained were fractionally distilled through the fractionating column of the Stedman type. Two main fractions were obtained being accompanied with a considerable amount of distillation residue. The physical properties of these main fractions were listed in Table I. Although the data for the first main fraction of molecular weight, analysis, and molar refraction were in good agreement with that of di(trimethylsilyl)ethane, those of boiling point, density, and refractive index showed marked differences from that of 1,2-di(trimethylsilyl)ethane (151–2°C, 0.7565, and 1.4199, respectively[5]). This discrepancy is thought to be due to the presence of the isomeric mixture, which will be shown later on in this paper. The second main fraction was considered to be di(trimethylsilyl)butene, but the structural proof was not undertaken. In any way, the occurrence of this compound might be explained to be due to the presence of vinylacetylene which might be produced under the reaction condition.

Addition of Trichlorosilane to Vinyltrichlorosilane.—In the course of the addition of trichlorosilane to acetylene leading to the formation of di(trichlorosilyl)ethane, vinyltrichlorosilane may be considered to be an indispensable intermediate. To make the situation simpler, vinyltrichlorosilane was used as the starting material instead of using acetylene and the reaction was carried out in glass tubes according to the following consideration: in the case of cyanoethylation of trichlorosilane published preceedingly, the reaction in an autoclave in the presence of pyridine could be well reproduced in glass tubes in the presence of tetrapyridine nickel chloride. Therefore, the analogous phenomenon was expected to occur here in the reaction of trichlorosilane and acetylene. In fact, that was the case. The typical examples of the experiments were summarized in Table II. This reaction did not take place in the presence of pyridine alone, but in the presence of a catalytic amount of tetrapyridine nickel

Table I

Products obtained from the reaction of acetylene and trichlorosilane in an autoclave in the presence of pyridine

	Fraction No. 1	Calcd. for $[(CH_3)_3Si]_2C_2H_4$	Fraction No. 3	Calcd. for $[(CH_3)_3Si]_2C_4H_6$
B. p. °C[a]	71–2 (43 mmHg), 155–6		82–5 (24 mmHg)	
d_4^{20}	0.7699		0.7933	
n_D^{20}	1.4280		1.4440	
Mol. Wt.	175	174.4	195	200.4
C %	55.30	55.05	59.53	56.92
H %	12.57	12.72	11.89	12.07
Double bond per mol.	0	0	1	1
MR_D	58.26	58.43	67.10	67.22

a) All temperature are uncorrected.

5) M. Kumada and A. Habuchi, *J. Inst. Polytech., Osaka City Univ.*, **3**, Ser. C, 65 (1952).

TABLE II

ADDITION OF TRICHLOROSILINE TO VINYLTRICHLOROSILANE AT 180–5°C

	Run 1	Run 2	Run 3	Run 4
$HSiCl_3$, g.	17.3	21.6	32.7	22.8
$CH_2=CHSiCl_3$, g.	22.6	24.0	38.0	25.8
Catalyst, g.	$NiCl_2 \cdot C_5H_5N \cdot HCl$, 0.2	C_5H_5N 0.1	$NiCl_2 \cdot C_5H_5N$ 0.1	$NiCl_2 \cdot 4C_5H_5N$ 0.1
Reaction time, hr.	8.0	5.4	7.3	7.5
B. p. of product, °C (mmHg)	110–5 (54)	—	111–5 (51)	111–4 (49)
Yield, %[a]	8.5	0	13	55[b]

a) The yields are based on the vinyltrichlorosilane used.

b) The chlorine content of the product was 70.4. (Calcd. for $C_2H_4Si_2Cl_6$, 71.7%).

chloride, the addition was realized to the extent of about 50 percent. The reaction product was then methylated by treating with methylmagnesium bromide and subjected to fractional distillation (Fig. 1). The physical data of two main fractions (fractions No. 3 and 9) were listed in Table III. As the lower boiling fraction (No. 3) shows physical constants which correspond closely to that described by Kumada[5], this fraction can probably be assigned as 1, 2-di(trimethylsilyl)ethane. The higher boiling fraction, which has a similar composition, may be assigned as 1, 1-di(trimethylsilyl)ethane. However, as it was generally unusual that the branched isomer has a higher boiling point than the normal one, the normal compound was synthesized according to the processes of Frisch and Young[6] as follows, and thus the structure of the lower boiling isomer was established conclusively:

$$2\ C_2H_5MgBr \xrightarrow{CH\ CH} BrMgC{\equiv}CMgBr \xrightarrow{(CH_3)_3SiCl} (CH_3)_3SiC{\equiv}CSi(CH_3)_3 \xrightarrow{H_2,\ Pt} (CH_3)_3SiCH_2CH_2Si(CH_3)_3 \quad \text{(Table III, B)}$$

From the comparison of these physical data, the structure of the lower boiling fraction (No. 3) is established to be 1, 2-di(trimethylsilyl)ethane. Further evidence for the identity of these compounds was obtained from the comparison of infrared spectra. Although the higher boiling compound could not be compared with the authentic sample because of the difficulty of synthesis, it may be reasonably considered to be the branched isomer. For the sake of comparison, the di(trimethylsilyl)ethane which is derived from the reaction of acetylene and trichlorosilane in the presence of platinized asbestos is also listed in Table III (A).

The author refers again to the aforementioned di(trimethylsilyl)ethane which was obtained from acetylene in the autoclave in the presence of pyridine. This compound proved to be a mixture of these two isomers through comparison of physical constants and infrared spectra. But at that time it could not be fractionated into the components, owing to its small amount.

As the results of the above experiments, the author is led to the conclusion that the main reaction in this condition may be represented as follows:

$$CH{\equiv}CH + HSiCl_3 \longrightarrow CH_2{=}CHSiCl_3$$

$$CH_2{=}CHSiCl_3 + HSiCl_3 \longrightarrow Cl_3SiCH_2CH_2SiCl_3 + Cl_3SiCHSiCl_3 \quad (CH_3)$$

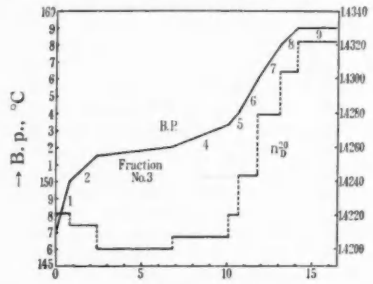

Fig. 1. Fractional distillation curve of the methylated product obtained from trichlorosilane and vinyltrichlorosilane.

TABLE III

PHYSICAL CONSTANTS AND ANALITICAL DATA OF DI(TRIMETHYLSILYL)ETHANE OBTAINED BY VARIOUS METHODS

	C[c] Fraction No. 3	C[c] Fraction No. 9	A[a]	B[b]
B. p. °C	151.5–2.0	159	150.0–0.5	150.5–1.0
d_4^{20}	0.7539	0.7808	0.7542	0.7532
n_D^{20}	1.4200	1.4322	1.4196	1.4194
Mol. Wt. in benzene	177	176	—	—
C %	55.53	54.66	54.55	55.68
H %	12.60	12.41	12.30	12.74
MR_D	58.54	57.95	58.46	58.51

a) A is the product of the reaction between acetylene and trichlorosilane in the presence of platinized asbestos.

b) B is the product obtained from acetylene via di-Grignard reagent of acetylene.

c) C is the product obtained from the reaction of trichlorosilane and vinyltrichlorosilane in the presence of tetrapyridine nickel chloride.

Experimental

Reaction of Trichlorosilane and Acetylene in an Autoclave.—The procedure described by Wagner and Strother[2] was followed by the author. One and a half grams of platinized asbestos[3] and 28 g. of trichlorosilane were charged into an autoclave of 100 ml. capacity. The air in the autoclave was replaced several times by acetylene, and then gradual heating was applied.

6) K.C. Frisch and R.B. Young, U.S. Pat. 2,671,099, Mar. 2 (1954); *C.A.* **49**, 2498g.

The initial pressure of acetylene was 12 kg./cm² at room temperature. The reaction started at 168°C, and the pressure at that time was 27.5 kg./cm² and decreased smoothly to the constant value of 3.2 kg./cm² at 174°C within three hours. After cooling, the contents of the autoclave was washed out by dry ether, filtered, and distilled, yielding 11.5 g. of 1,2-di(trichlorosilyl)ethane, b.p. 197–8.5°C.

In the other run, the pressure was maintained at above 15 kg./cm² throughout the operation by charging the acetylene intermittently, and the heating was stopped when the decrement of the pressure had amounted to 28 kg./cm² as a total. Distillation yielded 12.4 g. of vinyltrichlorosilane (b.p. 89.5–91.0°C) and 5.2 g. of higher boiling product.

Reaction of Trichlorosilane and Acetylene in an Autoclave in the Presence of Pyridine.—A half gram of pyridine and 55.8 g. of trichlorosilane (0.41 mol.) were charged into an autoclave of 240 ml. capacity, and treated in a similar manner as mentioned above. The reaction started at 184C° and 0.21 mol. of acetylene was consumed within 8.3 hr. Upon distilling the unreacted trichlorosilane, there remained 46 g. of a higher boiling product (Cl, 58.6%). The product was methylated in the usual manner with methyl magnesium bromide prepared from 23 g. of magnesium, and fractionally distilled through a Stedman column of about thirty theoretical plates, giving the following fractions: (1) b.p. 72°(70 mm.)–63°(27 mm.), 3.5 g.; (2) b.p. 59–76°C(23 mm.), 1.3 g.; (3) b.p. 76–88°C(23 mm.), 1.3 g.; (4) residue, 3.5 g. The first main fraction (No. 1) was purified by shaking it with concentrated sulfuric acid to remove the higher boiling unsaturated compound and by redistilling. The physical data of the purified compound are listed in Table I. The second main fraction (No. 3) was redistilled and its physical constants are also given in Table I.

Reaction of Trichlorosilane and Vinyltrichlorosilane.—Vinyltrichlorosilane was the product of Linde Air Products Co. and distilled at 89–90°C.

The reactions were carried out in sealed glass tubes and its procedure was as follows: trichlorosilane (b.p. 31.5–32.0°C), a vinylcompound, and catalyst were charged into a hard glass reaction ampoule of about 100 ml. capacity and cooled in an ice salt bath, and then the open end of the ampoule was sealed after the air had been replaced by dry nitrogen. Heating was carried out in an electric furnace equipped with an automatic controller. After cooling, the reaction tube was opened, the content was washed out with dry benzene, and the precipitate, if any, was filtered. The unreacted starting material and the solvent in the filtrate was distilled under atmospheric pressure, and then the product was distilled from a Claisen fiask under reduced pressure. The results are summarized in Table II.

The product of several runs are combined (35.4 g.) and methylated in the usual manner with methylmagnesium bromide prepared from 20.0 g. of magnesium, yielding 14.5 g. of di(trimethylsilyl)ethane, b.p. 150–8°C (70%). It (19.2 g.) was then distilled fractionally through a Stedman column (Fig. 1). The physical data of two main fractions (No. 3 and 9) are given in Table III.

Di(trimethylsilyl)ethyne.—This compound was synthesized according to the description of Frisch and Young[6]. Into the ethereal solution of ethylmagnesium bromide prepared from 30 g. of magnesium, dry acetylene was bubbled slowly for about six hours at room temperature. After boiling for a short time and then cooling, 1 g. of cuprous chloride was added, and stirred until the gas evolution settled down. Then, 30 g. of trimethylchlorosilane was added, stirred for half an hour, and refluxed for two and a half hours. After cooling, the reaction mixture was treated with ice and diluted hydrochloric acid, and the ether layer was separated, washed with water, and dried with calcium chloride. After filtration the ether solution was distilled through a Stedman column, yielding 2.1 g. of di(trimethylsilyl)ethyne, b.p. 136.0°C; d_4^{25}, 0.7578; n_D^{25}, 1.4231; MR_D, 57.25 (calcd. 56.82).

1,2-Di(trimethylsilyl)ethane.—A solution of 2.84 g. of di(trimethylsilyl)ethyne in 10 ml. of alcohol was reduced catalytically in the presence of palladium charcoal. The amount of hydrogen absorbed was quantitative. After the removal of the catalyst by filtration, 50 ml. of water was added, and the separating oily layer was extracted with ether. The ether extract was washed with a small amout of water and dried over calcium chloride. Distillation of the ether solution yielded 1.8 g. of the crude product. The crude product was shaken twice with about equal volume of concentrated sulfuric acid and then distilled, yielding 1.0 g. of the pure 1,2-di(trimethylsilyl)ethane, b.p. 150.5–151.0°C. The physical constants and analytical data are shown in Table III (B).

Summary

The addition reactions of trichlorosilane and acetylene in an autoclave were carried out in the presence of platinized asbestos or of pyridine. In the case of the former catalyst, 1,2-di(trichlorosilyl)ethane was obtained exclusively. In the case of the latter, on the other hand, the principal product proved to be a mixture of 1,2- and 1,1-di(trichlorosilyl)-ethane.

The addition of trichlorosilane to vinyltrichlorosilane in the presence of tetrapyridine nickel(II) chloride in glass tubes also led to the formation of a mixture of two isomers. Therefore, it might be considered that the reaction processes in the autoclave in the presence of pyridine was reproduced by the reactions in glass tubes. This situation seems to be analogous to that in the case of cyanoethylation of trichlorosilane which was previously reported.

The author is much indebted to Profs. S. Murahashi and N. Hagiwara for their many helpful suggestions, and to Mr. S. Konotsune for his help in the experiments. Appreciation is also expressed to Nihon Silicon Resin Co. for their kindness in supplying the trichlorosilane.

Department of Chemistry, Faculty of Science, Osaka University, Osaka

*Synthetic Amphoteric Polypeptide. II. Synthesis and Some Properties of a Reversibly Contractile Amphoteric Polypeptide**

By Heimei YUKI, Shumpei SAKAKIBARA, Toshio TAKI and Hisaya TANI

(Received February 27, 1956)

K. H. Meyer[1] has suggested that the contraction and relaxation of muscle may be attributed to the electrostatic attraction and repulsion of ionised ammonium and/or carboxyl groups in the molecule of myosin. Recently W. Kuhn and A. Katchalsky et al.[2] have synthesized vinyl-type polyanions as such mechanochemical systems. Studies concerning these substances are, of course, very useful and instructive, but a study of polypeptide-type polyampholyte would be more desirable. In this paper the synthesis of a three-dimensional amphoteric polypeptide network composed of L-glutamic acid, L-lysine and DL-cystine residues, and some properties concerning its reversible contractility are described.

Preparation

A mixture of N-carboxy anhydrides of ε-N-carbobenzoxy-L-lysine, γ-benzyl L-glutamate and DL-cystine, the molar ratio of which was 26:26:1, was polymerized in dry chlorobenzene-pyridine mixture. Reduction of the polymer by phosphonium iodide gave the hydriodide of a linear polypeptide consisting of L-glutamic acid, L-lysine and DL-cysteine residues. The amino acid composition of this polypeptide was approximately the same as that derived from the starting monomer mixture. This linear polypeptide hydriodide was soluble in water, methanol and ethanol, and gave positive biuret and nitroprusside reactions. The free polypeptide had an isoelectric point at pH 7.4 and was insoluble in the pH range between about 5.0 and 10.0.

When the foil, made on a glass plate from the methanol solution of this linear polypeptide hydriodide, was soaked in commercial (not purified) ether overnight, it turned insoluble in water and yellowish-brown in color, due to the liberation of iodine; this color vanished by soaking in dilute alkali. This insoluble foil may be considered to be a network polypeptide, in which cysteine residues were converted into cystine ones.

Measurements of the Contractility

A piece of this foil, which was swollen in distilled water, became greatly extended in dilute acids and in dilute alkalis, and then contracted to its initial length in pure water (see Table I).

TABLE I

Immersion medium*	Parallel to the orientation: Length (×55, cm.)	Parallel to the orientation: Ratio	Perpendicular to the orientation: Length (×55, cm.)	Perpendicular to the orientation: Ratio
dry sample	1.77	1.00	4.00	1.00
in water	2.07	1.17	4.70	1.18
in 0.01 N NaOH	2.99	1.69	6.80	1.70
in water	2.30	1.30	5.42	1.36
in 0.01 N HCl	2.75	1.55	6.42	1.61
in water	2.10	1.19	4.78	1.20

* The foil was immersed in the media in descending order.

An attempt was made to give an orientation to the foil by allowing the methanol solution to flow in one direction when casting it on a glass plate, but practically no effect on the swelling was observed.

A strip, cut from the foil, was fastened at one end and a load attached to the other end. It was then immersed in various media and its length measured as a function of time.

The elongation of the strip in dilute hydrochloric acid and in dilute aqueous sodium hydroxide and its contraction in a neutral medium are shown in Fig. 1. The strip was elongated more in the alkaline than in the acidic medium, and the time required for contraction by neutralising from the alkaline solution was longer than that from the acidic solution. This time of contracting from the alkaline solution was shortened by using dilute aqueous sodium chloride as a neutral medium instead of pure water and by slightly agitating the medium. This behavior suggests that sodium ions were more strongly adsorbed on the strip than chloride ions. When the strip, which was elongated in alkaline (or acidic) medium, was soaked in an acidic (or alkaline) one, it contracted strongly momentarily and then elongated in the usual manner in the latter medium.

The lengths of the strip at various pH values from 2 to 11 are shown in Fig. 2. The minimum length was at pH 3–4 in Clark-Lubs' buffer and at pH 5 in acetate buffer. It is noticeable that the strip contracted more strongly in phthalate

* A preliminary report of the part of this paper was published in *J. Am. Chem. Soc.*, 75, 3042 (1953).

1) K.H. Meyer, *Biochem. Z.*, **214**, 253 (1929); *Experientia* **7**, 361 (1951).

2) W. Kuhn, B. Hargitay, A. Katchalsky and H. Eisenberg, *Nature*, **165**, 514 (1950); A. Katchalsky and H. Eisenberg, ibid., **166**, 267 (1950); W. Kuhn and B. Hargitay, *Experientia*, **7**, 1 (1951); A. Katchalsky, *J. Polymer Sci.*, **7**, 392 (1951).

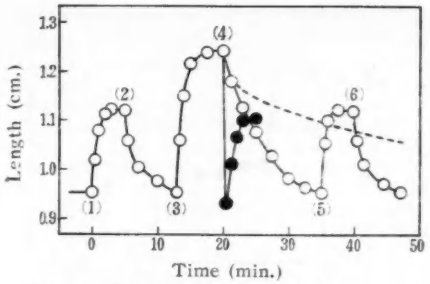

Fig. 1. Reversible lifting and lowering of a load by a strip.

Dry strip: $0.764\times0.038\times0.003$ cm^3, 0.065 mg. Load: 5.07 mg. Medium: (1) and (5), 0.005 N NaCl (15 ml.)+0.01 N HCl (3 ml.); (2) and (6), 0.005 N NaCl (18 ml.); (3), 0.005 N NaCl (15 ml.)+0.01 N NaOH (3 ml.); (4) ○, 0.005 N NaCl (slight agitation); (4) ●, 0.005 N NaCl (15 ml.)+0.01 N HCl (3 ml.); (4) dotted line, H_2O.

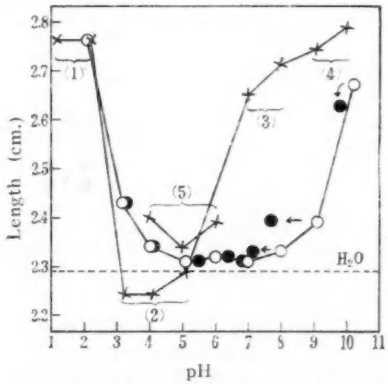

Fig. 2. Relationship between pH of the medium and length of a strip.

Dry strip: length, 1.974 cm.; weight, 0.4 mg. Load: 18 mg. Medium (70 ml.): ×, buffer solutions — (1), HCl-KCl; (2), potassium biphthalate-NaOH; (3), KH_2PO_4-NaOH; (4), H_3BO_3-KCl-NaOH; (5), AcOH-AcONa. ○, NaOH-HCl mixtures (ionic strength 0.01). ●, After immersion of the strip.

buffer than in pure water. This behavior is supposed to be attributable to the large bulk of the bivalent phthalate ions.

In the solutions made by mixing various proportions of 0.01 N hydrochloric acid and 0.01 N sodium hydroxide, the length of the strip was a minimum at pH from 5 to 7 and the pH of the media shifted towards pH 6.5 after immersion of the strip. These results demonstrate the adsorption of sodium and chloride ions on the strip, i.e., the ion-exchange ability of the strip. The maximum pH shift was found in solution of pH 9, in which the excess of the number of sodium ions over the number of chloride ions was approximately equal to the number of carboxyl groups in the strip used, and the length of the strip reached the equilibrium value only after a very long time.

The elongation of the strip was constant in the media so acidic (i.e., pH below 2) that no dissociation of the carboxyl groups in the strip could take place.

The elongation of the strip by a load up to about two thousand times the dry weight of the strip per 1 cm. of length was measured in 0.01 N hydrochloric acid and in 0.01 N aqueous sodium chloride. The results are shown in Fig. 3. In

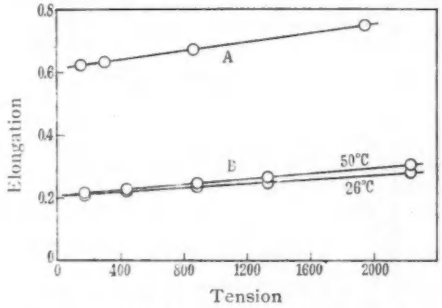

Fig. 3. Relationship between tension and elongation of a strip.

Elongation: $(l-l_0)/l_0$, where l and l_0 are the lengths of the immersed and the dry strip respectively. Tension: $W/(w_0/l_0)$, where W and w_0 are the weights of load and the dry strip respectively. A: In 0.01 N HCl at room temperature; l_0= 1.46 cm., w_0=0.30 mg. B: In 0.01 N NaCl at 26°C and 50°C; l_0=1.985 cm., w_0=0.23 mg.

these media the elongation was proportional to the weight of load; but after removing the load a slight hysteresis was observed, which vanished on prolonged standing.

The length of the strip increased slightly on raising the temperature. The relation of temperature *versus* tension, for a constant length of the strip, is shown in Fig. 4. This figure was ob-

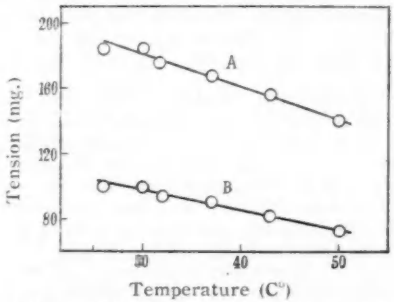

Fig. 4. Relationship between temperature and tension at constant lengths of a strip.

Dry strip: length, 1.985 cm.; weight, 0.23 mg. A: length=2.500 cm. B: length =2.450 cm.

tained graphically from the data of the measurements of load-elongation relationships at various temperatures from 20 to 50°C. It was found that the strip tends to decrease its tensile strength with increasing temperature.

It is interesting to study the effects of inorganic salts on the contractility of this strip compared with that of actomyosin.

The strip, immersed in water, was elongated by the addition of sodium chloride; the higher its concentration, the greater the elongation. The sodium chloride concentration was increased stepwise from 0.1 to 4 N and then decreased reversely. As shown in Fig. 5, the elongation

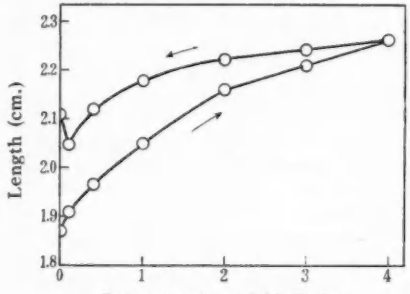

Fig. 5. Effect of concentration of NaCl on length of a strip.
Dry strip: length, 1.594 cm.; weight, 0.3 mg. Load: 18 mg.

of the strip was not reversible and its length could not return completely to its initial value. Upon immersing this strip in distilled water it was elongated. Subsequent immersion in dilute hydrochloric acid then caused it to contract rapidly, suggesting that the adsorption of sodium ions in the strip is rather strong.

The behavior of the strip in concentrated sodium chloride solution was somewhat complicated. When it was transferred directly into 4 N aqueous sodium chloride from distilled water, its length increased instantly; this was followed by a slow additional elongation proportional to the time, until the equilibrium length was approached. This elongated strip contracted now reversely by replacing it in distilled water; the rate of contraction was rapid at first and then slow (see Fig. 6).

Very striking and interesting phenomena were observed in the following series of experiments (see Fig. 6). The strip, which was elongated previously in 4 N aqueous sodium chloride as described above, contracted sharply on the addition of a small amount of dilute hydrochloric acid to the medium, and regained its original length in distilled water. When it was soaked again in 4 N aqueous sodium chloride, no change in length was observed, but on subsequent immersion in distilled water an instantaneous strong elongation and contraction was observed. On insertion of the strip into 4 N aqueous sodium chloride, it was lengthened in a manner similar to that when first immersed in this medium.

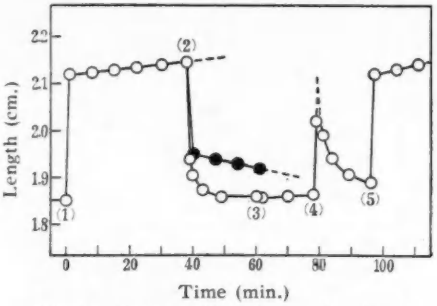

Fig. 6. Contractility of a strip in concentrated NaCl solution. I.
Dry strip: length, 1.594 cm.; weight, 0.30 mg. Load: 18.0 mg. Medium: (1), (3) and (5), 4 N NaCl; (4), H_2O; (2) ○, 4 N NaCl (15 ml.) +0.01 N HCl (3 ml.); (2) ●, H_2O.

This series of experiments was repeated by using 2 N aqueous sodium chloride (see Fig. 7).

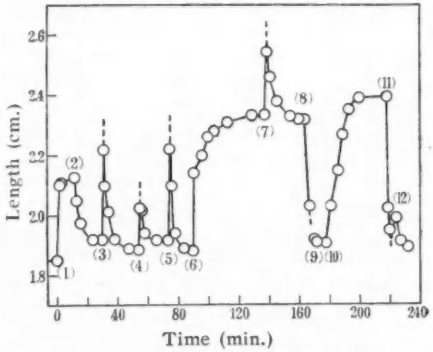

Fig. 7. Contractility of a strip in concentrated NaCl solution. II.
Dry strip: length, 1.594 cm.; weight, 0.30 mg. Load: 18.0 mg. Medium: (1), 2 N NaCl; (2) and (4), 2 N NaCl (16.5 ml.) +0.01 N HCl (1.5 ml.); (3), (5), (7), (9) and (12), H_2O; (6), 2 N NaCl (16.5 ml.)+0.01 N NaOH (1.5 ml.); (8) and (11), H_2O (16.5 ml.) +0.01 N HCl (1.5 ml.); (10), H_2O (16.5 ml.) +0.01 N NaOH (1.5 ml.).

When the strip was transferred from distilled water into 2 N aqueous sodium chloride solution containing a small amount of hydrochloric acid, an instantaneous elongation and contraction was observed. This phenomenon appeared to be an overlap of the elongation by the sodium chloride and the following contraction by the acidic sodium chloride solution.

The effect of the addition of a small amount of sodium hydroxide to aqueous sodium chloride was contrary to that of hydrochloric acid. The strip was elongated further stronger in the alkaline sodium chloride solution than was elongated in 2 N aqueous sodium chloride. Then, on soaking in distilled water, a strong elongation and

contraction was observed; but the final length of the strip was the same as that in the preceeding medium. Soaking the strip in dilute hydrochloric acid then caused it to return to the original length which it had had in distilled water. This process was similar to the contraction observed on the transfer of the strip into dilute hydrochloric acid from dilute aqueous sodium hydroxide (see Fig. 7).

A series of immersion media was prepared by dissolving various amounts of sodium chloride in 0.005 N hydrochloric acid, and the length of the strip was measured in these media (see Fig. 8). Though at the lower concentration (i.e., below 0.1 N) of sodium chloride the length of the strip was somewhat longer than that in hydrochloric acid alone, the strip contracted with an increase in the concentration of salt, and at the higher concentration (i.e., above 0.1 N) the extent of contraction was proportional to the logarithm of the concentration. This behavior is contrary to that in neutral sodium chloride solution.

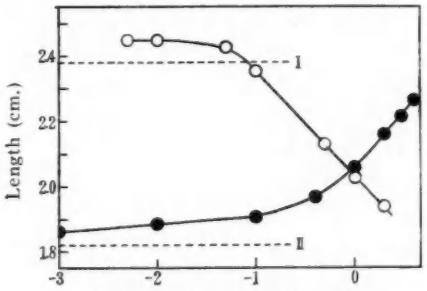

Fig. 8. Length of a strip in acidic and neutral NaCl solution.

Dry strip: length, 1.594 cm.; weight, 0.30 mg. Load: 18.0 mg. ○, Solution of NaCl in 0.005 N HCl. ●, Aqueous solution of NaCl. Dotted lines I and II represent the lengths of the strip in 0.005 N HCl and water, respectively.

The effects of neutral inorganic salts containing bivalent ions are shown in Fig. 9. The length-concentration relationships were similar for $CaCl_2$, $MgCl_2$, Na_2SO_4 and $(NH_4)_2SO_4$ solutions to that for aqueous sodium chloride. On the contrary, the strip contracted in aqueous $CuSO_4$ and in aqueous $ZnCl_2$ at the concentrations below and above 0.1 N respectively, and very strongly in aqueous $HgCl_2$ at the whole concentration tested. Since it has been known that these metal ions (Hg^{++}, Cu^{++} and Zn^{++}) are capable of forming complexes with amino groups and particularly that Hg^{++} ion can combine strongly with sulfur atoms, the contraction of the strip in these solutions appears to be due to the formation of cross-linkages of these complexes. In aqueous $KHCO_3$ the strip was elongated strongly as a result of its alkalinity. The strip was also slightly elongated with increasing temperature in all these salt solutions.

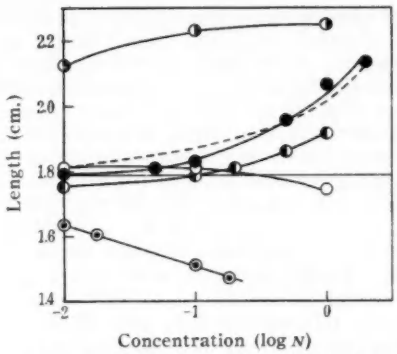

Fig. 9. Effects of various salts on length of a strip.

Dry strip: length, 1.47 cm.; weight, 0.30 mg. Load: 19.5 mg. ●, $CaCl_2$; ○, $ZnCl_2$; ◐, $CuSO_4$; ⊙, $HgCl_2$; ◑, $KHCO_3$; dotted line, NaCl. $MgCl_2$, Na_2SO_4, $(NH_4)_2SO_4$ gave curves similar to that for $CaCl_2$.

Discussion

W. Kuhn and A. Katchalsky et al.[2] reported with their three-dimensional polyanion network that a statistical consideration concerning the entropy of a three-dimensional network and considerations concerning the electrostatic energy of the ionised system are required for the theoretical treatment of the elongation and contraction phenomena. S. Asakura[3] and H. Noguchi[4] stated that the entropy force of counter-ions bound by the system plays a predominant role, tending to expand the system against the rubber-like elastic force.

In this experiment the phenomena shown by the strip-form polyampholyte system was, as expected, more complicated than that shown by the polyanion system. Contrary to the polyanion system, the strip of this amphoteric polypeptide decreased its restoring force with increasing temperature. This fact shows that at a given temperature the internal energy and the entropy increase with the elongation of the strip: that is,

$$(\partial E/\partial l)_T > 0 \quad \text{and} \quad (\partial S/\partial l)_T > 0$$

in the relation

$$K=(\partial E/\partial l)_T - T(\partial S/\partial l)_T$$
$$=(\partial E/\partial l)_T + T(\partial K/\partial T)_l$$

in which K, E, S, l, and T represent restoring force, internal energy, entropy, length and absolute temperature respectively.

It appears that there are some cross-linkages in the foil in addition to the cystine -S-S- linkages and that the number of the

3) S. Asakura, *Busseiron Kenkyu*, **62**, 39 (1953).
4) H. Noguchi, ibid., **62**, 30 (1953).

former changes with the increase and decrease of temperature by their rupture and reformation. Such linkages might include the salt linkages between carboxyl and ammonium ions and the hydrogen bonds between two amide linkages. This consideration is supported also by the strong elongation of this strip in concentrated salt solutions and by both the viscosity increase and the insolubility of synthetic linear polypeptide, reported in the preceeding paper[5], in neutral region. Furthermore, it was found that synthetic high molecular copoly-1 : 1-(L-glutamic acid, L-lysine)[6], which was insoluble in distilled water, could be dissolved in concentrated sodium chloride solution. The solubility and the viscosity behavior of these linear amphoteric polypeptides is closely related to the contractility of this strip and qualitatively coincide with it.

As found in most instances, the strip adsorbed cations more strongly than anions. This difference in adsorption appears to be caused by reasons such as the decrease in the number of amino groups during the formation of the foil, but the true reason remained unknown. The difference in the hydrations of cations and anions is also considered to be concerned with the above behavior of the foil. Although no satisfactory conclusion could be obtained, since the phenomena are too complicated, the contractility of this foil, e.g. the rapid elongation and contraction of the strip found in some instances, is very interesting as compared with the behavior of actomyosin.

Experimental

N, N'-Dicarbobenzoxy-cystine.—This was synthesized from L-cystine according to the Bergmann's method[7], but showed no optical rotation in acetic acid probably due to the racemisation during the reaction. Recrystallized from acetone-chloroform, it combined 1/4 mol. of chloroform m.p. 101–103° (sintered from 80°C).

Anal. Found: C, 49.83; H, 4.71; N, 5.14; SO_4 and Cl, 40.53. Calcd. for $C_{22}H_{24}N_2O_8S_2 \cdot 1/4\ CHCl_3$: C, 49.63; H, 4.54; N, 5.20; SO_4 and Cl, 40.63% (S and Cl were measured by Stragand's method[8] and obtained as the sum of converted SO_4 and Cl).

DL-Cystine Bis-(N-carboxy-anhydride).—To the solution of 2 g. of dicarbobenzoxy-cystine in 12 ml. of dry dioxane 4.4 g. of phosphorus pentachloride was added. After shaking for 15 min. at 10°C, the mixture was filtered and heated for one hour at 40°C. The crystallized anhydride was filtered and washed with ethyl acetate. Yield 1.0 g., colorless needles. m.p. 134° (decomp.). It contained 1 mol. of combined dioxane.

Anal. Found: C, 38.04; H, 4.18; N, 7.31; S, 16.65. Calcd. for $C_8H_6N_2O_6S_2 \cdot C_4H_8O_2$: C, 37.90; H, 4.24; N, 7.37; S, 16.84%.

Copolymerization.—A mixture of 2.104 g. (8.0 m mol.) of γ-benzyl N-carboxy-L-glutamate anhydride[5], 2,448 g. (8.0 m mol.) of ε-N-carbobenzoxy-L-lysine anhydride[5] and 0.117 g. (0.308 m mol.) of DL-cystine bis-(N-carboxy-anhydride) in 42 ml. of chlorobenzene and 3 ml. of dry pyridine was heated rapidly to 100°C in a sealed glass tube until in solution, and then kept for ninety hours at 50°C and for ten days at room temperature. The solution gradually increased in viscosity and finally became an opalescent gel. The polymer, precipitated by adding petroleum ether, was allowed to swell in acetone, and after reprecipitating by petroleum ether, it was obtained as a white powder. Yield 3.890 g. (99% of the theor.).

Anal. Found*: C, 63.86; H, 6.54; N, 8.70. Calcd. for $[26(C_{12}H_{13}NO_2), 26(C_{14}H_{18}N_2O_3), (C_3H_8N_2O_2S_2)]_n$: C, 64.37; H, 6.45; N, 8.81%.

The polymer swelled in chloroform, acetone, pyridine, dioxane, tetrahydrofuran, and hot glacial acetic acid, but could not be dissolved.

Reduction of the Polymer.—After 0.7 g. of the polymer was swelled by heating in 50 ml. of glacial acetic acid, 1.7 g. of phosphonium iodide was added in portions during five hours at 55°C, with dry hydrogen bubbling through the solution. The supernatant liquid was separated from the resultant precipitate by decantation, and a small amount of absolute alcohol was added. This dissolved the major part of the precipitate, but some swollen material remained. The polymer was reprecipitated from the solution by freshly distilled ether and was then extracted repeatedly with water. The extracts were combined and were concentrated in vacuo at 40°C. The polypeptide hydriodide was precipitated from the residual syrup by adding ethanol and ether, washed with ether and dried. White powder; yield 0.27 g. (48% of the theor.). It was soluble in water, methanol, and ethanol, and gave positive biuret and nitroprusside test.

Anal. Found: C, 33.77; H, 5.25; N, 10.83; I, 32.1; amino-N, 3.46. Calcd. for $[26(C_9H_7NO_2), 26\ C_7H_{12}N_2O \cdot HI), 2(C_3H_5NOS)]_n$: C, 34.25; H, 5.23; N, 10.96; I, 32.3; amino-N, 3.56%.

Preparation of the Foil.—The foil was made on a parraffin-treated glass plate by casting a 2% methanol solution of the above polypeptide hydriodide. After immersing overnight in commercial ether, the foil became orange-yellow in color and turned insoluble, but swelled in water. This foil gave no nitroprusside test, and was quite flexible and strongly elastic in water. It was decolorised by soaking in dilute alkali, and, after washing with dilute hydrochloric acid and water, it was contracted easily by alcohol and ether, and dried.

The powdered polypeptide hydriodide was treated with commercial ether as before and then

5) H. Yuki, S. Sakakibara and H. Tani, This Bulletin, 29, 654 (1956).
6) H. Yuki and H. Tani, Unpublished.
7) M. Bergmann and L. Zervas, *Ber.*, 65, 1192 (1932).
8) G.L. Stragand and H.W. Safford, *Anal. Chem.*, 21, 625 (1949).

with 0.001 N sodium hydroxide, washed with water, ethanol and ether, and dried. This substance contained a small amount of combined sodium.

Anal. Found: C, 49.99; H, 7.12; N, 14.77; Na, 3.92. Calcd. for $[16(C_5H_7NO_3), 10(C_5H_7NO_3 \cdot Na), 26(C_9H_{12}N_2O), (C_3H_8N_2O_2S_2)]_n$: C, 49.28; H, 6.98; N, 15.75; Na, 3.24%.

Swelling of the Foil (Table I).—A piece of the foil was immersed in the media and its length was measured by photographs (magnification 55×), taken after one hour of immersion.

Elongation and Contraction of the Strip.—The strips used for measurements were 1.5–2 cm. in length, 0.04–0.07 cm. in width, and 0.2–0.5 mg. in weight. Assuming the specific gravity to be approximately equal to unity its thickness was about 0.003 cm.

Glass clips were attached to the two ends of the strip. The upper clip was fastened to the hook of a glass rod. The lower clip was used itself as a load, and, if necessary, also used for hanging platinum rings, varied according to the desired additional load. The strip was immersed in the medium in a large test tube, held in a thermostat. The upper end of the strip was fixed and the change of the length was followed with a microscope.

To obtain the reproducibility the measurements were made after training the strip to elongate and contract, using successively dilute aqueous NaOH, water, dilute HCl and water. By this training the strip came to a constant length in a given medium. In most cases either the length of the strip in distilled water or that in dilute aqueous sodium chloride was used as a standard, from which each experiment was started. The strip was used in each experiment after recovering its standard length by washing it with dilute hydrochloric acid and then with water in order to remove any of the rather strongly adsorbed cations. The measurements were made at 25°C unless otherwise stated.

Summary

1. A reversibly contractile amphoteric polypeptide, copoly-26 : 26 : 1-(L-glutamic acid, L-lysine, DL-cystine), was synthesised.

2. The foil of this polypeptide contracted at its isoelectric region and extended in both acidic and basic media. This extension and contraction was pH-dependent and fully reversible.

3. The load-elongation relation of the strip of this foil was measured in aqueous media using the load up to about 2,000 times the dry weight per 1 cm. of length of the strip. This relation was linear in this range.

4. The temperature-elongation relation was measured in aqueous media at 20–50°C. From the data it was concluded that, at a given temperature, the internal energy and entropy increased with the elongation of the strip.

5. The change of length of the strip in aqueous media, containing hydrochloric acid, sodium hydroxide, sodium chloride and some other neutral salts individually or in pairs, was measured. Some peculiar and interesting phenomena were observed.

The authors express their hearty thanks to Prof. S. Akabori and Prof. S. Murahashi for their interest and encouragement throughout the work, to Dr. M. L. Huggins for reading the manuscript, and to Mr. Y. Hozumi and Miss S. Mori for a part of the experimental work. This research was financially supported by the Institute for Fibre Research and The Asahi Press.

Department of Chemistry, Faculty of Science, Osaka University, Osaka

Spectrophotometric Microdetermination of Arsenic in Natural Waters and its Application to Silicate and Biological Materials

By Ken SUGAWARA, Motoharu TANAKA and Satoru KANAMORI

(Received February 20, 1956)

Introduction

Ordinary natural waters are usually very poor in arsenic. As shown later, well water on the Higashiyama campus of Nagoya University contains only 0.4 μg./l. of this element and the sea water off Sugashima Island in Ise Bay contains 1.8 μg./l. For determining arsenic in such dilution, various methods[1,2,3] already proposed are not satisfactory. Some are liable to be contaminated, thus causing a considerable error while others are of low sensitivity. The neutron activation method by Smales and Pate[4] which boasts the highest sensitivity is usable only to those to whom a nuclear reactor is accessible.

After considering these points and closely examining the merits and defects of the current methods, the writers finally succeeded in establishing the following time-saving method fulfilling every requirement for water analysis with fair accuracy.

Our method consists of five steps; (a) coprecipitation with ferric hydroxide, (b) mineralization of the filtered precipitate, (c) extraction of arsenic xanthate by carbon tetrachloride, (d) oxidation of the xanthate into quinque-valent arsenic followed by extraction by water, and (e) final spectrophotometry of the extracted element as molybdenum blue.

Thus, usually using 3 l. of the sample, 2 μg. of arsenic can be safely determined with an error of only 5%. With appropriate pretreatment, the method is also applicable to silicate and biological materials.

Experimental

Reagents.—*Ferric Chloride.*—4.84 g. of arsenic-free ferric chloride ($FeCl_3 \cdot 6aq.$) is dissolved in 25 ml. of sulfuric acid and diluted to 100 ml. This solution contains 10 mg. of iron per ml.

Bromcresol Purple.—0.1% W/V solution.

Ammonia (1 : 3).—Reagent quality.

Nitric acid.—Reagent quality, freshly distilled.

Sulfuric acid.—Reagent quality, arsenic free.

Potassium iodide.—25% W/V solution.

Sodium thiosulfate.—5% W/V solution.

Carbon tetrachloride.—Reagent quality.

Potassium xanthate.—0.1% W/V solution, reagent quality.

Carbon tetrachloride containing bromine (1 : 25).—One part of bromine is mixed with 25 parts of carbon tetrachloride.

Sulfuric acid (1 : 9).

Ammonium molybdate.—2% W/V solution, reagent quality.

Hydrazine sulfate.—0.1% W/V solution, reagent quality.

Arsenic standard solution.—0.132 g. of arsenous oxide is dissolved in 2 ml. of 1 N sodium hydroxide solution, slightly acidified with dilute sulfuric acid, and diluted to 100 ml. This solution contains 1.00 mg. of arsenic per ml. A working standard solution is prepared by adequately diluting this solution.

Apparata.—Automatic Filtering Apparatus (Fig. 1).—This apparatus consists of three parts: a funnel (A), its receptacle (B), and a siphon (C).

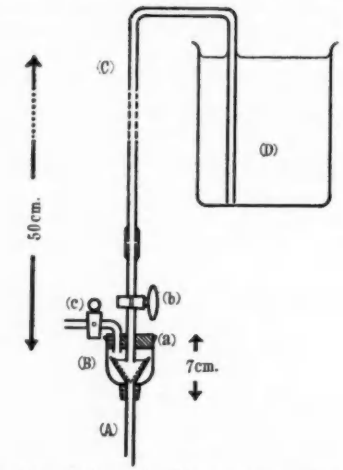

Fig. 1. Automatic filtering apparatus.

The funnel with a filter paper is fixed in the receptacle. A rubber stopper (a) with two leading tubes (b and c) is then tightly fixed into the mouth of the receptacle and the upper end of tube (b) is connected to the end of one of the arms of the siphon. Filteration is carried out as follows: Cocks (b and c) are opend and lips are placed to the end of tube (c) to gently suck,

1) R. Pieruccini, *Spectrochim. Acta*, **4**, 189-99 (1950).
2) M. Ishibashi, T. Shigematsu, Y. Nakagawa and Y. Ishibashi, *Bull. Inst. Chem. Research Kyoto Univ.*, **24**, 68 (1951).
3) A.K. Klein and F.A. Vorhes, Jr., *Assoc. Offic. Agr. Chemists*, **23**, 121-30 (1939).
4) A.A. Smales and B.D. Pate, *Analyst*, **77**, 188-95 (1952).

while the stem-end of the funnel is closed with a finger. When the liquid in vessel (D) flows down to the end of tube (b), both cocks are closed. Then the cock (b) is opend and the liquid is allowed to drop down into the funnel. Filtration continues under automatic control by the pressure change in the closed receptacle. Thus when the water level difference is kept at 50 cm., liquid continues to filter at a rate of about 500 ml. per hr.

Digestion Apparatus[5] (Fig. 2).—This apparatus

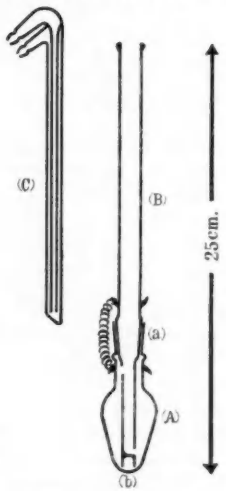

Fig. 2. Digestion apparatus.

consists of three parts: a digestion flask (A), a chimney (B), and a Schirm's[6] condenser (C). The chimney is so designed as to fit into the mouth of the digestion flask with ground joint (a). The small elongation of the chimney extending into the flask has a septum near its opening (b) bearing a small air space. When the chimney is fixed and the liquid in the flask is heated to boiling the open space immersed in the liquid continuously supplies air bubbles whereby bumping is avoided so that boiling continues smoothly. The chimney elongation has two openings, one near the mouth of the flask and the other just above the septum, through which the vapour evolving in the flask is led into the chimney where it is cooled and condensed by the previously inserted Schirm's condenser.

Procedure.—Co-precipitation.—To a suitable amount of the sample containing 1–5 μg. of arsenic, 1 ml. of ferric chloride solution is added per liter. After warming to 70–80°C, the solution is neutralized with ammonia (1 : 3) using bromcresol purple as indicator. While stirring vigorously, 1 ml. of the same reagent is added in excess per liter of the solution. When the solution is sufficiently cooled, the ferric hydroxide precipitate is filtered off through the automatic filtering apparatus just described.

5) M. Tanaka and S. Kanamori, *Anal. chim. Acta* **14**, 263 (1956).
6) E. Schirm, *Z. anorg. Chem.*, **25**, 1225 (1912).

Mineralization—The filter paper with precipitate is placed in the digestion flask and the chimney with Schirm's condenser is fixed in the flask. Gradually 2 ml. of nitric acid and 5 ml. of sulfuric acid are successively added through the chimney. A violent reaction occurs. When the reaction slows down, the contents of the flask are digested for 1–3 hr. During this digestion period repeated additions of nitric acid in small portions are necessary to avoid carbonization. After completion of mineralization, the contents of the flask are transferred into a quartz evaporating dish and heated on a water bath to drive off the excess nitric acid.

Extraction.—The residual solution in the dish is transferred into a 100 ml. beaker. After dilution with 25 ml. of water, it is warmed on a water bath and 2 ml. of potassium iodide solution added. After the solution is left to cool sufficiently for about thirty min., sodium thiosulfate solution is added with care in order to remove the liberated iodine. Any excess addition of the reagent must be avoided. Then the solution is transferred into a 100 ml. separatory funnel to which 5 ml. of potassium xanthate solution and 3 ml. of carbon tetrachloride were previously added. The funnel is vigorously shaken for two min. When carbon tetrachloride layer separates on the bottom, it is drawn out into a 25 ml. separatory funnel. The carbon tetrachloride extraction is repeated with 5 ml. of potassium xanthate solution and 3 ml. of carbon tetrachloride, and this second extract is joined to the first.

It is often the case that a part of the carbon tetrachloride is emulsified into numberless small droplets, their unification being difficult. This difficulty, however, is easily solved by filtering through a cotton plug 1 mm. thick placed at the bottom of the funnel. The droplets are united by passing through the plug and running down to form larger drops associated with some considerable amount of water. This water can be completely removed by repeated separatory funnel treatment.

To the joined carbon tetrachloride extract, are added 1.2 ml. of sulfuric acid (1 : 9), 2 ml. of water and one or more of carbon tetrachloride containing bromine (1 : 25), to give a deep red color to the organic layer. After thorough shaking, the funnel is left to stand until two perfectly separate layers form. A greater part of the oxidized arsenic has gone into the acid layer. The bottom carbon tetrachloride layer is separated into another 25 ml. separatory funnel and shaken with 3 ml. of water to remove the last trace of arsenic in carbon tetrachloride by the water. The acid extract and the water extract are united and washed with two portions of 3 ml. of carbon tetrachloride to remove the remaining bromine. Then the joined extract is transferred into a 10 ml. measuring flask. The separatory funnels are washed with 3 ml. of water and this washing is also added to the flask.

Determination.—After first adding 0.4 ml. of ammonium molybdate solution and 0.4 ml. of hydrazine sulfate solution and then making it up

to 10 ml., the flask is kept in boiling water for thirty min. and then cooled with tap water. Now the extinction measurement is made using a wave length greater than 700 mμ, preferably 840 mμ. The value obtained is corrected by referring to the value of a blank test which was conducted, omitting no step of the procedure. Finally the amount of arsenic is determined by referring to a standard curve constructed by using various known amounts of arsenic.

Discussion

In the analysis of minute quantities of arsenic, special care must be paid to avoid the slightest contamination. Glass and enamel vessels are sources of considerable contamination, particularly when they are warmed in the process of evaporation or co-precipitation. The following experiment proved this: 100 ml. of 1 N suluric acid was put in each of three beakers, glass, enamel, and porcelain, of equal size. They were heated on an electric plate for thirty min. Then the arsenic from each beaker was determined with the result that 2 μg., 50 μg., and below 0.1 μg. were the arsenic values for glass, enamel, and porcelain beakers respectively. Thus a porcelain vessel is recommended as the best for our purpose.

The reason why co-precipitation with ferric hydroxide was adopted is that it suffers the least from contamination and also saves considerable time when compared with evaporation.

Ferric hydroxide, however, co-precipitates not only dissolved arsenic but also other suspended particulates which might contain combined arsenic. Therefore the obtained arsenic value indicates the total amount of arsenic.

The recovery of tri-valent and quinquevalent arsenic in the co-precipitation process was separately examined as follows: Various quantities of each arsenic species were dissolved in 1 l. of water and co-precipitated with 10 mg. of ferric hydroxide. The precipitate filtered off through a fine glass filter was dissolved in dilute sulfuric acid and determined according to the prescribed procedure. The results given in Table I show that the recovery is between 98 and 100%. The experiment also proved that 10 mg. of ferric hydroxide is sufficient to complete co-precipitation of arsenic in ordinary waters even if they contain other substances susceptible to ferric hydroxide co-precipitation.

The optimum pH for the co-precipitation is around 9 and in order to bring the pH of the solution up to this value, approximately 1 ml. of ammonia (1: 3) must be added in excess beyond the neutral point for bromcresol purple. The addition must be made with vigorous stirring so that a uniform shifting of pH is ensured.

TABLE I

CO-PRECIPITATION OF ARSENIC WITH FERRIC HYDROXIDE

Fe used mg.	As^{III} added μg.	As^{III} co-pptd. μg.
10	2	1.9
10	5	5.2
10	100	97
10	1000	990
Fe used mg.	As^{V} added μg.	As^{V} co-pptd. μg.
10	2	2.1
10	5	4.8
10	100	98
10	1000	990

As for extraction of tri-valent arsenic, it is complete even with an acidity of 1 N sulfuric acid so long as co-existing elements are poor. With an increase of such elements, the pH range for a complete extraction is narrowed, a fact by the consideration of which the writers adopted an acidity of 6 N sulfuric acid in the present procedure.

Fig. 3 shows interferences with the extraction of arsenic xanthate by various elements.

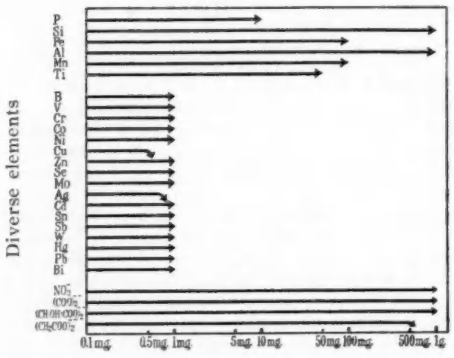

Fig. 3. Interferences of diverse elements.

Straight arrows indicate interference ranges no greater than 3%. A greater interference is first visible at the points where arrows begin to bend. Downward bending indicates a negative interference greater than 3%.

It is remarkable to find that phosphorus and silicon show no considerable interference despite the fact that they are likely to develop the same molybdenum blue as arsenic.

The interferences by alkalis, alkaline earths, aluminum, manganese, zinc, cadmium, vanadium, and boron cause no greater error than the minor unavoidable error straying in through mechanical treatment.

If selenium is in the original sample, it is reduced into metal partly during the course of potassium iodide treatment and in part in the hydrazine sulfate treatment. The first selenium metal can be easily removed by filtering off through a cotton plug similar to that used in the treatment of carbon tetrachloride droplets, while the second metallic selenium can be removed by adding a small amount of carbon tetrachloride and shaking.

The results of application of the method are given in Table II. They show the quantitative recoveries of arsenic which was previously added to the original sample.

TABLE II

EXAMPLES OF APPLICATION

Description	Sample taken	As added	As found
Ground water from a well on the campus of Nagoya Univ.	5 l. 5 l.	 10 μg.	2.1 μg. 12.0 μg.
Sea water at Sugashima Is., Mie pref.	2 l. 2 l.	 10 μg.	3.3 μg. 13.6 μg.
Serpentine (Sugashima Is., Mie pref.)	1 g. 1 g.	 5 μg.	0.4 μg. 5.6 μg.
Bottom deposit of Aburagafuchi, a brackish lake, Aichi pref.	1 g. 1 g.	 5 μg.	7.7 μg. 12.5 μg.
York	4.6 g. 4.6 g.	 5 μg.	0.6 μg. 5.4 μg.

Application to Silicate and Biological Materials

Silicate Materials.—To 0.5–1 g. of powdered silicate material weighed in a nickel crucible, 0.5 g. of sodium hydroxide and 1 ml. of water are added and placed on a water bath. When completely dried out, 0.5 g. of sodium peroxide and 2 g. of fused sodium hydroxide are successively added and the crucible is quickly covered with a lid. A violent reaction occurs. When the reaction is over, the crucible is heated to dull-red for 0.5–1 hr. until decomposition is supposed to be complete. The melt is digested with 20 ml. of water and then neutralized with 9 ml. of sulfuric acid (1 : 1). Disregarding any separation of silica, the solution is acidified with 5 ml. of sulfuric acid and processed according to the prescribed procedure.

Biological Materials.—A suitable amount of a biological material is first decomposed in the digestion apparatus. Then the digest is processed to the prescribed procedure.

Results of application of the method to silicate and biological materials are also given in Table II.

Chemical Institute, Faculty of Science
Nagoya University, Nagoya

On the Transport Number for Ion-exchange Resin Membranes

By Yoshio ODA and Tadashi YAWATAYA

(Received February 24, 1956)

Introduction

The ionic permselectivity of ion-exchange resin membrane has been expressed quantitatively by means of a transport number defined as the fraction of current carried by either cations or anions through it. The transport number for a membrane is generally computed from the membrane potential measurement which arises at a membrane separating two solutions of different concentrations. In this case, the Nernst's equation is generally used for correlating the membrane potentials with the transport number.

$$n_+ = \frac{1}{2}\left(1 + \frac{E_{obs}}{E_{th}}\right) \quad (1)$$

$$E_{th} = \frac{RT}{nF} \ln \frac{a_2}{a_1} \quad (2)$$

n_+: transport number (*t. n.*) of cations

E_{obs}: observed value of membrane potential

E_{th}: calculated value of membrane potential by use of Eq. (2)

a_1, a_2: activities of the solutions separated by the membrane. R, T, n, and F have their usual significances.

If an ion-exchange membrane is subjected to an electric field in an electrolyte solution, movement of a definite amount of solvent occurs simultaneously with ion transference[1]. Since the Nernst's equation holds in the case where only ion transference is considered, a correction should be made for the transport number in Eq. (1). This is identical with the "Hittorf transport number", which is calculated from the changes in concentra-

1) Y. Oda and T. Yawataya, This Bulletin, 28, 263 (1955).

tion of solution after the passage of the current, without taking account of transport of solvent molecules, and consequently expressed in terms of ionic velocities relative to an imaginary plane moving with the same speed as the solvent.

The errors arising from neglecting the solvent transference were already remarked by A. J. Staverman[2], and G. Scatchard[3], but experimental proof has not yet been reported.

As for the case of ion-exchange resin membranes, the difference between the Hittorf- and true-transport number is comparatively large and plays a very important role for practical applications.

In the present report, the Hittorf- and true-transport numbers of the various cation-exchange resin membranes were determined in sodium chloride solutions and the differences between them were discussed in view of electro-osmotic water transfer.

Experimental

Membranes.—Strong acid cation-exchange resin membranes of sulfonated type, the thickness being about 0.5 and 1.0 mm., and the water contents ranging from 30 to 60%. Prior to the measurement, membranes were thoroughly equilibrated with the solutions to be used. When a membrane is required to be interposed between two solutions of different concentration, as is the case with the membrane potential measurement, it had been equilibrated with the more dilute solution of the two. In such a case at least thirty minutes were needed to attain a stationary state after setting the membrane in the cell.

Hittorf Transport Number.—The potential was measured for a cell shown in Fig. 1, consisting of two glass half cells, a sample membrane, and calomel electrodes. Temperature was regulated at 25±0.2°C.

Calomel electrode	Satd. KCl soln.	NaCl soln. (m_1)	Membrane	NaCl soln. (m_2)	Satd. KCl soln.	Calomel electrode

Fig. 1.

The membrane potential was obtained by making a correction for the liquid junction potential at the boundaries, KCl (satd.) NaCl (m_1) and NaCl (m_2) KCl (satd.). This correction amounted to several millivolts under the conditions prevailing in the present experiments. From the membrane potential thus measured, the Hittorf *t. n.* was computed by the Eq. (1).

Although it is desirable to correlate the *t. n.* with the concentration of a solution, the measurement above described has to be made for a membrane placed between two solutions of different concentration. In order to obtain the *t. n.* as a function of a single concentration, an interpolating method was employed as follows. At first, fixing the concentration of a solution in one side of the cell constant, which being a parameter, membrane potentials were measured employing solutions of various concentrations in another side. And, as shown in Fig. 2 the *t. n.* computed therefrom

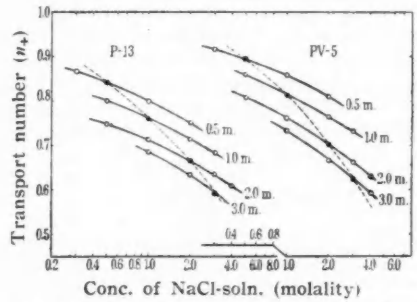

Fig. 2. Transport numbers for cation-exchange resin membranes, determined from membrane potential measurements.

were plotted on a diagram against the varied concentrations respectively for each parameter. Then the *t. n.* corresponding to a single concentration can be obtained by interpolating the curve to a point where the reading of the parameter and the abscissa coincides. In Fig. 2, these points are shown by black solid circles connected with a dotted line.

True Transport Number.—A cell made of methyl metacrylate resin was used (Fig. 3). The effective area of a membrane was 4.0 cm². A stirrer was provided in each compartment to keep the solutions as uniform as possible.

Prior to an experiment, the sodium chloride solution was filled in the cell to equilibrate the membrane with it. After the solution was taken out, the remaining solution on the cell wall was wiped out clean with filter paper. A weighed amount of the sodium chloride solution (W_S g.; NaCl: m_S mol.) of the same concentration as previously used, was put in the cell, and silver-silver chloride electrodes (weight of the cathode being W_E) were inserted. Then the circuit was closed, iodine coulometer being connected in series. After a certain amount of electricity (Q coulomb) passed, the solution in the cathode compartment and the cathode itself were taken out separately in dried weighing bottles and their weights were measured rapidly. Let the weight of cathode in wet state be W_E', and that of the solution W_S'. Next, the solution remaining on the cell wall and the membrane inside the cathode cell was blotted rapidly but cautiously with filter paper, and was titrated for chloride ion with silver nitrate standard solution (NaCl: m_S''). Sodium chloride in

2) A. J. Staverman, *Trans. Faraday Soc.*, **48**, 176 (1952).
3) G. Scatchard, *J. Am. Chem. Soc.*, **75**, 2883 (1955).

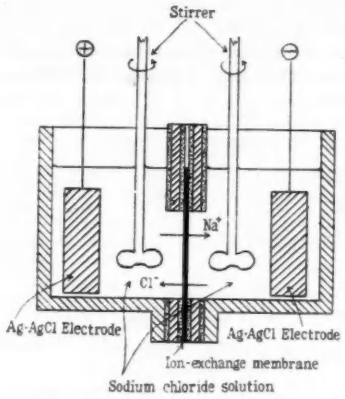

Fig. 3. Apparatus for measuring true transport number.

the main solution taken out from the cathode compartment (m_S') and that imbibed in the cathode material (m_E') were also determined by titration.

Then the material balance in the cathode cell is shown as follows.

NaCl increase $(\Delta m)=(m_S'+m_E'+m_S'')-m_S$

Total weight increase $(\Delta W)=(W_S'+W_E'+W_S'')-(W_S+W_E)$, where, $W_S''=W_S'\cdot\frac{m_S''}{m_S'}$.

From these, the true transport number and the amount of transferred water are computed by the next equations.

$$n_+'=\frac{\Delta m}{Q/F} \tag{3}$$

$$\beta_W=[\Delta W-\Delta m\times M_{Na}+(Q/F-\Delta m)\times M_{Cl}]/Q \tag{4}$$

M_{Na}, M_{Cl}: atomic weight of sodium-and chloride ion

The electrolysis was carried out for about thirty to sixty minutes with the current density of 5 A/dm². By preliminary experiments it was ascertained that the *t.n.* was scarcely dependent on current density over the range from 1 to 6 A/dm². Since the surface of the solution was inevitably exposed to the atmosphere during the experiment, the amount of water that might be lost by evaporation was not negligible. For this correction, the rate of water evaporation was measured for the same solution in an other vessel.

The β_W computed from the Eq. (4) is the amount of water transferred by one coulomb, i.e. the electro-osmotic water exclusive of solute. In the following part of this report, there will be discussed the relation between β_W and β, volume of transferred solution per unit coulomb, which was determined volumetrically in the previous report[1].

Water Content, Fixed Ion Concentration and the Donnan Absorption.—For the discussion on the transport numbers, measurements were made on water content, fixed ion concentration, along with the concentration of non-exchangeable ions absorbed in membrane due to the Donnan equilibrium, for each membrane in the similar manner to those reported by G. Manecke or W. Juda et al.[4,5].

Results

Transport Numbers.—In Figs. 4 and 5, are shown Hittorf *t.n.* (n_+) and true *t.n.* (n_+')

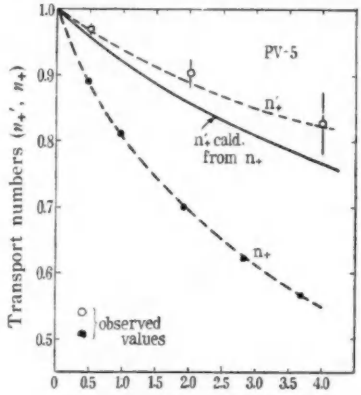

Conc. of outer NaCl-soln. (N)

Fig. 4. Transport numbers for cation-exchange resin membrane PV-5.

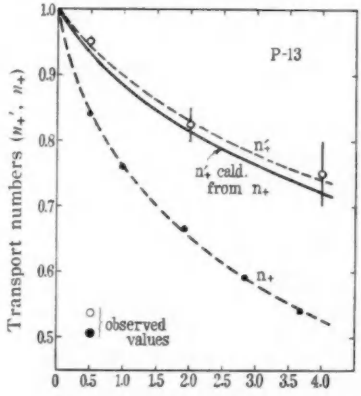

Conc. of outer NaCl-soln. (N)

Fig. 5. Transport numbers for cation-exchange resin membrane P-13.

determined by the procedures above described for two typical cation-exchange resin membranes against the concentration of outer solutions. Both *t.n.* show the similar tendency that they decrease with increase in outer concentration, but remarkable differences exist between their absolute values. True *t.n.*, the "dynamic transport number" so to speak, is much higher than Hittorf *t.n.* computed from nearly static thermodynamic membrane potentials.

4) G. Manecke, *Z. phys. Chem.* 201, 193 (1952).
5) W. Juda et al., *J. Am. Chem. Soc.*, 74, 3736 (1952).

Electro-osmotic Water Transference.—Measured values of β_W are plotted on Fig. 6 against the concentrations of outer solution. For the purpose of comparison, β are shown in Fig. 7.

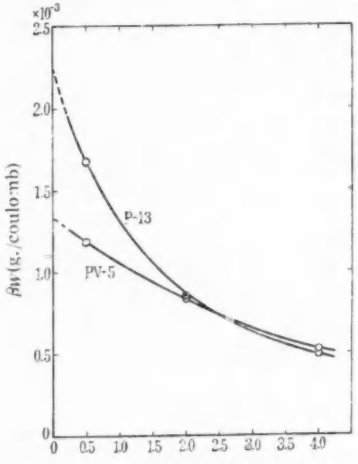

Fig. 6. Electro-osmotic water transference of cation-exchange resin membranes.

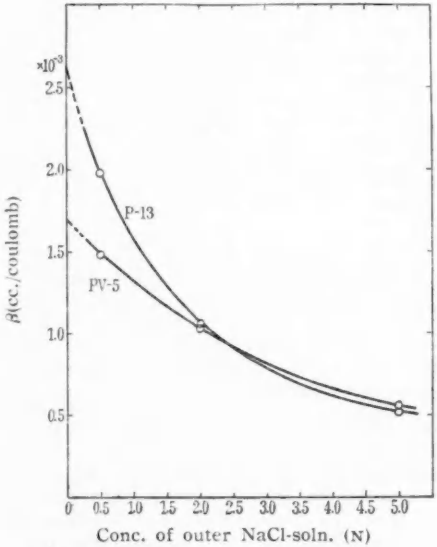

Fig. 7. Electro-osmosing solution transference of cation-exchange resin membranes.

When the concentration of the outer solution was raised from zero concentration upward, β_W and β, irrespective of membrane difference, tend to decrease rather sharply and converge to nearly constant values respectively.

Water Content, Fixed Ion Concentration and the Donnan Absorption.—These are shown in Figs. 8, 9 and 10. Here the Donnan

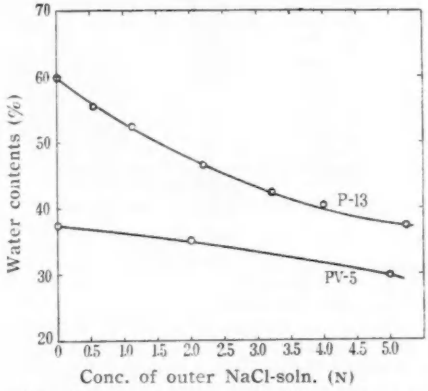

Fig. 8. Water contents of cation-exchange resin membranes.

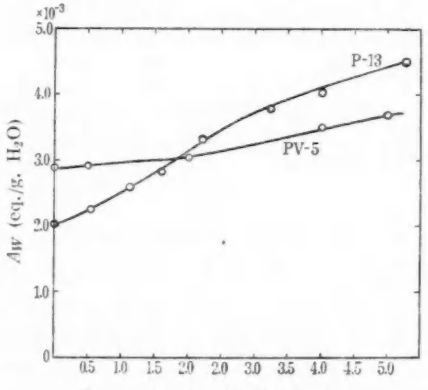

Fig. 9. Fixed ion concentration of cation-exchange resin membranes.

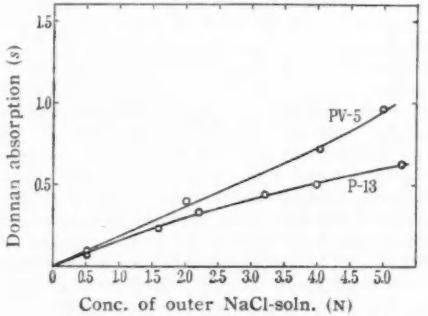

Fig. 10. Donnan absorption of cation-exchange resin membranes.

absorption (s) is expressed by the ratio of the concentration of absorbed chloride ion to that of fixed ion of the resin, both concentrations being computed in relation either to the weight of water taken up in the resin, or to the swollen volume of the resin.

$$s=[Cl^-]/[-SO_3^-]$$

Then, if the fixed ion concentration is expressed by A, which is the content of fixed ion per unit volume of swollen resin, $A(1+s)$ indicates the concentration of Na^+, and $A\cdot s$ that of Cl^-.

Discussion

Transport Numbers.—When a membrane is interposed between two solutions of different concentration, flow of materials takes place across it. Namely, solute molecules diffuse through the membrane from the more concentrated side to the dilute side, and at the same time solvent molecules in the reverse direction. As the membrane potential has to be measured under such a situation, the $t.n.$ derived therefrom may cause the erroneous result due to this material transference.

But, the error would be minimized by the application of the "interpolation method" as mentioned above. In fact, R. Schlögl[6] has shown that the $t.n.$ computed from membrane potential measurement* stands in good agreement with that derived from the rate of self-diffusion within a membrane, the latter being determined for the membrane placed between two solutions which are only differentiated with radioactive Na^{24} or Br^{82} on one side.

On the other hand, the water transport due to the current passage across the membrane is so large that its effect on the $t.n.$ can never be overlooked.

In order to consider the contribution of electro-osmosis to the passage of the current within a resin membrane, it will be assumed that ions are present in completely dissociated state in the resin. The assumption seems to be not so far from reality because of the strong acidic nature of the sulfonate type cation-exchange resin.

As G. Schmid has already reported[7], electric conduction within micro-porous membrane consists of electrolytic and convective conduction. If we denote the mobilities of cation and anion relative to the pore wall by u'_+ and u'_-, they are written as,

$$u'_+=u_+ + u_s,\quad u'_-=u_- - u_s \tag{6}$$

where u_+ and u_- are the mobilities relative to the solution, and u_s that of the solution.

In this way, ions seem to move in a similar manner to "a walking man on a running vehicle". In cation-exchange resin membranes, the velocity of cation is accelerated, that of anion retarded.

On this basis, the conductivity of a membrane, k', is derived as,

$$\begin{aligned} k' &= F[A(1+s)u'_+ + A\cdot s\cdot u'_-] \\ &= FA[(1+s)u_+ + s\cdot u_- + u_s]. \end{aligned} \tag{7}$$

On the other hand, the conductivity of a membrane, if without any electro-osmosis, is,

$$k=F\cdot A[(1+s)u_+ + s\cdot u_-]. \tag{8}$$

Therefore, the conductivity rise due to electro-osmosis is,

$$k'-k=F\cdot A\cdot u_s \tag{9}$$

On the basis of a similar concept, the transport numbers may be expressed as,

$$n'_+=\frac{(1+s)u'_+}{(1+s)u'_+ + su'_-} \tag{10}$$

$$n_+=\frac{(1+s)u_+}{(1+s)u_+ + su_-}. \tag{11}$$

Thus,

$$n'_+-n_+=(n_-+s)\frac{k'-k}{k'}. \tag{12}$$

Now, if we denote by β_E the volume of electro-osmosing solution under unit potential gradient applied to a membrane,

$$\beta_E=\beta\cdot k'=u_s S \tag{13}$$

where S is the total cross sectional area of pores of membrane resin. In this case, the spaces occupied by the hydration water of sulfonate group should be excluded from the pore volume, if it is considered as immobile even under electric field.

Hence, from Eqs. (9), (12) and (13),

$$\begin{aligned} n'_+-n_+ &= (n_-+s)\cdot FAu_s/k' \\ &= (n_-+s)\cdot(A/S)\cdot\beta\cdot F \\ &= (n_-+s)\cdot A_S\cdot\beta\cdot F \end{aligned} \tag{14}$$

where A_S is the content of fixed ion per unit volume of electro-osmosing solution, i.e. mobile solution in the resin.

In Eq. (14), the term $(n_-+s)\cdot A_S$ expresses the sodium chloride concentration of electro-osmosing solutions. This expression does eventually coincide with "strömende Konzentration"* by G. Schmid[8], which has been

6) R. Schlögl, *Z. Elektrochem.*, **57**, 199 (1953).

* He applied the interpolation method on the membrane potential vs. activity of outer solution curves.

7) G. Schmid, *Z. Elektrochem.*, **56**, 181 (1952).

* $C_s=(C_k-n_k\cdot A)=(C_A+n_A\cdot A)=[A(1+s)-n_k\cdot A]$
$=A(1+s-n_k)=A(n_-+s)$

G. Schmid used the notation A as the content of fixed ions per unit volume of solution within resin phase.

8) G. Schmid, *Z. Elektrochem.*, **56**, 35 (1952).

derived for the salt concentration of solution flowing out of a membrane when hydrostatic pressure is applied on one side.

Since it is difficult to determine A_S, a volumetric quantity, experimentally, one had better reform the expression (14) into Eq. (15) by use of gravimetric quantities,

$$n'_+ - n_+ = (n_- + s)A'_W \cdot \beta_W \cdot F \qquad (15)$$

where A'_W is the content of fixed ion per unit weight of the water contained in electro-osmosing solution. The transformation from Eq. (14) to Eq. (15) would be justified when it is considered that the term $A_S \cdot \beta \cdot F$ is a dimensionless quantity.

Here, let us examine the implication of A'_W in a little more detail. There are three kinds of water within ion-exchange resin, (1) hydration water of sulfonate ion, (2) that of free cations and anions, and (3) solvent water. The latter two are "mobile water"[1], and (1) is considered as immobile even under electric field. According to R. H. Stokes and R. A. Robinson[9], the former two have been called "bound water" and (3) "free water".

Basing on this concept, A'_W may be expressed in terms of (2)+(3), since the hydration water of sulfonate ion is considered to be almost indifferent to electro-osmosis. It follows, therefore, that the water which contributes to the "convective conduction" is the mobile water, i.e. (2)+(3).

For these reasons, in order to exactly compute the right-hand term of Eq. (15), it is necessary to know the distribution of water within the exchanger. But, since no satisfactory knowledge on the water distribution is available at present, Eq. (15) is approximately computed by substituting A_W for A'_W, the concentration of fixed ion in the total water within the resin.

In Figs. 4 and 5, the solid line shows the results of computation on n'_+ from observed values of n_+, A_W, β_W and s. The concordance of observed and computed values of n'_+ seems fairly good.

Since the water distribution in ion-exchanger, though neglected in the above treatment, seems very important to account for the nature of ion-exchange resin, it will be examined in more detail in the succeeding paper.

Electro-osmotic Transference of Water, β_W and β.—In the preceding paper the present authors reported on the electro-osmotic water transference through cation-exchange resin membranes. There, employing a volumetric procedure, observed data were expressed by β (cc./coulomb), volume of electro-osmotically transferred solution per unit coulomb.

During current passage, a solution containing excess sodium ion flows into a cathode cell across the membrane, and it is neutralized with chloride ion formed by the cathode reaction with the result that a certain amount of concentrated sodium chloride solution is added to the cathode solution. In this case, although the volume change occurs due to dilution, it may readily be seen that that is negligible for the sensitivity of the present electro-osmotic measurement. Also, the volume change due to the cathode reaction, $AgCl + e \longrightarrow Ag + Cl^-$, may be neglected.

Then, the relation between β_W and β is written as,

$$\beta = \frac{1}{d}(\beta_W + n'_+ \cdot M/F) \qquad (16)$$

where d is the density of the concentrated sodium chloride solution which is added to cathode cell due to electro-osmosis and electrode reaction combined, and M is molecular weight of NaCl.

A difficulty arises to know d, when the electro-osmosing solution is so concentrated in sodium ion that it, combined with chloride ion from cathode, is to form supersaturated solution. In such cases, the values of d were approximately calculated by use of the partial molal volume of sodium chloride at saturation.

In Fig. 11, the value of β calculated from β_W and n'_+ is shown by the solid line in com-

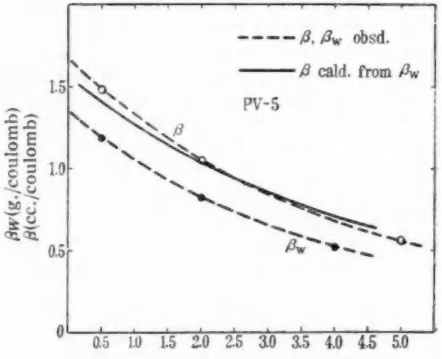

Fig. 11. Relation between β and β_W of a cation-exchange resin membrane.

9) *Annual Review of phys. Chem.*, 1954, p. 420.

parison with the experimentally observed values.

Conclusion

The cation transport numbers through cation-exchange resin membranes were determined experimentally by two methods, first, computation from membrane potential measurement, and second from analytical tracing of the concentration change which takes place, on current passage, in the solution separated by the membrane. The former, which is considered as "Hittorf transport number", is found to be far smaller than the latter, the true transport number. The difference between the two sorts of transport number was accounted for on the basis of the concept of convective conduction within the pores of ion-exchange resin.

The electro-osmotic water transference through the membrane was discussed on comparing the results of its volumetric- and gravimetric measurements.

The authors are grateful to Dr. M. Sekino, Dr. S. Uemura and Mr. M. Funaoka for their encouragement in this work.

Research Laboratory Asahi Glass Co. Ltd. Benten-cho Tsurumi-ku Yokohama

---

Flame Photometric Determination of Alkali and Alkaline Earth Elements in Waters. I. Sodium and Potassium

By Ken SUGAWARA, Tadashiro KOYAMA and Nobuko KAWASAKI

(Received March 20, 1956)

Introduction

It is our usual experience in a flame photometric determination of an element that when other elements and compounds co-exist they often interfere with that element, sometimes positively and other times negatively. The present investigation was commenced to develop sensitive methods for determining alkali and alkaline earth elements by making use of the positive interference phenomena toward one element in such a way that the determinable amount of that element is greatly lessened.

Thus the writers succeeded in establishing a more satisfactory method of determining sodium and potassium in which the minimum determinable amount is lowered to one-tenth for both these two elements in any comparison with the most sensitive methods hitherto proposed. A method for the simultaneous determination of calcium and strontium was also achieved in which the minimum determinable amount of strontium was lowered to one-tenth.

Determination of Sodium and Potassium

Preliminary Experiments.—Previous investigators have proved that the addition of methyl alcohol, ethyl alcohol or propyl alcohol to the solutions of gelatine and cane sugar increases the detectability of sodium and potassium in these solutions probably by intensifying the emissions of the two elements[1,2].

Based upon this information, and taking into consideration physical properties, the writers chose a number of alcohols, aldehydes and ketones. The same volume of one of these substances was added to a series of a solution containing sodium chloride or potassium chloride. Then the intensities of emissions of sodium and potassium in these solutions were determined with a Perkin-Elmer type flame photometer.

The results listed in Table I show that acetone, methyl ethyl ketone, propyl alcohol and ethyl alcohol are particularly effective and that the effectiveness decreases successively.

The next test was to compare the effectiveness by changing the added amount of these substances. It is evident from Fig. 1 that acetone is the most effective with the least amount added and that there is a particular range of concentration for each substance in which the effectiveness is the greatest.

The results also show that, as expected, the physical properties of the individual

1) J.W. Berry, D.G. Chppel and R.B. Barnes, *Ind. Eng. Chem., Anal. Ed.*, 18, 19 (1946).
2) R.D. Catom, Jr. and R.W. Bremer, *Anal. Chem.*, 26, 805 (1954).

TABLE I

EMISSION INTENSITIES OF Na AND K IN NaCl SOLUTIONS (0.05 ppm FOR Na) AND IN KCL SOLUTIONS (0.4 ppm FOR K) IN THE ADDITION OF OTHER SOLVENTS IN SINGLE OR IN COMBINATION. BRACKETED VALUES ARE FOR Na. INTENSITY OF THE ORIGINAL SOLUTION IS 8-9 FOR Na AND 6-7 FOR K.

	Acetone	Ethyl alcohol	Propyl alcohol	Methyl ethyl ketone	Butyl alcohol	Formal-dehyde	Acetic acid	Isooctyl phenol	Lauryl amine hydro-chloride
Acetone	13 (20)								
Ethyl alcohol	13	9 (10)							
Propyl alcohol	35	18	9 (15)						
Methyl ethyl ketone	35	7	27	10 (20)					
Butyl alcohol	10	20	16	15	—				
Formaldehyde	10	5	11	—	—	7 (9)			
Acetic acid	18	15	14	12	10	25	8 (9)		
Isooctyl phenol	20	15	13	14	12	10	20	10 (−)	
Lauryl amine hydrochloride	20	12	10	15	18	—	10	8	14 (16)

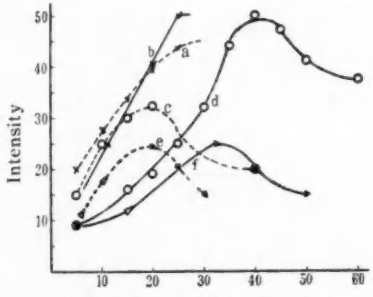

Fig. 1. Effectiveness of acetone, propyl alcohol and ethyl alcohol on the emissions of Na and K.

a Acetone Na b Acetone K
c Propyl alcohol Na d Propyl alcohol K
e Ethyl alcohol Na f Ethyl alcohol K

substances are closely connected with the intensifying effect.

As shown in Table II, acetone which has the greatest interference is the greatest in heat of combustion, small in heat of vaporization as well as in sulface tension, and exceedingly small in viscosity.

TABLE II

PHYSICAL CONSTANTS OF THE SOLVENTS RECOMMENDED

	Surface tension dyn./cm.	Viscosity	Heat of combustion cal./g.	Heat of vaporization cal./g.
Acetone	22.5	2.9×10^{-3}	7400	132.1
Methyl ethyl ketone	18.1	3.9×10^{-3}	5831	124.1
Propyl alcohol	23.8	17.2×10^{-3}	4821	159.0
Ethyl alcohol	22.3	12.0×10^{-3}	7090	224.6

The circumstances are interpreted as follows: Its smallness in surface tension and in viscosity makes it easy for a large amount to pass into the flame as finely atomized. The small heat of vaporization makes easy the vaporization whereby the emission intensity is increased. And its large heat of combustion contributes considerably to raising the flame temperature.

A further test was made on the effect produced by the binary combination of the most effective substances. By Table I it is shown that the best results are obtained in two combinations, one of the acetone-methyl ethyl ketone and the other of acetone-propyl alcohol.

The next test was carried out by changing the amounts of the components in the system of acetone-propyl alcohol. The results in Table III show that the intensity is halved

TABLE III

EMISSION INTENSITIES AT DIFFERENT COMPOSITIONS IN THE ACETONE-PROPYL ALCOHOL SYSTEM

Na ppm	K ppm	Acetone %	Pyropyl alcohol %	Intensity
0.05		20	40	40
0.05		10	40	32
0.05		20	30	20
0.05		0	0	8
	0.4	20	40	100
	0.4	10	40	65
	0.4	20	30	50
	0.4	0	0	6-7

for propyl alcohol when the amount is reduced by one-quarter, while a 35% drop in intensity is first seen for acetone when the amount drops to one-half. This finding points to the

fact that propyl alcohol is more essential to the intensifying action than acetone to the acetone-propyl alcohol system.

One point which must not be overlooked when acetone is applied to the flame photometry is that its relatively large amount might cause an incomplete combustion. As a matter of course the writers examined whether or not a part of the acetone in the acetone-propyl alcohol system could be replaced by ethyl alcohol. The examination shows that in order to keep the original degree of intensity, a large amount of ethyl alcohol is required (see Table IV).

TABLE IV

EMISSION INTENSITY FOR THE COMBINATION SYSTEM OF ACETON, PROPYL ALCOHOL AND ETHYL ALCOHOL

K ppm	Acetone %	Propyl alcohol %	Ethyl alcohol %	Intensity
0.4	15	40	20	100
0.4	15	40	25	100
0.4	0	0	0	6–7

Another approach to the positive interference is the addition of surface active agents. Two kinds of such agents, isooctyl phenol and lauryl amine hydrochloride, accidentally at hand, were tested.

The result (Table V) shows that at surface tension minimum, isooctyl phenol is more active than lauryl amine hydrochloride. However, the background of isooctyl phenol is considerably great. For this reason isooctyl phenol was rejected and the addition of lauryl amine hydrochloride at a concentration of 0.25% was recommended where it can give an intensifying effect with the least background comparable to isooctyl phenol.

TABLE V

EFFECTIVENESS OF SURFACE ACTIVE AGENTS

Agent	Concentration %	K ppm	Intensity	Background
Isooctyl phenol	0.5	0.4	32	20
Lauryl amine hydrochloride	0.25	0.4	16	1–2

The final experiment was to ascertain in the presence of this amount of lauryl amine hydrochloride to what extent the amount of propyl alcohol could be reduced with no heavy decrease in intensity. The answer was, as listed in Table VI, that the amount of propyl alcohol can be decreased to a concentration about 10% by an intensity decrease of 40% for sodium and 34% for potassium of the original values for the respective elements.

Hereupon arose another question: Can butyl alcohol replace at least in part the propyl alcohol? Primarily, butyl alcohol is more effective than propyl alcohol but because of its low solubility in water it has not been recommended by the writers. This situation was changed when lauryl amine hydrochloride was introduced. The introduction of this substance promises a great solubility of butyl alcohol in the system whereby the effectiveness of the system is considerably

TABLE VI

EFFECTIVENESS OF THE COMBINATION SYSTEM OF ACETONE, PROPYL ALCOHOL, BUTYL ALCOHOL, METHYL ETHYL KETONE AND LAURYL AMINE HYDROCHLORIDE

Na ppm	K ppm	Acetone %	Propyl alcohol %	Butyl alcohol %	Lauryl amine HCl %	Methyl ethyl ketone %	Intensity	gain
0.05		5	40	0	0.25	0	80	
0.05		5	30	0	0.25	0	70	
0.05		5	20	0	0.25	0	56	
0.05		5	10	0	0.25	0	48	
0.05		5	0	10	0.25	0	110	18:10
0.05		5	0	5	0.25	0	100	18:30
0.05		0	0	5	0.25	5	100	18: 8
0.05		0	0	0	0	0	10–11	18: 8
	0.4	5	40	0	0.25	0	80	
	0.4	5	30	0	0.25	0	75	
	0.4	5	20	0	0.25	0	60	
	0.4	5	10	0	0.25	0	55	
	0.2	5	0	10	0	0	60	
	0.2	5	0	5	0	0	45	
	0.4	5	0	5	0.25	0	100	20: 6
	0.4	0	0	5	0.25	5	100	20: 0
	0.4	0	0	0	0	0	6–7	

increased. The result of the examination actually evidenced that a system, 5% of acetone, 5% of butyl alcohol and 0.25% of lauryl amine hydrochloride, gives an intensity comparable to the highest value ever obtained among many combinations. Thus was established the system upon which the following analytical method of sodium and potassium determination is constructed.

Temperature Regulation in the Environment.—Table VII shows that the emission intensity drops by 17-23% when the thermometer, inserted in the space between the atomizer and the photometer cover, drops from 30°C to 10°C.

TABLE VII
INTENSITY OF EMISSION AND ENVIRONMENTAL TEMPERATURE

Na ppm	K ppm	10°C		30°C	
		Intensity	Gain	Intensity	Gain
20		100	12:68	100	11:25
10		100	13:27	100	13:47
2		100	17:28	100	17:68
0.1		100	21: 9	100	21:20
0.1		22±1	18:36	22±1	18:51
	2.0	60	21: 0	97	21: 0
	1.0	35	21: 0	50	21: 0
	0.4	12	21: 0	28	21: 0

Thus it is advisable in winter to heat the atomizer by placing an adjustable electric plate at the bottom whereby the constancy and consequently the accuracy of the meter reading are secured.

Stock Solutions.—Stock solutions are prepared different in concentration for sodium and potassium and different in their proportions. Here the maximum concentration is 10 ppm. for both sodium and potassium. The solutions are kept in polyethylene bottles with a cap.

Calibration Curves.—From the stock solutions several series of standard solutions are prepared as follorwed: To a suitable amount of the stock solution, 25 ml. of acetone, 25 ml. of butyl alcohol and 1.25 g. of lauryl amine hydrochloride are added. After shaking thoroughly, the solution is made up to 500 ml. Each series consists of solutions different in dilution but definite in the ratio Na/K. Then a calibration curve is made for each of these series (see Figs. 2 and 3).

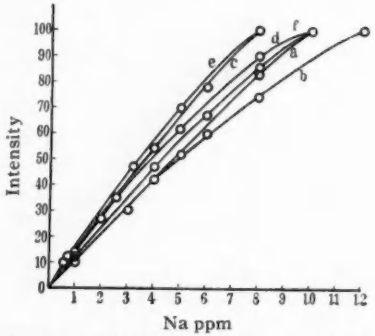

Fig. 2. Calibration curves for sodium at different Na/K. Ratios on the map are Na/K values for the individual curves.

a 1:1 b 3:1 c 4:1
d 5:1 e 8:1 f 10:1

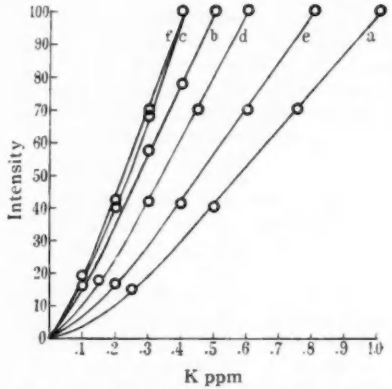

Fig. 3. Calibration curves for potassium at different Na/K. Ratios on the map are Na/K values for the individual curves.

a 1:1 b 3:1 c 4:1
d 5:1 e 8:1 f 10:1

Method of Processing Samples.—Originally the writers' attempt was to afford a method to meet the requirements for determining minor amounts of sodium and potassium as found in rain and other terrestrial waters in which both sodium and potassium are often found in quantities of 0.1 ppm or below. Thus the method of processing will be described so that it can easily be applied to such materials.

From a rain sample previously filtered through absorbent cotton and freed from all contamination such as soot and other dusts, an accurately measured amount (at least 40 ml.) is transferred to a 50 ml. measuring flask. To this are successively added 2.5 ml. of acetone 2.5 ml. of butyl alcohol and 2.5 ml. of a 5% aqueous solution of lauryl amine hydrochloride. After thorough shaking, the solution is made up to 50 ml., put to the flame photometer and the intensities of sodium and potassium are read.

Accuracy of Method.—The accuracy of the method was tested as follows: To rain water samples, the sodium and potassium contents of which were previously determined, a certain amount of sodium or potassium is added and sample content is determined.

As shown in Tabe VIII, for sodium the deviation of the observed value from the theoretical is from 0 to −8.6% with an average error −4.7%, while for potassium the deviation is from −1.9 to +7.5% with an average error +3.6%.

Interferences by Other Elements.—Among the interferences by other elements, those by

TABLE VIII

APPLICATION TO RAIN WATER AND ACCURACY OF DATA

Collected on	Fraction	Original content Na ppm	Original content K ppm	Added Na ppm	Added K ppm	Theoretical Na ppm	Theoretical K ppm	Found Na ppm	Found K ppm	Error in % Na	Error in % K
July 23, '55	1	0.35	0.10	0.30	0.30	0.65	0.40	0.60	0.43	−7.7	+7.5
	2	0.45	0.11	0.30	0.30	0.75	0.41	0.75	0.41	0.0	0.0
	3	0.65	0.18	0.30	0.30	0.95	0.48	0.90	0.49	−5.2	+2.1
	4	0.50	0.10	0.30	0.30	0.80	0.40	0.78	0.43	−2.5	+7.5
	5	0.30	0.10	0.30	0.30	0.60	0.40	0.55	0.42	−8.3	+5.0
	6	0.23	0.075	0.30	0.30	0.52	0.375	0.50	0.38	−5.8	+1.4
	7	0.28	0..63	0.30	0.30	0.58	0.363	0.53	0.38	−8.6	+2.8
	8	0.30	0.081	0.30	0.30	0.60	0.38	0.58	0.38	−3.3	+0.26
Aug. 27, '55	2	0.35	0.24	0.30	0.30	0.65	0.54	0.63	0.53	−3.1	−1.9
	3	0.24	0.11	0.30	0.30	0.54	0.44	0.51	0.45	−5.6	+9.1
	4	0.20	0.18	0.30	0.30	0.50	0.48	0.51	0.49	−2.0	+2.1
								Average		−4.7	+3.6

TABLE IX

APPLICATION TO ONTOLOGICAL MATERIAL

Lymph of Animal	Sample taken mg.	Na ppm	K ppm
Internal ear Guineapig	0.59	85.5×10^{3}	13.5×10^{4}
External ear Guineapig	0.31	13.7×10^{3}	14.5×10^{3}
Internal ear Corpse (Labyrinthin fluids)	0.96	1.99×10^{3}	7.99×10^{3}
External ear Calf	1.22	2.05×10^{3}	3.98×10^{3}
External ear Shark	0.02	37.5×10^{3}	11.2×10^{3}

calcium and magnesium are particularly notable. The presence of 20 ppm. of calcium causes an error −2% to sodium and −1% to potassium, wile 25 ppm of magnesium causes an error −2% to sodium and −1% to potassium. Consequently, the method can be directly applied to ordinary fresh waters in which the portions of calcium or magnesium to sodium or potassium are not large. Other elements in the ordinary fresh waters show no interference.

Chemical Institute, Faculty of Science
Nagoya University, Nagoya

Flame Photometric Determination of Alkali and Alkaline Earth Elements in Waters. II. Calcium and Strontium

By Ken SUGAWARA, Tadashiro KOYAMA and Nobuko KAWASAKI

(Received March 20, 1956)

Preliminary Experiments

It is known that sodium, potassium and calcium intensify the emission of strontium while strontium has no interference with calcium[1,2,3]. In making use of this fact the writers started to elaborate a method of simultaneous determination of calcium and strontium in a solution sufficiently free from sodium and potassium in which the boundary concentration of the determinable amount, at least for strontium, is considerably lowered.

As the first step in this investigation, the writers examined in vain the possible effectiveness of additional solvents, i.e. acetone, butyl alcohol and lauryl amine hydrochloride which have proved to be very effective for

1) O.N. Hinsvark, S.H. Wittwer and H.M. Sell, *Anal. Chem.*, 25, 320 (1953).
2) T.J. Chow and T.G. Thompson, *Anal. Chem.*, 27, 18 (1955).
3) T.J. Chow and T.G. Thompson, *Anal. Chem.*, 27, 910 (1955).

the determination of sodium and potassium as reported above.

On the contrary, we found quite unexpectedly great effectiveness in oxalic acid which is used as a precipitant for separating calcium and strontium from a solution containing sodium and potassium. As suggested by these findings, other substances belonging to the same category were tested with the result that among them formic acid, acetic acid and propionic acid are found to be particularly effective. (See Table I).

TABLE I
EFFECTIVENESS OF ORGANIC ACID ON STRONTIUM EMISSION

Agent	Added amount in volume %	Intensity
Formic acid	5.0	60
	10	46
Tartaric acid	0.5	60–70
	1.0	30–35
Propionic acid	5.0	25
	10	40

Further, a comparative study of these three substances at different concentrations showed that tartaric acid especially in a 0.5% solution is the most effective of all and finally a one % solution was recommended as the best because of its greater constancy in meter reading.

On the other hand, the dependence of the intensifying effectiveness of calcium toward strontium was explored on calcium concentration with the result that strontium emission was found to increase uniformly with calcium increase (see Fig. 1).

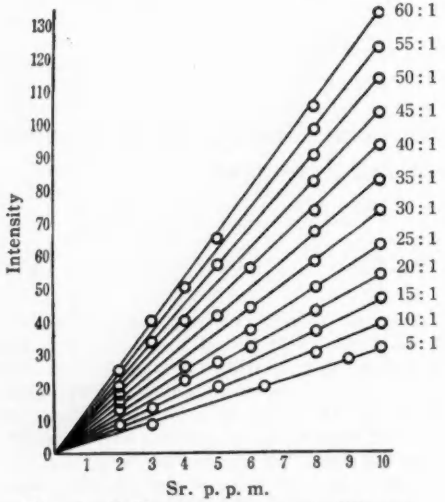

Fig. 1. Calibration curves at different Ca/Sr. Ratios on the map are Ca/Sr values for the individual curves.

Based upon these results the fundamentals of the anticipated procedure for the simultaneous determination of calcium and strontium were determined as follows: By using a precipitated mixture of oxalates of calcium and strontium with the addition of a suitable amount of tartaric acid, calcium is first determined and then after the addition of a quantity of calcium, (if necessary), the emission of strontium is determined.

Stock Solutions.—There are prepared stock solutions which contain 10% of tartaric acid, various amounts of chlorides of calcium and strontium in various proportions. Each solution is preserved in a polyethylene bottle with a cap.

Calibration Curves.—From stock solutions there are prepared several series of standard solutions as follows: A suitable amount of the stock solution is taken into a measuring flask. Suitable amounts of oxalic acid, tartaric acid and hydrochloric acid are added and the solution is made up to 500 ml. so that the final solution contains 10 ml. of hydrochloric acid (1 ; 1) and 5 g. of tartaric acid with a quantity of oxalic acid equivalent to the total of calcium and strontium. Each series of the standard solutions consists of members different in dilution but with a definite ratio Ca/Sr. For each series a calibration curve is constructed at a constant gain because of the fact that the emission of calcium itself is never influenced by the change in the amount of strontium (see Fig. 1).

Preparation of Samples.—For its lower concentration, rain water usually needs a previous concentration especially for strontium. Measured amounts, usually from 100 to 500 ml. for calcium and 1.5 to 2 liters for strontium, of the collected rain water which has passed through the pretreatment mentioned in Part I of the present paper are, if necessary, evaporated down to a volume of about 100 ml.

The next step is to prepare separate samples for determining calcium and strontium by using these condensed rain waters or any river or lake water.

To a measured amount of such a water, 2 ml. of hydrochloric acid (1 : 1), 20 ml. of a saturated solution of ammonium oxalate, 10 g. of urea and 2 drops of a methyl red solution are added successively. The solution is warmed on an electric plate until its color changes to orange-yellow.

After cooling at room temperature, the precipitate consisting of the oxalates of calcium and strontium is filtered off through a filter paper and washed five times with 10 ml. of an ammoniacal ammonium oxalate solution. With distilled water it is rinsed out into a beaker. After the addition of 2 ml. of hydrochloric acid (1 : 1), the contents of the beaker including the filter paper are warmed until thr precipitate completely dissolves. Then the solution is filtered. To the combined filtrate 2.5 ml. of a 20% tartaric acid solution is added.

TABLE II

APPLICATION TO THE SOLUTIONS WITH KNOWN AMOUNTS OF CALCIUM AND STRONTIUM

Theoretical		Observed		Error in ppm.		Error in %	
Ca ppm	Sr ppm	Ca ppm	Sr ppm	Ca	Sr	Ca	Sr
25	1	23.5	1.0	−1.5	0.0	−6.0	0.0
50	1	48.5	1.0	−1.5	0.0	−3.0	0.0
40	5	37.0	4.8	−3.0	−0.2	−7.5	−4.0
25	5	23.0	4.9	−2.0	−0.1	−8.0	−2.0
200	10	198.5	9.8	−2.0	−0.2	−1.0	−2.0
50	10	50.0	10.0	0.0	0.0	0.0	0.0
50	2	48.0	2.0	−2.0	0.0	−4.0	0.0
40	2	39.0	2.3	−1.0	+0.3	−2.5	+1.5
				Average		−4.0	−0.81

TABLE III

Collected on	Fraction	Sample content Ca ppm	Added Ca ppm	Theoretical Ca ppm	Found Ca ppm	Error in
July 23, '55	1	4.1	60	64.1	65.3	+1.9
	2	8.2	60	68.2	68.0	−0.29
	3	4.0	50	54.0	55.4	+2.6
	6	9.3	20	29.3	29.3	+1.7
Aug. 27, '55	2	3.5	40	43.5	42.3	−2.8
	3	7.0	40	47.0	46.0	−2.1
Sept. 7, '55	2	1.5	40	41.5	41.0	−1.2
				Average		−0.02

Collected on	Fraction	Sample content Sr ppm	Added Sr ppm	Found Sr ppm	Error in ppm	Error in %
July 23, '55	1	5.8	5	11.0	+0.2	+2
	2	4.9	5	10.0	+0.1	+1
	4	5.5	6	11.7	+0.2	+2
				Average		+2

Samples have previously been condensed down to one-sixtieth of the original volumes. Consequently, values for calcium and strontium are sixty-times greater than those in the original samples.

The solution is made up to 50 ml. and ready for flame photometry of calcium.

Samples for strontium determination are prepared as follows: To a measured amount of sample water, a suitable amount of calcium chloride solution, 2 ml. of hydrochloric acid (1 : 1), 20 ml. of a saturated ammonium oxalate solution, 10 g. of urea and 2 drops of a methyl red solution are added successively. Then the solution is processed as indicated for the samples for calcium determination.

Flame Photometry.—Calcium is determined first by reading the emission intensity at about 5600 Å. Then the strontium emission is read at 4607 Å. The strontium content can be determined from the reading of the strontium emission and total calcium, calcium determined plus calcium added.

Accuracy of the Method.—The accuracy of the present method was tested in two different ways: a) The method was applied to a number of solutions containing chlorides of calcium and strontium of known composition. b) To rain water samples, the calcium or strontium content of which was previously known, certain amounts of calcium and storontium chlorides of definite concentration were added and determination was conducted.

As listed in Tables II and III, in test (a), error is from 0.0 to −8.0% with an average −4.0% for calcium and from +1.5 to −4.0% with an average −0.81% for strontium, while in test (b) it is from +2.6 to −2.8% with an average −0.02% for calcium and from +1 to +2% with an average +1.5% for strontium.

Interferences by Other Elements.—As previously mentioned, magnesium interferes considerably with both calcium and strontium. This is why we precipitate calcium and strontium in the presence of urea.

The presence of this substance secures the complete separation of calcium and strontium from magnesium. This caution is particularly essential when the method is applied to sea water.

Chemical Institute, Faculty of Science
Nagoya University, Nagoya

*Notes on the Geochemistry of Germanium**

By Hiroshi ONISHI

(Received April 7, 1956)

To Goldschmidt and Peters[1] we owe most of the present knowledge of the geochemistry of germanium. A value of 7 ppm. for the abundance of germanium in the lithosphere was reported by Goldschmidt[2,3]. This value is based on the content of a composite of shales in which germanium was found to be enriched. Goldschmidt and Peters showed that germanium replaces silicon and forms GeO_4 tetrahedra. Wickman[4] pointed out that, on the whole, germanium is preferably substituted for silicon in the least-linked silicate tetrahedra. Harris[5] found that germanium is enriched relative to silicon, in olivines (isolated tetrahedra), and pyroxenes (silicate chains), but is impoverished in feldspars and quartz (silicate networks). This confirms Wickman's supposition. In view of this new fact, it appeared to the present author that Goldschmidt and Peters' earlier observation indicating that silicic rocks are richer than subsilicic rocks in germanium, should be reexamined. This would lead to a further study on the germanium content of common igneous rocks (compare Fleischer[6]). Fortunately a sensitive and accurate photometric method for determination of germanium has now been made available.

The more pertinent abundance data for germanium are summarized in Table I. Goldschmidt and Peters' values were obtained by the spectrographic method having a sensitivity limit of about 1 ppm. Ge. This limit is not considered very sensitive. The spectrographic method of Preuss[7] involves fractional distillation of 1-3 g. samples. Harris used the spectrochemical determination after chemical concentration. His method had a sensitivity limit of 0.1 ppm. and the accuracy of ±10%. The results of the Noddacks[8,9] were obtained by an unspecified method. In the paper of the geochemistry of rhenium[10], they gave the germanium content of various geomaterials including meteorites. However, those values are not shown in Table I.

TABLE I
SUMMARY OF LITERATURE DATA ON ABUNDANCE OF GERMANIUM

Material	Ge, ppm.	Author
Igneous Rocks		
Igneous rocks, average	1	Noddacks (1930)[8]
Granites, average	3.5	Goldschmidt and Peters (1933)[1]
Composite of 14 German granites	3	Preuss (1940)[7]
Pitchstones, 3 samples	1.5, 1.4, 1.4	Harris (1954)[5]
Hypersthene-augite-dacite-pumice, Japan	1.7	Harris (1954)[5]
Andesite, New Zealand	1.4	Harris (1954)[5]
Nephelin syenites, average	2	Goldschmidt and Peters (1933)[1]
Basic plagioclase rocks, average	2	Goldschmidt and Peters (1933)[1]
Composite of 11 German gabbros	2	Preuss (1940)[7]
Greisen, average	35	Goldschmidt and Peters (1933)[1]
Sedimentary Rocks		
36 Shales, average	7	Goldschmidt and Peters (1933)[1]
Composite of 36 German shales	7	Preuss (1940)[7]
Red clay, Challenger Exp., Station 353	3.5	Goldschmidt and Peters (1933)[1]
Composite of 23 German sandstones	2	Preuss (1940)[7]
Meteorites		
Nickel-iron, average	500	Goldschmidt and Peters (1933)[1]
Troilite, average	40	Goldschmidt and Peters (1933)[1]
Meteorites, average	79	Goldschmidt (1937)[2]
Meteorites, average	55	Goldschmidt (1954)[3]
Chondrites, average	31	Noddacks (1934)[9]

* Presented at the 9th Annual Meeting of the Chemical Society of Japan in April, 1956.

1) V.M. Goldschmidt and C. Peters, *Nachr. Ges. Wis. Göttingen, Math.-physik. Kl.* IV, 1933, 141.

2) V.M. Goldschmidt, *Skr. Norske Videnskaps-Akad. Oslo, I. Mat.-naturv. Kl.*, No. 4. Geochemische Verteilungsgesetze der Elemente, IX (1937).

3) V. M. Goldschmidt, ed. by A. Muir, "Geochemistry", Oxford Univ. Press, London (1954), p. 379.

4) F. Wickman, *Geol. Foren. Stockh. Förh.*, 65, 371 (1943).

5) P.G. Harris, *Geochim. et Cosmochim. Acta*, 5, 185 (1954).

6) M. Fleischer, *Geol. Soc. Amer. Sp. Paper*, No. 62, 145 (1955).

7) E. Preuss, *Z. angew. Mineral.*, 3, 8 (1940).

8) I. Noddack and W. Noddack, *Naturw.*, 18, 757 (1930).

9) I. Noddack and W. Noddack, *Svensk. Kem. Tid.*, 46, 173 (1934).

10) I. Noddack and W. Noddack, *Z. physik. Chem.*, A154, 207 (1931).

Goldschmidt and Peters[11] found a strong enrichment of germanium in coals. Due to the growing importance of this element in the electrical industry, a few extensive studies on the occurrence of germanium in American[12] and Japanese coals[13] have recently been made. The germanium contents of coals are variable, ranging from a few parts per million to as much as several per cent in the ashes. It appears that there is a regional variation in the abundance of germanium. Occurrence of germanium in ore-minerals has been studied by Kimura and some other workers[14,15,16,17].

The present paper supplies data on the germanium content of the common igneous and sedimentary rocks, and of chondrites.

Analytical Method

For determination of germanium in silicate rocks, the photometric procedure described by Schneider and Sandell[18] was adopted with minor modifications. The method consists in decomposition of a 0.5 g. sample with sulfuric-nitric-hydrofluoric acid, extraction of germanium tetrachloride from 9 M hydrochloric acid solution of the residue, transfer of germanium to aqueous solution by shaking the carbon tetrachloride with water, and final photometric determination with phenylfluorone. Instead of gum arabic to disperse germanium-phenylfluorone complex, aqueous polyvinyl alcohol solution[19] was used. Absorbance measurements were made with a Hirama photoelectric colorimeter (517 mμ filter) in a 1 cm. cell. Recoveries of germanium were slightly low, and a correction of 10% was made. For 1 to 2 ppm. Ge the error should be within 20 to 10%.

Shale composites (0.4 g. each) were heated in an oven at 550°C[20] for about one hour to destory organic matter. The residue was then treated with sulfuric-nitric-hydrofluoric acid. To ensure the validity of this method, 3.0 μg. of Ge and 1 mg. of sodium chloride were added to a 0.50 g. shale sample (1.0 ppm. Ge) containing a considerable amount of organic matter, and after carrying out the above procedure, duplicate values of 7.8 and 7.8 ppm. Ge were obtained.

For determination of total germanium in chondrites, the sample (0.25 g.) was first treated with nitric and sulfuric acid and the solution was evaporated to slight fumes. The residue was treated with hydrofluoric acid and germanium extracted with carbon tetrachloride after elimination of hydrofluoric acid, followed by photometric determination.

Discussion

Igneous Rocks.—Table II–VI list the germanium content of igneous rocks arranged according to rock class. Silica contents of some silicic rocks are based on Shibata, Okada, and Hara's analyses[21]. A summary of igneous averages is given in Table VII. The frequency distribution of germanium in silicic, mafic, and ultramafic rocks is shown in Fig. 1.

TABLE II
GERMANIUM IN RHYOLITES AND GRANITIC ROCKS

	SiO_2, %	Ge ppm.
Rhyolites		
Rhyolite, composite of 12 beach pebbles, 5 miles east of Grand Marais, Minn.		1.0
Rhyolite, White Pine, Nevada		1.3
Granitic Rocks		
Japan		
Quartz porphyry, Hatasa, Okumyo-mura, Gifu Prefecture		1.2
Quartz porphyry, Hatasa, Okumyo-mura, Gifu Pref.		0.9
Quartz porphyry, Hatasa, Okumyo-mura, Gifu Pref.		1.0
Two mica-granite, Ouchi, Ishikawa-machi, Fukushima Pref.	73.89	1.3
Granite, pink, Fusamata, Kawamata-machi, Fukushima Pref.	71.29	1.2
Granite, Ono-shinmachi, Fukushima Pref.		1.0
Granite, Soma-gun, Fukushima Pref.		1.4
Granite, Soma-gun, Fukushima Pref.		1.5
Granite, Tanakura-machi, Fukushima Pref.		1.0
Granite, Tanakura-machi, Fukushima Pref.		1.3
Granite, Higashishirakawa-gun, Fukushima Pref.		1.1
Two mica-granite, Yamamoto, Nanae-mura, Ibaraki Pref.	72.82	1.3, 1.3
Two mica-granite, Hongo, Sanso-mura, Ibaraki Pref.	72.30	1.4

11) V.M. Goldschmidt and C. Peters, *Nachr. Ges. Wis. Göttingen, Math.-physik. Kl.* IV, 1933, 371.
12) T. Stadnichenko, K.J. Murata, P. Zubovic and E.L. Hufschmidt, *U.S. Geol. Survey Circ.*, 272 (1953). A considerably extensive bibliography is found there.
13) M. Inagaki, *J. Chem. Soc. Japan* (*Pure Chem. Sect.*) **74**, 19 (1953).
14) K. Kimura, T. Nakamura and T. Kushibe, ibid., 52, 55 (1931).
15) K. Kimura and Y. Koyama, ibid., 57, 1190 (1936).
16) K. Kimura, O. Nagashima, K. Saito, M. Shima and S. Nakai, ibid., 73, 589 (1952).
17) E.H. Strickland, *Analyst*. 80, 548 (1955).
18) W.A. Schneider, Jr. and E.B. Sandell, *Microchim. Acta*, 1954, 263.
19) Y. Oka and T. Kanno, *J. Chem. Soc. Japan* (*Pure Chem. Sect.*) 76, 874 (1955).
20) Cf. H. Almond, H.E. Crowe and C.E. Thompson, *U.S. Geol. Survey Bull.*, 1036-B (1955).
21) H. Shibata, S. Okada and K. Hara, *Sci. Repts. Tokyo Kyoiku Daigaku*, Sect. C. 3, No. 22, 141-172 (1954).

	SiO_2, %	Ge, ppm.
Two mica-granite, Mito, Higashinaka-mura, Ibaraki Pref.	73.05	1.4
Two mica-granite, Kitanaka-yama, Nishiyamauchi-mura, Ibaraki Pref.	72.32	1.4
Biotite granite, Higashiiida, Amabiki-mura, Ibaraki Pref.	71.66	1.3
Biotite granite, Ogoto, Kita-yamauchi-mura, Ibaraki Pref.	73.03	1.6
Hornblende biotite granite, Ashio-machi, Tochigi Pref.	67.68	1.1
Granite, Hotokezakikannon, Omachi-shi, Nagano Pref.	75.79	1.2
Hornblende biotite granite, Akazawa, Agematsu-machi, Nagano Pref.	71.27	1.2
Hornblende biotite granite, Haizawa, Agematsu-machi, Nagano Pref.	69.81	1.4
Granite, Kariyasutoge, Oyama-mura, Toyama Pref.	74.52	1.3
Granite, Shomyogawa, Tate-yama, Toyama Pref.	65.08	1.2
Gneissic granite, Mizutani, Tateyama-mura, Toyama Pref.	69.84	0.7
Granodiorite, Tamanoyu, Ono-mura, Fukushima Pref.	62.86	1.2
Granodiorite, Ono-shinmachi, Fukushima Pref.		1.4
Granodiorite, Ono-shinmachi, Fukushima Pref.		1.4
Granodiorite, Ono-shinmachi, Fukushima Pref.		1.4
Granodiorite, Tanakura-machi, Fukushima Pref.		1.8
Granodiorite, Soma-gun, Fukushima Pref.		1.2
Granodiorite, Higashishira-kawa-gun, Fukushima Pref.		1.2
Granodiorite, Higashishira-kawa-gun, Fukushima Pref.		1.2
Granodiorite, Ishikawa-machi, Fukushima Pref.		1.4
Granodiorite, Senzai, Yoshi-hama-mura, Iwate Pref.	66.72	1.6
Granodiorite, Yokoishi, Yoshi-hama-mura, Iwate Pref.	65.18	1.0
Average		1.3
U.S.		
Granite, red, Lower Falls, Snake River, Kanabec Co., Minn.		1.4
Granite, grey, coarse-grained, Benton Co., Minn.		0.9
Granite, red, Stearns Co., Minn.		1.5
Hornblende granite, Freed-hem, Minn.		1.1
Quartz monzonite, Warman, Minn.		1.0
Granite, near Pierz, Minn		1.0
Hornblende granite, Rockport, Mass.		1.8
Granite (standard G-1), Westerly, R.I.		0.9, 1.0
Average		1.2
Average of all		1.3

TABLE III

GERMANIUM IN INTERMEDIATE ROCKS

	SiO_2, %	Ge, ppm.
Japan		
Quartz diorite, Rajotoge, Yoshihama-mura, Iwate Pref.	61.94	1.6
Quartz diorite, Namiita, Okirai-mura, Iwate Pref.	55.96	1.4
Quartz diorite, composite of 7 samples, Miho, Yamakita-machi, Kanagawa Pref.		1.3
Diorite, Soma-gun, Fukushima Pref.		1.6
Diorite, Soma-gun, Fukushima Pref.		1.7
Diorite, Soma-gun, Fukushima Pref.		1.6
Diorite, Tanakura-machi, Fukushima Pref.		1.6
Diorite, Ono-shinmachi, Fukushima Pref.		1.2, 1.4
Diorite, Higashishirakawa-gun, Fukushima Pref.		1.6
Biotite-hornblende gabbro diorite, Kamioka-machi, Gifu Pref.		1.3
Average		1.5
U.S.		
Porphyritic syenite, Wausau, Wis.		2.0
Hornblende tonalite, medium texture, Freedhem, Minn.		0.9
Average of all		1.5

TABLE IV

GERMANIUM IN BASALTS AND DIABASES

	Ge, ppm.
Japan	
Basalt, Ajiro-machi, Shizuoka Prefecture	1.6
Basalt, Ajiro-machi, Shizuoka Pref.	1.7
Basalt (1951 lava) Miharayama, Oshima Volcano, Izu	1.7
Basalt, Tateyama, Toyama Pref.	1.0
Basalt, Tateyama, Toyama Pref.	1.3
Average	1.5

	Ge, ppm.
Localities outside Japan	
Diabase, Grand Marais, Minn.	1.4*
Basalt and diabase, composite of 4 samples, Minn.	1.2
Diabase (standard W-1), Fairfax Co., Va.	1.6, 1.6
Basalt, Columbia River (Nat. Bur. Standards sample no. 4978)	1.2
Triassic diabase (Nat. Bur. Standards sample no. 4984)	1.3
Trap, Deccan (Nat. Bur. Standards sample no. 4985)	1.4
Diabase porphyry, Mt. Etna, Sicily	1.1
Average	1.3
Average of all	1.3

* Triplicate values of 1.4, 1.4, and 1.4_5 have independently been obtained by El Wardani[33].

TABLE V

GERMANIUM IN GABBROS

	Ge, ppm.
Japan	
Gabbro, Higashishirakawa-gun, Fukushima Prefecture	1.3
Gabbro, Higashishirakawa-gun, Fukushima Pref.	0.9
Gabbro, Higashishirakawa-gun, Fukushima Pref.	1.3
Gabbro, Tanakura-machi, Fukushima Pref.	1.3
Gabbro, Miharu-machi, Fukushima Pref.	1.0
Gabbro, Miharu-machi, Fukushima Pref.	1.7
Gabbro, Soma-gun, Fukushima Pref.	1.4
Gabbro, Soma-gun, Fukushima Pref.	1.4
Olivine gabbro, Kamioka-machi, Gifu Pref.	0.9
Gabbro, olivine-bearing? Kamioka-machi, Gifu Pref.	0.9
Gabbro, olivine-free, Kamioka-machi, Gifu Pref.	0.8
Microgabbro, Kamioka-machi, Gifu Pref.	1.3
Average	1.2
Localities outside Japan	
Gabbro, Duluth, Minn., above cement plant	0.8
Gabbro, Duluth, Minn.	1.3
Gabbro, composite of 5 samples, Minn.	1.2
Olivine gabbro, Cripple Creek, Colo.	1.3
Hornblende gabbro, near Shelby, N. Car.	1.8
Hypersthene gabbro (Norite), near Sudbury, Ontario	1.1
Weighted average excluding the first two samples	1.3
Average of all	1.2

TABLE VI

GERMANIUM IN ULTRAMAFIC ROCKS

	Ge, ppm.
Japan	
Peridotite, Horoman, Hidaka, Hokkaido	0.9
Peridotite, Horoman, Hidaka, Hokkaido	1.0
Peridotite, Horoman, Hidaka, Hokkaido	0.8
Peridotite, Miharu-machi, Fukushima Prefecture	0.8
Peridotite, Ogawa-machi, Saitama Pref.	1.1
Cortlandite, Miharu-machi, Fukushima Pref.	1.6
Average	1.0
Localities outside Japan	
Dunite, Balsam, N. Car.	0.7
Dunite (Nat. Bur. Standards sample no. 4975)	1.0
Average	0.9
Average of all	1.0

TABLE VII

IGNEOUS AVERAGES

Rock (number of samples)	Range	Avg. Ge, ppm.
Granitic rocks (43)	0.7–1.8	1.3
Japanese (35)	0.7–1.8	1.3
U.S.A. (8)	0.9–1.8	1.2
Intermediate rocks (12)	0.9–2.0	1.5
Japanese (10)	1.3–1.7	1.5
Basalts and diabases (15)	1.0–1.7	1.3
Japanese (5)	1.0–1.7	1.5
Other localities (10)	1.1–1.6	1.3
Gabbros (20)	0.8–1.8	1.2
Japanese (12)	0.8–1.7	1.2
Other localities (8)	0.8–1.8	1.3
Ultramafic rocks (8)	0.7–1.6	1.0

The amounts and the distribution patterns are much the same for granitic rocks, basalts and diabases, and gabbros. The granitic average (1.3 ppm. Ge) does not differ from the basaltic and gabbroic averages (1.3 and 1.2 ppm.). This is in contrast with the finding of Goldschmidt and Peters showing a larger concentration of germanium in granitic rocks (3.5 ppm.) than plagioclase rocks (2 ppm.).

The average germanium content of the lithosphere probably lies in the range 1–2 ppm., and we may give the most reasonable figure as 1.5 ± 0.5 ppm. Ge. Although the samples studied were mostly from Japan, the same distribution patterns and a small dispersion in the germanium contents are observed for both Japanese and some other samples. Thus, for example, among the granitic and gabbroic rocks analyzed, there are a good number of samples from Fukushima Prefecture or Abu-

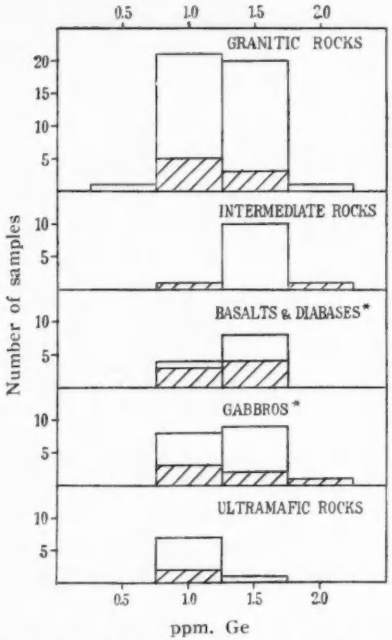

Fig. 1. Frequency distribution of germanium in igneous rocks.

▨ Outside Japan

* Minnesota composite taken as one sample

kuma Plateau. The average of 6 granites from this area is 1.2 ppm. compared to 1.2 ppm. as the average of 8 American granitic rocks. Nine granodiorites from Fukushima Prefecture gave an average of 1.2 ppm. Among 12 Japanese gabbro samples analyzed, 8 were from the same prefecture and an average of 1.3 ppm. is obtained for the latter samples. This value very favorably compares to the weighted average of 1.3 ppm. for 8 American and Canadian gabbros. Such an uniform distribution of germanium in igneous rocks (also compare Fig. 1) is the very basis of the new estimate of the terrestrial abundance of this element. Analysis of a larger number of samples from well-scattered areas of the globe is naturally desirable to get more exact averages. This will also serve as an inter-laboratory test of analyses.

The new igneous values are consistently lower than those of Goldschmidt and Peters and of Preuss. The reason for this discrepancy is not entirely evident: difference in the standardization could explain it to some extent, and some difference could be attributed to a lower limit of sensitivity of the spectrographic method. For the reason that will be discussed on **Sedimentory Rocks,** a possibility of regional variation may not be so great as one would suspect. As for intermediate rocks, two values obtained by Harris, i. e., 1.7 and 1.4 ppm., are just in the right range of the germanium content of this class of rocks obtained by the present author. Values for three pitchstones reported by Harris, i. e., 1.5, 1.4, and 1.4 ppm. and for rhyolites by the present author (Table II), seem to indicate that silicic volcanic rocks are not particularly high in germanium. This is opposite to the behavior of arsenic which shows a higher arsenic content in silicic volcanic rocks[22].

Goldschmidt's estimate in 1937[2] was based on the results of 12 igneous rocks and 13 sedimentary rocks, but several of the samples were composites. He found an average of 4 ppm. for igneous and 7 ppm. for sedimentary rocks but he preferred the latter for some reason as the abundance of germanium in the lithosphere. Recently Fleischer[5] stated that the Noddacks value for igneous rocks (1 ppm.) would probably be closer to the truth. He did not, however, mention the reason why he preferred Noddacks to Goldschmidt in the germanium abundance. The present data happen to confirm Fleischer's supposition.

Logarithms of the atomic abundances, expressed as parts per million atomic weight, of elements of atomic numbers 29 to 35 and 47 to 53 in igneous rocks are plotted in Fig. 2. The value for tellurium is quite uncertain. The data for selenium, silver, and iodine are not definitely established.

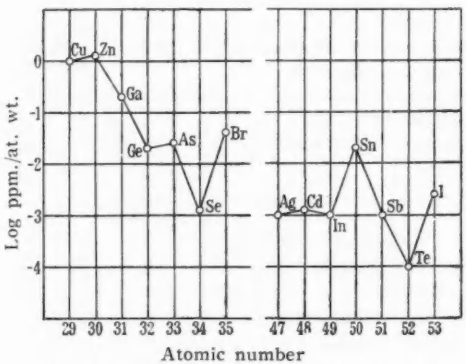

Fig. 2. Log of the atomic abundance, expressed as parts per million/atomic weight, of elements 29–35 and 47–53 in igneous rocks.

The average of 1.5 ppm. of germanium for igneous rocks arrived at above makes the

22) H. Onishi and E.B. Sandell, *Geochim. et Cosmochim. Acta*, 7, 1 (1955).

element definitely less abundant than gallium (15 ppm.), but comparable to arsenic (2 ppm.) in the upper lithosphere. The terrestrial abundances of germanium and tin (2–3 ppm.[23]) are much the same.

As already mentioned in the introductory part of this paper, germanium (using Ahrens' 1952 values for ionic radii[24], Ge^{4+} 0.53 Å) replaces silicon (0.42 Å). The valency of germanium in igneous rocks and magmas is usually quadrivalent, although, according to Ahrens[25], divalent germanium may apparently be found in some sulfide minerals that were formed at low oxidation potentials. Goldsmith[26] has synthesized and determined some of the crystal-chemical properties of Ge^{4+} substituted feldspars. Harris[5] studied the distribution of germanium among coexisting phases of partly glassy rocks such as pitchstone and andesite. Although his findings may not be applied to minerals formed at different stages of the crystallization of the different parent magmas, they deserve careful attention. His results showed that feldspar usually contained ~1 ppm. Ge, whereas olivines and pyroxenes 2–4 ppm. Thus a greater enrichment of germanium relative to silicon, takes place in the latter two minerals. Quartz may contain a fraction of a part per million of germanium, as one would infer from the presence of germanium in cherts and novaculites (0 to 3.0; average 0.4 ppm.)[27]. Also a few parts per million of germanium may be found in sandstones (Table VIII). The feldspar of igneous rocks probably accounts for one-half or more of the total germanium. However, the contribution of olivines and pyroxenes is also considerable, and this is probably the reason that germanium does not show any marked enrichment in a particular class of igneous rocks as shown by the present work.

For granitic rocks whose content of silica had been determined, no relation between germanium and silica was apparent.

In Fig. 3 the germanium contents of some igneous rocks are plotted against arsenic. The substitution of arsenic for silicon has already been indicated. As germanium behaves in the same way, a correlation between the two elements is not unexpected. A general tendency for germanium to rise with arsenic seems to exist, and it may be concluded that the process increasing the arsenic

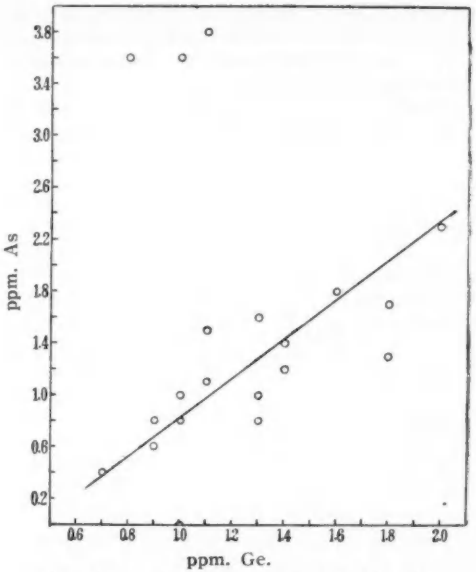

Fig. 3. Germanium as a function of arsenic in igneous rocks.

content of magmas also tends to increase the germanium content. Both germanium and arsenic are known to concentrate in the end stages of magmatic differentiation.

Replacement of iron (Fe^{3+} 0.64 Å) by germanium appears very probable since 1–3 ppm. Ge was found in magnetites[5]. The ionic radius of Al^{3+} (0.51 Å) suggests the possible substitution of germanium for aluminum. If substitutional disorder (Si–Al) in aluminosilicate is proved, this substitution of germanium for aluminum becomes a good possibility. This is, however, a mere speculation

TABLE VIII

GERMANIUM IN SEDIMENTARY ROCKS

	Ge, ppm.
Graywacke, Hatasa, Okumyo-mura, Gifu Prefecture	0.9, 0.9
Graywacke, Hatta, Hokuse-machi, Mie Prefecture	3.1, 3.5
Sandstone, Mitani-mura, Shiga Pref.	0.8, 0.8
Sandstone, Mitani-mura, Shiga Pref.	1.6, 1.5
Shale, Mitani-mura, Shiga Pref.	1.6, 1.6
Shale, Hatta, Hokuse-machi, Mie Pref.	1.7, 1.6
Shale, Hatta, Hokuse-machi, Mie Pref.	1.5, 1.4
Shale, Hatta, Hokuse-machi, Mie Pref.	1.6, 1.8
Composite of 14 Japanese Paleozoic shales (Minami)	1.6
Composite of 10 Japanese Mesozoic shales (Minami)	1.8
Composite of 36 European Paleozoic shales (Noll)	2.2

23) H. Onishi and E.B. Sandell, *Geochim. et Cosmochim. Acta*, To be published.
24) L.H. Ahrens, ibid., 2, 155 (1952).
25) L.H. Ahrens, ibid., 3, 1 (1953).
26) J.R. Goldsmith, *J. Geol.*, 58, 518 (1950).
27) J.A. Maxwell, Ph. D. Thesis, Univ. of Minnesota (1953).

unless a larger number of analyses of rock-forming minerals have been carried out and more pertinent information on the substitution has been obtained.

Sedimentary Rocks.—Tables VIII and IX list germanium values for sedimentary materials.

TABLE IX
GERMANIUM IN DEEP-SEA DEPOSITS

	Location		Depth, m	
Composite of red clays, Pacific Ocean	30°28.0′N	135°47.0′E	4363	Ge, ppm.
	15°10.0′	154°34.5′	5219	
	31°33.5′	136°20.5′	4096	1.6,
	13°39.5′	158°49.0′	5794	1.6*
Composite of red clays, Pacific Ocean	5°13.0′N	140°40.0′E	4884	
	9°25.5′	126°40.5′	5844	1.4,
	6°47.0′	139°27.0′	4293	1.6*
	6°43.0′	141°27.5′	4743	

* Most of the sodium chloride removed with water before hydrofluoric acid treatment.

The average of 4 shales, of which 3 are from Mie Prefecture and 1 from Shiga Prefecture, is 1.6 ppm. This figure is in good agreement with the weighted average of the two composites prepared by Minami[28] to represent 24 Japanese shales (1.7 ppm.). The composite of 36 European shales prepared by Noll[29] contained 2.2 ppm. The weighted average of the three composites above, based on 60 European and Japanese shales is 2.0 ppm. Here attention should be called to a difference in the results obtained by the previous workers and the present author. Goldschmidt and Peters[1], and Preuss[7] did not describe in detail the shale composites analyzed, but it appears that all three of the samples are the same. As shown in Table I, Goldschmidt and Peters reported 7 ppm. Ge or 0.001% GeO_2. Judging from the description of the analytical procedure they used, it is the impression of the present author that their value is rather approximate; the accuracy may well be 50% or more. However, Preuss' value of 7 ppm. Ge for 36 German shales is claimed to be obtained by a quantitative intensity measurement of the spectrogram. He mentions that the average error of ±50% was obtained for 10 determinations of germanium (as well as of other rare elements) in a shale sample. Considering this, the Preuss' value could be regarded as 7±4 ppm. or 3–11 ppm. Ge. In the present work, the procedure for shales was studied carefully, and, as mentioned in the *Analytical Method*, the recoveries were satisfactory. So the present figure of 2.2 ppm. could well be ±0.4 or 1.8–2.6 ppm. The agreement with Preuss' value is not very satisfactory, and the cause for this discrepancy may be sought elsewhere.

If we adopt the value of 7 ppm. Ge for European shale composite, the result is that it indicates that an extraordinary enrichment of germanium occurred in this sample (compare the data for Japanese shales and oceanic red clays). Of course it may be pointed out that too few shales have been examined in the present work to enable a satisfactory average to be established. Local concentration of germanium may be possible; two Chattanooga shales in which germanium-rich coals (average 470 ppm. in 4 samples) occurred, contained 8 and 18 ppm. Ge[30]. Further investigations of the germanium content of sedimentary rocks, particularly of shales, are very desirable.

The average germanium content of 2 pelagic red clay composites representing 8 individual samples from the Pacific Ocean, is 1.6 ppm. Antimony determination was already made on these composites[31]. A sample of deep-sea red clay contained 2 ppm. according to the analysis of J. A. Maxwell, Geological Survey of Canada[32]. El Wardani[33] has independently obtained the same value for the same sample. A value of 2 ppm. is thus indicated for red clays and this average is comparable to that of shales examined.

As a result of the above observations, it can be pointed out that shales and red clays tend to be rich in germanium compared to igneous rocks. This may be understandable from the fact that some germanium compounds are volatile at relatively low temperatures. Germanium is found in some waters of hot springs. In a mineral water of Senami Spring, Niigata Prefecture, Kuroda[34] found 0.03 mg. Ge per liter or 0.03 ppm. Data of germanium for sea water are scanty. El Wardani found 0.05 μg. Ge in a liter of sea water, corresponding to $\sim 10^{-5}$ ppm.[33] Arsenic is much more abundant in sea water (1–3 μg. As/l.[35,36]) than germanium. The escaping tendency of germanium is less than that of arsenic.

Chondrites.—Table X contains the chandrite data. The frequency distribution is shown

28) E. Minami, *Nachr. Ges. Wis. Gottingen, Math.-physik. Kl.* IV, N.F. 1, 143 (1935).
29) W. Noll, *Chem. Erde*, 8, 537 (1934).
30) I. A. Breger and J. M. Schopf, *Geochim. et Cosmochim. Acta*, 7, 287 (1955).
31) H. Onishi and E. B. Sandell, ibid., 8, 213 (1955).
32) J. A. Maxwell, Private communication to E. B. Sandell.
33) S. A. El Wardani (Scripps Inst. Oceanography, Univ. of Calif.), Private communication to E. B. Sandell.
34) K. Kuroda, This Bulletin, 14, 303 (1939).
35) A. A. Smales and B. D. Pate, *Analyst*, 77, 188 (1952).
36) K. Sugawara, Distribution of some minor bio-elements in western Pacific Waters, Regional Symposium on physical oceanography, Tokyo, October, 1955.

in Fig. 4. For the description of some samples, the readers are referred to Prior and Hey[37] or Onishi and Sandell[38].

TABLE X
GERMANIUM IN CHONDRITES

	Ge, ppm. Present work	El Wardani, analyst
Alamogordo, N. Mex.	10.3	
Arriba, Colo.	10.3	9.2*
Cope, Colo.	9.6	9.1*
Gladstone, N. Mex.	11.6	
Gruver, Texas	10.6	
Haven. Kans.	12.4	
Hesston, Kans.	9.6	
Hugoton, Kans.	9.6	
Kanzaki-gun, Saga Prefecture, Japan	10.6	
Kingfisher, Okla.	11.3	
Ladder Creek, Kans.	9.2, 9.2	6.1
Melrose, N. Mex.	10.0	9.4*
Miller, Kans.	12.4	
Morland, Kans.	10.6	
Oshima-gun, Kagoshima Pref., Japan	9.0	
Plainview, Texas	11.2	12.0
Potter, Neb.	11.9	
Roy, N. Mex.	11.2, 11.2	8.8
Average	10.6	
Composite I (Arriba, Benham, Cope, Cotesfield, Morland, Plainview, Roy)	9.5, 10.0	10.6*
Composite II (Alamogordo, Estacado, Gladstone, Gruver, Kingfisher, Ladder Creek, Melrose)	11.7, 10.9	9.4*

* Average of duplicate analyses.

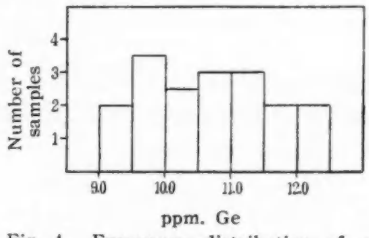

Fig. 4. Frequency distribution of germanium in chondrites.

El Wardani's[33] values were obtained by a photometric method with phenylfluorone after decomposing the sample with hydrofluoric acid only, followed by fusion of the residue with potassium pyrosulfate, and distillation of germanium tetrachloride. The agreement is generally good and this fact was already discussed from the standpoint of the present day trace analysis[39]. The worst agreement is found in the Ladder Creek chondrite which contains 6.1 ppm. (single analysis) according to El Wardani and 9.2, 9.2 ppm. (duplicate analyses) according to the author. For Composite I, a difference between the two analysts' values, taking an average respectively, is 8% with respect to the author's value. For Composite II, it is −17%. The average given by El Wardani for the two composites is 10.0 ppm. and by the author 10.5 ppm. The difference is only −5% which should, in the opinion of the author, be considered very satisfactory.

The average for 18 chondrites is 10.6 ppm. Ge, with a range from 9.0 to 12.4 ppm. The germanium content is uniform and it is probable that this average is not far from the truth. If we take the average for Haven, Hesston, Hugoton, Kanzaki, Miller, Oshima, and Potter chondrites, all of which are not included in either Composite I or II, a value of 10.8 ppm. is obtained and is comparable with 9.8 and 11.3 ppm. of those composites.

In the present work, no attempt was made to separate silicate, troilite, and metal phases of chondrites, or to determine germanium in these phases.

Some of the chondrite samples used in the present work are considerably weathered and the effect of this alteration on the gallium content was previously discussed[38]. We believed that no important change in the gallium content has occurred. In the case of germanium, no definite relation between the degreen of alteration and the germanium content is apparent. Thus, for example, the Kingfisher chondrite, which is the freshest in our collection, contains 11.3 ppm. Ge, as compared to 11.2 ppm. in the weathered Roy chondrite.

There seems to be no relation between the germanium and arsenic contents of chondrites, and this is in contrast with igneous rocks (see Fig. 3).

The new average germanium content of chondrites or approximate cosmic abundance (10.6 ppm. Ge) is much smaller than the values of 31 ppm. reported by the Noddacks[9] and of 55 ppm. by Goldschmidt[3]. The last value is based on the ratio 10 silicate phase : 2 metal : 1 troilite.

In Fig. 5 the meteoritic abundances of germanium, tin, and their neighbors of both even and odd atomic numbers are plotted. The

37) G. T. Prior and M. Hey, "Catalogue of Meteorites", 2nd ed., British Museum (Natural History), London (1953).

38) H. Onishi and E. B. Sandell, *Geochim. et Cosmochim. Acta* **9**, 78 (1956).

39) H. Onishi, *Kagaku*, **26** 306 (1956).

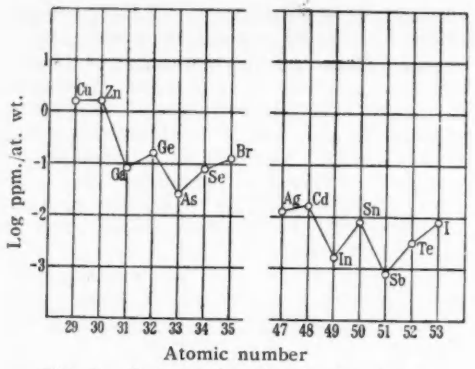

Fig. 5. Log of the atomic abundance, expressed as parts per million/atomic weight, of elements 29–35 and 47–53 in meteorites.

abundances of copper[40], gallium[38], arsenic[22], tin[23], and antimony[31] referred to chondrites. Other values are based on the Goldschmidt's ratio as representing the average of meteorites. Some of the values, e. g., bromine and iodine, are very uncertain. The value for tellurium is an estimate (0.5 ppm.) by the author.

If we adopt the Urey-Craig[41] average for silicon in chondrites, i. e., 18% Si, we obtain the weight ratio $Ge/Si=10.6/18\times10^4=5.9\times10^{-5}$ or the atomic ratio 2.3×10^{-5}.

Germanium (atomic number 32) is more abundant than gallium (A. N. 31) and arsenic (A. N. 33) if the respective contents are taken as 5.3 and 2 ppm. in chondrites.

40) J.M. Shreeve, Unpublished work, Univ. of Minnesota (1955).

41) H.C. Urey and H. Craig., *Geochim. et Cosmochim. Acta*, **4**, 36 (1953).

Summary

Chondrites have uniform germanium contents: the average of 18 samples is 10.6 ppm. Ge, with the range 9.0–12.4 ppm.

The common igneous rocks do not differ greatly in germanium content as shown by the averages: granitic rocks 1.3 ppm., intermediate rocks 1.5 ppm., basalts and diabases 1.3 ppm., gabbros 1.2 ppm., and ultramafic rocks 1.0 ppm. The average for the lithosphere or the crustal rocks may be taken as 1.5 ± 0.5 ppm. Ge.

Shales contain 2 ppm. Ge. Oceanic red clay also contains the similar amount. The germanium content of sedimentary materials seems to be somewhat higher than that of igneous rocks because of the possible escape of germanium in hydrothermal and volcanic emanations.

Special thanks are due Professor E. B. Sandell for generous cooperation in providing rock and meteorite samples and helpful suggestions. Dr. E. Minami kindly provided three composites of European and Japanese shales. Drs. S. S. Goldich, M. Gorai, H. Hamaguchi, and H. Shibata, and Messrs. R. Kuroda and S. Sato supplied various rock samples. Two Japanese meteorites were vigne through the courtesy of the Director, Geological Survey of Japan.

Government Industrial Research Institute, Nagoya

Spectrochemical Study of Microscopic Crystals. XII[1]. *Polarized Absorption Spectra of Cupric Complexes with Tropolone and Related Compounds*[2]

By Shoichiro YAMADA and Ryutaro TSUCHIDA

(Received April 10, 1956)

In the previous papers[3], the present authors studied the dichroism of planar quadri-co-ordinate complexes of platinum (II) and palladium (II), and induced the common rules on the dichroisms of these compounds. Besides those complexes of platinum and palladium, a number of cupric quadri-co-ordinate complexes are also known to possess planar configuration, for which a definite dichroism may be expected. In connection with the earlier studies on the planar complexes, it was supposed to be desirable to determine

1) Part XI of this series, S. Yamada and R. Tsuchida, This Bulletin, **29**, 421 (1956).

2) Presented in part at the sixth annual meeting of the Japan Chemical Society, Kyoto, April, 1953.

3) S. Yamada, H. Yoneda and R. Tsuchida, *J. Chem. Soc. Japan*, **69**, 145 (1948) (in Japanese); S. Yamada, *J. Am. Chem. Soc.*, **73**, 1182 (1951); S. Yamada and R. Tsuchida, This Bulletin, **26**, 489 (1953).

the dichroism of planar complexes of copper (II). As ligands we have taken up tropolone[4] and its derivative, which were kindly donated by Prof. T. Nozoe. In the study with compounds of tropolone and its derivative, it also seemed of great interest to make comparison of these metallic compounds with complexes of some β-diketones which bear resemblance to the former. In the present work, we have determined dichroisms of cupric complexes with tropolone, hinokitiol[5], acetylacetone and salicylaldehyde[6], all of these chelate groups co-ordinating to the metal through oxygen atoms, and the results have been discussed in relation to the above points.

Experimental

Materials.—Bis-(tropolonato)-copper(II).—The sample, which was kindly supplied by Professor T. Nozoe of Tohoku Univ., was recrystallized from alcohol. The green prismatic crystals belonging to the monoclinic system show an oblique extinction in the prism face. A marked dichroism was observed under the microscope. Measurement of the dichroism was made in the (110)-plane with polarized light vibrating along the directions of extinction the extinction angle being about 19.5° with reference to the *c*-axis.

Bis-(hinokitiolato)-copper (II).—The sample supplied by Prof. Nozoe was recrystallized from alcohol. The crystals obtained in green, monoclinic prisms show in the prism face a dichroism similar to that of the tropolonato-compound. Measurement of the dichroism was made in the prism face along the directions of extinction. The crystals exhibit an oblique extinction, the extinction angle being about 36° referred to the needle axis.

Bis-(acetylacetonato)-copper (II).—Was prepared from an aqueous solution of copper acetate and an alcoholic solution of acetylacetone[7]. Blue, monoclinic crystals of this compound, elongated along the *b*-axis, show a striking dichroism; they appear indigo with the electric vector along the *b*-axis, and greenish yellow with the electric vector perpendicular to the *b*-axis. The dichroism measurement was made with polarized light having its electric vector along the above two directions.

Bis-(*o*-formylphenolato)-copper (II).—Was prepared in green, monoclinic prisms according to the method of Tyson et al[8]. The crystals thus obtained exhibit a marked dichroism in the prism face; they appear yellow and brownish yellow, respectively, with the electric vector along and normal to the direction of elongation. The measurement was made with reference to the above two directions.

Measurements.—Quantitative dichroism measurements were made at room temperature in the region covering from 2400 to 7500 Å by Tsuchida-Kobayashi's microscopic method[9]. The symbol, α, represents absorption coefficient per mm. of a crystal.

Absorption spectrum in solution was determined with a Beckman DU quartz-spectrophotometer. ε represents extinction coefficient of the solution.

Results

Bis-(tropolonato)-copper (II).—The results of the measurements are shown in Fig. 1 and Table I. According to the X-ray analysis of

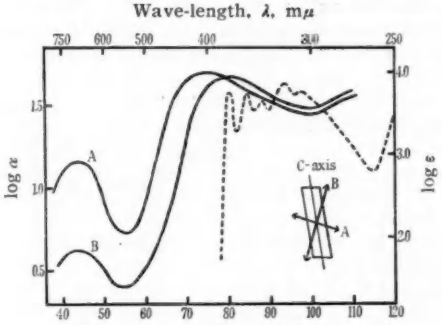

Fig. 1. Ultra-violet absorption spectra of bis-(tropolonato)-copper (II) and tropolone. The absorption spectrum of tropolone in hexane (dotted curve) is taken from J. W. Cook, A. R, Gibbs, R. A. Raphael and A. R. Somerville, *J. Chem. Soc.* **1951**, 503.

TABLE I

ABSORPTION MAXIMA OF BIS-(TROPOLONATO)-COPPER (II)

	ν, 10^{13}/sec.	$\log \alpha$	ν, 10^{13}/sec.	$\log \alpha$
A-abs	43.8	1.16	76	1.88
B-abs	44	0.71	81	1.88

the crystal structure by Robertson[10], a copper atom and four oxygen atoms around it form a square, the whole molecule containing the tropolone-rings being planar. The normal to the planes of the complexes makes an angle of about 26.5° with the *c*-axis. The X-ray analysis indicated that the A-absorption involves more ||-absorption of the molecule[11], and the B-absorption involves more ⊥-absorption (Fig. 1). The tropolonato-copper (II) complex in the crystalline state shows an absorption

4) Tropolone represents cycloheptatriene-2, 4, 6-one-1-ol.

6) Salicylaldehyde may be regarded as *o*-formylphenol. The latter is preferred, when it is necessary to stress that this is one of the phenolic compounds.

7) W. C. Fernelius, "Inorganic Syntheses", Vol. 2 (1946), p. 14.

8) G.N. Tyson, Jr. and S.C. Adams, *J. Am. Chem. Soc.*, **62**, 1228 (1940).

9) R. Tsuchida and M. Kobayashi, This Bulletin, **13**, 388 (1938); "The Colour and the Structure of Metallic Compounds", Zoshindo, Osaka (1944), p. 180 (in Japanese).

10) J.M. Robertson, *J. Chem. Soc.*, **1951**, 1223.

11) The ||- or ⊥-absorption represents absorption with polarized light having its electric vector along the plane of the complex or perpendicular to it, respectively.

band at about 44×10^{13}/sec. and another band at about 80×10^{13}/sec. and shorter wave-length. The former band (band A) may be considered as due to the copper atom in co-ordination with the ligand groups. The latter band may be due to the electronic transition in the ligand bound to the metal atom and should be designated as a specific band[12].

The following rules are obtained on the dichroism. (1) For the band A, the ||-absorption is remarkably hyperchromic to the ⊥-absorption, and (2) for the specific band, the ||-absorption is highly bathochromic to the ⊥-absorption.

Bis-(hinokitiolato)-copper (II).—The results of the measurements are shown in Fig. 2 and Table II. The compound shows a band

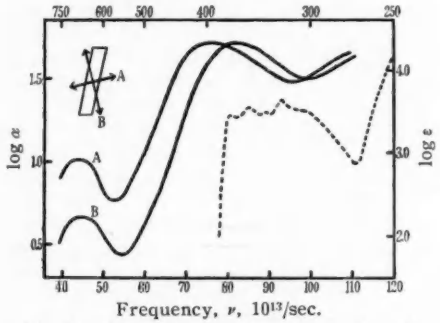

Fig. 2. Ultra-violet absorption spectra of bis-(hinokitiolato)-copper (II) and hinokitiol. The absorption spectrum, of hinokitiol in iso-octane (dotted curve) is taken from M. Tsuboi, This Bulletin, **25**, 369 (1952).

TABLE II

ABSORPTION MAXIMA OF BIS-(HINOKITIOLATO)-COPPER (II)

	ν, 10^{13}/sec.	log α	ν, 10^{13}/sec.	log α
A-abs.	44.2	1.0	76	1.70
B-abs.	44	0.62	80	1.72

at about 44×10^{13}/sec. and the other band at about 80×10^{13}/sec. and shorter wave-length region. The crystal structure has not yet been determined. The dichroism of the compound, however, may be understood in a way similar to the case of the tropolonato-compound, assuming that the A-absorption involves the characteristics of the ||-absorption and the B-absorption involves those of the ⊥-absorption. On the basis of the assumption, we are led to the rules, the same as those of the tropolonato-compound.

12) About the specific band, see, for example, R. Tsuchida and M. Kobayashi, This Bulletin, **13**, 476 (1938), etc.

Bis-(acetylacetonato)-copper (II).—The results of the measurements are shown in Fig. 3 and Table III. The analysis of the crystal

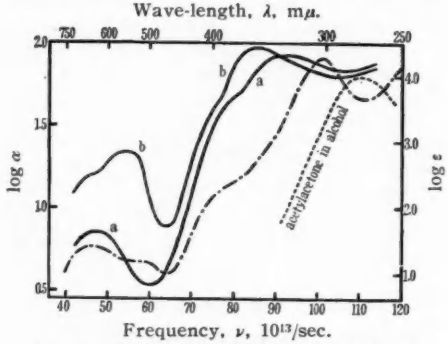

Fig. 3. Ultra-violet absorption spectra of bis-(acetylacetonato)-copper (II): ——— crystal; – – – – chloroform solution. The absorption spectrum of acetylacetone in alcohol (– – – – – –) is taken from P. Grossmann, *Z. physik. Chem.*, **103**, 305 (1924).

TABLE III

ABSORPTION MAXIMA OF BIS-(ACETYLACETONATO)-COPPER (II)

	ν, 10^{13}/sec.	log α	ν, 10^{13}/sec.	log α
b-abs.	55.8	1.39	94	2.04
c-abs.	48	1.05	98	2.00

structure was performed by Koyama et al.[13], indicating that the planes of the complex molecules inclined by about 53.5° to the *b*-plane. It is seen from the X-ray study that the *a*-absorption, absorption with the electric vector along the *a*-axis, involves more ⊥-absorption, and the *b*-absorption, absorption with the electric vector along the *b*-axis, involves more ||-absorption. The crystal shows two absorption bands, one at about 50 to 55×10^{13}/sec. and the other in the region shorter than 70×10^{13}/sec. The band at shorter wave-length apparently corresponds with the specific band which is due to the electronic transition of the π-electron system in combination with the copper atom. From the result of the measurement, we obtain the following rules on the dichroism of the planar complex. (1) For the band A, the ||-absorption is greatly hyperchromic to the ⊥-absorption, the former being slightly hypsochromic to the latter, and (2) for the specific band, the absorption with the electric vector along the π-electron system is bathochromic to the absorption with the electric vector normal to the π-electron system.

13) H. Koyama, Y. Saito and H. Kuroya, *J. Inst. Polytech. Osaka City Univ.*, Vol. 4, No. 4, Series C, p. 43 (1953).

Bis-(*o*-formylphenolato)-copper (II). — The results of the measurements are shown in Fig. 4 and Table IV. The crystal is found to show a band at about 50×10^{13}/sec. (band A) and another band at about 65×10^{13}/sec. and shorter wave-length. The latter band may be considered as due to the electronic transition in the *o*-formylphenolate ion co-ordinating to the copper atom, and should be designated as a specific band. The analysis of the crystal structure is not available as yet. Comparing the polarized absorption spectra of this compound with those of the other cupric complexes, however, we can readily assign the A- and B- absorption as representing the characteristics of the ||- and ⊥-absorption. Assuming the above assignment, the following relationships may be derived on the dichroism of the bis-(*o*-formylphenolato)-copper (II). (1) For the band A, the ||-absorption is greatly hyperchromic to the ⊥-absorption. (2) For the specific band, the ||-absorption is bathochromic to the ⊥-absorption.

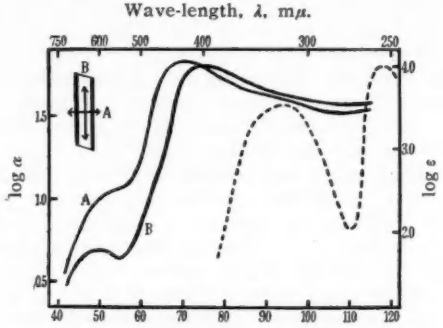

Fig. 4. Ultra-violet absorption spectra of bis-(*o*-formylphenolato)-copper (II). The absorption spectrum of *o*-formylphenol in hexane (dotted curve) is taken from R. A. Morton and A. L. Stubbs, *J. Chem. Soc.*, **1940**, 1347.

TABLE IV

ABSORPTION MAXIMA OF BIS-(*o*-FORMYLPHENOLATO)-COPPER (II)

	ν, 10^{13}/sec.	log α	ν, 10^{13}/sec.	log α
A-abs.	51	1.01	69	1.82
B-abs.	51	0.70	73	1.84

Discussion of the Results

General Rules on the Polarized Absorption Spectra of the Cupric Complexes.—The planar complexes of copper (II) that have been examined in the present work are seen to show analogous absorption spectra and a quite similar type of dichroism. The four complexes exhibit two kinds of absorption bands, one in the visible region and the other in the ultra-violet.

The former (band A) may be considered as originating from the copper atom bound to the ligands. Reviewing the experimental data, the following rules which are common for the four cupric complexes may be derived for the band A. *The ||-absorption is much higher in intensity than the ⊥-absorption.* The same rule was also shown to hold for bis-(ethylenediamine)-copper (II) complexes[14] and bis-(dimethylglyoximato)-copper (II)[15]. In the previous papers[3], a similar relation on the dichroism was obtained with planar complexes of palladium (II) for the absorption band which was assumed to be due to the co-ordinate linkage between the metal and the ligands. The above rule on the dichroism implies that the electric moment responsible for the band in question is greater along the plane of the complex than that normal to the complex plane. This relationship seems to be readily understandable in a qualitative way. Thus, since the linkage lies in the plane of the complex, the electrons concerned with the linkage would be excited more readily with the electric vector along the plane of the complex than with the electric vector normal to the plane.

It is seen that with the four cupric complexes there are two types of dichroism for the band A. For the one, the ||- and ⊥-absorption show a band A at almost identical wave-lengths, and for the other, the ||- and ⊥-absorption show their band A at different wave-lengths. To the latter type, for example, belongs the acetylacetonato-complex. In the crystal of bis-(ethylenediamine)-copper (II) perchlorate also was observed a similar splitting of the band A, which was ascribed to the perturbations from the surrounding complex ions and anions[14]. According to the X-ray study, the closest distance between the copper atom and one CH group in the α-position of an adjacent molecule is 2.84 Å in the crystal of the acetylacetonato-complex, suggesting a kind of weak interaction between them. Therefore, the splitting of the band A in this compound might be ascribed mainly to the interaction between the *d*-electron of the copper atom in one molecule and the π-electron of the CH group in another in the crystalline state. Thus, the above interaction acting perpendicularly to the plane of the cupric complex is expected to give rise to the bathochromic shift with the ⊥-absorption.

14) S. Yamada and R. Tsuchida, This Bulletin, 29, 289 (1956).
15) S. Yamada and R. Tsuchida, ibid., 27, 156 (1954).

In connection with this, it also seems noteworthy that the absorption maximum for the band A of the acetylacetonato-copper (II) in the crystalline state is found at a wavelength considerably shorter than that in the solution. This fact suggests some bathochromic effect of the solvent molecules on the complex in solution. This effect may be due to close approach of the solvent molecules to the copper atom along the direction normal to the plane of the complex. The interaction between the complex molecules in the crystalline state might also be possible. The effect of the solvent molecules on the planar complexes, however, seems to be more probable, since the interaction between the complex molecules would be expected to cause bathochromic effect. This phenomenon would be similar to the bathochromic shift with the aqueous solution of bis-(ethylenediamine)-copper (II) complexes, where weak linkage of the solvent molecules to the copper atom was assumed in the direction along the normal to the plane of the complex[14].

The absorption band at the shorter wavelength may be considered as due to the characteristic absorption of the isolated ligands. It is seen that the characteristic absorption, which is exhibited by the isolated ligand in the ultra-violet region, is modified and displaced toward the longer wave-length when it is combined with the metal atom to form a complex molecule. As to the specific band of the ligand in the cupric complex, the present measurement shows (1) that *the absorption parallel to the π-electron system of the ligand is bathochromic to the absorption normal to the π-electron system*, and (2) that *the intensity is of almost equal magnitude for both the ∥- and ⊥-absorption.*

For the isolated molecules of the ligands that have been treated in the present work, we may expect a dichroism which is similar to that for the benzene ring, since all of them involve a conjugated π-electron system. It was formerly established for the isolated benzene derivatives that the absorption parallel to the benzene ring is highly hyperchromic and slightly bathochromic to the absorption normal to the ring[16]. The above rule (1) seems to be similar to the relation derived for the isolated benzene derivatives. The polarization property of the ligand is retained in this respect, when the ligand combines with the metal. The rule (2), however, is quite different from that with the benzene derivatives or from what would be expected for the isolated π-electron systems. Thus, the ⊥-absorption which is forbidden in the isolated system of the ligand is seen to be allowed in forming the metallic complex. This change as to the polarization property of the specific band may be ascribed to the disturbance caused on the ligand when combining with the metal atom.

Absorption Spectra and Electronic Structure.—Comparison of the frequency at the maximum of the band A among the cupric complexes with different ligand ions gives the following hypsochromic order of the ligands: acetylacetone>salicylaldehyde>tropolone, hinokitiol. This order may be taken as one measure for the effect of the ligand on the electronic state about the copper. Thus, it is supposed that the effect of the ligand ion on the copper atom decreases in the above order.

The oxygen atoms directly attached to the metal atom would be greatly influenced by the neighbouring carbon atoms in the same ligand. According to Calvin et al.[17], who extensively studied stability constants of cupric complexes with a number of β-diketones, the most profound change within a ligand on its complex formation may be in the nature of the double bond between the two carbon atoms of the three-carbon systems forming the conjugated chain between the two oxygen atoms. They found a straightforward correlation between the stability constant of the cupric complexes and the nature of the double bond in the three-carbon systems of the conjugated chain. In those compounds which are treated in the present paper, the linkage between the oxygen and copper atom might involve, besides the ordinary σ-bond, some amount of additional π-binding which would be due to an overlap of atomic orbitals of the oxygen and copper atom. Thus, the chelate-ring system comprising the metal atom in the above type of compounds may be supposed to involve the conjugation of more or less unsaturated linkages, which would be somewhat analogous to that in the aromatic ring[17]. Going further on this assumption, the greater conjugation the many-carbon system between the two oxygen atoms would involve, the greater would be the contribution of the π-bond between the copper and oxygen atom, resulting in the stronger linkage between the metal and the ligand, which would yield

16) R. Tsuchida, M. Kobayashi and K. Nakamoto, *J. Chem. Soc. Japan*, 70, 12 and 14 (1949) (in Japanese); K. Nakamoto, *J. Am. Chem. Soc.*, 74, 390 (1952), etc.; G. Scheibe, S. Hartwig and H. Müller, *Z. Elektrochem.*, 49, 372 (1943).

17) M. Calvin and K.W. Wilson, *J. Am. Chem Soc.*, 67, 2003 (1945).

the more hypsochromic shift of the absorption band A[18].

Following the hypothesis[19] that tropolone is a vinylog of an enolized β-diketone, with the linkage of a small bond order between the carbon atoms 1 and 2 (Fig. 5), the seven-

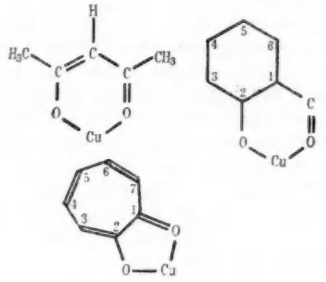

Fig. 5.

carbon system of tropolone might be assumed to have a structure similar to that of acetylacetone, involving considerable conjugation between the two oxygen atoms. The present measurement, however, indicates that with respect to the absorption band A, which is supposed to be closely connected with the linkage between the copper and the ligand, the tropolonato-copper complex is highly bathochromic to the acetylacetonato-copper. The wave-length difference between them seems to be so marked that it would be reasonable to suppose that the linkages around the copper atom in the tropolonato-complex are considerably different from those in the acetylacetonato-complex. That is, besides the contribution of the vinylog structure, we can not overlook the contribution in tropolone of a structure which involves linkage between carbon atoms 1 and 2 having a bond order considerably larger than a single bond. This assumption appears to be in agreement with the hypothesis that the tropolone ring involves some amount of aromaticity[20].

On the other hand, the present measurement also indicates that the cupric complex of salicylaldehyde shows its absorption band A at the shorter wave-length than the complex of tropolone, suggesting a stronger effect on the copper atom of salicylaldehyde than that of tropolone. Assuming for the compounds of the above type a similar criterion to that proposed by Calvin et al.[17], the stronger effect on the copper atom of salicylaldehyde seems to indicate a higher bond order of the carbon-to-carbon linkage (C_1—C_2) between the two oxygen atoms in salicylaldehyde than the corresponding C_1—C_2 linkage in tropolone (Fig. 5). This appears to be in agreement with the current concept on the structure of the tropolone ring.

When the ligand combines with a metal atom, the absorption of the ligand is seen to undergo some change or other according to the magnitude of the effect on the ligand. The magnitude of the change in the specific absorption band as compared with the original absorption of the isolated ligand may be taken roughly as one measure of the change in the electronic state of the ligand within the complex as compared with the free ligand. As the conjugation of the linkages would become greater within the chelate-ring involving the metal atom, the greater effect might be caused on the electronic state of the ligand and, in consequence, on its characteristic absorption. Thus, inspection of the previous data with the complexes in solution shows that the shift of the specific band of the metallic complex from the characteristic absorption of the free ligand molecule is smaller with the compound of tropolone than with the corresponding compound of acetylacetone and salicylaldehyde (Table V). This is parallel with the results described in the foregoing part of the present paper, leading to the same conclusion as that derived in the above.

TABLE V

WAVE-LENGTH SHIFT OF THE CHARACTERISTIC BAND OF THE LIGAND ON COMPLEX FORMATION WITH THE COPPER ATOM

Ligand	$\Delta\nu$, 10^{13}/sec.	ref.
Tropolone	1.2	(a), (b)
Salicylaldehyde	1.9	(c), (d)
Acetylacetone	8	(d), (e)

(a) J.W. Cook, A.R. Gibbs, R.A. Raphael and A.R. Somerville, *J. Chem. Soc.*, **1951**, 503.
(b) M. Tsuboi, This Bulletin, **25**, 369 (1952).
(c) R.A. Morton and A.L. Stubbs, *J. Chem. Soc.*, **1940**, 1347.
(d) K. Sone, *J. Am. Chem. Soc.*, **75**, 5207 (1953).
(e) P. Grossmann, *Z. physik. Chem.*, **109**, 305 (1924).

A similar frequency shift of the absorption band of the ligand may be expected in the infra-red spectra. Thus, the carbonyl stretching frequency of the free ligand molecule undergoes a shift to the lower frequency on its complex formation. As shown in Table VI, inspection of previous data seems to indicate that frequency shift is greatest for acetylacetone and smallest for tropolone. This is again coincident with the above hypsochromic order, giving another piece of

18) Such arguement is not strictly valid in every case, but may be applicable to those compounds which have a structure closely related to each other.
19) See, for example, W. von E. Doering and L.H. Knox, *J. Am. Chem. Soc.*, **74**, 5684 (1952), etc.
20) See, for example, T. Nozoe, *Proc. Japan Acad.*, **26**, 30 (1950), etc.

TABLE VI

FREQUENCY SHIFT OF THE C=O STRETCHING ON COMPLEX FORMATION

Compound	Free, cm^{-1}	Cu(II)-compd., cm^{-1}	ref.
Acetylacetone	1639–1538	1550–1562	a
Salicylaldehyde	1661	1600	b
Tropolone	1615	1510, 1595	c

(a) R.S. Rasmussen, D.D. Tunnicliff and R.R. Brattain, *J. Am. Chem. Soc.*, **71**, 1068 (1949); J.Le Comte, *Discuss. Faraday Soc.*, **9**, 125 (1950).
(b) I.M. Hunsberger, ibid., **72**, 5626 (1950).
(c) H.P. Koch, *J. Chem. Soc.*, **1951**, 512.

evidence for the conclusion on the electronic state of the ligands which has been reached in the former part of the present paper.

Summary

Polarized absorption spectra of cupric complexes with tropolone, hinokitiol, acetylacetone and salicylaldehyde have been determined in the visible and ultra-violet by Tsuchida-Kobayashi's microscopic method. The above compounds all exhibit two bands at about 40 to 55×10^{13}/sec. (band A) and at about 70×10^{13}/sec. or shorter wave-length (specific band). The following rules on the dichroism which are common for the above complexes, have been induced:

For the band A, the absorption parallel to the complex plane is highly hyperchromic to the absorption normal to the complex plane. For the specific band, the absorption parallel to the π-electron system is found considerably bathochromic to the absorption normal to the plane.

With different ligand ions, the wave-length of the band A of the cupric complexes have been compared, and the following hypsochromic order has been derived: acetylacetone> salicylaldehyde>tropolone, hinokitiol. The same order has been found for the wave-length shift of the specific band from the corresponding band of the free ligand.

The above results have been discussed in relation to the electronic state of the complexes and the ligands.

We thank Professor T. Nozoe and his collaborators for supplying us with the samples of the tropolonato- and hinokitiolato-complexes and drawing our attention to these compounds. We are also indebted to Professor M. Nakagawa for helpful discussions. The financial support of this work by the Education Ministry is gratefully aknowledged.

Department of Chemistry, Faculty of Science, Osaka University, Osaka

---

Determination of Nitrate Nitrogen by the Strong Phosphoric Acid-Iodic Acid Decomposition Method

By Shigeru OHASHI and Hiroshi MAKISHIMA

(Received April 24, 1956)

In the previous papers[1,2] one of the authors reported new methods for the determination of nitrogen in organic compounds by the strong phosphoric acid (SPA)-iodic acid decomposition. Organic compounds such as amines and azo-compounds or ammonium salts are decomposed by heating with a mixture of SPA and potassium iodate to liberate the nitrogen contained in them. By sending the liberated nitrogen with carbon dioxide into an azotometer, filled with potassium hydroxide solution, the nitrogen can be determined gas-volumetrically. The nitrogen in nitro or oxime compounds can also be determined by the SPA-iodic acid decomposition method after their reduction with a mixture of metallic iron powder and diluted sulfuric acid to the corresponding amines.

The purpose of the present investigation is to extend these methods to the determination of nitrogen in nitrates. Since nitrates or nitro compounds can not be directly decomposed to free nitrogen by the SPA-iodic acid decomposition method, nitrates should be converted into amines or ammonium salts prior to the decomposition.

A recent paper of T. Nakamura and F. Yamazoe[3] describing various methods for the determination of nitrate nitrogen in fertilizers concluded that the iron reduction method followed by the Kjeldahl distillation

1) S. Ohashi, This Bulletin, **28**, 177 (1955).
2) S. Ohashi, This Bulletin, **28**, 537 (1955).
3) T. Nakamura and F. Yamazoe, *The Bulletin of the National Institute of Agricultural Sciences* (Japan), Series B, No. 2, 1 (1953).

was the best. In the first place it was tried in the present investigation to combine the iron reduction method with the SPA-iodic acid decomposition method. However, when a small amount of iron was used, the authors obtained low values for nitrogen, due to incomplete reduction of nitrate. In the case of a large amount of iron, high values for nitrogen resulted, probably because some iron remained in the reaction medium and hydrogen was liberated during the decomposition with a mixture of SPA and potassium iodate. So it was difficult to find out the optimum amount of iron to be used.

It was then tried to combine the modified Gunning method[4] with the SPA-iodic acid decomposition method. The modified Gunning method involves three main steps as follows: (1) Solution of the nitrate in salicylic-sulfuric acid, for converting the nitrate into nitrosalicylic acid. (2) Treatment of the nitro compound with sodium thiosulfate to reduce it to an amino or ammonium compound. (3) The Kjeldahl digestion and distillation of the resulting compound. In this investigation the Kjeldah digestion and distillation in the above mentioned steps were replaced by the SPA-iodic acid decomposition and statisfactory results were obtained.

Apparatus and Reagents

The apparatus used in the present experiment was almost the same as that described in the previous papers, but as shown in Fig. 1 a gas-safety bulb, filled with 42% aqueous solution of glycerine, was inserted between the reaction vessel and a Kipp's carbon dioxide generator in order to prevent a possible leak of the liberated nitrogen from the reaction vessel.

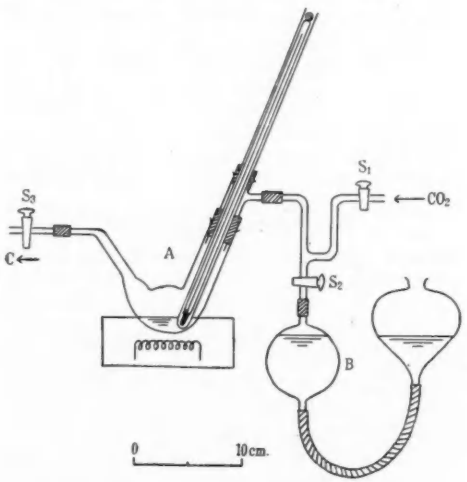

Fig. 1. Apparatus.
A: Reaction vessel B: Gas-safety bulb
C: Azotometer S_1–S_3: Stopcocks

The reagents were all of extra pure grade. The method for the preparation of strong phosphoric acid was described in the previous paper[1].

Results and Discussion

Since the decomposition process is carried out in a SPA medium, it seems to be convenient for the nitration process to be also done in the same medium. Therefore, at first, a mixture of salicylic acid and SPA was employed as a nitration reagent, but low results were given. Probably this may be due to the fact that salicylic acid is not easily dissolved in SPA. Using a common 89% orthophosphoric acid, also similar results were obtained. For this reason salicylic acid dissolved in concentrated sulfuric acid was used for the nitration. In the modified Gunning method the nitration is carried out by standing a reaction mixture for thirty minutes at room temperature. In the present study, however, according to the procedure suggested by W. E. Dickinson[5], the nitration was done by heating the reaction mixture for about fifteen seconds. For the reduction of the resulting nitrosalicylic acid, iron metal powder was tested as the reducing agent, but it was not favorable, as it required too much time and patience for the complete reaction. Thus, according to the general procedure, sodium thiosulfate was employed in its place. After examining several conditions for the determination of these facts, the following procedure was recommended.

Procedure.—Weigh a sample corresponding to about 6 to 12 mg. of NO_3 in a small weighing tube; place it in a reaction vessel and add 1.5 to 2.0 ml. of concentrated sulfuric acid containing 70 mg. of salicylic acid. Rotate the contents in the tip of a Bunsen burner for about fifteen seconds to dissolve all nitrate. To the still hot contents in the vessel add nearly 50 mg. of sodium thiosulfate and heat the contents with a small electric heater for four to five minutes until sufficient white fumes of sulfuric acid are produced. Add 5 ml. of strong phosphoric acid into the vessel. After completely cooling the contents, add 1.5 g. of potassium iodate to it. Now connect the reaction vessel with a carbon dioxide generator through the gas-safety bulb. After elevating the head of the liquid in the bulb slightly to the stopcock S_2, remove the air present in the vessel and connect it with an azotometer. Heat the mixture in the vessel with a small electric heater at 200 to 250°C and transfer the produced gas into the bulb. After the complete decomposition, transfer

4) H.C. Moore, *Ind. Eng. Chem.*, 12, 669 (1920).

5) W.E. Dickinson, *Anal. Chem.*, 26, 777 (1954).

the liberated nitrogen into the azotometer by sweeping it with carbon dioxide. From the volume of the nitrogen collected in the azotometer deduct the blank value (about 0.04 ml. in the authors' experiment) and calculate the percentage of the nitrogen.

The data obtained for potasium nitrate by means of this method were shown in Table I. The calculated value of nitrogen in the

TABLE I

DETERMINATION OF NITROGEN IN POTASSIUM NITRATE

Sample Weight mg.	N, Calcd. %	N, Found %	Deviation %
10.4	13.47	13.2	−0.3
12.3	〃	13.6	+0.1
17.1	〃	13.5	0.0
18.2	〃	13.5	0.0
18.8	〃	13.3	−0.2
19.8	〃	13.3	−0.2

Table was gravimetrically obtained by the nitron method. The accuracy for the results obtained is within ±2%. The time taken for an analysis is fifty to sixty minutes.

Since it was expected that this method can be effectively adopted to the analysis of nitrogenous fertilizers, some problems concerning this aspect were investigated. As shown in Table II, the presence of consider-

TABLE II

EFFECT OF SEVERAL SUBSTANCES ON DETERMINATION OF NITROGEN IN POTASSIUM NITRATE

KNO_3-Sample Weight mg.	Other Salts	mg.	N, Calcd. %	N, Found %	Deviation %
17.2	KCl	20	13.47	13.5	0.0
15.9	〃	30	〃	13.7	+0.2
15.7	〃	30	〃	13.4	−0.1
19.4	$FeSO_4$	20	〃	13.3	−0.2
18.6	$Fe_2(SO_4)_3$	20	〃	13.3	−0.2
19.1	〃	20	〃	13.2	−0.3
19.4	$CaCO_3$	20	〃	13.6	+0.1
18.5	〃	20	〃	13.2	−0.3

able amounts of chloride, ferrous and ferric iron, and calcium does not produce a serious error in the determination of nitrate nitrogen by this method. Of course a large amount of sulfate or phosphate has no injurious effect on this method. Nitrite can not be directly determined by this method. Therefore it seems that nitrite must be oxidized to nitrate prior to the nitration process.

When both nitrate and ammonium salt are present the total nitrogen can be determined by this method and only the ammonium nitrogen can be directly determined by the SPA-iodic acid decomposition method after expelling nitric acid by heating with SPA. When nitrate, ammonium salt, and urea are present together the total nitrogen and the sum of nitrogen in ammonium salt and urea can similarly be determined. These results are summarized in Table III and IV.

TABLE III

DETERMINATION OF NITROGEN IN POTASSIUM NITRATE AND AMMONIUM SULFATE

Sample Weight mg.	Total N: Calcd. %	Found %	Deviation %
20.0	17.17	17.2	0.0
〃	〃	17.0	−0.2
〃	〃	16.8	−0.4
〃	〃	17.4	+0.2
〃	〃	17.1	−0.1
Sample Weight mg.	**Ammonium N: Calcd. %**	**Found %**	**Deviation %**
20.0	10.44	10.4	0.0
〃	〃	10.3	−0.1
〃	〃	10.4	0.0
〃	〃	10.4	0.0
〃	〃	10.4	0.0

TABLE IV

DETERMINATION OF NITROGEN IN POTASSIUM NITRATE, AMMONIUM SULFATE, AND UREA

Sample Weight mg.	Total N: Calcd. %	Found %	Deviation %
15.7	27.92	27.2	−0.2
15.0	27.00	26.7	−0.3
15.9	28.12	27.8	−0.3
15.1	27.06	26.7	−0.4
Sample Weight mg.	**Ammonium N+Urea N: Calcd. %**	**Found %**	**Deviation %**
15.1	22.69	22.2	−0.5
15.4	23.08	23.4	+0.3
14.6	21.77	21.9	+0.1

Summary

(1) The strong phosphoric acid-iodic acid decomposition method for the determination of nitrogen in organic compounds, which was already reported, has been extended to the analysis of nitrate nitrogen.

(2) In a reaction vessel salicylic acid was nitrated by heating with the sample and concentrated sulfuric acid and the product was reduced by heating with sodium thiosulfate. The resulting mixture was decomposed by heating with a mixture of strong phosphoric

acid and potassium iodate. The liberated nitrogen was measured gas-volumetrically.

(3) In the presence of nitrate, ammonium salt, and urea, the total nitrogen and the nitrogen except nitrate could be determined by the strong phosphoric acid-iodic acid decomposition method, respectively.

Acknowledgments are made to Prof. T. Kiba for his interest and encouragement. The expense for the experiment has been defrayed from a grant given by the Ministry of Education, to which the authors' thanks are due.

Department of Chemistry, Faculty of Science, Kanazawa University
Kanazawa

Calculation on the Changes of Vibrational Frequencies due to Electronic Excitation in Several Organic Molecules

By Tosinobu ANNO*, Akira SADÔ and Ikuo MATUBARA

(Received April 4, 1956)

Introduction

In the vibrational analysis of the electronic spectrum it is important to know the correspondence between the vibrational frequencies in the ground electronic state and those in the excited state. This correspondence together with the Franck-Condon principle enables one to know about the change of the shape and dimension of the carrier molecule caused by an electronic excitation. This correspondence has hitherto been determined on the basis of the empirical facts found in similar molecules. To contribute a theoretical basis to this problem, a method will be proposed and will be applied to benzene, mesitylene, 1,3,5-trichlorobenzene and *p*-dichlorobenzene. The method is of the first approximation, as will be discussed later, but it can explain the frequency changes at least qualitatively.

Method of Calculation

The essential idea of the present method is that the bond-order is calculated by the empirical LCAO MO method for the two electronic states and the bond-length is deduced from the bond-order bond-length relation. Badger's relation[1,2] is used to calculate the stretching force constant, and the deformation force constant is deduced from a rather well established frequency. These force constants are then used to calculate the vibrational frequencies in the valence-force-field approximation.

Excepting the mesitylene molecule, the calculation of the orbital coefficients in the LCAO form was performed with the assumptions described elsewhere[3]. In the case of mesitylene, only the hyperconjugation perpendicular to the plane of the benzene ring was taken into account, assuming that the coulomb integral of the quasi H_3 "atom" is equal to the coulomb integral of the carbon atom in benzene[4], and that the resonance integral of $C{\equiv}H_3$ bond is equal to 4.83 times the resonance integral of the C–C bond in benzene[5]. The definition of the bond-order is the same as that of Coulson and Longuet-Higgins[6].

Bond-lengths were deduced from bond-orders with the help of Coulson's curve[7] for C–C bonds, taking into account the effect of hybridization[8]. For C–Cl bonds the order-length curve due to Anno and Sadô[3] was used with an appropriate modification which takes account of the effect of hybridization of carbon σ-atomic orbital only.

---

* Department of Chemistry, College of General Education, Kyushu University, Fukuoka.

T.A. is greatly indebted to the Dean of the Faculty of Science and Professor S. Imanishi for permitting him to continue his work in the Faculty.

1) R.M. Badger, *J. Chem. Phys.* **2**, 128 (1934).

2) R.M. Badger, *J. Chem. Phys.* **3**, 710 (1935).

3) T. Anno and A. Sadô, This Bulletin, **28**, 350 (1955).

4) R.S. Mulliken, C.A. Rieke and W.G. Brown, *J. Am. Chem. Soc.* **63**, 41 (1941).

5) Mulliken et al. (ref. (4)) took the resonance integral β^* of the $C{\equiv}H_3$ bond equal to 4.06 times the β_{CC} at $r = 1.33$ Å. Since β_{CC} in benzene ($r = 1.39$ Å) is 0.84 times β_{CC} at 1.33 Å according to Mulliken, we took $\beta^* = (4.06/0.84)\beta_{benzene} = 4.83\beta_{benzene}$.

6) C.A. Coulson and H. C. Longuet-Higgins, *Proc. Roy. Soc.* (London), **A191**, 39 (1947).

7) C.A. Coulson, *Proc. Roy. Soc.* (London) **A169**, 413 (1939).

8) C.A. Coulson, "Victor Henri Memorial Volume", Meson Desoer, Liège (1948), p. 15.

Badger's relation[1,2] of the following form was used to obtain the stretching force constant from the above-obtained values of bond-length:

$$r_e=(C/k_e)^{1/3}+d, \qquad (1)$$

where r_e and k_e are the equilibrium distance and the force constant of the bond, respectively, and C and d are constants. The physical meaning proposed by Badger[1] for d is that it represents the most approachable distance of the atom pair. It varies considerably from pair to pair. The meaning of C is not obvious. It remains rather constant as compaired with d. In fact Badger took it as a universal constant in the first paper of his series[1]. In Fig. 1 the inverse third power of the force constants of C–C bonds in several molecules are plotted against bond-lengths. In the same figure a line (b) is drawn through the point for benzene with the slope of $(1.86)^{1/3}$ (this is equal to the value of $C^{1/3}$ taken as a universal constant in Badger's first paper[1]) and it is seen that the line passes through the point for ethylene. If we draw straight lines parallel to the line b through points for acetylene and ethane, two lines a and c are obtained, which cut the r_e-axis at 0.717 and 0.798 Å, respectively, while the line b cuts the same axis at 0.765 Å. These values may be considered to represent three different d-values for C–C bond corresponding to three different states of hybridization of carbon atoms (a, b, c correspond to sp, sp^2, sp^3, respectively). Since Coulson[8] has shown that the carbon atom takes different covalent radii depending on its state of hybridization, it may be considered that this causes the change of the most approachable distance in the C–C bonds in the respective states of hybridization. If this is correct, the d-values for carbon atom pairs corresponding to sp, sp^2 and sp^3 hybridizations should have a sequence $d(\text{sp-sp})<d(sp^2\text{-}sp^2)<d(sp^3\text{-}sp^3)$. This is actually the case for lines a, b and c in Fig. 1. For this reason we assume that the relation (1) holds, where C is a universal constant but d may have different values depending upon the species and the states of hybridization of the participating atoms.

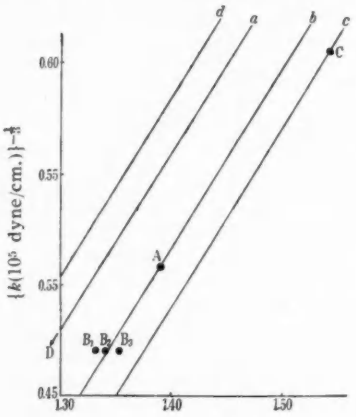

Fig. 1. Badger's rule for the C–C bonds.
a Drawn parallel to line *d* through the point for acetylene (not shown in the figure).
b Drawn parallel to line *d* through the point for benzene.
c Drawn parallel to line *d* through the point for ethane.
d From Badger's original paper (reference 1).

$$r=(1.86/k)^{\frac{1}{3}}+0.68$$

A: Benzene
(r=1.39 Å[a], k=7.61×10⁵ dyne/cm.[b]).
B_1: Ethylene
(r=1.331 Å[c], k=9.57×10⁵ dyne/cm.[d]).
B_2: Ethylene
(r=1.340 Å[e], k=9.57×10⁵ dyne/cm.[d]).
B_3: Ethylene
(r=1.353 Å[f], k=9.57×10⁵ dyne/cm.[d]).
C: Ethane
(r=1.543 Å[g], k=4.50×10⁵ dyne/cm.[h]).
D: Acetylene
(r=1.207 Å[i], k=15.80×10⁵ dyne/cm.[i]).

a V. Schomaker and L. Pauling, *J. Am. Chem. Soc.*, **61**, 1769 (1939).
b F.M. Garforth, C.K. Ingold and H.G. Pool, *J. Chem. Soc.*, **1948**, 491.
c H. W. Thompson, *Trans. Faraday Soc.*, **35**, 697 (1939).
d G. Herzberg, "Infrared and Raman Spectra of Polyatomic Molecules", D. Van Nostrand Co. Inc., New York (1945) p. 184.
e C.A.Coulson, "Victor Henri Memorial Volume", Meson Desoer, Liège, (1948) p. 15.
f W. S. Gallaway and E. F. Barker, *J. Chem. Phys.*, **10**, 88 (1942).
g G.H. Hansen and D. M. Dennison, *J. Chem. Phys.*, **20**, 313 (1952).
h Reference d p. 193.
i Reference d p. 398.
j Reference d p. 180.

In Fig. 2 the inverse third power of the force constants and the bond-lengths of the C–Cl bonds in chloroacetylene and methyl chloride are plotted as in Fig. 1 for C–C bonds. The straight lines a and c passing through the points for chloroacetylene and methyl chloride, respectively, are drawn with the slope of $1.86^{1/3}$ (see above). The line a gives a smaller d-value than the line c. This difference may result from the difference of the state of hybridization of the carbon atom. The state of hybridization of the carbon atom attached to the chlorine atom in chlorobenzenes is undoubtedly the intermediate of those in chloroacetylene and methyl chloride. Unfortunately, since we have neither the

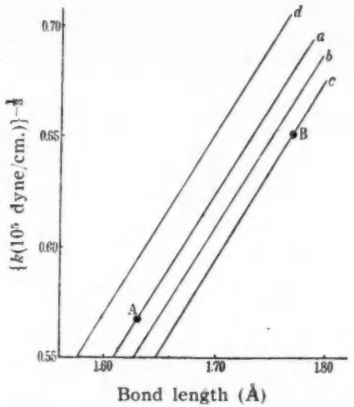

Fig. 2. Badger's rule for the C–Cl bonds.
a Drawn parallel to line *d* through the point for chloroacetylene.
b Drawn parallel to line *d* and at the middle of lines *a* and *c*.
c Drawn parallel to line *d* through the point for methyl chloride.
d From Badger's original paper (reference 1).

$$r=(1.86/k)^{\frac{1}{3}}+0.900.$$

A: Chloroacetylene (r=1.63 Å[a], k=5.52×10^5 dyne/cm.[b]).
B: Methyl chloride (r=1.77 Å[a], k=3.64×10^5 dyne/cm.[c]).

a Landolt-Börnstein, "Zahlenwerte und Funktionen", Springer, Berlin, (1951).
b W.S. Richardson and J.H. Goldstein, *J. Chem. Phys.*, 18, 1314 (1950).
c G. Herzberg, "Infrared and Raman Spectra of Polyatomic Molecules", D. Van Nostrand Co. Inc., New York (1945) p. 193.

precise knowledge of the hybridization of the carbon atoms in these molecules nor the quantitative knowledge about the variation of the *d*-values as a function of the state of hybridization, the line *b*, which we use throughout this paper, is drawn just in the middle of the lines *a* and *c*. Our conclusion may be little affected by the arbitrariness of drawing the line *b*, since we are concerned only with the change of vibrational frequencies in the two electronic states of a particular molecule, and not with the calculation of the absolute values of the vibrational frequency themselves.

Furthermore, we assume implicitly that the states of hybridization of the atoms are not affected by the electronic excitation. Briefly, we deduce the force constants from the calculated bond-lengths using the lines *b* of Figs. 1 and 2 for C–C and C–Cl bonds, respectively, both for the ground and the excited electronic states.

Bond-order, Bond-length and Bond-force-constant

The calculated values of bond-order, bond-length, and bond force-constant are shown in Tables I and II for the ground and the first excited states, respectively. Numberings of atoms are shown in Fig. 3. One thing should be mentioned in regard to the calculations for the first excited states of benzene, mesitylene and 1, 3, 5-trichlorobenzene. It can be shown that the first excited states of these molecules are accidentally degenerate and single configurations do not represent the excited states for these molecules even when the configurational interaction is neglected, because the wave functions corresponding to single configurations do not form the bases of the irreducible representations of the

Table I
Calculated values of bond-orders, bond-lengths, and bond-force-constants in the ground electronic states

Molecule	Bond	Total bond-order	Bond-length (in Å)	Bond-force-constant (in 10^5 dyne/cm.)
Benzene	C_1–C_2	1.667	1.390	7.61
Mesitylene	C_1–C_2	1.661	1.390	7.61
	C_1–C_1'	1.125	1.498	5.05
1, 3, 5-Trichlorobenzene	C_1–C_2	1.635	1.395	7.40
	C_1–Cl_1	1.320	1.687	4.68
p-Dichlorobenzene	C_1–C_2	1.633	1.395	7.45
	C_2–C_3	1.675	1.388	7.70
	C_1–Cl_1	1.298	1.691	4.60

Table II
Calculated values of bond-orders, bond-lengths, and bond-force-constants in the first excited states

Molecule	Bond	Total bond-order	Bond-length (in Å)	Bond-force-constant (in 10^5 dyne/cm.)
Benzene	C_1–C_2	1.500	1.416	6.75
Mesitylene	C_1–C_2	1.497	1.415	6.79
	C_1–C_1'	1.138	1.496	5.08
1, 3, 5-Trichlorobenzene	C_1–C_2	1.523	1.413	6.90
	C_1–Cl_1	1.334	1.684	4.73
p-Dichlorobenzene	C_1–C_2	1.555	1.407	7.04
	C_2–C_3	1.481	1.418	6.68
	C_1–Cl_1	1.472	1.665	5.11

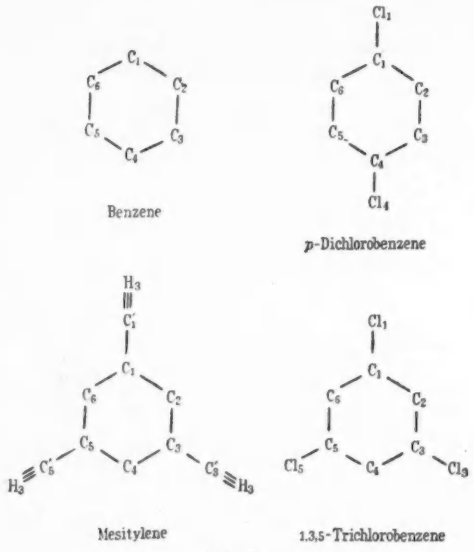

Fig. 3

point groups appropriate to these molecules. But it is easy to obtain, by linearly combining the configurational functions, the wave functions which do form the bases of the irreducible representations of the molecular point groups. These combinations involve only two configurational functions, which differ from each other in the assignment of two electrons so that the bond-orders for the states result only from superpositions of the participating configurations. Thus, the bond-order is found to be the same in the accidentally-degenerate first-excited states of particular one of these molecules.

Calculation of Vibrational Frequencies

In this paper we shall confine ourselves to the totally symmetrical skeleton vibrations since these appear more prominently in UV spectra for those molecules treated in the present paper than the other types of vibration.

Benzene.—For the benzene molecule the value of the C–C stretching force constant is only required to calculate the totally symmetrical skeleton vibrational frequency. The results are shown in Table III. Since the ground-state value is used to establish the line *b* in Fig. 1, the corresponding calculated value is in brackets. Comparison of the calculated values with the observed ones will be discussed later.

Mesitylene, 1, 3, 5-Trichlorobenzene and *p*-Dichlorobenzene.—In the case of the mesitylene molecule as well as other molecules than benzene, the totally symmetrical skeleton-vibrational frequencies are determined not only by bond-stretching force constants but also by bending force constants. These bending force constants come into the secular equation for each molecule as the combination of only one kind among them. So, one vibrational frequency for each molecule is sufficient to determine the value of the combination of bending force constants, and the other frequencies may be calculated. The results are shown in Table IV. The frequencies used for calculating deformation force constants are in brackets. The choice of the frequency from which the value of the deformation force constant was calculated was made on the basis of the following two conditions:

(i) Assignment of the frequency must be certain.

(ii) The corresponding vibrational mode must be mainly of deformation, in which case a large change in frequency yields only a small change in deduced deformation force constant, or a combination of such constants.

The first singlet-singlet absorption spectrum of mesitylene has been analyzed by Sponer and Stallcup[9]. There seems to be no question in correlating the 968- and 555-cm^{-1} frequencies in the upper state with the 997- and 575-cm^{-1} ground-state values, respectively. They obtained as an upper-state frequency 1300 cm^{-1} and correlated it with the observed Raman shift of 1299 cm^{-1} rather than the alternative one of 1378 cm^{-1}. The former correlation gives a frequency drop by −0.1%, while the latter gives a drop of 5.7%. Sponer and Stallcup preferred the former, commenting that it is not improbable for the corresponding vibrational frequencies in the two electronic states to have nearly

TABLE III
CALCULATED AND OBSERVED VALUES OF TOTALLY SYMMETRICAL SKELETON VIBRATIONAL FREQUENCY OF THE BENZENE MOLECULE

		Calculated	Observed[a]
Ground state (cm^{-1})	A_{1g}	(993)	992
	B_{2u}	937	923
Excited state (cm^{-1})	B_{1u}	937	965
	E_{1u}	937	—
	A_{1g}–B_{2u}	5.6	7.0
Drop(%)[b]	A_{1g}–B_{1u}	5.6	2.7
	A_{1g}–E_{1u}	5.6	—

a Taken from reference 14 and 15 in text.

b $\text{Drop}(\%) = \frac{\nu_{(\text{G.S.})} - \nu_{(\text{E.S.})}}{\nu_{(\text{G.S.})}} \times 100.$

9) H. Sponer and M. J. Stallcup, Ref. (8), p. 222.

TABLE IV

CALCULATED AND OBSERVED VALUES OF TOTALLY SYMMETRICAL SKELETON VIBRATIONAL FREQUENCY OF THE MESITYLENE, 1,3,5-TRICHLOROBENZENE, AND *p*-DICHLOROBENZENE MOLECULES (THE FORCE CONSTANTS USED IN CALCULATION ARE TAKEN FROM TABLE I AND II)

		Calculated			Observed[a]		
		G.S.(cm^{-1})	E.S.(cm^{-1})	Drop(%)[b]	G.S.(cm^{-1})	E.S.(cm^{-1})	Drop(%)[b]
Mesitylene	ν_1	1427	1422	0.4	1299	1300	−0.1
	ν_2	(997)	(968)	—	997	968	2.9
	ν_3	571	537	6.0	575	555	3.5
1,3,5-Trichlorobenzene	ν_1	1351	1332	1.4	1146	1122	2.1
	ν_2	(995)	(963)	—	995	963	3.2
	ν_3	365	360	1.4	375	369	1.6
p-Dichlorobenzene	ν_1	1675	1584	5.4	1589	1461/66	8.1/7.8
	ν_2	1186	1166	1.7	1102	1051	4.6
	ν_3	(755)	(725)	—	755	725	4.0
	ν_4	275	241	12.4	331	244	26.3

a a Taken from: mesitylene, reference 9; 1,3,5-$C_6H_3Cl_3$, reference 10, *p*-$C_6H_4Cl_2$, reference 11, in text.

b See footnote b in Table III.

the same values. According to our calculation the drop amounts to 0.4%, in favor of the correlation by Sponer and Stallcup.

The UV absorption spectrum of 1,3,5-trichlorobenzene was studied by Sponer and Hall[10]. In this case, the correlations of the 963- and 1122-cm^{-1} upper-state frequencies with the 995- and 1146-cm^{-1} ground-state values seem to be certain. The frequency difference of 369 cm^{-1} found in UV spectrum was correlated with the 375-cm^{-1} ground-state value with some reservations. This correlation gives only a small drop of 1.6%, which is not impossible according to Sponer and Hall. The present calculation shows this drop to be 1.4%.

The vibrational analysis of the longest wave length singlet-singlet absorption of *p*-dichlorobenzene was carried out by Anno and Matubara[11]. There can be no doubt in correlating 725 and 1051 cm^{-1} in the excited state with 755 and 1102 cm^{-1} in the ground state. It is reported there that the upper-state frequency corresponding to the 331-cm^{-1} ground-state value may be taken as 244 cm^{-1}, the 331-cm^{-1} frequency being considered as an alternative. The former choice gives a drop of 26.3%, while the latter would give no drop at all. The present calculation gives a drop of 12.4%, in favor of Anno and Matubara's analysis. To the remaining upper-state frequency 1461/66 cm^{-1} the ground-state frequency 1589 cm^{-1} may correspond. It is not certain which component of the band gives the fundamental frequency in the excited electronic state. This correlation gives a drop of 8.1/7.8%. The present calculation gives a drop of 5.4%.

Discussion

The calculated values of bond-order are naturally affected by the assumed values of the coulomb and resonance integrals. Anno and Sadô have recently found the best values of α_{Cl} and β_{CCl} by fitting the calculated shift of the UV spectrum of *p*-dichlorobenzene with experiment and the calculated value of the π-electron loss at the chlorine atom in vinyl chloride with quadrupole coupling data[12]. These values of α_{Cl} and β_{CCl} are also consistent with the experimental data for other chlorinated hydrocarbons. They have also found that the order-length relation holds as well on the basis of these values of α_{Cl} and β_{CCl}, and the relative calculation of C–Cl bond-length from the bond-order is little affected, whether we use these new values of α_{Cl} and β_{CCl} or whether we make the previously described assumption[3]. In order to show the effect of the assumed values of α_{Cl} and β_{CCl} on the changes of the vibrational frequencies of chlorinated benzenes, the calculated values of bond-order, bond-length and force constants for *p*-dichlorobenzene and 1,3,5-trichlorobenzene are listed in Table V. It may be seen in the table that the changes of the force constants for 1,3,5-trichlorobenzene are nearly the same as those given in

10) H. Sponer and M.B. Hall, Ref. (8), p. 211.

11) T. Anno and I. Matubara, *J. Chem. Phys.*, **23**, 796 (1955).

12) T. Anno and A. Sadô, To be published in *J. Chem. Phys.*, July (1956).

TABLE V

CALCULATED VALUES OF BOND-ORDERS, BOND-LENGTHS, AND BOND-FORCE-CONSTANTS FOR 1,3,5-TRICHLOROBENZENE AND *p*-DICHLOROBENZENE BASED ON α_{Cl} AND β_{CCl} DERIVED FROM EXPERIMENTAL DATA (SEE TEXT).

Molecule	Bond	Ground states: Total bond-order	Ground states: Bond-length (in Å)	Ground states: Bond-force-constant (in 10^5 dyne/cm.)	First excited states: Total bond-order	First excited states: Bond-length (in Å)	First excited states: Bond-force-constant (in 10^5 dyne/cm.)
1,3,5-Trichlorobenzene	C_1–C_2	1.626	1.396	7.42	1.548	1.408	7.02
	C_1–Cl_1	1.242	1.686	4.69	1.256	1.683	4.75
p-Dichlorobenzene	C_1–C_2	1.647	1.393	7.54	1.495	1.416	6.76
	C_2–C_3	1.670	1.388	7.72	1.515	1.413	6.87
	C_1–Cl_1	1.230	1.688	4.65	1.367	1.664	5.15

Tables I and II. As for *p*-dichlorobenzene the changes of the force constants are somewhat different from those listed in Tables I and II. Therefore we have calculated the vibrational frequencies of *p*-dichlorobenzene from the force constants given in Table V in the same manner as described previously. The results are given in Table VI. The calculated values of the changes of the frequency are in accordance with the values listed in Table IV at least qualitatively.

ing of different configurations are not found in the literature except for the ground A_{1g}– and the lowest E_{1u}–states of this molecule[13]. Therefore, we must be content with qualitative considerations. We hope to have another opportunity to discuss this effect more quantitatively.

Our calculated values of bond-orders for benzene are correct in so far as CI is neglected, and are independent of the method of calculation (e. g. simple LCAO MO, anti-

TABLE VI

CALCULATED AND OBSERVED VALUES OF TOTALLY SYMMETRICAL SKELETON VIBRATIONAL FREQUENCY OF *p*-DICHLOROBENZENE (THE STRETCHING FORCE CONSTANTS USED IN CALCULATION ARE TAKEN FROM TABLE V).

		Calculated: G.S. (cm^{-1})	Calculated: E.S. (cm^{-1})	Calculated: Drop (%)[b]	Observed[a]: G.S. (cm^{-1})	Observed[a]: E.S. (cm^{-1})	Observed[a]: Drop (%)[b]
p-Dichlorobenzene	ν_1	1677	1587	5.4	1589	1461/66	8.1/7.8
	ν_2	1190	1173	1.4	1102	1051	4.6
	ν_3	(755)	(725)	—	755	725	4.0
	ν_4	272	250	8.1	331	244	26.3

a Taken from reference 11 in text.
b See footnote b in Table III.

It is implicitly assumed in the present calculation that the molecules have planar configurations in both the electronic states. All molecules treated here have undoubtedly planar structures in their electronic ground states (treating each H_3 " atom " in mesitylene as a mass point). The vibrational analysis shows that these molecules seem also to be planar in their first excited electronic states, in which we are interested.

As to the effect of configurational interaction (CI) we are considering the case of the benzene molecule only, as for obvious reasons it is difficult at present to estimate such an effect in other molecules.

The effect of CI on the energy levels of the benzene molecule is well known. Unfortunately, however, the coefficients of mix-

TABLE VII

LOWER SINGLET LEVELS OF THE BENZENE MOLECULE CALCULATED WITH AND WITHOUT CONFIGURATIONAL INTERACTION (eV.).

Level	Roothaan and Parr[a]	Parr, Craig and Ross[b]	Observed[c]
$^1A_{1g}$	0.0	0.0	0.0
$^1B_{1u}$	7.3	9.0	6.0
$^1B_{2u}$	5.9	4.4	4.9
$^1E_{1u}$	9.8	9.9	7.0

a) Configurational interaction is neglected. All the integrals are included. (*J. Chem. Phys.*, 17, 1001 (1949)).
b) Configurational interaction and all the integrals are included. (*J. Chem. Phys.*, 18, 1561 (1950)).
c) Taken from Pariser and Parr, *J. Chem. Phys.*, 21, 767 (1953).

13) C.W.L. Bevan and D.P. Craig, *Trans. Faraday Soc.*, 47, 564 (1951). In this paper many-center integrals are neglected.

symmetrized products of molecular orbitals with or without many center integrals, etc.). However, CI produced by the higher energy configurations in which the C–C bonds have smaller bond-orders should decrease the bond-orders in the original configuration. It is to be noted that the bond-orders even in the ground state should more or less decrease. However, as can be seen in Table VII, the magnitudes of the energy changes produced by CI fit in the following sequence:

$$B_{2u} > A_{1g} \approx E_{1u} > B_{1u}.$$

If the same sequence applies to the bond-order changes, we can expect that for A_{1g}–B_{2u} or A_{1g}–B_{1u} transitions the bond-order decrease caused by the electronic excitation may be greater or smaller than when the CI is neglected, while for A_{1g}–E_{1u} transition it may be nearly the same, whether CI is considered or not. The same applies to the totally symmetrical ringvibrational frequency. Thus we can expect that the above-calculated value of 937 cm^{-1} should represent the upper and the lower limit for the vibrational frequency in the B_{1u}- and B_{2u}-state, respectively. The observed values are 923 and 965 cm^{-1} for the B_{2u}- and B_{1u}-state, respectively[14,15].

Errors due to Badger's relation appear to be small. As for the effect of d-values it may not be serious in calculating the change of the frequency caused by the electronic excitation as described above. The effect of C-values may have to be considered even for the calculation of the frequency change. According to Badger's second paper[2], this constant varies among atom pairs with the maximum deviation of 10%, which results in the error of 30% in the difference of the force constants. Therefore, the error in the frequency difference is estimated to be less than 20%.

Errors due to the valence-force-field (VFF) approximation are difficult to estimate. According to Wilson[16] the following equation holds:

$$\Lambda = L^{-1}GFL = L'FL, \qquad (2)$$

where Λ is a diagonal matrix whose diagonal elements are the characteristic roots of the secular equation $|GF - E\lambda| = 0$. G is the inverse kinetic energy matrix and F is the force constant matrix. L is the transformation matrix defined by

$$R = LQ,$$

where R and Q represent the internal and normal coordinates, respectively, prime and reciprocal denoting the transpose and the inverse matrices, respectively. In the case of the symmetrical molecules, each symmetry type can be treated separately, and in such cases R represents the symmetry coordinate formed by an appropriate linear combination of the equivalent internal coordinates. Taking the ii element of Eq. (2) it follows that

$$\lambda_i = \sum_{k,m}(L')_{ik}F_{km}L_{mi} = \sum_{k,m}L_{ki}L_{mi}F_{km}. \qquad (2')$$

From this equation the first order change of λ_i produced by small changes of F_{km}'s is given by

$$\delta\lambda_i = \sum_{k,m}L_{ki}L_{mi}\delta F_{km}. \qquad (3)$$

Now, from Eqs. (2') and (3) the relative change of λ_i is

$$\frac{\delta\lambda_i}{\lambda_i} = \frac{\sum_{k,m}L_{ki}L_{mi}\delta F_{km}}{\sum_{k,m}L_{ki}L_{mi}F_{km}}$$

$$= \frac{\sum_{k}L_{ki}L_{ki}\delta F_{kk} + \sum_{k,m\neq k}L_{ki}L_{mi}\delta F_{km}}{\sum_{k}L_{ki}L_{ki}F_{kk} + \sum_{k,m\neq k}L_{ki}L_{mi}F_{km}}. \qquad (4)$$

The use of the VFF approximation implies that in the last expression of Eq. (4) the second sums in the denominator and numerator can be neglected as compared with the corresponding first sums. In order to investigate the error due to the VFF approximation, four cases may be considered.

(i) If λ_i refers to the characteristic frequency of the stretching internal coordinate R_k, it holds that[17]

$$\lambda_i \approx (L_{ki})^2F_{kk}.$$

In general, for planar vibrations the magnitude and the change are greater for stretching force constants than those for deformation force constants and interaction constants[18]. Therefore,

$$\delta\lambda_i \approx (L_{ki})^2\delta F_{kk}.$$

Accordingly, the error due to the VFF approximation does not seem to be serious in this case.

(ii) If λ_i refers to the characteristic frequency of two (or more) stretching internal coordinates R_k and R_l, it holds that[17]

$$\lambda_i \approx (L_{ki})^2F_{kk} + (L_{li})^2F_{ll} + 2(L_{ki}L_{li})F_{kl},$$

where the first and the second terms of the right hand side are of the same order of

14) H. Sponer, G. Nordheim, A. L. Sklar and E. Teller, *J. Chem. Phys.*, 7, 207 (1939).
15) G. Nordheim, H. Sponer and E. Teller, *J. Chem. Phys.*, 8, 455 (1940).
16) E. B. Wilson, Jr., *J. Chem. Phys.*, 7, 1047 (1939); 9, 76 (1941).
17) Y. Morino and K. Kuchitsu, *J. Chem. Phys.*, 20, 1809 (1952).
18) J. Duchesne, *J. Chem. Phys.*, 21, 548 (1953), 22, 1464 (1954), *Bull. Acad. Roy. Belg.*, 39, 697 (1953), *J. phys. radium*, 15, 211 (1954), *Acad. Roy. Belg., Classe sci. Mem. Collection in* 8°, 28, 3 (1955) and J. Duchesne and L. Burnelle, *J. Chem. Phys.* 21, 2005 (1953).

magnitude. From considerations similar to those in the previous case

$$\delta\lambda_i \approx (L_{ki})^2\delta F_{kk}+(L_{li})^2\delta F_{ll}+2(L_{ki}L_{li})\delta F_{kl}.$$

Taking into account the fact that the magnitude and the change are greater for stretching force constants than those for bond-bond interaction constants it follows that

$$\frac{\delta\lambda_i}{\lambda_i} \approx \frac{(L_{ki})^2\delta F_{kk}+(L_{li})^2\delta F_{ll}+2(L_{ki}L_{li})\delta F_{kl}}{(L_{ki})^2 F_{kk}+(L_{li})^2 F_{ll}+2(L_{ki}L_{li})F_{kl}}$$

$$\approx \frac{(L_{ki})^2\delta F_{kk}+(L_{li})^2\delta F_{ll}}{(L_{ki})^2 F_{kk}+(L_{li})^2 F_{ll}},$$

in which the relative error in the frequency change due to the second approximation may be of the same order of magnitude as the relative error due to the VFF approximation in the calculation of the absolute values of vibrational frequency.

(iii) If λ_i refers to the characteristic frequency of the deformation internal coordinate R_δ, it holds that[17]

$$\lambda_i \approx (L_{\delta i})^2 F_{\delta\delta}.$$

In general, the magnitude and the change of the in-plane deformation force constants are small and are comparable with those of the interaction constants. Therefore, it is doubtful whether the following approximation holds fairly well:

$$\delta\lambda_i \approx (L_{\delta i})^2\delta F_{\delta\delta}.$$

In addition, in the method described in the present paper, various effects due to interaction constants are included in $F_{\delta\delta}$ when it is deduced form the experimental frequency. Furthermore, if we use this value of $F_{\delta\delta}$ in calculating another vibrational frequency the error included may be great, since the contributions from interaction constants to the latter frequency may be different from the contributions to the frequency from which $F_{\delta\delta}$ is calculated. Therefore, the error due to the VFF approximation is expected to be great in this case.

(iv) If λ_i refers to the characteristic frequency of the deformation (R_δ) and stretching (R_k) internal coordinates,

$$\lambda_i \approx (L_{\delta i})^2 F_{\delta\delta}+(L_{ki})^2 F_{kk}+2(L_{\delta i}L_{ki})F_{\delta k},$$

where the first and the second terms in the right hand side are nearly equal in magnitude. The error due to the VFF approximation is expected to be great also in this case on account of the error in $F_{\delta\delta}$ as described above.

Thus, it may be concluded that the use of the VFF approximation does not produce serious errors for the vibration whose mode is almost bond-stretching.

To summarize although the present approach to the problem of the changes of the vibrational frequencies in the course of the electronic excitation involves many sources of error, the results obtained are encouraging at least qualitatively. In other words, the present calculation cannot be expected to predict precisely the frequency changes in these molecules, but it is of some use in understanding or interpreting the observed frequency changes.

Finally, we express our sincere thanks to Professor S. Imanishi for his encouragement throughout this work and for his kindness in reading the manuscript.

Department of Chemistry, Faculty of Science, Kyushu University
Fukuoka

A Thermistor Method for the Determination of Velocity Coefficients of Vinyl Polymerization. I

By Hajime MIYAMA

(Received December 10, 1955)

Introduction

Various methods have been described for the measurement of the rate of vinyl polymerization. Dielectric constant[1] and refractive index[2] methods are suitable to follow rapidly the rate of exothermic polymerization in liquid-phase since these methods are sensitive to the slight rise in temperature during the reaction. However, these methods are applicable only with difficulty, therefore it is desirable to measure the small temperature rise with an easier operation. Thus recently the thermocouple method[3] was investigated by H. W. Melville et al. for the measurement of the rate of vinyl porymerization. Instead of using a thermocouple, the author used a bridge consisting of two thermistors, one of which was equipped at the center of a reaction vessel and the other was placed at the center of a standard vessel, to obtain better results from the point of view of sensitivity in temperature, adiabatic period of the system, response time of the instrument and saving the space of the reaction vessel.

This paper is concerned with the measurement of the ratio of the propagation constant to the termination constant for styrene polymerization which is catalyzed by 2, 2′-azobispropane. The data are compared with the values obtained by other methods.

Theoretical

Since the theory of this work is the same as that used in Melville's thermocouple method, the author describes briefly the outline of the theory. When the reaction vessel, which contains monomer M, is irradiated and photopolymerization takes place, the relationship between time t and fractional conversion $\Delta M/M$, is shown as follows.

$$\Delta M/M = k_p/k_t \ln \cosh (t/\tau) \qquad (1)$$

where k_p and k_t are the propagation and termination rate constants respectively and τ is the lifetime of the active species before they are removed by mutual termination. When t exceeds 3τ this relation becomes approximately linear.

$$\Delta M/M = k_p/k_t(t/\tau - \ln 2) \qquad (2)$$

The values of $\tau \ln 2$ and $k_p/k_t \times 1/\tau$ can be obtained from the interception of the time axis and the slope of this straight line. While the reaction remains adiabatic, the rise in temperature is directly proportional to the fractional conversion. Thus, provided that the heat of polymerization and the heat capacity of the system are known, the accurate values of k_p/k_t and τ can be obtained. Because of the lag in response of the instrument itself, however, the intercept does not represent $\tau \ln 2$, but the measured intercept X is given by

$$X = C + \tau \ln 2 \qquad (3)$$

where C is the lag in response of the instrument. From the kinetics of polymerization, the following formula can be obtained

$$\tau = k_p/k_t \times 1/V \qquad (4)$$

where V is the fractional rate of polymerization. From Eqs. (3) and (4)

$$X = C + k_p/k_t \times 1/\mathrm{V} \times \ln 2 \qquad (5)$$

Hence the plot of the measured interception X aginst the reciprocal of the rate $1/V$ is a straight line. The value of k_p/k_t depends only upon the slope of the line and therefore is independent of the response lag of the instrument, when this is of the same order with or less than the lifetime. But to use the theory described above, it is necessary to plot the logarithm of the light intensity $\log I$ against the logarithm of the fractional rate $\log V$ and to verify that the intensity exponent is 0.5 in this plot, as poved by Melville[3].

Experimental

The reaction vessel, shown in Fig. 1, made of transparent quartz and equipped with a thermistor is ca. 9 cc. in capacity. Its inside diameter is 38 mm., inside depth is 8 mm. and this vessel can be connected to the vacuum system by the softglass-quartz joint A. B and C are both softglass-quartz joints. This vessel can be cleaned easily after the reaction by removing the joints B and

1) C. M. Burnell, T.G. Majury and H.W. Melville, *Proc. Roy. Soc. London*, **A 205**, 309 (1951); T.G. Majury and Melville, ibid., **A 205**, 323 (1951).
2) N. grassie and H.W. Melville, ibid., **A 207**, 285 (1951).
3) W.I. Bengough and H.W. Melville, ibid., **225**, 331 (1954).

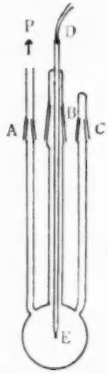

A, B, C: Softglass-quartz joints
D: Thermistor's lead wires
E: Thermistor
P: To vacuum

Fig. 1. Reaction vessel.

C. The lead-wires of thermistor are covered by very thin softglass tube which is sealed at the upper end of the joint B and the thermistor is placed at the center of the reaction vessel. One of such reaction vessels is used as a standard of temperature. Each thermistor, made by Ohizumi Factory, has the same characteristics shown in Fig. 2, of the temperature-resistance relation.

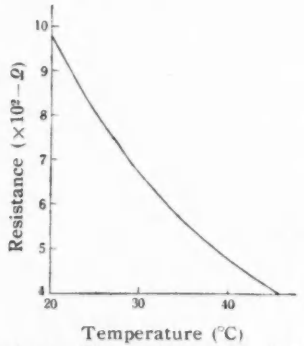

Fig. 2. Thermistor's charactestics.

A diagram of arrangement is shown in Fig. 3. In this figure, the oscillator A supplies the constant voltage 700 c/s sine waves to the bridge B and at the same time it is connected to the phase-discriminator of the amplifier C for detecting plus or minus sign of temperature difference. The bridge consists of two identical thermistors, X and S, two equally valuable resistance R, a variable resistance r and a variable condensor c. When two thermistors X and S are situated at the same temperature, the bridge can be balanced by varying the value or r and c. Then, if the temperature of S does not change but that of X changes, the balance of the bridge is broken up and the bridge supplies the output voltage e to the amplifier c. By a simple calculation, e is represented as follows.

$$e=(\Delta r/4r_0)E \qquad (6)$$

where E is the input voltage to the bridge, r_0 is the resistance value of thermistors and Δr is a

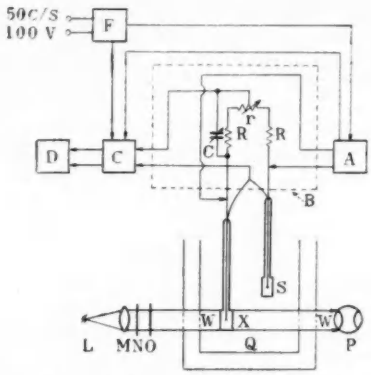

Fig. 3. Diagram of arrangement.
A; 700 c/s Oscillator B; Bridge
C; 700 c/s Amplifier
D; Penwriting-Oscillograph
F; Regulated power supply
L; Light-source M; Quartz lense
N; Shutter O; Filter
P; Photo-cell
Q; Double-thermostat W; Quatz-windows
X, S; Thermistors

resistance-change of one thermistor caused by the temperature change. When $E=2.0$ V is used $e=20\,\mu$V. for the temperature change of 0.001°C, provided that the resistance-change is ca. 4% for the temperature change of 1°C as shown in Fig. 2. The degree of amplification can be controlled from 1 to 1000 by gain-controller and multiplier of the amplifier. As to the amplifier, frequency is 700 c/s, gain is ca. 110 db and noise is ca. 1.5 μV. expressed in the same unit of the input signal. Therefore noise is neglegible for the temperature change of 0.001°C. The output from the amplifier is displayed on the galvanometer, the direct current resistance of which is 8 kΩ and amplitude per current is 15 mm./mA, of the pen-writing oscillograph D. Velocity of recording-paper can be varied in ten steps from 120 mm./sec. to 5 mm./min. The regulated power supply F is constructed so as to eliminate the outer noise and to stabilize the filament- and B-Voltage of the oscillator and the amplifier.

The source of light is a 400 watt high pressure mercury lamp (Japan Storage Battery Co. Type HL-400) fed from a constant voltage transformer. The light is passed through a quartz lens and then a Matsuda UVD_1 filter to obtain parallel and monochromatic (3660 Å) light. During the experiment the constancy of light is checked by a photocell 931 A.

Two vessels with thermistors are placed in a double water thermostat equipped with quartz-windows, which is regulated to ±0.001°C.

Commercial styrene is purified and distilled into the reaction vessel according to the method of Fujii[4].

2, 2'-Azobispropane was prepared by M. Shinichi Taira of Tokyo Metropolitan University and

4) Saburō Fujii, This Bulletin, 27, 216 (1954).

was used after distillation, b.p. 88.5°C, n_D^{25} 1.3890. In Fig. 4 is shown its absorption spectrum.

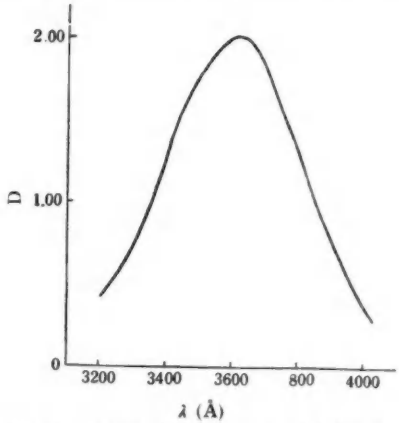

Fig. 4. Absorption spectrum of 2, 2′-azobispropane at the concentration of 0.099 Mol./L in styrene.
D; Optical density measured by Hitachi spectrophotometer EPB-U

The experimental procedure is as follows. The outputs of two thermistors are balanced by using a variable condensor c and resistance r of the bridge. A light through a lens and a filter UVD_t, irradiates the reaction vessel. At the same time, the time-mark is written on the recoreing-paper by an electric switch. After the reaction proceeds in a measurable amount, the shutter is closed and the time-mark of cutting-off light is recorded. The degree of amplification is adjusted so that the curve on the recording paper can be analyzed. This procedure is repeated until the results are reproducible.

Results

As a blank test, the reaction vessel which contained air or benzene but not monomer, was irradiated by light through a UVD_t filter. The temperature-rise of the order of 10^{-3}°C was observed and this was supposed to be caused by the direct irradiation on the thermistor. Therfore a center of the outer surface of the reaction vessel was covered by a white-paint spot of ca. 5 mm. diameter to eliminate this effect by shutting out the direct irradiation on the thermistor. Then no temperature-rise was observed.

One of the curves of the recording-paper is shown in Fig. 5, in which A and B are the marks of opening shutting the and shutter respectively. This measurement was performed at 30°C, using 0.0202 mol./l. of 2, 2′-azobispropane. Another vessel, used as a standard, was filled with benzene. Even if monomer

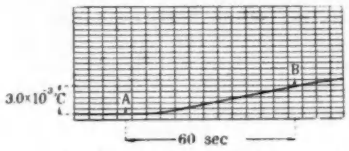

Fig. 5. A recorder trace of a typical experiment for the polymerization of styrene sensitized by 2, 2′-azobispropane.

and sensitizer were placed in that vessel as well as in the reaction vessel, the curve was the same as that when only benzene was used. This means that the dark reaction is neglegible within the experimental error, compared with the light reaction. Accordingly all measurements were carried out under the condition that the standard cell was filled with benzene.

According to the theory equation (2) is true when t exceeds 3τ, but many measurements showed that this equation could be used when t exceeds approximately 1.5τ.

The necessary constants of styrene at 30°C are as follows[5].

Heat capacity	43.9 cal./mol.
Heat of polymerization	16.76 kcal./mol.

Therefore the relation between the conversion of monomer and the temperature-rise is

$$1\% = 3.82°C \qquad (7)$$

The relation between the temperature-rise of the reaction vessel and the amplitude of the oscillograph was checked experimentally at various temperature differences. The resistance-temperature curve of the thermistor as shown in Fig. 2 is not correctly lineart and therefore the amplitude-temperature-rise relation is not the same at different temperature-rise relation is not the same at different

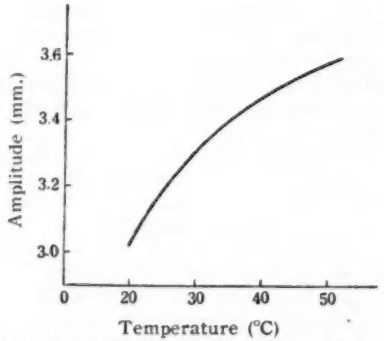

Fig. 6. The amplitude corresponding to the temperature difference of 0.001°C at maximum sensitivity.

5) Ray H. Boundy and Raymond F. Boyer, "Styrene", Reinhold, New York (1952), pp. 67, 68.

temperatures. Provided that the amplification is at its maximum sensitivity, the amplitude necessary to detect the temperature difference of 0.001°C is shown in Fig. 6. Therefore at 30°C, the amplitude of the recording paper is shown as follows.

$$1\,\text{mm.} = 3.0\times10^{-4}\text{°C} \qquad (8)$$

Since the amplitude can be read easily within the accuracy of 0.2 mm. on the recording paper, the sensitivity in temperature is 0.6×10^{-4}C. From Eqs. (7) and (8), the following relation can be obtained.

$$1\,\text{mm/s} = 0.785\times10^{-4}\%/\text{s} = 0.785\times10^{-6}/\text{s} \qquad (9)$$

To check this relation, the velocity measured by thermistor method was compared with the one measured dilatometrically. A dilatometer shown in Fig. 7, which was made from transparent quartz and of the same size as the

Fig. 7. Dilatometer.

reaction vessel shown in Fig. 1, was used. Under the same conditions, the values measured by the thermistor agreed with the one measured dilatometrically within the error of ±2%. Accordingly the value measured by thermistor method will be used without checking hereafter.

Various filters, of which the transparency factor is known, were used to change the light-intensity.

In Fig. 8 the relation between log I and log V is shown. From this line's slope, it can be shown that the exponent is 0.5 and therefore the theory already described is applicable.

The relation between $1/V$ and X is shown in Fig. 9. In Fig. 8 and Fig. 9, marks × and ○ are points obtained by using 0.0202 mol./l. and 0.0101 mol./l. of sensitizer respectively.

From the straight line's intercept in Fig. 9, it can be seen that instrument's lag in response is ca. 0.6 sec. This lag is possibly the thermistor's, because the maker of the thermistors gives ca. 0.5 sec. as the lag in response.

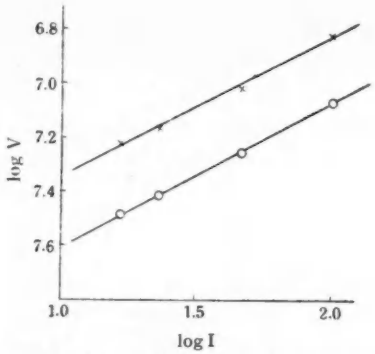

Fig. 8. The relation between log I and log V.

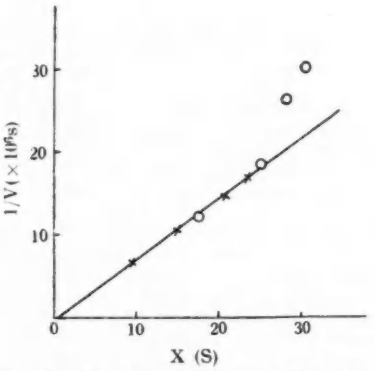

Fig. 9. The relation between X and 1/V.

The time period in which the reaction system remains adiabatic is about 70 sec., from the results of many measurements. One of these result is shown in Fig. 10. Beyond this period, the curve deviates from the straight line. As Melville showed experi-

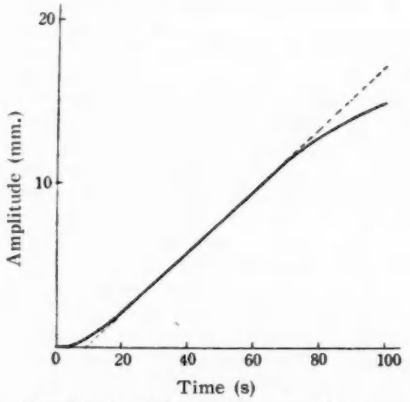

Fig. 10. Deviation of a recorcler trace from the straight line.

mentally the reaction, in which the lifetime is smaller than ca. 1/3 of this period, can be completely analyzed by using his theory. And Fig. 10 shows that the measurements, in which the lifetime is smaller than 25 sec., are all acceptable.

From the slope of Fig. 10, the value of k_p/k_t of styrene at 30°C is 2.02×10^{-3}.

Discussion

Compared with the thermocouple method, the results obtained are better in the points of sensitivity in temperature, adiabatic period of the system and instrument's lag in response. They are shown in Table I compared with the thermocouple method.

TABLE I
THE COMPARISON OF THIS METHOD WITH THE THERMOCOUPLE METHOD

	This method	Thermocouple method
Sensitivity in temperature	0.6×10^{-4}°C	2×10^{-4}°C
Adiabatic time period	70 sec. (9 cc. vessel)	60 sec. (15 cc. vessel)
Instrument's lag in response	0.6 sec.	1–3 sec.

The k_p/k_t value of styrene does not depend upon the concentration of sensitizer used. This value is reasonable in comparison with others obtained by a different method[3].

Summary

To measure the rate of vinyl polymerization, a thermistor method was devised and better results were obtained compared with the thermocouple method, in the points of sensitivity of temperature, adiabatic time period, instrument's lag in response and saving the space of the reaction vessel. The k_p/k_t value of styrene at 30°C obtained by this method was 2.02×10^{-3} and reasonable in comparison with other values obtained by different methods.

The auther wishes to express his hearty thanks to Dr. Momotato Suzuki of this Academy for his helpful advice and encouragement and to Mr. Shinichi Taira of Tokyo Metropolitan University for his kind proparation of 2,2′-azobispropane.

Department of Chemistry, Defense Academy, Yokosuka

6) Other values are summarized in ref. 2).

A Thermistor Method for the Determination of Velocity Coefficients of Vinyl Polymerization. II

By Hajime MIYAMA

(Received January 11, 1956)

Introduction

In the 1st paper[1] of this series the author described a thermistor method for the measurement of the rate of vinyl polymerization and good results were obtained compared with the thermocouple method. According to this measurement, the k_p/k_t value of styrene at 30°C, when 2,2′-azobispropare used as photosensitizer, was 2.02×10^{-3}. However, this sensitizer was not very effective and the rate of polymerization was very slow especially when irradiation was weak. Thus the analysis of the curve of oscillograph was very difficult.

In this paper, α-azobisisobutyronitrile which is a very effective photosensitizer for vinyl polymerization is used. The measurement was fulfilled on styrene, vinyl acetate and methyl methacrylate at 30°C, 35°C and 40°C. And, from the value of k_p/k_t at various temperatures, the activation energy difference E_p-E_t of these monomers was obtained, where E_p was the activation energy of propagation process and E_t was the activation energy of termination process.

Experimental

The experimental apparatus and procedure are the same as those described in the previous paper.

The monomers were prepaped according to Fujii's meteod[2] as described in the first paper.

α-Azobisisobutyronitrile was a commercial product (Kanto Chemical Co. Inc.) and used after three recrystallizations from carbon tetrachloride.

1) H. Miyama, This Bulletin, 29, 711 (1956).

2) S. Fujii, This Bulletin, 27, 216 (1954); 27, 238 (1954).

In Fig. 1, its ultraviolet absorption spectrum is shown.

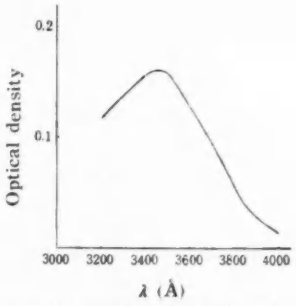

Fig. 1. Ultraviolet absorption Spectrum of α-azo-bisisobutyronitrile α-azolisisobutyronctrile at the concentration of 0.0122 mol./l. in CCl_4.

Results

Styrene.—As shown in Fig. 6 of the first paper, the amplitude of oscillograph corresponding to the temperature difference of 0.001°C is not the same at different temperatures. These values at 30°C, 35°C and 40°C obtained from that figure are as follows.

$$\begin{aligned} 1\text{ mm.} &= 3.00\times10^{-4}\text{°C at 30°C} \\ 1\text{ mm.} &= 2.94\times10^{-4}\text{°C at 35°C} \\ 1\text{ mm.} &= 2.88\times10^{-4}\text{°C at 40°C} \end{aligned} \quad (1)$$

Although heat capacity and heat of polymerization of styrene depend on the temperature, the values at 30°C are used, since the error caused by these values is small compared with the experimental error[3]. From the relation (1) and constants of styrene at 30°C, the following relations between amplitude-change per second and fractional rate of polymerization can be obtained.

$$\begin{aligned} 1\text{ mm./sec.} &= 0.785\times10^{-6}\text{/sec. at 30°C} \\ 1\text{ mm./sec.} &= 0.770\times10^{-6}\text{/sec. at 35°C} \\ 1\text{ mm./sec.} &= 0.755\times10^{-6}\text{/sec. at 40°C} \end{aligned} \quad (2)$$

In Fig. 2 a recorder trace of a typical experiment is shown, in which A and B are respectively the marks of lighting on and lighting off. This measurement was carried out at 30°C by using 0.0122 mol./l. of α-azoisobutyronitrile as a photosensitizer and other conditions were the same as those described for Fig. 5 of the first paper. From

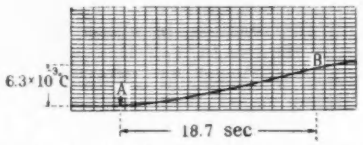

Fig. 2. A reconder trace of a typical experiment for the polymerization of styrene sensitized by α-azobisisobutyronitrile at 30°C.

Fig. 5 of the first paper and Fig. 2 it can be shown that the rate of polymerization photosensitized by 0.0122 mol./l. of α-azoisobutyronitrile is sixfold larger than the rate of polymerization photosensitized by 0.0202 mol./l. of 2,2′-azobispropane and thus the analysis of the curve can be more correctly preformed.

By varying the intensity of light, the relation between log I and log V at 30°C, 35°C and 40°C were obtained as shown in Fig. 3. From this

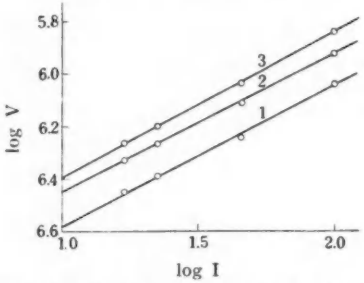

Fig. 3. Variation of the rate with the light intensity for styrene; Curve 1, at 30°C; Curve 2, at 35°C; Curve 3, af 40°C.

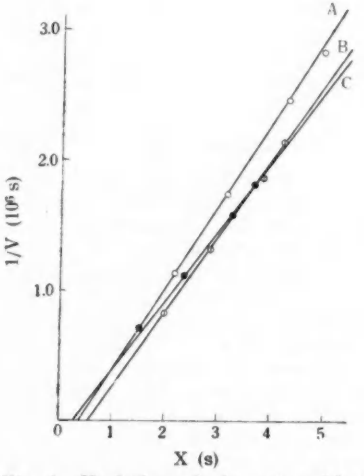

Fig. 4. Variation of the rate with the measured intercept for the polymerization of styrene.
○ Curve A, at 30°C; ⓘ Curve B, at 35°C; ● Curve C, at 40°C.

3) Heat capacities and heat of polymerization of styrene at different temperatures are as follows[4].

Heat Capacity	Heat of Polymerization
30°C 43.9 cal./mol.	16.76 kcal./mol.
35°C 44.3 cal./mol.	16.84 kcal./mol.
40°C 44.6 cal./mol.	16.90 kcal./mol.

From these values and (1), the relations between the amplitude-change per second and the fractional rate can be obtained.

$$\begin{aligned} 1\text{ mm./sec.} &= 0.785\times10^{-6}\text{/sec. at 30°C} \\ 1\text{ mm./sec.} &= 0.775\times10^{-6}\text{/sec. at 35°C} \\ 1\text{ mm./sec.} &= 0.760\times10^{-6}\text{/sec. at 40°C} \end{aligned}$$

These Values coincide with (2) within the error of ca. ±0.3%, which is small compared with the usual experimental error.

4) Ray H. Boundy and Raymond F. Boyer; "Styrene", Reinhold, New York (1952), pp. 67, 68.

straight-line's slope, it can be shown that the exponent is 0.53 at 30°C, 0.53 at 35°C and 0.54 at 40°C. Therefore the theory described in the first paper is applicable.

The relation between $1/V$ and X is shown in Fig. 4 and from this straight-line's intercept the instrument's lag in response is 0.25–0.5 sec. This value coincides approximately with 0.6 sec. obtained in the first paper. From the slope of this line, the values k_p/k_t of styrene are 2.28×10^{-6} at 30°C, 2.50×10^{-6} at 35°C and 2.77×10^{-6} at 40°C.

Vinyl Acetate.—The rate of polymerization of vinyl acetate was ca. ninefold larger than that of styrene under the same conditions. Hence the sensitivity of the amplifier was lowered as follows.

$$\begin{aligned} &1\text{ mm.}=1.20\times10^{-3}\text{°C at 30°C}\\ &1\text{ mm.}=1.18\times10^{-3}\text{°C at 35°C}\\ &1\text{ mm.}=1.15\times10^{-3}\text{°C at 40°C} \end{aligned} \quad (4)$$

The necessary constants of vinyl acetate are as follows[5]).

Heat capacity 40.5 cal./mol.
Heat of polymerization 21.3 kcal./mol.

From these values the relation between the conversion and the temperature-rise can be obtained.

$$1\% = 5.28\text{°C} \quad (4)$$

From (3) and (4) the following relations were obtained.

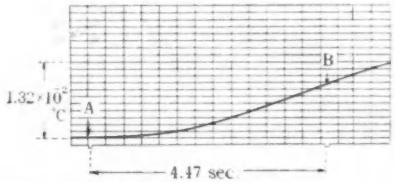

Fig. 5. A recorder trace of a typical experiment for the polymerization of vinyl acetate sensitized by α-azobisisbutyronitrile at 30°C.

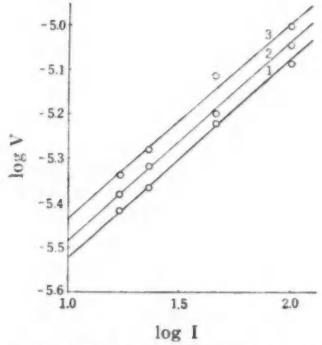

Fig. 6. Variation of the rate with the light intensity for the polymerization of vinyl acetate. Curve 1, at 30°C; Curve 2, at 35°C; Curve 3, at 40°C.

5) W.I. Bengough and H.W. Melville, *Proc. Roy. Soc.*, **A225**, 330 (1954).

$$\begin{aligned} &1\text{ mm./sec.}=0.228\times10^{-5}\text{/sec. at 30°C}\\ &1\text{ mm./sec.}=0.223\times10^{-5}\text{/sec. at 35°C}\\ &1\text{ mm./sec.}=0.218\times10^{-5}\text{/sec. at 40°C} \end{aligned} \quad (5)$$

In Figs. 5, 6 and 7, the exprimental results

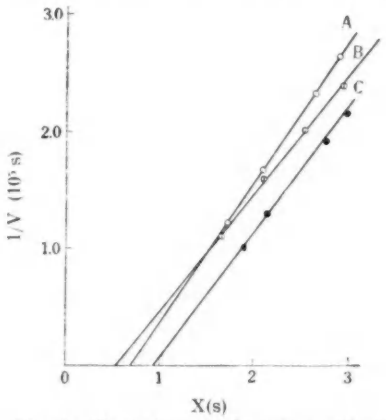

Fig. 7. Variation of the rate with the measused intercept for the polymerization of vinyl acetate.
○ Curve A, at 30°C; ① Curve B, at 35°C; ● Curve C, at 40°C.

obtained under the same conditions as in styrene are shown. From Fig. 7 the instrument's lag in respones is 0.5–0.9 sec. and the k_0/k_t values of vinyl acetate are 1.21×10^{-5} at 30°C, 1.34×10^{-5} at 35°C and 1.44×10^{-5} at 40°C.

Methyl Methacrylate.—The rate of polymerization of methyl methacrylate was ca. threefold larger than styrene under the same conditions. As the sensitivity of amplifier, (1) was used. The constants of methyl methacrylate used were as follows[5]).

Heat capacity 49.0 cal./mol.
Heat of polymerization 13.0 kcal./mol.

From these values the relation between the conversion and the temperature-rise is

$$1\% = 2.65\text{°C} \quad (6)$$

From (1) and (6), the following relations were obtained.

$$\begin{aligned} &1\text{ mm./sec.}=1.132\times10^{-6}\text{/sec. at 30°C}\\ &1\text{ mm./sec.}=1.110\times10^{-6}\text{/sec. at 35°C}\\ &1\text{ mm./sec.}=1.078\times10^{-6}\text{/sec. at 40°C} \end{aligned} \quad (7)$$

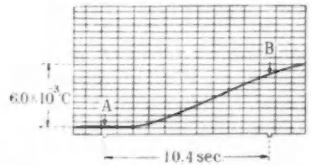

Fig. 8. A recorder trace of a typical experiment for the polymerization of Methyl Methacrylate sensitized by α-azobisisobutyronitrile at 30°C.

6) C.H. Bamford and Dewer, *Proc. Roy. Soc. London*, **A 192**, 309 (1948).

In Figs. 8, 9 and 10, the experimental results are shown and the experimental condition is the same as in styrene and vinyl acetate. From Fig. 10 the instruments's lag is 0.5–0.6 sec. and k_p/k_t values of methyl methacrylate are 7.41×10^{-5} at 30°C, 8.08×10^{-5} at 35°C and 8.92×10^{-5} at 40°C.

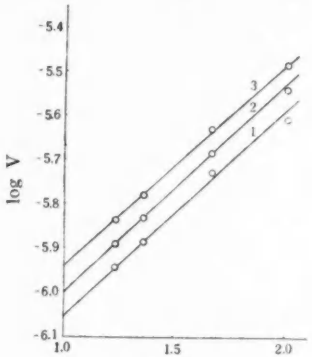

Fig. 9. Variation of the rate with the light intensity for the polymerization of methyl methacrylate. Curve 1, at 30°C; Curve 2, at 35°C; Curve 3, at 40°C.

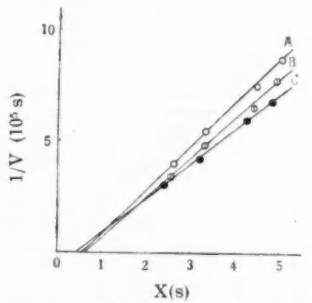

Fig. 10. Variation of the rate with the measured intercept for the polymerization of methyl methacrylate.
○ Curve A, at 30°C; ◐ Curve B, at 35°C; ● Curve C, at 40°C.

Discussion

From the k_p/k_t value at various temperatures, the difference between the activation energies E_p and E_t, where E_p and E_t are respectively the activation energy of propagation and termination processes, can be calculated. Thus the values of E_p-E_t are 3.71 kcal./mol., 3.25 kcal./mol. and 3.54 kcal./mol. for styrene, vinyl acetate and methyl methacrylate respectively. Using these values and k_p/k_t values at values temperatures, the following equations can be obtained.

$$k_p/k_t=1.09\times10^{-3}\times e^{-3710/RT} \quad \text{for styrene}$$
$$k_p/k_t=2.72\times10^{-3}\times e^{-3250/RT} \quad \text{for vinyl acetate}$$
$$k_p/k_t=2.66\times10^{-3}\times e^{-3540/RT} \quad \text{for methyl methacrylate} \qquad (8)$$

These equations obtained by other workers are as follows.

$$k_p/k_t=3.33\times10^{-3}\times e^{-3700/RT} \quad \text{for styrene}^{3)}$$
$$k_p/k_t=5.34\times10^{-3}\times e^{-2080/RT} \quad \text{for vinyl acetat}^{7)}$$
$$k_p/k_t=3.78\times10^{-3}\times e^{-3470/RT} \quad \text{for methyl methacrylate}^{8)}$$

Using equations (8), the k_p/k_t values at 15°C can be obtained and they are compared with other worker's values in Table I, Table II and Table III.

Since the above results were, as described in the previous paper, obtained from measurements after the reaction system attained the stationary state and was then irradiated, the reaction in the dark is supposed to be canceled out. However heat-decomposition of α-azobisisobutyronitrile at higher temperature is considerable and accelerates the polymerization in the dark, hence the effect of

TABLE I
THE k_p/k_t VALUE OF STYRENE AT 15°C

Method	Sensitizer	$k_p/k_t\times10^5$	Ref.
Thermistor	Azobisisobutyronitrile	1.3	This work
Interferometer	Benzoyl Peroxide	2.0[9]	Grassie & Melville (1951)
Sector	Benzoyl Perxide	3.6[9]	Valentine & Melville (1950)
Sector	Azopropane	0.65[9]	Matheson (1950)
Dilatometer	None	5.26[9]	Burnett (1950)
Dielectric Constant	Azobisisobutyronitrile	0.68[9]	Majury & Melville (1951)
Viscosity	None	5.3[9]	Bamford & Dewer (1948)

7) M.S. Matheson, E.E. Auer, E.B. Bevilacpuer and E.T. Hart, *J. Am. Chem. Soc.*, **71**, 497 (1949).
8) ibid., **71**, 497 (1949).
9) N.G. Grassie and Melville, *Proc. Roy. Soc. London*, **A 207**, 285 (1951).
These values are summarized in this paper and corrected to 15°C assuming an activation energy of 4 kcal./mol. for the k_p/k_t term.
10) These values are summarized in ref. 5) and corrected to 15°C assuming an activation energy of 4.1 kcal./mol. for the k_p/k_t term.
11) These values are summarized in ref. 5) and corrected to 15°C assuming an activation energy of 3.7 kcal./mol. for the k_p/k_t term.

TABLE II

THE k_p/k_t VALUE OF VINYL ACETATE AT 15°C

Method	Sensitizer	$k_p/k_t \times 10^5$	Ref.
Thermistor	Azobisisobutyronitrle	0.92	TGis work
Thermocouple	Azobiscyclohexanecarbo-nitrile	2.5[10]	Bengough & Melville (1954)
Refractometric	Azobisisobutyronitrile	2.0[10]	Grassi & Melville (1951)
Dielectric Constant	Azobisisobutyronitrile	0.35[10]	Majury & Melville (1951)
Sector	None	0.11[10]	Burnett & Melville (1947)
Sector	None	1.1[10]	Bartlett & Melville (1946)
Sector	Azobisisobutyronitrile	1.1[10]	Matheson, Bevilacqua, Auer, & Hart (1949)
Viscosity	None	1.9[10]	Dixon-Lewis (1949)
Dilatometer	Azobiscyclohexanecarbo-nitrile	2.4[10]	Bengough (unpublished)
Sector	None	1.4[10]	Bartlett, Broadbent & Kwart (1950)

TABLE III

THE k_p/k_t VALUE OF METHYL METHACRYLATE AT 15°C

Method	Sensitizer	$k_p/k_t \times 10^5$	Ref.
Thermistor	Azobisisobutyronitrile	5.4	This work
Thermocouple	Azobiscyclohexanecarbo-nitrile	9.8[11]	Bengough Melville (1954)
Interferometer	None	6.1[11]	Grassie & Melville (1951)
Secto:	None	3.8[11]	Mackay & Melville (1949)
Sector	Benzoine	8.9[11]	Chinmayanandam & Melville (1954)
Viscosity	None	20[11]	Bamford & Dewer (1948)
Sector	Bnnzoyl Peroxide	7.9[11]	Melville & Valentine (1950)

reaction in the dark must be taken in consideration. It is desirable, therefore, to use a photosensitizer which does not accelerate the reaction in the dark but the one in the light only.

Summary

The k_p/k_t value of styrene, vinyl acetate and methyl methacrylate was obtained by using thermistor method reported in the first paper of this series. Moreover from the k_p/k_t values at various temperatures, the activation energy difference between propagation and termination processes was calculated. They were 3.71, 3.25 and 3.54 kcal./mol. for styrene, vinyl acetat and methyl methacrylate respectively. The characteristics of this apparatus were almost the same as described in the first paper, although various monomers were used.

The author wishes to thank Dr. Momotaro Suzuki for his useful advice and encouragement.

Department of Chemistry, Defense Academy, Yokosuka

A Thermistor Method for the Determination of Velocity Coefficients of Vinyl Polymerization. III

By Hajime MIYAMA

(Received January 17, 1956)

Introduction

In the previous papers of this series[1] the author described, a thermistor method for the measurement of the rate of vinyl polymerization and obtained the values of k_p/k_t for styrene, vinyl acetate and methyl methacrylate in the initial stages of polymerization. As well as the thermocouple method, this method is not only applicable to the initial stages of polymerization, but can be used equally well for the study of the later stages when the reaction mixture becomes a viscous syrup or solid gel. Recently velocity coefficients for the later stages of the polymerization of vinyl acetate were evaluated by Melville and his co-worker with the use of a thermocouple[2].

In this paper, the author uses the thermistor method for studying the later stages of vinyl acetate polymerization. The monomer was photosensitized by the addition of 1,1'-azobiscyclohexanecarbonitrile, which is a better sensitizer than α-azobisisobutyronitrile, from the points of view of effectiveness and lack of accelaration of polymerization in the dark.

Theoretical

From the kinetics of polymerization[3], the fractional rate of polimerization is represented by equation (1).

$$V=-1/M.\quad \mathrm{d}M/\mathrm{d}t=k_p(V_{init}/k_t)^{1/2} \tag{1}$$

where k_p, k_t, V_{init}. and M are propagation constant, termination constant, velocity of of initiation and concentration of monomer respectively. Because V_{init}. of this equation is not varied by temperature-change in the photopolymerization, the difference between activation energy of propagation and the one half of activation energy of termination $E_p-1/2E_t$ can be obtained by measuring the variation of the fractional rate V with the temperature.

The lifetime of the active species τ is shown as follows.

$$\tau=(k_p/k_t)\times 1/V \tag{2}$$

From Eqs (1) and (2) the following equation can be obtained.

$$\tau=(k_t\times V_{init})^{-1/2} \tag{3}$$

Since V_{init} is not varied by the temperature-change in the photopolymerization, the activation energy of termination can be obtained by measuring the value τ at various temperatures.

An estimate of the extent of conversion can be obtained by the next formulas. Thus M of Eq. (1) is replaced by the initial concentration of monomer M_0,

$$V_0=-1/M_0\quad \mathrm{d}M/\mathrm{d}t \tag{4}$$

If the variation of V_0 against time t is measurable, M at any time t can be calculated according to the following equation.

$$M_0-M=M_0\int_{t_0}^{t}V_0\mathrm{d}t \tag{5}$$

where t_0 is the initial time. Thus the extent of conversion φ is expressed as follows.

$$\varphi=(M_0-M)/M_0=\int_{t_0}^{t}V_0\mathrm{d}t \tag{6}$$

Using the thermistor method, the value of V_0 can be obtained when specific heat of the system and heat of polymerization are known, as shown in the previous papers of this series. But the correct values of V_0 at various degrees of conversion are unknown, because the specific heat of the system varies with the extent of conversion. Approximately, the extent of conversion can be obtained by assuming that the specific heat does not change with conversion. Then using the specific heat at these values of conversion, the values of V_0 are corrected and therefore values of ρ are corrected. Repeating these procedures the correct values of V_0 and φ can be, obtained, although the extent of conversion cannot be measured directly and the specific heat of the system varies with the degree of conversion.

1) H. Miyama, This Bulletin, **29**, 711 (1956). H. Miyama, ibid., **29**, 715 (1656).
2) W.I. Bengough and H.W. Melville, *Proc. Roy. Soc.*, **230**, 429 (1955).
3) C.E.H. Bawn, "The Chemistry of High Polymers", London (1948), p. 68.

Experimental

The experimental apparatus and the preparation of vinyl acetate are the same as described in the previous papers[1]. 1,1'-azobiscyclohexanecarbonitrile was purified through recrystallization from ethanol and its ultraviolet absorption spectrum is shown in Fig. 1. The variation of the rate of

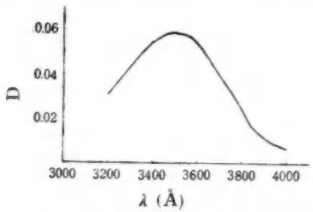

Fig. 1. Ultraviolet absorption spectrum of 0.003 mol./l. 1,1'-azobiscyclohexanecarbonitrile in vinyl acetate.

polymerization and that of the lifetime with the intensity of irradiation was usually studied at 20°C. The temperature was then raised as rapidly as possible to other temperatures, and measurements of the rate and of the corresponding lifetime were performed. As soon as the necessary measurements had been done, the thermostat was cooled rapidly to 20°C. The rate and the lifetime at 20°C were then measured and compared with the values obtained before heating. The monomer was then polymerized to a further stage by continuous irradiation using an ultra high pressure mercury lamp. When the next arbitrary stage of the polymerization was attained, irradiation was discontinued and the sequence of measurement of rates and lifetimes was repeated. This procedure was repeated until the rate became so slow and the lifetime so great that accurate determination was impossible. The extent of conversion was obtained from the fractional velocity change with time, using Eq. (6). As specific heat of vinyl acetate, the next value[2] was used. (p. 2)

$$\text{Specific heat} = 0.470 - 0.081\,\varphi \qquad (7)$$

where φ is the extent of conversion.

Experimental Results

All measurements were carried out by using 0.003 mol./l. 1,1'−azobiscyclohexaecarbonitrile as photosensitizer.

The variation of velocity V_0 during continuous polymerization is shown in Fig. 2. Using Eq. (6), the variation of velocity V_0 with the extent of conversion is shown in Fig. 3. These values of V_0 and φ were corrected using the already described theory and specific heat (7). The first correction is shown by broken curves I in Fig. 2 and 3 and the second correction by broken curves II. In these figures, curves I and II are almost the same. To check these values of conversion the reaction mixture was dissolved in acetone; the polymer was precipitated by addition of methanol and weighted. The comparison is shown in Table I.

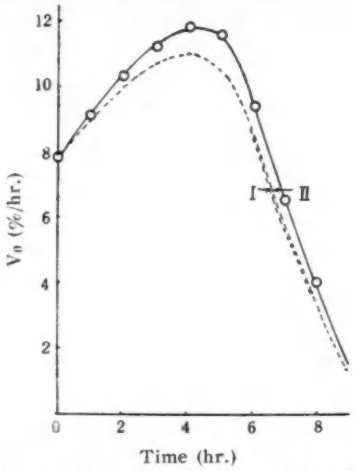

Fig. 2. Variation of the rate V_0 during the continuous polymerization at 20°C.

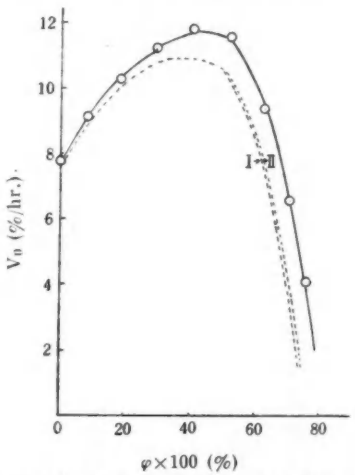

Fig. 3. Variation of the rate V_0 with conversion at 20°C.

TABLE I

COMPARISON OF CALCULATED CONVERSION WITH MEASURED ONE

Uncorr.	1st Corr.	2nd Corr.	Meas.
78.80%	73.60%	73.80%	75.20%

From these results it is seen that the first correction is good enough for use, within the experimental error. Therefore the first corrected values of V_0 and φ will be used hereafter.

The variation of the rate with intensity of irradiation at various stages of the reaction is shown in Fig. 4. From this figure, the exponent is 0.5 until 49.80% conversion. As polymerization proceeds over this conversion, the exponent exceeds 0.5, therefore the theory described in

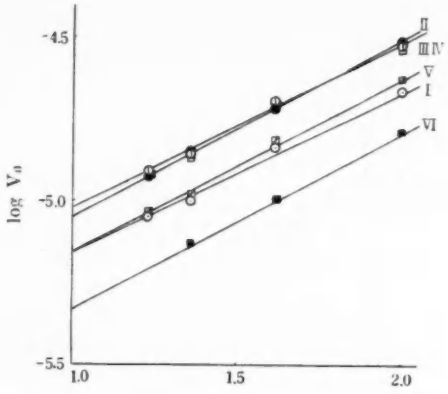

Fig. 4. Variation of the rate with the light intensity at 20°C, where V_0 is expressed in the unit of sec^{-1}.
○ Curve I, at 0% conversion; ◐ Curve II, at 28.15% conversion; ● Curve III, at 39.00% conversion; □ Curve IV, at 49.80% conversion; ▨ Curve V, at 59.30% conversion; ■ Curve VI, at 66.40% conversion.

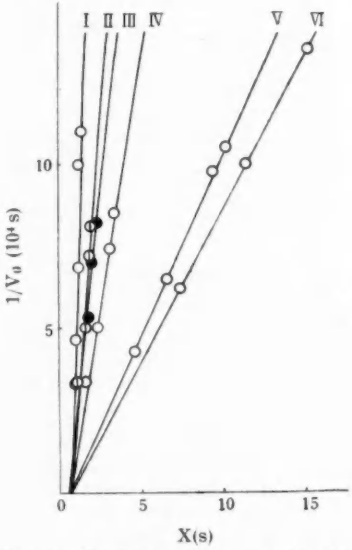

Fig. 5. Variation of the rate V_0 with the measured intercept at 20°C.
○ Curve I, at 0% conversion; ◐ Curve II, at 28.15% conversion; ● Curve III, at 39.00% conversion; ○ Curve IV, at 49.80% conversion; ○ Curve V, at 59.30% conversion; ○ Curve VI, at 66.43% conversion.

the first paper of this series cannot be applied correctly and the results at later stages are less accurate than those at initial stages.

The variation of the rate with the measured intercept X is shown in Fig. 5. From this intercept, the instrument's lag in response can be obtained and is 0.6–0.9 sec. From the slope of this line the values of k_p/k_t can be calculated. But at the conversion of 71.10%, the linearity between X and $1/V_0$ cannot be seen, because the lifetime becomes greater and velocity becomes slower. The values of V_0 and X at this conversion are shown in Table II.

TABLE II

VARIATION OF RATE AND LIFETIME WITH INTENSITY OF IRRADIATION AT 20°C AND AT 71.10% CONVERSION

Light Intensity	$V_0(s^{-1})$	$X(s)$	k_p/k_t
100	1.00×10^{-5}	14.5	20.0×10^{-5}
46	0.62×10^{-5}	19.7	19.0×10^{-5}
		Average	18.5×10^{-5}

The value of k_p/k_t in Table II is calculated by assuming that instrument's lag in response C in equation $X=C+(k_p/k_t)\times(1/V_0)\times\ln 2$ is 0.7 sec. The k_p/k_t value at various conversions is summarized in Table III.

TABLE III

THE VALUE OF k_p/k_t AT VARIOUS CONVERSION AT 20°C

Conversion (%)	$k_p/k_t\times10^{-5}$
0	1.08
28.15	2.02
39.00	2.72
49.80	4.78
59.30	13.1
66.40	16.3
71.10	18.5

The variation of rate V_0 with the extent of conversion at 30°C and 40°C is shown in Fig. 6.

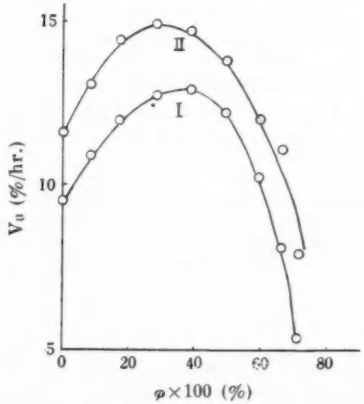

Fig. 6. Variation of the rate V_0 with conversion at 30°C and 40°C.
Curve I, at 30°C; Curve II, at 40°C.

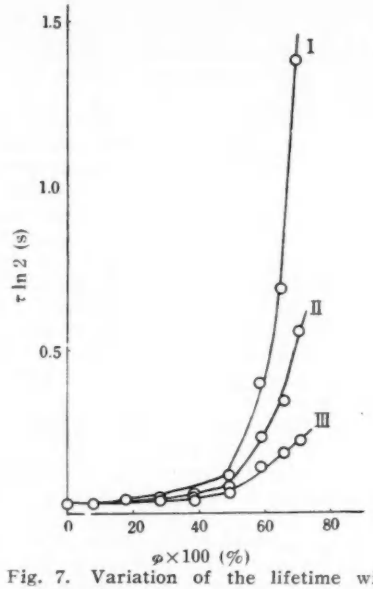

Fig. 7. Variation of the lifetime with conversion.
Curve I, at 20°C; Curve II, at 30°C; Curve III, at 40°C.

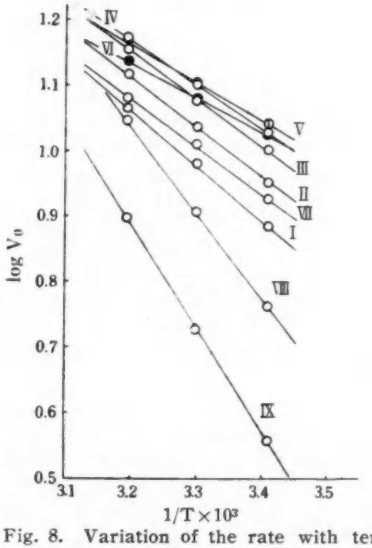

Fig. 8. Variation of the rate with temperature, where V_0 is expressed in the unit of %/hr.
Curve, I, at 0% conversion; Curve II, at 8.3% conversion; Curve III, at 17.8% conversion; Curve IV, at 28.15% conversion; ⓘ Curve V, at 39.00% conversion; ● Curve VI, at 49.80% conversion; Curve VII, at 59.30% conversion; Curve VIII, at 66.40% conversion; Curve IX, at 71.10% conversion.

where φ is the first corrected value. At these temperatures, the measurement of rate and lifetime at various light intensities was not carried out and the instrument's lag was unknown. But by using the lag at 20°C, the value of the lifetime was calculated according to the equation $X=C+\tau \ln 2$. The value of $\tau \ln 2$ at various conversions is shown in Fig. 7. The lifetime does not vary remarkably until 50% conversion is attained, but beyond this point it increases rapidly.

From Figs. 3 and 6 the variation of the rate with temperature can be obtained as shown in Fig. 8. And from Fig. 7 the variation of the lifetime with the temperature can be obtained as shown in Fig. 9.

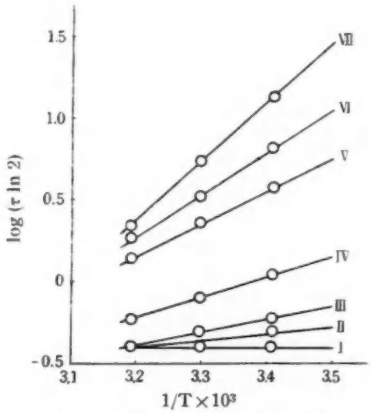

Fig. 9. Variation of the lifetime with temperature.
I, at 17.8% conversion; II, at 28.15% conversion; III, at 39.00% conversion IV, at 49.80% conversion; V, at 59.30% conversion; VI, at 66.40% conversion; VII, at 71.10% conversion.

Discussion

Because the value of k_p/k_t in Table III is calculated by using V_0 of Eq. (4), it is neccessary to correct these values by using the true fractional rate V. From Eqs. (1) and (4) V can be expressed as follows.

$$V=V_0\times(M_0/M)=V_0/(1-\varphi) \qquad (8)$$

Since $k_p/k_t=V\times\tau$, the true k_p/k_t values can be obtained through multiplication $1/(1-\varphi)$ by the values of Table III. These values are summarized in Table IV, comparing with Melville's results[2].

From both the results it is clear that the value of k_a/k_t increases gradually until 50% conversion and beyond this point increases rapidly. But the author's values are lower than the values obtained by Melville.

The overall activation energy $E_p-\frac{1}{2}E_t$ and activation energy of termination E_t are

obtained from figures 7 and 8 and compared with Melville's values[2] in Table V.

TABLE IV
THE CORRECTED VALUE OF k_p/k_t COMPARED WITH MELVILLE'S VALUE AT VARIOUS CONVERSIONS

Conversion	$k_p/k_t \times 10^5$	
%	This Work[a]	Thermocouple Method[b]
0	1.08	
4		3.72
23		10.2
28.15	2.82	
39.00	4.13	
46		22.1
49.80	9.55	
57		82.8
59.30	32.3	
65		75
66.40	48.6	
71.10	64.2	

a) This measurement was carried out at 20°C.
b) This measurement was carried out at 25°C.

TABLE V
THE VALUE OF $E_p - 1/2\ E_t$, E_t AND E_p AT VARIOUS CONVERSIONS, COMPARED WITH MELVILLE'S VALUE

Conversion	$E_p - \frac{1}{2} E_t$ (kcal./mol.)		E_t (kcal./mol.)		E_p (kcal./mol.)	
(%)	This Work	Melville	This Work	Melville	This Work	Melville
0	3.7		0		3.7	
4		4.2		<1		≥4.2
6		4.2		<1		≥4.2
8.3	3.4		0		3.4	
17.8	3.4		0		3.4	
20		4.0		—		≥4.0
23		3.5		1.4		4.2
28.15	2.8		2.2		3.9	
39.00	2.6		3.8		4.5	
46		1.9		3.4		3.6
49.80	2.5		5.6		5.3	
54		2.0		10.8		7.4
57		2.7		11.8		8.6
59.30	3.3		9.4		8.0	
65		>4.9		>13.0		>11.4
66.40	6.0		12.2		12.1	
71.10	7.2		16.8		15.6	
73		>6.7		>15.4		>14.4

Where E_p is calculated from $E_p - 1/2\ E_t$ and E_t. In both values, the overall energy of activation remains constant up to 20% conversion and then gradually decreases to a minimum value in the region of 50% conversion. It then increases rapidly beyond this region. The activation energy of termination is very low at the initial stages but it gradually increases at 20–30% conversion and then increases through the polymerization. On the other hand, the activation energy of propagation remains constant until 40–50% is reached and then increases very rapidly as further polymerization takes place.

Although differences between the author's and Melville's values are, to some extent, observed in Tables IV and V, the qualitative tendency coincides satisfactorily in spite of the differences of methods and temperature.

From these results, it seems that as the polymerization proceeds, increasing viscosity effects the termination process to slow down, but the effect of viscosity upon the propagation process is not so marked and becomes appreciable only at high conversions. But this conclusion must be proved by further study and in the next paper the author will describe the variation of k_p and k_t with the extent of polymerization.

Summary

The author used a thermistor method to study the later stages of polymerization of vinyl acetate, which was photosensitized with 1,1'-azobiscyclohexanecarbonitrile and obtained the variation of k_p/k_t, E_p and E_t with conversion.

From these results it was observed that the value of k_p/k_t increases gradually until about 50% conversion is reached and beyond this point increases rapidly. At the same time, the extent of conversion effects E_t in the region of 20–30% conversion, but the effect upon E_p is not so marked in these stages and becomes appreciable at high conversions.

The author wishes to express his hearty thanks to Dr. Momotaro Suzuki of this Academy for his helpful advice and encouragement and Mr. Shinichi Taira of Tokyo Metropolitan University for his kind supply of 1,1'-azobiscyclohexanecarbonitrile.

Department of Chemistry
Defense Academy
Yokosuka

The Reaction between Diphenylalkanes and Maleic Anhydride by the Friedel and Crafts Method

By Wataru KOGA

(Received April 25, 1956)

Introduction

It is a well-known fact that the Friedel and Crafts reaction between maleic anhydride and an aromatic compound results in the formation of a β-aroylacrylic acid. For example, benzene reacts with maleic anhydride to produce β-benzoylacrylic acid. In this case, an excess of maleic anhydride does not lead to the production of any detectable quantity of acids of the types, $C_6H_4(COCH=CHCOOH)_2$, $C_6H_3(COCH=CHCOOH)_3$, etc., nor can such products be obtained by the action of maleic anhydride on benzoylacrylic acid in any solvent with alminum chloride as catalyst[1]. This is also the case in the reaction between maleic anhydride and diphenyl[2]. This fact is illustrated as an E-effect of a carbonyl group by the electronic theory. Therefore, it is expected that the reaction between maleic anhydride and such a compound as one in which two benzene rings are separated by some methylene groups, e. g. diphenylmethane or bibenzyl, should result in substitution of each benzene ring by $-COCH=CHCOOH$ radicals. But some investigators[3] reported that the reaction between diphenylmethane and succinic anhydride, similarly to the reaction under consideration, gave only β-(p-benzyl) benzoyl propionic acid. On the other hand, there are some reports which support the first opinion. For instance, in addition to $C_6H_5-(CH_2)_n-C_6H_4COOH$ (n is 1 or 2), Liebermann[4], and Liebermann and Zsuffa[5] obtained $HOOCC_6H_4-(CH_2)_n-C_6H_4COOH$ (n is 1 or 2) by the reaction of diphenylmethane or bibenzyl and oxalyl chloride, and Duval[6] produced p-benzylacetophenone and p,p'-diacetyldiphenylmethane from diphenylmethane and acetyl chloride by the Friedel and Grafts reaction. But hitherto the reaction of diphenylalkanes and maleic anhydride has not been reported.

Now, in the present work the Friedel and Crafts reaction between diphenylmethane and bibenzyl, and maleic anhydride were studied, and diphenylmethane-4, 4'-di-γ-oxocrotonic acid and bibenzyl-4, 4'-di-γ-oxocrotonic acid were obtained respectively. The reduction of these compounds by zinc and acetic acid was examined and diphenylmethane-4, 4'-di-γ-oxobutyric acid and bibenzyl-4, 4'-di-γ-oxobutyric acid respectively were obtained. Furthermore these saturated ketoacids were reduced by a modified Clemmensen reduction method to diphenylmethane-4, 4'-dibutyric acid and bibenzyl-4, 4'-dibutyric acid, respectively.

Experimental Part

(1) Synthesis of Diphenylmethane and Bibenzyl.—a) Diphenylmethane was produced by the reaction between benzyl chloride and benzene in the presence of aluminium amalgam as catalyst according to the method of Hartman and Phillips[7]. The reaction product was purified by fractional distillation under reduced pressure and distillate boiling at 97–98°C/1.5 mmHg was collected. The yield was 49–54.6% of the theoretical amount.

b) Bibenzyl was produced by the reaction of 1, 2-dichloroethane with benzene in the presence of anhydrous aluminium chloride as catalyst according to the method described in "Organic Synthetic Chemistry"[8]. The reaction product was also purified by fractional distillation under reduced pressure and distillate boiling at 105–6°C/3 mmHg (m.p. 51–52°C) was collected. The yield was 66.2–74.6% of the theoretical amount.

(2) Diphenylmethane-4, 4'-di-γ-oxocrotonic acid.—The Friedel and Crafts condensation of maleic anhydride with various aromatic hydrocarbons was extensively studied by the use of such a solvent as carbon disulfide, nitrobenzene, and chlorinated hydrocarbons or aromatic hydrocarbon itself. It was found in the previous work[9] that 1, 2-dichloroethane gave the best result. So it was also used here as a solvent.

In a 1 l. four-necked, round-bottomed flask fitted with a mechanical stirrer, a reflux condenser, a dropping funnel, and a thermometer, were placed

1) M.T. Bogert and J.T. Ritter, *J. Am. Chem. Soc.*, 47, 526 (1925).
2) H.G. Oddy, *J. Am. Chem. Soc.*, 45, 2156 (1923).
3) J.W. Cook, A.M. Robinson and E.M. Roe, *J. Chem. Soc.*, 1939, 266; L.F. Fieser, et al., *J. Am. Chem. Soc.*, 70, 3201, Table C (1948).
4) C. Liebermann, *Ber.*, 45, 1186 (1912).
5) C. Liebermann and M. Zsuffa, *Ber.*, 45, 852 (1911).
6) M.H. Duval, *Bull. chim. soc.*, [4], 7, 789 (1913).
7) W.W. Hartman and R. Philips, "Organic Syntheses, Coll. Vol.", John Wiley & Sons, Inc., New York, N.Y. (1943), II, p. 232.
8) R. Oda, "Organic Synthetic Chemistry", Kyoritsusha, Tokyo (1949), p. 92.
9) W. Koga, *J. Chem. Soc. Japan (Pure Chem. Sect.)* 76, 1053 (1955).

49 g. (0.5 mol.) of maleic anhydride and 200 g. of dichloroethane. With cooling 105 g. of powdered, anhydrous aluminium chloride was added and stirred for about ten minutes, during which period most of the solid matter went into solution. Forty two grams (0.25 mol.) of diphenylmethane was then added slowly through a dropping funnel with efficient cooling and stirring. During this period the reaction mixture had to be kept below 3°C. After the addition had been completed, stirring was continued for about two hours at 5–6°C; at the end of this period the reaction mixture became very viscous and finally could not be stirred. The reaction mass was poured onto ice and hydrochloric acid and the solvent was removed by steam distillation. After cooling, the solid mass was collected and was dissolved in soda solution. The insoluble mass was filtered and the filtrate was acidified to Congo red by hydrochloric acid. The precipitated diphenylmethane-4, 4′-di-γ-oxocrotonic acid was filtered and washed with water. After drying for a day in vacuum desiccator, it weighed 42–53 g. (46–58% of the theoretical amount). It was purified by recrystallization from ethanol.

The purified acid is straw-yellow needles and melts at 255–6°C (from temperature at 220°C it turns from yellow to brown). It is soluble in hot alcohol and acetic acid but slightly in cold. It is practically insoluble in any other organic solvents or water.

Neutralization equivalent. Found: 304, 303. Calcd.: 308.

Anal. Found: C, 69.29; H, 4.36. Calcd. for $C_{21}H_{16}O_5$: C, 69.23; H, 4.40%.

Oxidation of this acid with alkaline permanganate gave colorlese crystals, which did not melt up to 300°C. The esterification of this acid in methanol gave colorless crystals which melted at 224–5°C (recrystallized from methyl ethyl ketone). This melting point agrees with that of dimethyl ester of benzophenone dicarboxylic acid-4, 4′ reported by Limplicht[10] and Staudinger[11] and analytical data is also in accordance with the calculated value as shown below.

Anal. Found: C, 68.45; H, 4.89. Calcd. for $C_{17}H_{14}O_5$: C, 68.46; H, 4.70%.

Furthermore alkaline fusion of the colorless acid melting above 300°C gave benzoic acid, m.p. 120°C, and terephthalic acid, identified as the methyl ester, m.p. 140–41°C; mixed m.p. 141–42°C.

Dimethyl ester of diphenylmethane-4, 4′-di-γ-oxocrotonic acid was made under the usual variety of conditions. The purified ester is a straw-yellow needle and melts at 128–128.5°C (recrystallized from methyl ethyl ketone).

Anal. Found: C, 70.38; H, 5.03. Calcd. for $C_{23}H_{20}O_5$: C, 70.41; H, 5.10%.

This colored isomeric ester (*trans*) rearranges slowly to the *cis*-isomer when its methyl ethyl ketone solution is exposed to sunlight for a few days. The *cis*-isomer is a colorless needle melting at 84–84.5°C.

(3) Bibenzyl-4, 4′-di-γ-oxocrotonic acid.—Bibenzyl-4, 4′-di-γ-oxocrotonic acid was produced similarly to diphenylmethane-4, 4′-di-γ-oxocrotonic acid. The yield was 56–69 g. (57.8–70.3% of the theoretical amount.)

This acid is practically insoluble in most organic solvents and water. So the purification is carried out in such a way that it was disssolved in soda solution and filtered and the filtrate was acidified by hydrochloric acid, or by the hydrolysis of the purified dimethyl ester of the acid by mineral acid.

The purified acid is a straw-yellow crystal and does not melt up to 300°C.

Nentralization equivalent. Found: 296, 292. Calcd.: 297.

Anal. Found: C, 69.89; H, 4.73. Calcd. for $C_{22}H_{18}O_5$: C, 69.84; H, 4.76%.

Oxidation of this acid with alkaline permanganate gave terephthalic acid, identified as the methyl ester, m.p. 140–41°C, mixed m.p. 141–42°C.

Dimethyl ester is formed in the same way as above. The purified ester is a straw-yellow needle melting at 137–8°C (recrystallized from methyl ethyl ketone).

Anal. Found: C, 70.88; H, 5.38. Calcd. for $C_{24}H_{22}O_5$: C, 70.94; H, 5.42%.

This colored isomer (*trnas*) also rearranges to the *cis*-isomer when its methyl ethyl ketone solution is exposed to sunlight for a few days. The *cis*-isomer is a colorless needle melting at 175.5–6.5°C.

(4) Diphenylmethane-4, 4′-di-γ-oxobutyric acid.—Ten grams of diphenylmethane-4, 4′-di-γ-oxocrotonic acid was suspended in 80 g. of acetic acid and to this was added a small portion of 15 g. of zinc dust with stirring After threee to four hours the reaction mixture became colorless; then it was poured in 1 l. of soda solution and dissolved. The insoluble mass was filtered and the filtrate was acidified with hydrochloric acid. The precipitated diphenylmethane-4, 4′-di-γ-oxobutyric acid was filtered and washed with water. After drying, it was purified by recrystallization from ethanol. The yield was 6.2–7.5 g. (61.3–74.3% for theoretical amount). The purified acid is a colorless needle melting at 224–5°C.

Anal. Found: C, 68.45; H, 5.56. Calcd. for $C_{21}H_{20}O_5$: C, 68.48; H, 5.43%.

Dimethyl ester is formed by refluxing methanol solution of the acid in the presence of concentrated sulfuric acid as catalyst. The purified ester (recrystallized from methanol) is a colorless thin plate and melts at 95°C.

Anal. Found: C, 69.23, H, 6.11. Calcd. for $C_{23}H_{24}O_5$: C, 69.70; H, 6.06%.

(5) Bibenzyl-4, 4′-di-γ-oxobutyric acid.—The reduction of the diphenylethane-4, 4′-di-γ-oxocrotonic acid was carried out in the same way as above. The yield was 5.5–7.6 g. (54.4–75.2% for theoretical amount). The purified acid is a colorless needle (recrystallized from a large amount of ethanol) and melts at 259–60°C.

10) H. Limpricht, *Ann.*, **312**, 97 (1900).
11) H. Staudinger and G.A.R. Kon, *Ann.*, **384**, 98 (1911).

Anal. Found: C, 69.06; H, 5.58. Calcd. for $C_{24}H_{22}O_5$: C, 69.11; H, 5.76%.

Dimethyl ester is formed by refluxing suspension of the acid in methanol in the presence of a small amount of concentrated sulfuric acid as catalyst. The purified ester (recrystallized from methyl ethyl ketone) is a colorless needle melting at 114.5°C.

Anal. Found: C, 70.40; H, 6.36. Calcd. for $C_{24}H_{26}O_5$: C, 70.24; H, 6.34%.

(6) Diphenylmethane-4, 4′-dibutyric acid and Bibenzyl-4, 4′-dibutyric acid.—The reduction of the carbonyl group of the above saturated keto acids according to Clemmensen's method or modified Martin-Clemmensen's method was unsuccessful, for these acids were insoluble in water, hydrochloric acid, or toluene. So the reduction was carried out according to Koelsch[12] who used ethanol as a solvent.

To the mixture of 45 cc. of ethanol, 45 cc. of concentrated hydrochloric acid, and amalgamated zinc, which was prepared from 15 g. of zinc dust and 1.5 g. of murcuric chloride, 5 g. of the acid, which should be reduced, was added and then was refluxed for one hour. A second portion of 45 cc. of concentrated hydrochloric acid was then added and refluxing was continued for six hours. The mixture was cooled and the solid mass was collected and dissolved in boilling 500 cc. of 5% aqueous sodium hydroxide. After filtration and acidification of the filtrate, the reduced acid was separated. It was purified recrystallization from ethanol.

Diphenylmethane-4, 4′-dibutyric acid.—The yield was 2.5–2.7 g. (54.1–58.4% for theoretical amount). Colorless needles, m.p. 199.5–200°C.

12) C.F. Koelsch, *J. Am. Chem. Soc.*, **55**, 3885 (1933).

Anal. Found: C, 73.76; H, 6.97. Calcd. for $C_{21}H_{24}O_4$: C, 74.12; H, 7.06%.

Bibenzyl-4, 4′-dibutyric acid.—The yield was 2.2–2.5 g. (54.1–58.4% for theoretical amount). Colorless needles, m.p. 182–3°.

Anal. Found: C, 74.86; H, 7.44. Calcd. for $C_{22}H_{24}O_4$: C, 74.58; H, 7.36%.

Summary

(1) By the reaction of diphenylmethane and diphenylethane with maleic anhydride in the presence of aluminium chloride, diphenylmethane-4, 4′-di-γ-oxocrotonic acid and bibenzyl-4, 4′-di-γ-oxocrotonic acid were produced, respectively. And *cis* and *trans* isomers of dimethyl esters of these acids were prepared.

(2) By the reduction of the above two acids by zinc and acetic acid, diphenylmethane-4, 4′-di-γ-oxobutyric acid and bibenzyl-4, 4′-di-γ-oxobutyric acid were prepared.

(3) These saturated keto acids were reduced by amalgamated zinc in the mixture of ethanol and hydrochloric acid to diphenylmethane-4, 4′-dibutyric acid and diphenylethane-4, 4′-dibutyric acid.

The author wish to express his gratitude to Dr. Tomoyoshi Miura and Dr. Shiro Tsuruta for their helpful advice in performing these experiments.

Hitachi Research Laboratory, Hitachi Ltd., Hitachi

A New Method for Radiochemical Prospecting of Uranium Ore. I. Estimation of the Amount of Uranium

By Yūji YOKOYAMA

(Received April 2, 1956)

Introduction

The economic importance of uranium and thorium has been stimulating extensive investigations of terrestrial occurrence and distribution of these elements. One of the important parts of these investigations is prospecting for uranium and thorium ores.

For many years, radioactive survey with a Geiger-Müller counter has been extensively used for this purpose. Recently, the development of a scintillation counter has made it possible to prospect radioactive deposits by the airborne radioactive survey.

However, these methods are effective only for the cases in which a uranium deposit is cropping out on the surface of the ground, because gamma radiation from these elements can not penetrate thick layers of rocks and soils. Furthermore, it is considerably difficult to distinguish between uranium and thorium ores by these methods.

Therefore, practically there has been no method to prospect and evaluate an underground uranium deposit without a test boring of the ground. The aim in the present work is to establish a new radiochemical method in which naturally radioactive elements in natural waters are used as a kind of tracer for the purpose of estimating the amount and the depth of uranium layer under the ground.

It is well known that the uranium content of mineral waters is less than that of sea water, but radon and radium content of some mineral waters is much higher than that of sea water. (Table I)

TABLE I
RADIOACTIVE ELEMENTS IN NATURAL WATERS

	U (g./l.)	Ra (g./l.)	Rn (curie/l.)
Sea Water[1]	10^{-6}	10^{-13} to 10^{-14}	10^{-13}
Mineral Water[2]			
Hot Spring			
Arima	10^{-6} to 10^{-7}	10^{-10}	10^{-10}
Mineral Spring			
Masutomi	10^{-7} to 10^{-8}	10^{-11} to 10^{-12}	10^{-8} to 10^{-10}

The content of radon and radium in mineral waters could be explained as follows; mineral water passes through a uranium-rich layer under the ground, dissolving radon and radium which have greater solubility than their ancestors. Based on these facts, the author considered that the radiochemical studies of mineral waters can be used as a tool for prospecting a uranium-rich layer under the ground.

The Presence of Two Radioactive Strata

It has been suggested, in some of the previous reports[3], that there must be two radioactive strata under the ground of mineral springs. A deep stratum, which is probably related to the uranium or thorium ores, may be located at a depth of the order of several kilometers. This stratum is considered as a supplying zone of radium and its isotopes, such as thorium X, mesothorium 1 and actinium X, for mineral waters. The other radioactive stratum, which is considered to be the source of radon and thoron for mineral waters, is located very close to the surface of the earth at a depth from 10 to 50 meters below the ground.

When radium-containing mineral waters come close to the surface of the earth, deposition of the sinter deposits takes place, which is caused by the escape of carbon dioxide, contact with air, decrease in temperature etc. Then a part of radium and its isotopes is precipitated with sinter deposits.

The porous zones of the sinter deposits, which are as radioactive as ordinary radioactive minerals such as monazite, etc., are often found in the areas of radioactive springs. The radio activity of sinter deposits is mainly due to radium and its isotopes, and it is a very important fact that the uranium content of these deposits is much lower than the value expected from radium content. For example, the uranium content of sinter deposits from a mineral spring in Japan ranges from 0.004 to 0.05 p. p. m.[4] (both extremes for Masutomi Mineral Springs), whereas these sinter deposits contain about 10^{-10} g. Ra per gram.

The very low content of uranium in mineral waters and sinter deposits was apt to lead us to a faulty conclusion that there was probably no uranium-rich ore in the areas of radioactive springs of Japan. But the occurrence of a remarkably uraniumbearing layer is concluded by the author's present estimation.

Estimation of the Amount of Uranium Reserves

It is possible to estimate the amount of uranium, which occurs in a supplying zone of radium, by calculating the amount of supply of radium to mineral waters per second. The estimation may be carried out by two different ways.

In the first one, it is assumed that the atoms of radium, which are generated by the radioactive decay of uranium, are directly supplied into mineral waters.

The amount of radium, G_{Ra} which is generated from 1 g. of uranium per second, is calculated as follows.

$$G_{Ra} = \frac{226}{238}\lambda_U = 4.6\times10^{-18}\ \text{g./sec.} \qquad (1)$$

where λ_U is a decay constant of uranium and 226 and 238 are mass number of radium and uranium respectively.

On the other hand, the amount of radium,

1) F. Herneggar, *Anz. Akad. Wis. Wien*, **1**, 19 (1933), R.D. Evans, A.F. Kip and E.G. Moberg, *Am. J. Sci.*, **36**, 241 (1938), I. Iwasaki and T. Ishimori, *J. Chem. Soc. Japan*, **72**, 14 (1951), M. Nakanishi, This Bulletin, **24**, 36 (1951), E. Rona and W.D. Urry, *Am. J. Sci.*, **250**, 241 (1952).

2) T. Nakai, This Bulletin, **15**, 333 (1940), P.K. Kuroda and Y. Yokoyama, ibid., **22**, 34, 43 (1949), M. Nakanishi, ibid., **24**, 33 (1951), Y. Yokoyama, *J. Chem. Soc. Japan*, **76**, 558 (1955).

3) P.K. Kuroda and Y. Yokoyama, This Bulletin, **21**, 52, 58 (1948); **22**, 34, 43 (1949); *Anal. Chem.*, **26**, 1509 (1954); Y. Yokoyama, *J. Chem. Soc. Japan*, **70**, 399 (1949).

4) M. Nakanishi, This Bulletin, **24**, 33 (1951).

which is supplied into mineral waters per second, is $C_{Ra} \cdot F$, where C_{Ra} is the radium content of mineral waters (g./l.), and F is the amount of flow (l./sec.).

From the supplying rate of radium, therefore, one can expect that the following amount of uranium, W, is present in supply zone.

$$W = \frac{C_{Ra} \cdot F}{G_{Ra} \cdot K} \text{ g.} \quad (2)$$

where K is a dissolving coefficient of radium into mineral waters from uranium ore. In the case of perfect dissolving, the value of K is 1.00.

For example, in Hot Spring Arima, which has the highest radium content in Japan, C_{Ra} is 2×10^{-10} g./l. and F is 5 l./sec. Then one can obtain the following equation.

$$W = \frac{2\times10^{-10}\times5}{4.6\times10^{-18}\times K} = \frac{2\times10^{8}\text{g.}}{K} = \frac{200\text{ ton}}{K} \quad (3)$$

From the foregoing calculation, one might expect that 200 ton or 2,000 ton of uranium is present under the ground of Hot Spring Arima, on the assumption that K=1.00 or 0.10 respectively.

The exact value of K is unknown, but it may be not unreasonable to suppose that the value of K is of the order of 0.1. It was found by the present author that mineral waters contain usually a comparable amount of thorium X with mesothorium 1[5].

Table II

Isotopes of radium in mineral waters

Name of Spring		^{226}Ra 10^{-12} c./l.	^{224}Ra(Th X) 10^{-12} c./l.	^{228}Ra(MsTh I) 10^{-12} c./l.	^{225}Ra(Ac X) 10^{-12} c./l.	Th X/MsTh I
Arima	Shin-onsen	170±5	560±20	580±10	9±0.5	0.97±0.04
〃	Ariake-no-yu	170±7	310±10	380±20	9±0.9	0.82±0.05
Ikeda	No. 1	33±1	100±2	85±8	——	1.18±0.07
〃	No. 2	36±3	113±12	53±7	——	2.12±0.36
Masutomi	A 5	66±3	200±7	230±10	——	0.87±0.05
〃	B 7	24±1	66±2	240±1	1.3±0.1	3.6 ±0.1
Misasa	Misasa-kan	14±1	34±2	38±4	——	0.90±0.11
〃	Ōhashi-sotoyu	9±2	95±6	30±6	——	3.2 ±0.7
Tamagawa	Ōbuki	16±1	144±2	109±3	——	1.32±0.04
〃	Kobuki	24±0.5	160±6	131±2	——	1.22±0.05

Table III

Amount of uranium estimated by radiochemical method

Name of Spring	Pref.	Ra Content 10^{-12} g./l.	Amount of flow l./sec.	Ra Discharge 10^{-12} g./sec.	Amount of Uranium K=1.00 ton	Amount of Uranium K=0.10 ton
Springs with Ra Content $> 10^{-11}$ g./l.						
Tamagawa	Akita	20	150	3,000	700	7,000
Arima	Hyōgo	300	5	1,000	200	2,000
Masutomi	Yamanashi	30	2	60	10	100
Matsunoyama	Niigata	15	4	60	10	100
Misasa	Tottori	15	3	45	10	100
Yugakae	Shimane	30	1	30	7	70
Ikeda	Shimane	40	0.25	10	2	20
Takarazuka	Hyōgo	25	0.4	10	2	20
Isobe	Gumma	15	0.3	5	1	10
Springs with Ra Content $\leq 10^{-11}$ g./l.						
Onogawa	Yamagata	8	600	4,800	1,000	10,000
Toyotomi	Hokkaido	10	300	3,000	700	7,000
Yuzaki	Wakayama	8	15	120	30	300
Kawatana	Yamaguchi	10	8	80	20	200
Wakura	Ishikawa	5	10	50	10	100
Ōshio	Fukushima	4	3	12	3	30

5) Y Yokoyama, *J. Chem. Soc. Japan*, **76**, 558 (1955).

This fact indicates that the dissolving coefficient of radium and its isotopes is not very large. The reason can be explained as follows. If mesothorium 1 dissolves prefectly into mineral waters, it would be impossible to supply thorium X in mineral waters from supply zone. Because, in such case, no mesothorium 1 and its descendants (radiothorium and thorium X etc.) are present in supply zone.

Another method of calculation for the amount of uranium is as follows.

It is assumed that at first, uranium of supply zone is in radioactive equilibrium with radium, then mineral waters dissolve radium. The amount of radium, which is in equilibrium with 1 g. of uranium, is

$$E_{Ra} = \frac{\lambda_U \cdot 226}{\lambda_{Ra} \cdot 238} = 3.4 \times 10^{-7}\ \text{g.} \qquad (4)$$

where λ_U and λ_{Ra} are decay constants of uranium and radium respectively.

During the time interval T second, the amount of radium brought to the surface of the earth by mineral waters is $C_{Ra} \cdot F \cdot T$(g.). From the total supplying amount of radium, therefore, one can expect that the following amount of uranium, W', is present in the supply zone.

$$W' = \frac{C_{Ra} \cdot F \cdot T}{E_{Ra} \cdot K'} \qquad (5)$$

where K' is a portion of radium, which is soluble in mineral waters, to total radium.

For example, on Hot Spring Arima, assuming $T=100$ year (3×10^9 sec.) and $T=1{,}000$ year (3×10^{10} sec.) we get

$$W' = \frac{2\times10^{-10}\times5\times3\times10^{9}\text{g.}}{3.4\times10^{-7}\times K'} = \frac{10\ \text{ton}}{K'}, \text{ for } T=100 \text{ year},$$

$$W' = \frac{2\times10^{-10}\times5\times3\times10^{10}\text{g.}}{3.4\times10^{-7}\times K'} = \frac{100\ \text{ton}}{K'}, \text{ for } T=1{,}000 \text{ year} \qquad (6)$$

The foregoing calculation shows that the value of W' in Eq. (6) becomes close to the value of W in Eq. (3) when the time interval T is as long as the order of the half life of radium (1622 years). Therefore these two calculating methods will give practically the same value, if issue of mineral waters continues during some long time in which a kind of equilibrium state takes place between leaching and supplying of radium. More general discussions about these points will be reported in future in detail. But it may be supposed that the times required for equilibrium will be shorter than the values expected from the half life of radium, because those times are determined not with physical half life but with actual half life in which geochemical half life by leaching effect is also considered.

Using Eq. (2), the author estimates the amount of uranium in the supplying zone of the main mineral springs, containing radium, in Japan. The results are shown in Table III. It must be noticed that the amount of uranium, calculated in this way, is not the weight of minerals but the weight of uranium metal only. In Table III, two values are shown for the amount of uranium, where K is supposed to be 1.00 and 0.10.

The largest amount of uranium ore in Japan, discovered in the past, is Suishō-yama at Ishikawa, Fukushima Pref. The amount of uranium reserves in Suishō-yama is estimated as about 1 to 2 ton as uranium metals, or 2,000 to 4,000 ton as minerals. The mean uranium content of ore is estimated as 0.05% in Suishō-yama.

It is found in Table III that the amounts of uranium in some mineral-spring areas estimated by the author, are very much higher than that of Suishō-yama.

Recently a new uranium deposit has been discovered at Ogamo Mine near the Hot Spring Misasa, which is one of the largest radioactive springs in Japan. This fact may support the author's opinion.

Summary

A radiochemical method for the prospecting and the estimation of the amount of uranium layer under the ground based upon the determination of radium in mineral waters, is described. Results show, 700 to 7,000 ton of uranium may occur in Hot Spring Tamagawa and 200 to 2,000 ton of uranium in Hot Spring Arima. The natural radioactive elements in mineral waters will give valuable information on the geological structures, especially the nature of the underground radioactive strata.

The authour expresses his hearty thanks to Prof. Kenjirō Kimura of the University of Tokyo for his kind guidance in the course of this study, to Prof. Masatake Kozaki of Yokohama National University, to Dr. Paul K. Kuroda of the University of Arkansas, to Dr. Nobufusa Saitō of the University of Tokyo and Dr. Jean Delloue of the Atomic Energy Committee of France for their valuable advice and encouragement.

Faculty of Liberal Arts and Education
Yokohama National University
Kamakura

The Adsorption of Water Vapor by Gelatin-Detergent Complexes

By Kunio TAMAKI and Bun-ichi TAMAMUSHI

(Received May 29, 1956)

In the previous investigation[1] on the interaction of gelatin with detergent anions or cations, we have found that hydrophobic complexes are formed between them under appropriate conditions. Observing the sedimentation velocity as well as the sedimentation volume in both cases of gelatin-detergent anion complex and gelatin-detergent cation complex, it has been found that the sedimentation velocity of the former complex is greater than that of the latter, while the sedimentation volume of the former is smaller than that of the latter. This suggests that there must be some difference in the hydrophobic nature of these two types of complexes. It is the purpose of this paper to detect such a difference by measuring the adsorption of water vapor by these two types of complexes.

Experimental

Materials.—Gelatin, sodium dodecyl sulfate and dodecyl ammonium chloride used in this experiment are the same samples as used in the previous work[1].

Samples for Adsorption Experiments.—The gelatin, purified by use of ion exchange resins, was precipitated by the addition of methanol to its aqueous solution, and the precipitate was dried in a vacuum desiccator. The detergent-gelatin complex was separated from the solution by centrifugation after the precipitate was formed, repeatedly washed with water and centrifugated, and then dried in a vacuum desiccator. The nitrogen content of the complex was determined by the Kjeldahl method. As the complex may be considered as a compound between gelatin molecule and dodecyl sulfate ion ($C_{12}H_{25}OSO_3^-$= 265.4) or dodecyl ammonium ion ($C_{12}H_{25}NH_3^+$= 186.3), the detergent content in the complex is calculated from the nitrogen percentage. The combined detergent, calculated in this way, was found to agree very well with that obtained by direct analysis in the previous investigation[1]. The data are given in Table I.

TABLE I

	Sample	pH of Solution	Nitrogen Content (%)	Detergent Content (mM/g. Gel.) Cal.	Detergent Content (mM/g. Gel.) Exp.	Gelatin Content (%)
No. 1	Pure Gelatin	4.8	16.26	0	0	100
2	Gelatin-Dodecyl	2.0	12.96	0.96	0.92	79.7
3	Sulfate Ion	3.6	13.80	0.67	0.68	84.9
4	Complex	4.0	14.70	0.40	0.40	90.4
5	Gelatin-Dodecyl	8.0	15.56	0.41	0.40	92.8
6	Ammonium Ion	9.3	15.20	0.65	0.63	89.2
7	Complex	10.6	14.80	0.94	0.98	85.0

Adsorption Experiment.—Adsorption experiment was carried out by the desiccator method similar to that adopted by H. Bull[2], who first studied in detail the adsorption of water vapor by several purified proteins. A definite quantity —between 0.5 g. and 0.9 g.—of each samples of complexes was taken in a weighing bottle, which was then placed in a desiccator containing sulfuric acid of a definite concentration. The desiccator was submerged in a thermostat maintained at 25±0.1°C. After the attainment of the equilibrium, the weighing bottle was weighed, and the density of the sulfuric acid was measured, from which the relative vapor pressure was calculated. The amount of the water vapor adsorbed by a given weight of protein was obtained from the increase in weight of the weighing bottle. In order to allow for the dilution effect of the added detergent, the amount of adsorbed water was calculated on the basis of protein portion.

According to Bull[2], it requires about two weeks for the attainment of equilibrium, but as Robinson[3], Benson et al[4]. have remarked, the equilibrium can be attained in a shorter time, if the adsorption takes place under diminished air pressure. In our experiment, it was sufficient, to wait under the pressure of 10—20 mmHg for about twentyfour hours.

Fig. 1 shows some of the isotherms obtained, one with a sample of pure gelatin and two with samples of different type complexes.

1) K. Tamaki and B. Tamamushi, This Bulletin, 28, 555 (1955).

2) H. Bull, *J. Am. Chem. Soc.*, 66, 1499 (1944).

3) R.A. Robinson, *J. Chem. Soc.*, 1948, 1083.

4) S.W. Benson, D.A. Ellis and R.W. Zwanzig, *J. Am. Chem. Soc.*, 72, 2102 (1950).

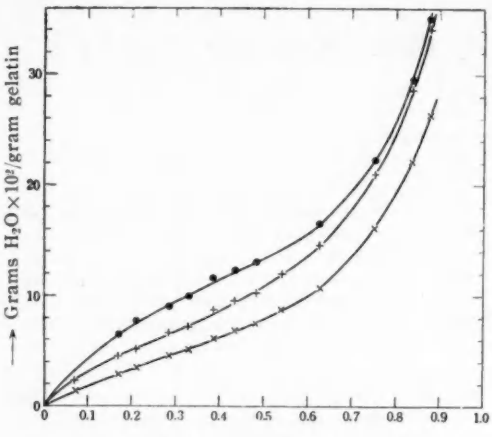

Fig. 1. Water vapor adsorption isotherms
·No. 1; ×No. 2; +No. 7

Discussion

As Fig. 1 indicates, the amount of water vapor adsorbed by gelatin is markedly reduced by the combination of detergent ion with it. However, the amount adsorbed by the gelatin-dodecyl sulfate ion complex is less than that by gelatin-dodecyl ammonium ion complex over the whole range of relative vapor pressures. From this fact, it is concluded that the former is more hydrophobic than the latter, which is in accord with the experimental results obtained in the measurement of sedimentation volume and sedimentation velocity. For both types of complexes, it was found that the complexes containing detergent in greater amount adsorb water vapor in less degree.

As has been reported by many investigators, adsorption isotherms of water vapor on proteins are generally S-shaped, and these are represented by the Brunauer-Emmett-Teller (B.E.T.) equation[5] in the range of relative vapor pressure from 0.05 to 0.5. The isotherms obtained in our experiment have been found too in accord with the B.E.T. theory as shown by Fig. 2. The amount of the first monolayer coverage V_m as well as the constant C in in the B.E.T. equation are listed in Table II.

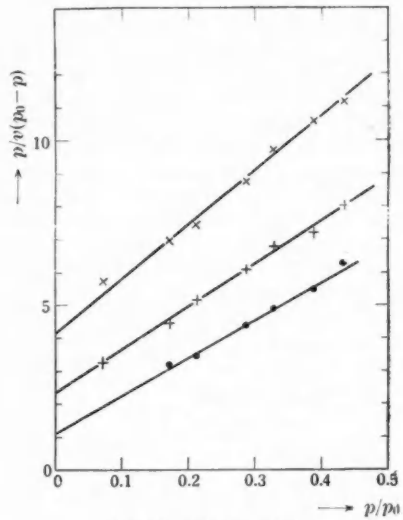

Fig. 2. B.E.T. plot.
·No. 1; ×No. 2; +No. 7

According to Dunford and Morrison[6], the isotherms obtained by Bull[2] are represented by the Harkins-Jura equation[7], while the isotherms obtained in our experiment do not obey that equation except the isotherm for pure gelatin.

Many workers have discussed the mechanism of the adsorption of water on proteins. Pauling[8] suggested that the amount of the first monolayer adsorption V_m could be interpreted in terms of the number of polar

TABLE II

	Sample	($g.H_2O$/g. Gel.) V_m	C	Decrease in V_m (mM/g. Gel.)	Detergent Combined (mM/g. Gel.)
No. 1	Pure Gelatin	0.0821	9.54		
2	Gelatin-Dodecyl	0.0493	4.85	1.82	0.96
3	Sulfate Ion	0.0503	5.73	1.76	0.67
4	Complex	0.0512	6.13	1.71	0.40
5	Gelatin-Dodecyl	0.0654	7.66	0.93	0.41
6	Ammonium Ion	0.0648	7.45	0.96	0.65
7	Complex	0.0632	7.00	1.05	0.94

5) S. Brunauer, P.H. Emmett and E. Teller, ibid., 60, 309 (1938).
6) H.B. Dunford and J.L. Morrison, *Can. J. Chem.*, 32, 558 (1954).
7) W.D. Harkins and G. Jura, *J. Am. Chem. Soc.*, 66, 1366 (1944).
8) L. Pauling, ibid., 67, 555 (1945).

amino-acid side-chains in protein molecules. Benson et al[4]. inferred from their experimental result that the adsorption of water vapor on proteins should be qualitatively different from that of non-polar gases such as nitrogen, and the adsorption of water would take place at specific sites on protein molecules. According to the work of Mellon, Korn and Hoover[9], a reduction in the amount of adsorption takes place over the whole range of relative vapor pressures, when the amino-groups of casein are benzoylated. By the B.E.T. treatment of the data, they have shown that the amount of reduction in V_m roughly correspnds to the amounts benzoylated on the protein molecule. On the other hand, Green and Ang[10] came to the conclusion, on the basis of their study of the adsorption of water vapor by acetyl derivatives of collagen and of silk fibroin, that the change in V_m caused by acetylation is independent of number the of acetyl groups introduced.

As indicated in Table II, there is a certain parallel correlation, but no stoichiometrically definite relation between the reduction in V_m and the amount of the combined detergent in our experimental data. For both complexes, the decrease in V_m is always greater than the amount of combined detergent.

9) E.F. Mellon, A.H. Korn and S.R. Hoover, ibid., 70, 3040 (1948).
10) R.W. Green and K.P. Ang, ibid., 75, 2733 (1953).

Summary

1. The adsorption of water vapor by gelatin-dodecyl sulfate ion complexes and gelatin-dodecyl ammonium ion complexes has been measured.
2. The adsorption of water vapor by both those kinds of complexes has been found to be less than that by pure gelatin.
3. The amount of adsorption on the gelatin-dodecyl sulfate ion complexes is always smaller than on the gelatin-dodecyl ammonium ion complexes, and this fact indicates that the former complexes are more hydrophobic than the latter.
4. The adsorption isotherms have been interpreted by the B.E.T. theory and the amount of the first monolayer adsorption has been calculated.
5. In both types of complexes, there is a certain parallel correlation but no stoichiometric relationship between the reduction in the amount of the first monolayer adsorption and the amount of combined detergent.

We should like to express our sincere thanks to Armour and Co., U.S.A. and Nezu Chemical Laboratory, Tokyo, for their kind supply of pure detergents.

Chemistry Department, College of General Education; and Institute of Science and Technology, The University of Tokyo, Tokyo

Dielectric Studies on Colloidal Solutions. II. The Behavior of Small Counter Ions in the Aqueous Solutions of the Hydrochlorides of Homologous Long-chain Amines

By Michio SHIRAI and Bun-ichi TAMAMUSHI

(Received June, 6, 1956)

In the previous work[1] of this series the high-frequency conductivity of aqueous solutions of paraffin-chain salts has been measured and the results have been interpreted in terms of the Debye-Falkenhagen's theory of strong electrolytes. The sudden rise of the high-frequency effect as well as the fall of the low-frequency equivalent conductivity of these solutions have been considered to be due to the electrostatic interaction between ionic micelles and small counter ions. It is, however, probable that some fraction of counter ions associate with the micelle, and consequently, the valence of the ionic micelle does not agree with the number of single ions contained in the micelle. The fraction of counter ions associated with the micelle has been estimated from the data of conductivity and transference number[2,3], from those of electro-

1) M. Shirai and B. Tamamushi, This Bulletin, 28, 545 (1955).

2) G.S. Hartley, B. Collie and C. S. Samis, *Trans. Faraday Soc.*, 32, 785 (1936).
3) A.P. Brady and D.J. Salley, *J. Am. Chem. Soc.*, 70, 914 (1948).

motive force measurement[4], from those of self-diffusion coefficient[3], etc. Chandler and McBain[5] have recently estimated, based on the results of anomalous osmosis, that the effective charge on the micelle is only two or three, whereas Hartley and his collaborators[2] came to the conclusion that the micelles behave as polyvalent ions having a large number of effective charges.

In the present paper we discuss this problem on the basis of the experimental data of low-frequency and high-frequency conductivities, and those of transference number obtained for the hydrochlorides of homologous long-chain amines.

Experimental

Procedure.—The method and apparatus applied for the high-frequency conductivity measurement are the same as described in the previous paper[1].

The determination of transference number was carried out by the moving boundary method. The principle of that method was fully discussed by McInnes et al.[6], and the method suitable for the measurement of transference number of large radical-ions was developed by Hartley et al.[7] A brief outline of the method used in our present work is as follows. The micellar solution which is to be investigated acts as a following solution and potassium chloride solution is used as a leading one. The transference number of the following radical-ion, T_F, is determined by the concentration, C_L, and the transference number of the leading ion, T_L, and the concentration of the following radical-ion left behind the boundary, C_F, according to the following relation:

$$\frac{T_F}{C_F}=\frac{T_L}{C_L}$$

Thus, if C_F is determined, T_F is calculated by using the known values of C_L and T_L[8].

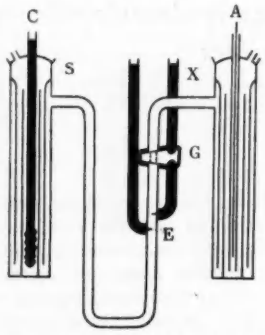

Fig. 1. Moving boundary apparatus.

The apparatus used is shown in Fig. 1. The initial boundary is formed at the position of the stopcock G. The platinum wire C immersed in a strong ferric chloride solution is used as the cathode, while the silver wire A serves as the anode. The electrodes must be nonpolarizable, which condition is fulfilled in this case. The part S of the vessel is filled with potassium chloride solution and the part X with the colloidal electrolyte solution which is to be investigated. After letting electric current flow for a few hours by connecting the apparatus in series with a constant current regulator, the concentration of the colloidal electrolyte solution left behind the boundary is determined by measuring its conductivity. This is performed by using the platinum electrodes E and the alternating-current bridge employing the frequency of 1000 cycle/sec. As it is difficult to measure the high-frequency conductivity at higher temperatures, all these measurements have been carried out at 30°C.

Materials.—Octyl-, decyl-, dodecyl-, tetradecyl-, and hexadecylamine hydrochlorides were prepared from the corresponding amines supplied by Armour & Co., U. S. A., by passing gaseous hydrogen chloride through their benzene solutions. The products were subjected to careful recrystallization from ethanol, and then they were dried in a vacuum desiccator over calcium chloride. All dissolution and dilution processes were carried out with conductivity water but no special precautions were taken to prevent access of carbon dioxide in the transference number measurement.

Results and Discussion

The experimental data of the equivatent conductivity at the frequency of 1000 cycle/sec. and the high-frequency effect at the frequency of 30 Mc./sec. for the electrolytes under investigation are tabulated in Table I, where the high-frequency effect denotes the increase of the equivalent conductivity at the applied high-frequency expressed in terms of the percentage as defined in the previous paper[1]. The measurement of the high-frequency conductivity was carried out only in the range of concentration shown in Table I, on account of the great increase of the conductance in higher concentrations.

The increase of equivalent conductivity at high-frequency is attributable to the relaxation effect of the ionic atmosphere surrounding the micelle ion, and therefore, that increase is expected to be the larger, the greater the electric charge of the micelle, and the smaller its radius. As is seen from Table I, dodecyl-, tetradecyl-, and hexadecylamine hydrochlorides show considerable increase of equivalent conductivity at high-frequency in spite of their large ionic

4) J.W. McBain and M.D. Betz, ibid., 57, 1909 (1935).
5) C. Chandler and J.W. McBain, *J. Phys. & Colloid Chem.*, 53, 930 (1949).
6) D.A. McInnes and L.G. Longsworth, *Chem. Reviews*, 11, 171 (1932).
7) G.S. Hartley, E. Drew and B. Collie, *Trans. Faraday Soc.*, 36, 648 (1934).
8) L.G. Longsworth, *J. Am. Chem. Soc.*, 54, 2741 (1932).

TABLE I

LOW-FREQUENCY CONDUCTIVITY AND HIGH-FREQUENCY EFFECT

Substance	Conc. (mole/1.)	Equivalent Conductivity at 1000 c./sec.	High-frequency Effect at 30 Mc./sec.
Octylamine	0.005	133	0
Hydrochloride	0.01	129	0
	0.02	120	0
	0.05	99	—
	0.1	85	—
	0.2	78.5	—
Decylamine	0.005	122	0
Hydrochloride	0.01	116	0
	0.02	108	0
	0.05	76	—
	0.1	64	—
	0.2	59	—
Dodecylamine	0.005	110	0
Hydrochloride	0.01	105	0
	0.02	75	4.2
	0.05	52	—
Tetradecylamine	0.002	107	0
Hydrochloride	0.005	102	0
	0.01	68	4.5
	0.02	48.5	6.6
Hexadecylamine	0.0001	102	0
Hydrochloride	0.001	100	0
	0.003	64	4.8
	0.005	40.4	8.6

micelles. This result can be accounted for only if the micelles behave themselves as polyvalent ions. In the case of octyl- and decylamine hydrochlorides the high-frequency effect is very small, and this fact can be considered to be due to the imperfect formation of micelles on account of the shortness of their paraffin-chains. Moreover, throughout all these electrolytes, the lower the low-frequency equivatent conductivity, the higher the high-frequency effect. This experimental fact is also in accord with the conclusion that the critical fall of equivalent conductivity is mainly due to the electrostatic interaction between large micelle ions and small counter ions, which has been inferred in the previous paper[1].

The results of transference number measurements are listed in Table II. The values of transference numbers shown in Table III are obtained from those in Table II by interpolation. For all the solutions under investigation, the transference number at an infinite dilution is about 0.2 or 0.3, but it rises very rapidly in the range where the total conductivity falls, and then tends towards a constant value. However, for the solutions of tetradecyl- and hexadecylamine hydrochlorides, the constant values could not be determined on account of their small solubilities. The mobility of each ion in the free state can be determined by using the value of the transference number and that of the equivalent conductivity at an infinite dilution, the result of calculation being shown in the last column of Table II. The mobility of chlorine ion at an infinite dilution for each solution is almost constant as is to be expected.

The critical rise of the transference number should come mainly from the association of counter ions to micelle ions. This association may take place mainly by electrical force in the low potential region around each micelle, because some other interactions, such as chemisorption or van der Waals adsorption, are unlikely to take place, taking into account the small effect of the nature of counter ions on the critical micelle concentration. The fact that the transference number reaches a nearly constant value with increasing concentration can be interpreted as follows: The fraction of counter ions which associate to the micelle will be governed by their

TABLE II

TRANSFERENCE NUMBER

Substance	Conc. (mole/l.)	Transference Number of Cation	Mobility at Infinite Dilution ($\times 10^4$ cm^2/v.sec.)	
			Cation	Anion
Octylamie Hydrochloride	0.008	0.39	(5.6)	(8.8)
	0.0166	0.40		
	0.032	0.40		
	0.050	0.42		
	0.090	0.45		
Decylamine Hydrochloride	0.0068	0.34	(4.4)	(8.7)
	0.014	0.34		
	0.057	0.71		
	0.086	0.72		
Dedecylamine Hydrochloride	0.00053	0.26	(3.1)	(8.7)
	0.0053	0.26		
	0.0172	0.42		
	0.052	1.04		
	0.067	1.11		
	0.090	1.12		
Tetradecylamine Hydrochloride	0.00092	0.23	(2.5)	(8.7)
	0.0019	0.23		
	0.0033	0.27		
	0.018	1.12		
Hexadecylamine Hydrochloride	0.000074	0.181	(2.0)	(8.7)
	0.0014	0.34		
	0.0042	0.84		

TABLE III

TRANSFERENCE NUMBER AND RELATED QUANTITIES

Substance	Conc. (mole/l.)	Transference Number of Cation	Apparent Conductivity of		C^B/C
			Cation	Anion	
Octylamine Hydrochloride	0.005	0.39	51.9	81.1	—
	0.01	0.40	51.6	77.4	—
	0.02	0.39	50.4	69.6	—
	0.05	0.40	50.5	48.5	—
	0.1	0.45	52.7	32.3	—
Decylamine Hydrochloride	0.005	0.34	40.9	81.1	—
	0.01	0.34	39.8	76.2	—
	0.02	0.33	35.6	72.4	—
	0.05	0.60	45.6	30.4	0.23
	0.1	0.72	46.0	1.8	0.38
Deodcylamine Hydrochloride	0.005	0.26	28.6	81.4	—
	0.01	0.26	27.3	77.7	—
	0.02	0.50	37.5	37.5	0.31
	0.05	1.10	57.2	− 5.2	0.57
	0.1	1.12	44.8	− 4.8	0.66
Tetradecylamine Hydrochloride	0.002	0.22	23.6	83.4	—
	0.005	0.24	24.5	77.5	—
	0.01	0.65	44.2	23.8	0.38
	0.018	1.12	54.3	− 5.8	0.59
Hexadecylamine Hydrochloride	0.0001	0.18	18.4	83.6	—
	0.001	0.28	28.0	72.0	0.09
	0.003	0.59	37.8	26.2	0.46
	0.0042	0.84	33.9	6.5	0.65

concentration near its surface, and this must be greater than their concentration in bulk, and as the ratio of the former concentration to the latter is given by the Boltzmann-Poisson equation, the concentration of counter ions near the surface of the micelle will tend towards a constant value, and consequently, its transference number will tend towards a constant value as the bulk concentration increases. The greater-than-unity value of the transference number means, of course, that more chlorine ions are being carried towards the cathode than towards the anode.

In order to calculate the fraction of small ions bound to the micelle, some assumptions are necessary. It is first assumed, that the critical rise of the transference number arises only from the association of counter ions to the micelle. This assumption is equivatent to that of "square well potential" around the micelle. In the second place, it is assumed that, above the critical micelle concentration, the number of free cations is equal to the total number of cations existing in solution just before the critical micelle concentration. The second assumption will, however, have little effect on the result of the calculation except in the range near the critical micelle concentration. The equation obtained under these two assumptions is the same type as that obtained by Brady and Salley[3], which is expressed as follows:

$$\frac{C^B_-}{C} = 1 - \frac{\Lambda - (C^0_+/C)(T_-\Lambda + \Lambda^0_+)}{\Lambda^0_- + T_+\Lambda - (C^0_+/C)\Lambda^0}$$

where C, C^B_-, C^0_+ are the concentrations of total ions, bound anions, and free cations, respectively, and Λ, Λ^0, Λ^0_+, Λ^0_- denote the equivalent conductivity of total ions, total free ions, free cations, and free anions, respectively. T_+ and T_- are the transference number of the cation and the anion, respectively.

In Table III, calculated values of C^B_-/C are listed, together with the values of the apparent conductivities of the cation and the anion. It is shown here that at the concentration far above the critical micelle concentration, 60 or 70% of small ions are bound to the micelle. These bound ions can be considered to have no kinetic independence, and therefore, the valence of a micelle is about one third of the number of single molecules contained in a micelle. If we assume for dodecylamine hydrochloride the molecular weight determined by Debye[9] on the basis of his light scattering measurement, a micelle of this colloidal electrolyte is regarded to consist of 55 single molecules, so that it may possess an electrical charge of about 18 units.

If it is further assumed that the mobility of a free ion is not altered with increasing concentration; the mobility of the micelle ion of dodecylamine hydrochloride can be calculated by using the above mentioned data. The value thus obtained is 5.2×10^{-4} cm^2/v.sec., which is the same order of magnitude as simple ions. According to a simple consideration, the mobility of a micelle ion is proportional to its electric charge and is inversely proportional to the cubic root of the number of molecules composing it, so that the micelle is expected to have a greater mobility than that above obtained. In order to explain the above obtained value, it should be supposed that the mobility of a micelle ion is considerably reduced by the electrostatic interaction with small ions forming an ionic atmosphere.

From Tables I and III, it is suggested that, in the solution which has a large high-frequency effect, the micelle includes many associated counter ions as its kinetic unit, and consequently, has a compact structure. Generally, the greater the number of single ions forming a micelle, the greater the number of counter ions associated and the more compact the micelle structure. The association of counter ions, being probably an evidence for the electrostatic association in Bjerrum's sense[10], should play an important role in micelle formation, in such a way that it makes the polar heads of long-chain molecules forming a micelle less repulsive to each other.

Summary

The high-frequency and low-frequency equivalent conductivities and transference numbers for aqueous solutions of octyl-, decyl-, dodecyl-, tetradecyl-, and hexadecylamine hydrochlorides have been measured.

For the latter three solutions a considerable increase of the high-frequency concuctivity was observed, and for these three solutions it has been shown that the transference numbers of cations abruptly rise at the critical concentration for the micelle formation, and then tend towards a constant value.

These experimental facts have been accounted for from the electrostatic point of view of the micelle structure. It has been inferred from the experimental results that the counter ion association may be essential to the formation of the micelle.

We are grateful to Armour & Co., U.S.A. for the kind supply of the samples of the electrolytes used in our present work.

Chemistry Dept., College of General Education, and Institute of Science and Technonogy, The University of Tokyo, Tokyo

9) P. Debye, *J. Phys. & Colloid Chem.*, **53**, 1 (1949).

10) N. Bjerrum, *Erg. exakt. Naturwiss.*, **6**, 125 (1926).

Physical Properties and Crystal Structure of 1,1,1,2-Tetrachloro-2-methylpropane

By Tsutomu KOIDE, Tsutomu ODA and Isamu NITTA*

(Received March 9, 1956)

Hexamethylethane and hexachloroethane are known to undergo phase transition, the transition points being −125°C for hexamethylethane[1] and 43°C and 71°C for hexachloroethane[2]. The high temperature modifications are characterized by relatively high melting points, 100.6°C and 185°C, respectively. These phases are also characterized by high volatility, high plasticity and optical isotropy. The X-ray study of these cubic modifications was made by C. D. West[3] and C. Finbak[4] and other investigators[5], who concluded that the molecules are in rotational motion in a rough sense. It seems of interest to examine what will occur in the phase just below the melting point of a hexa-substituted ethane of the type of $(CH_3)_xCl_{3-x}CC(CH_3)_{x'}Cl_{3-x'}$. We have carried out an X-ray diffraction study of 1,1,1,2-tetrachloro-2-methylpropane, which was reported[6] to have high volatility and a relatively high melting point such as 169°C.

Experimental

Sample.—The sample used was prepared by the method of C. Willgerodt and F. Dürr[6] and a modified method by S. M. McElvain and C. L. Stevens[7]. In a flask with a reflux condenser 26 g. of purified chloretone was allowed to react with 60 g. of phosphorus pentachloride for twelve hours, the temperature of the water bath being kept at about 80°C. The reaction mixture was then cooled and the solidified excess of phosphorus pentachloride was filtered off. The solid was washed with benzene. The filtrates were subjected to fractional distillation. At the final stage the compound came out as solidified distillate. The solid thus obtained was pressed with filter paper to remove liquid impurities contained in it, and then refined by sublimation at a pressure of 30 mmHg.

Physical Properties.—It was observed that it melts at 173°C, and boils at almost the same temperature. The vapour of this solid is irritating to the eyes and nose. The solid is soft and shows plasticity, and we have found it to be optically isotropic. It sublimed readilly in a closed vessel to give well-formed rhombic prisms. These properties are very much like those of cubic hexamethylethane and cubic hexachloroethane. By suspending the crystals in a mixture of chloroform and carbon tetrachloride, the density of the solid was found to be 1.52 g./cc. at 10°C.

X-Ray Crystallographic Analysis.—As the solid is volatile, we used single crystals sealed in thin-walled glass capillary tubes. Such a sample was mounted on a goniometer-head of an X-ray camera. Using Cu radiation, we took Laue photographs and a group of 20° oscillation photographs over a range of 60° about [001] as the axis of rotation. Laue photographs taken with the X-ray beam parallel to [100], [110] and [111] showed holotesseral symmetry, and thus the point group of the crystal should be T_d-$\bar{4}3m$, O-43 or O_h-$m3m$. All spots appearing on the oscillation photographs were indexed satisfactorily by a cubic reciprocal lattice corresponding to a=7.4Å. All spots were extinguished except those for which $h+k+l=2n$. This classifies the crystal as being body-centered cubic. Thus the space group should be T_d^3-$I\bar{4}3m$, O^5-$I43$ or O_h^9-$Im3m$.

The density indicates the existence of two molecules in the unit cell, the calculated one 1.59 bing in agreement with the value mentioned above.

The apparent feature of the present X-ray data as well as such properties mentioned above lead us to imagine that this crystal will be isomorphous with cubic $C_2(CH_3)_6$ and cubic C_2Cl_6. Therefore we may also expect that this solid would undergo phase transition similar to those[1,2] of the hexa-substituted ethanes. In this respect we have carried out a differential thermal analysis.

Differential Thermal Analysis.—The apparatus used for the differential thermal analysis was almost the same as that previously reported by H. Chihara and S. Seki[8], so that only a brief account may be given here. As shown in Fig. 1, two thin-walled glass tubes are fitted separately in two drilled holes in a copper block A. One of the glass tubes contains NaCl as a standard

* Faculty of Science, Osaka University, Nakanoshima, Osaka.

1) G.S. Parks, H.M. Huffman and B. Thomas, *J. Am. Chem. Soc.*, **52**, 1032 (1930).

2) I. Nitta and S. Seki, *J. Chem. Soc. Japan*, **62**, 581 (1941); K.J. Ivin and F.S. Dainton, *Trans. Faraday Soc.*, **43**, 32 (1947); S. Seki and M. Momotani, This Bulletin, **23**, 30 (1950). See also O. Lehman, *Z. Krist.*, **1**, 106 (1877); ibid., **6**, 584 (1882).

3) C.D. West, *Z. Krist.*, **88**, 195 (1934).

4) C. Finbak, *Tids. Kiem. Bergv.*, **17**, No. 9, 2 (1937).

5) M. Atoji, T. Oda and T. Watanaté, *Acta Cryst.*, **6**, 868 (1953).

6) C. Willgerodt and F. Dürr, *Ber.*, **20**, 539 (1887).

7) S.M. McElvain and C.L. Stevens, *J. Am. Chem. Soc.*, **69**, 2667 (1947).

8) H. Chihara and S. Seki, This Bulletin, **26**, 88 (1953).

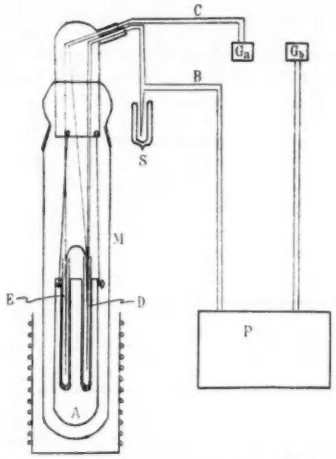

Fig. 1. A schematic diagram of the apparatus for differential thermal analysis. D: a reference cell containing NaCl; E: a sample tube; Ga, Gb: galvanometers; M: a mantle; P: a potentiometer; S: the standard temperature (ice).

material and the other the sample to be investigated. B and C are copper constantan thermocouples for the measurement of the temperature of NaCl, operated with a cotentiometer, and of the temperature difference between NaCl and the sample, operated with a galvanometer and a lamp-scale.

We have observed the anomalous heat effect at −62.2°C when the sample was cooled starting at a room temperature, and at −39.7°C. when heated starting at the temperature of solid CO_2. One of the typical curves is given in Fig. 2.

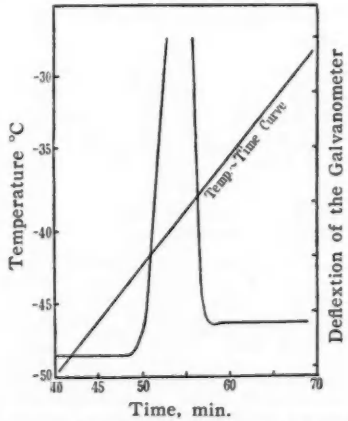

Fig. 2. Curves of differential thermal analysis of $Cl_3C{\cdot}C(CH_3)_2Cl$.

Discussion

Since there are two molecules in the unit cell with the body-centered translation, it is reasonable to place the centers of the molecules at the positions 0, 0, 0 and $\frac{1}{2}, \frac{1}{2}, \frac{1}{2}$, of which the symmetry should be T_d-$\bar{4}3m$, O-43 or O_h-$m3m$. On the other hand, as the rigid molecule of $Cl_3CC(CH_3)_2Cl$ can have at highest only one plane of symmetry which contains the central C–C bond axis, it becomes necessary to consider some statistical explanation of the structure, as is always so in plastic crystals[3,4,5,9]. In order that the statistical symmetry of the molecule be as high as T_d-$\bar{4}3m$ at 0, 0, 0 and $\frac{1}{2}, \frac{1}{2}, \frac{1}{2}$, the molecule should orientate its central C–C axis parallel to each one of the four body-diagonals statistically equally and at the same time laterally so that the C–C axis acquires a statistical symmetry of $3m$ at least. Such statistical symmetry can also be gained by a model of molecule in rotation about the C–C axis. In the cases of O^5-$I43$ and O_h^9-$Im3m$, it is necessary to add the antiparallel orientations of the polar C–C axis along the four body-diagonals, these directions having the symmetry of 3 or $3m$. It is also conceivable that the observed feature of X-ray diffraction can be explained by molecules in free spherical rotation. Which one of these possibilities is the case for the present statistical structure seems indiscernible from the consideration of intensity data, since the observable reflexions are few. However it may be said that the structure found for the present crystal is statistically analogous to those of the high temperature modifications of C_2Cl_6 and $C_2(CH_3)_6$.

The rapid decrease in intensity of the X-ray reflexions with increasing angle of scattering is evidently due to the disordered orientation of molecules in intense thermal motion. In accordance with these X-ray observations the crystal shows softness, plasticity, high volatility and relatively high melting point. The transformation observed at about −62.2°C may be attributed to a kind of order-disorder transition.

9) J. Timmermans, *J. Chim. Phys.*, **35**, 331 (1938); I. Nitta and T. Watanabé, This Bulletin, **13**, 28 (1938); T. Oda and T. Watanabé, *J. Chem. Soc. Japan*, **65**, 154 (1944); R.S. Schwartz, B. Post and I. Fankuchen *J. Am. Chem. Soc.*, **73**, 4490, 5113 (1951); T.B. Reed and W.N. Lipscomb, *Acta Cryst.*, **6**, 108 (1953); H.J. Backer and W G. Perdok, *Rec. Trav. Chim.*, **62**, 533 (1943).

Summary

1, 1, 1, 2-Tetrachloro-2-methylpropane is cubic at room temperatures. X-ray date may be interpreted on the basis of a body-centered packing of molecules in disorder, orientational or rotational. The cube edge of the unit containing two molecules is $a=7.4$Å. The crystal undergoes transition at about -62.2°C, when cooled, and at -39.7°C, when heated starting at a lower temperature.

The authors are grateful to the Ministry of Education for the Research Encouragement Grant in aid of this work.

Chemical Laboratory, Osaka University of Liberal Arts and Education
Tennoji, Osaka

SHORT COMMUNICATIONS

Precipitation of Silica in the Presence of Aluminum

By Katsumi Goto

(Received December 12, 1955)

It is commonly received among geologists[1] that silica in river water is colloidal and precipitated by electrolytes in sea water as a result of coagulation. It was shown in our previous reports[2-4], that colloidal silica, unless its concentration is very high, can not be precipitated even in sea water, where colloidal silica rather depolymerizes into molecularly dispersed state, owing to the high solubility of silica.

On the other hand, molecularly dispersed silica is precipitated by the addition of a small amount of aluminum salt, which hydrolyses into aluminum hydroxide and coprecipitates the silica, as has been employed to remove silica from boiler-feed water[5,6].

Thus a considerable literature has grown up around the subject of precipitation of molecularly dispersed silica by aluminum hydroxide, but little is known about the precipitation of colloidal silica.

Experimental

To a solution of silica, a known amount of aluminum was added as acidic solution of $AlCl_3$ or $Al_2(SO_4)_3$. The hydrogen ion concentration was adjusted to a pH 4 to 11 by the addition of dilute NaOH solution. The resulting solutions were filtered after about thirty minutes and analysed for the concentration of residual silica. As a similar effect was observed with $Al_2(SO_4)_3$ as well as with $AlCl_3$, the results obtained with $Al_2(SO_4)_3$ are described below. The colloidal solution of silica was prepared from sodium silicate solution containing 20 g. SiO_2 per litre by the ion-exchange method[2] followed by aging for several months at pH about 8.

Figs. 1. and 2 show the effects of pH on the

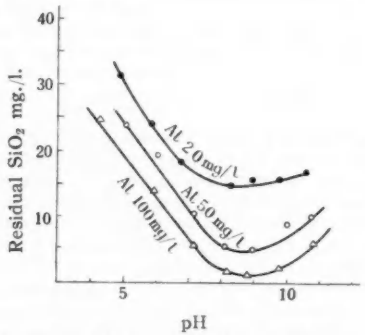

Fig. 1. Precipitation of molecularly dispersed silica. SiO_2 35 mg./l.

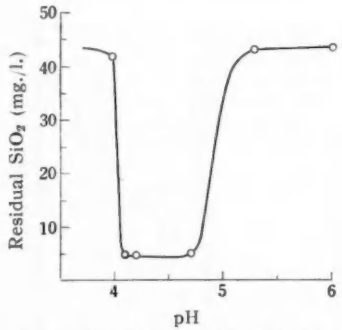

Fig. 2. Precipitation of colloidal silica SiO_2 45 mg./l., Al 1 mg./l.

precipitation of molecularly dispersed silica as well as colloidal silica, by aluminum. It is interesting to note that the optimum pH for the precipitation of molecularly dispersed silica is about 9, while colloidal silica is precipitated most

effectively at pH about 4.5. Much smaller amount of aluminum is sufficient for the precipitation of colloidal silica compared with that for molecularly dispersed silica. One milligram of aluminum precipitates as much as 40 mg. of colloidal silica. This may be closely connected with the fact that colloidal silica has a electrophoretic mobility much greater than that of molecularly dispersed silica[2,7].

Colloidal silica can not be precipitated, in the case where the ratio of colloidal silica to aluminum exceeds a certain value, as will be seen in Fig. 3. Neither aluminum nor colloidal silica precipitates in this case.

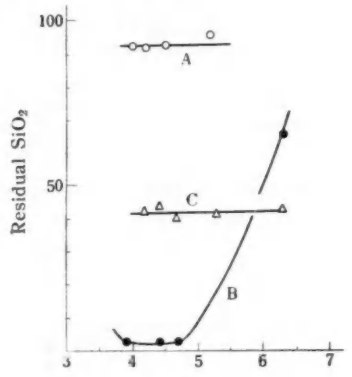

Fig. 3. Presipitation of colloidal silia.

A	SiO_2	92 mg./l.	Al	1 mg./l.
B	SiO_2	〃	Al	2 〃
C	SiO_2	43 mg./l.	Al	0.5 mg./l.

According to the results shown above, it is clear that a trace amount of aluminum plays an important role in the precipitation of silica, especially when the silica is colloidal. Biological sedimentation[1] of silica must also be taken into account, but at least in some cases, precipitation of colloidal silica by a trace amount of aluminum will successfully explain the sedimentation of silica in natural waters.

The author wishes to express his thanks to prof. Y. Uzumasa, Prof. G. Okamoto, Prof. I. Kayama, and Assist. prof. T. Okura for their invaluable advice and encouragement. The author is also indebted to T. Ogawa for carrying out a part of the experiments.

Faculty of Engineering, Hokkaido University, Sapporo

1) W.H. Twenhofel, "Principles of Sedimentation", McGraw-Hill (1950), p. 398.
2) K. Goto, T. Okura and I. Kayama, *Kagaku*, **23**, 428 (1953).
3) K. Goto, *J. Chem. Soc. Japan (Pure Chem. Sect.)*, **76**, 729 (1955).
4) K. Goto, ibid., **76**, 1364 (1955).
5) L.D. Betz, C.A. Noll and J.J. Maguire, *Ind. Eng. Chem.*, **32**, 1320 (1940).
6) G. Okamoto, T. Okura and N. Sudo, *J. Electrochem. Soc. Japan*, **19**, 289 (1951).
7) R.K. Iler, "The Colloid Chemistry of Silica and Silicate", Cornell Univ. Press (1955), p. 248.

Adiabatic Compressibility of Aqueous Solution. III. Egg Albumin

By Yutaka MIYAHARA

(Received March 12, 1956)

R. J. Urick[1] has pointed out empirically that the adiabatic compressibility of a suspensoid could be computed from the compressibilities of dispersed phase and dispersion medium. His treatment was based on the assumption that the compression of the suspension is the arithmetic sum of compressions of components. The extension of this idea to the hydrophilic colloids has been tried by the present author in a preliminary study on a starch sol[2].

In this paper the ultrasonic velocity in the aqueous solution of egg albumin was measured and the numerical value of the compressibility of the albumin molecule in the aqueous solution at its isoelectric point was estimated approximately. Along this line of the investigation, Jacobson[3] has determined the compressibilities of oxyhemoglobin, hemocyanin and serum albumin molecules.

The ultrasonic velocity was measured with an ultrasonic interferometer, the detailed description of which and the experimental procedures have been reported previously[4]. The frequency of the ultrasonics was 1090 KC and the measurement was made at 20.0°C.

The egg albumin used was prepared from the white of a fresh hen's egg by the usual procedure, using ammonium sulphate as a salting out agent. After recrystallizing several times, the electrolytes' impurities were removed by dialysis with redistilled water until no trace of ammonia was detected by the Nessler reagent. The concentration of the egg albumin in the solution was determined by the density measurement. The relation between density and concentration used here was obtained from the partial specific volume, numerical values of which had been given as 0.749 cc./g. by T. Svedberg et al.[5]

The experimental results of the measurements of the ultrasonic velocities and other related quantities are listed in Table I. The physical meaning of the notations here used was given in the previous paper[6].

The numerical value of K/x, the specific compression of the albumin solution at an infinite dilution, was calculated from the present data by using the method of least squares and is found to be -0.16.

To get the numerical value of the com-

TABLE I

No.	D_S/D_O	x	c/c_O	κ/κ_O	K
1	1.0034	0.0134	1.0022	0.9922	−0.0022
2	1.0005	0.0019	1.0003	0.9989	−0.0003
3	1.0062	0.0247	1.0041	0.9857	−0.0041
4	1.0045	0.0179	1.0031	0.9893	−0.0027
5	1.0030	0.0117	1.0019	0.9933	−0.0020
6	1.0025	0.0100	1.0019	0.9937	−0.0012
7	1.0032	0.0125	1.0024	0.9922	−0.0015
8	1.0027	0.0107	1.0017	0.9939	−0.0019
9	1.0026	0.0104	1.0016	0.9942	−0.0019
10	1.0005	0.0020	1.0003	0.9988	−0.0003

pressibility of the albumin molecule itself, we should estimate the effect of hydration on the compressibility of the solution. The necessary equation has already been given in the previous paper[4]. However, we have not obtained sufficient data for these terms, because we could not measure the hydration effect and compressibility separately. In the present investigation, the data of amino acid solutions were used for this purpose. As was shown in the previous paper[4], the hydration effect of amino acids is nearly independent of their species, and their numerical values are almost constant. The molar value, K_m ($=M\cdot K_h/x$, M being molecular weight) is about 6·10 on an average. In the albumin molecule, the radicals which give the dominant effects upon the compressibility of the solution by the hydration effect may be its ionized radicals only, and the effects of non-ionic groups could be neglected as in the case of amino acid solution. Further we assume here that the hydration effect of polar groups which are ionized perfectly in the solution at its isoelectric point is not greatly different from the effect of free amino acids in the solution. Of course this assumption should be subjected to further discussion. The number of pairs of ionized radicals in an albumin molecule at its isoelectric point could be determined from the data of potensiometric titration. The value adopted here is 9.10^{-4} gram equivalent per gram[7]. Using these data, the effect of hydration, K_h/x for albumin molecule is estimated as 0.05, about thirty per cent of K/x. That means that the deviation due to the above assumption produces not so much difference from the right value, if we expect just semi-quantitative discussion. The actual volume occupied by albumin molecule in the aqueous solution, which is necessary for the present purposes, was calculated as well from the specific volume obtained by Svedverg[5]. The value is $v_m=0.749\ x$ per one cc. solution.

The molecular compressibility of albumin molecule in the aqueous solution at its isoelectric point is then found to be 13.10^{-12} cgs. The values of oxyhemoglobin, hemocyanin and serum albumin were recalculated from Jacobson's data[3] by using the same procedure are 11, 17 and 11 cgs. respectively. These values are in the order of the compressibilities of organic molecular crystals and they are of reasonable magnitudes, considering that protein molecules have some special structures, not like artificial polymermolecules which stretch in the solution. The extension of the present survey is thought to deserve further investigation.

Chemical Institute, Faculty of Science
Nagoya University, Nagoya

1) R.J. Urick, *J. Applied Phys.*, **18**, 983 (1947).
2) Y. Miyahara and H. Shiio, *J. Chem. Soc. Japan (Pure Chem. Sect.)*, **73**, 1 (1953).
3) B. Jacobson, *Arkiv För Kemi.* **2**, 177 (1950).
4) Y. Miyahara, *Bull. Chem. Soc. Japan*, **26**, 390 (1953).
5) T. Svedberg and J.B. Nichols, *J. Am. Chem. Soc.*, **48**, 3081 (1926).
6) Y. Miyahara, *Bull. Chem Soc. Japan*, **25**, 326 (1952).
7) E.J. Cohn and J.T. Edsall, "Protein, Amino Acids and Peptides", (1943), p. 498.

*Studies on the Oxy-acid Phosphors. VI. Antimonate Phosphors**

By Yoshihide KOTERA, Tadao SEKINE and Michiko YONEMURA

(Received March 13, 1956)

Few reports have ever been published on the antimonate phosphors. K. H. Butler et al. reported the formation of calcium pyroantimonate during the preparation of calcium halophosphate phosphor, but he did not find any emission for this material[1]. R. Bernard and J. Janin observed recently the luminescence of calcium metaantimonate activated by manganese[2], and M. Tomono et al. reported the green luminescence of calcium metaantimonate activated by manganese[3], but the full details of their preparation, characteristics etc. remain still unknown.

In the preparation of antimonate phosphors, a commercially available pure grade of antimony chloride was used as one of the starting materials and purified by the process described in a previous paper[4]. As for the other starting materials, respective metallic salts were used, which were purified by the process described in another previous paper[5]. Their purity was established spectrographically. Purified antimony oxide and metallic oxide

TABLE I

THE OPTIMUM MIXING RATIO FOR THE PREPARATION OF ANTIMONATE PHOSPHORS

	Sb_2O_3 : (MO or $M(NO_3)_2$)	Firing Coditions
Ca antimonate	1 : 2.4 mol.	1100°C 2 hr.
Sr antimonate	1 : 2.2 mol.	1100°C 2 hr.
Ba antimonate	1 : 2.2 mol.	1100°C 2 hr.
Mg antimonate	1 : 4.8 mol.	1150°C 1 hr.
Zn antimonate	1 : 2.2 mol.	1100°C 1 hr.

or carbonate were mixed in an agate mortar in the molar ratio as shown in Table I and, if necessary, an appropriate salt was also added as an activator; then the mixture was fired for one to two hours at 1100°C in air.

5 weight % of NH_4NO_3 was added to the batch so as to increase the brightness[6].

The properties of antimonate phosphors are shown in Table II. The $Ca_2Sb_2O_7$: Bi phosphor gives the highest brightness among them, the spectral distribution of its emission under cathode-rays excitation being shown in Fig. 1. Data showing the X-ray diffraction pattern for $Ca_2Sb_2O_7$ are presented on Table III together with the results by K. H. Butler et al.[1].

TABLE II

THE EMISSIONS COLOURS OF ANTIMONATE PHOSPHORS

	3650 Å	2537 Å	Cathode rays
$Ca_2Sb_2O_7$	pink f	pink f	orange f
$Sr_2Sb_2O_7$	none	bluish white ff	none
$Ba_2Sb_2O_7$	none	white ff	none
$Mg_2Sb_2O_7$	none	none	orange ff
$Zn_2Sb_2O_7$	yellow ff	none	yellow ff
$Ca_2Sb_2O_7$: Bi	blue m	blue m	blue m
$Sr_2Sb_2O_7$: Bi	green f	green f	green f
$Mg_2Sb_2O_7$: Bi	green f	green f	none
$Zn_2Sb_2O_7$: Bi	green f	none	yellow f

m: medium, f: faint, ff: very faint

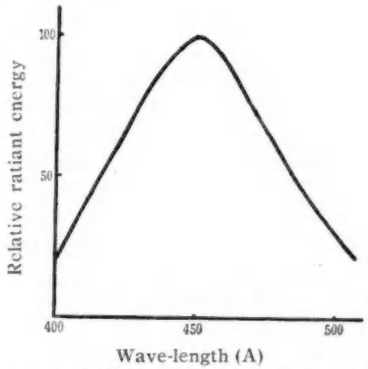

Fig. 1. Emission of $Ca_2Sb_2O_7$: Bi with cathode-rays excitation.

The formation of $Ca_2Sb_2O_7$ during the preparation of calcium halophosphate phosphors was verified by K. H. Butler et al. 's X-ray diffraction analysis. We found that various antimonates without any intentional activator are able to luminesce and give blue, green or yellow luminescence when bismuth is employed as an activator. The emission of samples without activators might be due to the activation by antimony itself, although such a possibility is not definitely ascertained. From the mixing molar ratio shown in Table I and the X-ray diffraction patterns in Table III, it is concluded that these phosphors are composed of pyroantimonate. The emissions of haloantimonates are expected from the

TABLE III

X-RAY DIFFRACTION PATTERN OF $Ca_2Sb_2O_7$ PHOSPHOR

Phosphor		$Ca_2Sb_2O_7$*		Phosphor		$Ca_2Sb_2O_7$*		Phosphor		Phosphor		Phosphor	
d	I	d	I	d	I	d	I	d	I	d	I	d	I
		10.05	0.4	2.58	s	2.607	0.6	1.72	w	1.435	w	1.141	m
6.05	m	5.97	0.7			2.551	0.4	1.70	w	1.400	w	1.127	vw
5.13	m	5.19	0.6	2.37	vw	2.351	0.1	1.66	vw	1.364	w	1.092	vw
4.51	w			2.31	m	2.290	0.1	1.64	vw	1.344	vw	1.085	vw
3.99	w					2.132	0.1	1.61	vw	1.299	m	1.066	m
3.62	m	3.633	0.5	2.09	vw	2.106	0.2	1.57	s	1.266	w	1.049	m
3.29	s			2.00	s	2.009	0.4	1.55	s	1.225	vw	1.041	w
3.08	w	3.105	0.4	1.85	w	1.867	0.4	1.53	m	1.204	vw	1.029	w
2.97	s	3.009	0.9	1.81	vs	1.824	1.0	1.499	m	1.175	vs	1.015	w
2.93	s	2.960	0.9	1.74	w			1.475	m	1.157	m	1.003	m

* Data by K.H. Butler et al.

In all columns "d" and "I" represent the interplanar spacing in Angstrom and its intensity respectively. The abbreviations in columns "I" mean:

vs: very strong. s: strong. m: medium. w: weak. vw: very weak.

fact, that the change of emission colour was observed when halide was employed as a flux, but their details are not yet investigated.

We wish to thank Dr. Shoji Makishima for the general discussion on the subject and the experimental work he and his associates have done.

Government Chemical Industrial Research Institute, Tokyo
Hatagaya-honmachi, Tokyo

* Read before the Seventh Annual Meeting of the Chemical Society of Japan 1954. Report V was published in This Bulletin.

1) K.H. Butler, M.J. Bergin and V.M.B. Hannaford, *J. Electrochem. Soc.*, **97**, 117 (1950).
2) R. Bernard and J. Janin, *Compt. rend.*, **237**, 798 (1953); **239**, 489 (1954); **240**. 614 (1955).
3) M. Tomono et al., Read before the Eighth Annual Meeting of the Chemical Society of Japan, 1955.
4) Y. Kotera and T. Sekine, *J. Electrochem. Soc.*, **102**, 390 (1955).
5) Y. Kotera and T. Sekine, This Bulletin, **27**, 13 (1954).
6) Y. Kotera and T. Sekine, *J. Chem. Soc. Japan (Ind. Sect.)* **54**, 625 (1951).

Lattice Constant of Digenite

By Tsuguyasu WADA

(Received June 19, 1956)

Digenite, $Cu_{1.8}S$, was first discovered by Buerger[1] in copper-sulfur system. The crystal structure of this phase is known as a cubic lattice of anti-fluorite type, in which half of the copper atoms are statistically distributed in the interstices of the sulfur atoms, forming so-called *averaged structure*[1,2]. Ramdohr[3] has thereafter discovered the naturally occurring mineral of this composition, and named it *Neodigenite*.

The Buerger's phase diagram of copper-sulfur system shows that the digenite phase has no range of solid solution at room temperature. However, some investigators[4] have maintained that this is not the case but that the digenite has some range of solid solution.

In this communication, the lattice constant of digenite at room temperature is measured using the samples of various compositions, and it is confirmed that the digenite has a range of solid solution.

The sample used was synthesized from electrolytic copper and thoroughly-distilled sulfur. The stoichiometric Cu_2S and CuS were first prepared by heat-treatment of copper and a corresponding amount of sulfur sealed in a vacuum Pyrex tube for about two hundred hours at 400°C. Then, these materials were mixed in appropriate ratio, sealed in vacuum, and heat-treated by the same procedure as above, with gradual cooling to the room temperature. Thus the samples of desired compositions were obtained.

X-ray powder photographs were obtained for these samples using Straumanis-type camera of 90 mm. diameter and CuK_α radiation. The line of (551) (711) is very suitable to determine the lattice constant, since its Bragg angle for CuK_α is about 81°, although its intensity is very weak. Sometimes, (440) line was measured by focusing backreflection camera and FeK_α radiation. The Bragg angle of this case is about 80°. As the wave lengths of X-rays, the values of Siegbahn's table[5] were used.

In the Figure, the lattice constants observed are plotted against the composition, and it is shown that these vary from 5.554 to 5.544 kX with the increase of sulfur content. The accuracy for the measurement of the lattice constant is estimated to be ±0.001 kX, and that of the composition to be ±0.2 atomic percent of sulfur.

From this result, it is obvious that the digenite has a range of solid solution, though it is relatively narrow, at room temperature. The range seems to cover the compositions from 35.7 to 36.1 atomic percent of sulfur, but more sufficient experimental points are necessary to determine it precisely. The fact

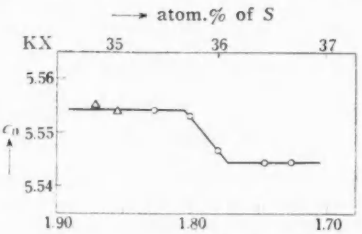

—○— From (551) (711), by CuK_α.
—△— From (440), by FeK_α.

Fig. 1. Lattice constant of digenite.

that the lattice contracts when the atomic fraction of cation is decreased suggests that the variation of composition may be caused by the escape of cations from their lattice sites.

Department of Chemistry, Faculty of Science, Hokkaido University
Sapporo

1) N.W. Buerger, *J. Chem. Phys.*, **7**, 1067 (1939); *Econ. Geol.*, **36**, 19 (1941).
2) P. Rahlfs, *Z. phys. Chem.*, **(B) 31**, 157 (1936).
3) P. Ramdohr, *Z. prakt. Geol.*, **51**, 1 (1943); *Chem. Abstr.*, **38**, 4500 (1944).
4) L. Eisenmann, *Ann. Phys.*, **6. Folge, 10**, 129 (1952).
5) M. Siegbahn, "Spektroscopie der Röntgenstrahlen". Berlin (1931).